

Original document stored on the publication server of the University of Basel

edoc.unibas.ch



This work is licenced under the agreement „Attribution Non-Commercial No Derivatives – 2.5 Switzerland“. The complete text may be viewed here:

creativecommons.org/licenses/by-nc-nd/2.5/ch/deed.en

Contributions to a science based expert system for solid dosage form design

Inauguraldissertation

ZUR

Erlangung der Würde eines Doktors der Philosophie
vorgelegt der
Philosophisch-Naturwissenschaftlichen Fakultät
der Universität Basel

von

Etienne Krausbauer
aus Strasbourg (Frankreich)

Basel, 2009



Attribution-Noncommercial-No Derivative Works 2.5 Switzerland

You are free:



to Share — to copy, distribute and transmit the work

Under the following conditions:



Attribution. You must attribute the work in the manner specified by the author or licensor (but not in any way that suggests that they endorse you or your use of the work).



Noncommercial. You may not use this work for commercial purposes.



No Derivative Works. You may not alter, transform, or build upon this work.

- For any reuse or distribution, you must make clear to others the license terms of this work. The best way to do this is with a link to this web page.
- Any of the above conditions can be waived if you get permission from the copyright holder.
- Nothing in this license impairs or restricts the author's moral rights.

Your fair dealing and other rights are in no way affected by the above.

This is a human-readable summary of the Legal Code (the full license) available in German:
<http://creativecommons.org/licenses/by-nc-nd/2.5/ch/legalcode.de>

Disclaimer:

The Commons Deed is not a license. It is simply a handy reference for understanding the Legal Code (the full license) — it is a human-readable expression of some of its key terms. Think of it as the user-friendly interface to the Legal Code beneath. This Deed itself has no legal value, and its contents do not appear in the actual license. Creative Commons is not a law firm and does not provide legal services. Distributing of, displaying of, or linking to this Commons Deed does not create an attorney-client relationship.

Genehmigt von der Philosophisch-Naturwissenschaftlichen Fakultät
auf Antrag von

Professor Dr. H. Leuenberger
und
Professor Dr. I. Caraballo

Basel, den 11. December 2007

Professor Dr. H-P Hauri
Dekan

To Luiza

Acknowledgements

I wish to express my deepest gratitude to my supervisor Professor Dr. H. Leuenberger to have given me the opportunity to perform this thesis and for his trust and great support during the work.

Sincere thanks go to Professor Dr. I. Caraballo who accepted to assume the co-reference of this work.

Many thanks to Dr. M. Puchkov for his help and for the very interesting collaboration that we had together during this PhD. I learned a lot from Dr. Puchkov, especially about cellular automata modeling and percolation theory.

I deeply thank Dr. Gabriele Betz for her support, advices and for the great atmosphere and the team that she installed in the Industrial Pharmacy Lab.

Many thanks go to my colleagues and friends at the Institute of Pharmaceutical Technology (IPT) and Industrial Pharmacy Lab (IPL). I am especially grateful to Mrs. S. Šehić, Mrs. M. Pašić, Mrs. E. Hadzovic, Dr. K. Chansanroj, Mrs. F. Müller, Mr. V. Balzano, Mr. M. Rumman, Mr. M. Saeed, Mr. H. Mojo, Mr. H. Yamaguchi and Mr. T. Meyer for their help, suggestions and companionship. It was a real pleasure to work in IPL with such a warm and congenial atmosphere.

A special thank to Mr. S. Winzap for his great availability and helpful presence.

Many thanks to Mrs. E. Darronqui for her help in IT management of IPT.

I would like to thank also Mr. M. Schneider, Dr. H. Nalenz and Dr. J. von Orelli for their advice in sterile liquid dosage forms practical course.

I am very grateful to Mr. K. Eichler for his interest to my work, and his kind invitations to speak and participate in numerous workshops in Technology Training Center.

My warmest thanks go to my family and friends. I am deeply grateful to my girlfriend Luiza Nedelcu for her love, help and patience during these 3 years. I would like to thank very much my mother for her encouragement and for teaching me the value of hard work and studies. I thank also my father for his constant interest in my work and his encouragements. I am very grateful to my dear grandmothers for always showing me their pride and love. My thanks go also to all my other family members for their affection and encouragements. I would like to express as well my gratitude to Mr. V. Gass, Mr. J. Fuchs, Mr. S. Fischer and Mr. Y. Bourgeois for our precious friendship.

*"Le vrai point d'honneur n'est pas d'être toujours dans le vrai.
Il est d'oser, de proposer des idées neuves, et ensuite de les vérifier."*

*"The real point of honor is not to be always right.
It is to dare, to propose new ideas, and then to verify them."*

**Pierre-Gilles de Gennes (1932-2007)
Nobel Prize winner for physics in 1991**

Table of contents

Symbols and abbreviations.....	IV
1. Summary	1
2. Introduction.....	3
3. Theoretical section.....	5
3.1. Solid dosage formulation design	5
3.1.1. Solid dosage preformulation and formulation	5
A. Preformulation testing.....	5
B. Tablet formulation and design	11
3.1.2. Compression of pharmaceutical powder into tablets	15
A. The compression process.....	16
B. Bonding in tablets	18
C. Compression equipment.....	20
D. Description of densification cycle	24
E. Energy and power occurring during compression.....	25
F. Pressure distribution within a compact	26
G. Mathematical characterisation of the compression process	27
3.1.3. Solubility of solids	28
A. Definition of the solubility	28
B. Solubility of drugs.....	29
C. Solvation process.....	29
D. Factors influencing solubility.....	30
E. Determination of the solubility.....	31
3.1.4. Disintegration of pharmaceutical tablets	32
A. Importance of the disintegration process in drug absorption	32
B. Mechanisms of disintegration	33
C. Types of disintegrants.....	39
D. Method of addition of disintegrants.....	41
E. Mathematical description of disintegration	41
F. In vitro disintegration test.....	42
G. The role of water uptake in the disintegration process.....	42
H. Rules to design fast disintegrating tablets	44
3.1.5. Dissolution of pharmaceutical compacts	48
A. Importance of the dissolution process in drug absorption.....	48
B. Surface area	48
C. Dissolution process.....	50

D. Mathematical description of the dissolution process	51
E. Dissolution testing methodology.....	59
F. Setting for <i>in vitro</i> dissolution measurements.....	61
G. Biopharmaceutical Classification System (BCS).....	63
3.2. Expert systems and solid dosage formulation design.....	63
3.2.1. General knowledge.....	63
3.2.2. Application of expert systems in pharmaceutical formulation	66
3.3. Main theories and models considered to develop a general (or non biased) expert system ...	71
3.3.1. Percolation theory.....	71
A. Main concepts of percolation theory.....	71
B. Fractals	82
C. The renormalisation group.....	89
D. Applications in pharmaceutical technology	91
3.3.2. Cellular automata	93
A. What are cellular automata?.....	93
B. Fundamental properties of CA.....	95
C. Two simple examples	96
D. CA For Modeling Physical Systems	102
4. Conception and implementation of the expert system	105
4.1. General conception	105
4.1.1. Reasons to develop an new innovative expert system for pharmaceutical solid dosage formulation design .	105
4.1.2. Non-biased expert system: a ES backbone based on general mathematical and physical models.....	105
4.1.3. Modular architecture: a toolbox for solid dosage formulation design	106
4.1.4. Quality evaluation of the modeling results from ES modules.....	108
4.2. Material and method of implementation	112
4.3. Developed modules description.....	114
4.3.1. Exact prediction of the optimal percentage of disintegrant for a minimal disintegration time of a tablet	114
A. Solution for non-fibrous disintegrants	114
B. Fibrous disintegrants	128
4.3.2. Dissolution simulation of a pharmaceutical compact using CA modeling.....	134
A. General concept and innovative aspect of the simulation.....	134
B. Tablet pattern design and discretisation using Tablet Designer (TD) module.....	135
C. Setting up composition of a virtual tablet.....	140
D. Databases of components, (DB module).....	145
E. Cellular automaton for <i>in silico</i> solid dosage form dissolution	146
F. Operating mode for calibration of solubility and swelling constants of the CA.	153

5. Experimental validation	154
5.1. Material and methods	154
5.1.1. Model drugs and excipients	154
A. Drug substances	154
B. Excipients	157
5.1.2. Characterisation of the substances	161
A. Particle size distribution	161
B. True density	161
C. Characterisation of the drug substances	161
D. Characterisation of the excipients	163
5.1.3. Tableting	164
A. Compaction technology	164
B. Tablet formulations for disintegration testing and water uptake measurement	164
C. Preparation of the tablet formulations for dissolution testing	168
5.1.4. Characterisation of the tablets	169
A. Porosity calculation	169
B. Characteristics of the tablets used for disintegration and water uptake testing	170
C. Characterisation of the tablets for dissolution testing	171
5.1.5. Tablet testing methods	172
A. Disintegration testing	172
B. Water sorption measurement	172
C. Dissolution testing	173
5.2. Results and discussion	174
5.2.1. Validation of Disintegration Optimisation module	174
A. Non-fibrous disintegrants	174
B. Fibrous disintegrants	185
5.2.2. Validation of the dissolution simulation module	190
A. Determination of CA solubility constants of the drugs	190
B. Comparison of <i>in silico</i> and experimental dissolution profiles	194
6. Conclusions and outlook	203
7. References	206
8. Image credits	221
9. Appendix	224
CURRICULUM VITAE	267

Symbols and abbreviations

CA	Cellular Automaton(a)
DB	DataBase module of ES
DO	Disintegration Optimisation of ES
DS	Dissolution Simulation module of ES
DT	Disintegration Time
ES	Expert System
FDA	Food and Drug Administration
GIT	Gastro-Intestinal Tract
IPL	Industrial Pharmacy Lab
IPT	Institute of Pharmaceutical Technology
PAT	Process Analytical Technology
SoC	Solubility Constant of an ingredient in DS
SwC	Swelling Constant of an ingredient in DS
TD	Tablet Designer module of ES
ϵ	Porosity of tablets
ϵ_t	Targeted porosity of tablets
p_c	Percolation threshold
%(v/v)	Volumetric percentage
%(w/w)	Mass percentage
WU	Water Uptake

1. Summary

The following work gathers different contributions to a science based expert system for solid dosage form design.

Within the context of PDA's Process Analytical Technology (PAT) initiative, quality by design of dosage forms is an ultimate objective for pharmaceutical companies. Significant returns on investment (ROI) were already realised in pharmaceutical industry by using modeling software tools and formulation expert systems. It was decided to develop an innovative expert system (ES) for solid dosage form design in order to help formulators to narrow the search for optimal formulations.

The scientific backbone of the system uses only mathematical and physical models in order to propose a general and non-biased ES. Moreover, it was decided to build the ES on a modular architecture in order to set up formulation toolbox elements. The modules developed and used during this PhD work are mathematical models and a discrete mechanistic modeling technique (i.e. cellular automata). Each module is constituted of a program or set of programs which enable the optimisation of one specific property (e.g. disintegration, dissolution rate, etc.). However it should be possible to link all modules to each other and to test at the same time the different properties of a formulation in order to choose at the end of the process the best compromises.

The main task of the ES backbone is to evaluate if simulation and modeling results obtained with each module meet the requirements of pharmacopoeia. A quality evaluation unit should thus use optimisation algorithms (e.g. Simplex or Nelder-Mead methods) to minimise the difference between required and *in silico* results.

Different models and three modules are presented in this PhD work. Disintegration optimisation (DO) module, dissolution simulation (DS) module and a module using databases to store ingredients' information (DB module) and to communicate information to the other modules.

Mathematical solutions based on geometrical models and using percolation theory are proposed for disintegration optimisation of tablet. The DO module enables to calculate the optimum amount of disintegrant (disintegrant threshold) in a formulation to minimise the disintegration time of a tablet. Comparison of experimental and calculated disintegrant thresholds has shown a good correlation and encourages using this model for disintegrant formulation.

The DS module for *in silico* drug release testing uses cellular automata (CA) modeling method to simulate the dissolution of a virtual tablet with respect to its physical characteristics, to the mean particle size of the ingredients and to the composition of the formulation. It is composed of different programs. Pattern of the virtual tablet must be first designed and discretised within a dissolution cubic matrix using “Tablet Designer” program. Virtual tablet composition is then set up using DB module. A program was implemented to pack randomly particles of the different selected ingredients and to mimic their compressed state in the compact. While CA dissolution algorithm is running, dissolution profile is drawn at the same time in the main interface of the module. Comparisons of *in silico* with experimental dissolution profiles showed encouraging correlations for most of the formulations tested.

Further developments are however required for complete automation of the formulation process with ES, for loading up the databases with more ingredients and for completing the module set of the toolbox.

These first contributions to an innovative ES for solid dosage forms design could be used as a base for computer aided formulation design to find alternative solutions to already existing simulation methods.

2. Introduction

The most commonly used dosage forms are still tablets. A tablet is a mixture of active pharmaceutical ingredients (API) and excipients, usually in powder form, compacted at certain shape. Tablets offer many advantages: manufacture is cost effective, convenient to dispense and store, easy to administer, and provide a versatile means of delivering the drug.

Tablets are manufactured by applying force to a powder bed, which compresses the powder into a robust compact. The powder may consist of either primary particles or aggregated particles (i.e. granules). During compression process, bonds are established between the particles or granules, thus conferring a certain mechanical strength to the compact. The properties of the tablet (e.g. mechanical strength, disintegration time and drug release characteristics) are affected by the properties of the constituent materials (API and excipients), but also by the manufacturing process. The excipients include binders, glidants (flow aids) and lubricants to ensure efficient tableting; disintegrants to ensure that the tablet breaks up in the digestive tract; sweeteners or flavours to mask the taste of bad-tasting APIs; and pigments to make uncoated tablets visually attractive. A coating may be applied to hide the taste of the tablet's components, to make the tablet smoother and easier to swallow, and to make it more resistant to the environment, extending its shelf life.

Tablets should be sufficiently strong to withstand handling during manufacturing and usage, but should also disintegrate and release the drug in a predictable and reproducible manner. For this reason it is important to choose the appropriate excipients and manufacturing process when developing a new tablet formulation.

However, tablets produced by pharmaceutical industry still currently exhibit variability in quality, e.g. API dosage, weight or hardness. Formulation of solid dosage forms is in fact currently closer to an art than to a science. The Sigma value which describes the performance of a process is laying between 2 and 3 for pharmaceutical industry (i.e. 4.6 % defectives), whereas semiconductor industry has this value of 6 (less than 2 per billions defectives). The reason for this is the poor understanding of many pharmaceutical processes, which causes sometimes unpredictable manufacturing.

In the last recent years, FDA's Process Analytical Technology (PAT) initiative has pushed forward the idea of improving the quality of pharmaceutical products by a deeper understanding of the processes involved in drug manufacturing. The ultimate goal is to achieve quality by design of pharmaceutical dosage forms. The guideline published by the FDA (2004) concerning the PAT-initiative presents a framework with two components: (1) set of scientific

principles and tools supporting innovation and (2) strategy for regulatory implementation that will accommodate innovation. The goal of FDA's PAT initiative is to achieve scientifically based decisions, i.e. to design the quality of the product and not to "test-in" the quality by eliminating the bad items at the end of the production, creating waste of time and money (Leuenberger et al., 2005). The PAT-initiative is however a recommendation to the pharmaceutical industry and not a compulsory regulation.

In this sense, FDA promotes as well the use of better manufacturing toolkit, in particular IT tools: "Scientists involved in reviewing medical devices at FDA report an urgent need for predictive software to model the human effects of design changes for rapidly evolving devices. We believe that such software may be attainable with a concentrated effort, by assembling currently available data and identifying existing data gaps." (Challenge and Opportunity on the Critical Path to New Medical Products, FDA).

Furthermore, it has been reported that there is a significant return on investment (ROI) to be realised from the use of modeling and simulation software tools (Louie et al., 2007) and that several key benefits were identified from use of pharmaceutical product formulation expert systems (Rowe et al., 1998).

Within this context, it was decided to develop innovative expert system (ES) software to help formulators to narrow the search for optimal solid dosage formulations. The innovative aspect of this project is the system using only mathematical and physical models as a scientific backbone in order to propose a general and non-biased ES. Moreover, it was decided to build the system on a modular architecture in order to set up the formulation toolbox elements. The algorithms used to model and simulate properties of pharmaceutical tablets should be based on mathematical methods (e.g. cellular automata) using only mechanistic models or first principles (see figure 2.1).

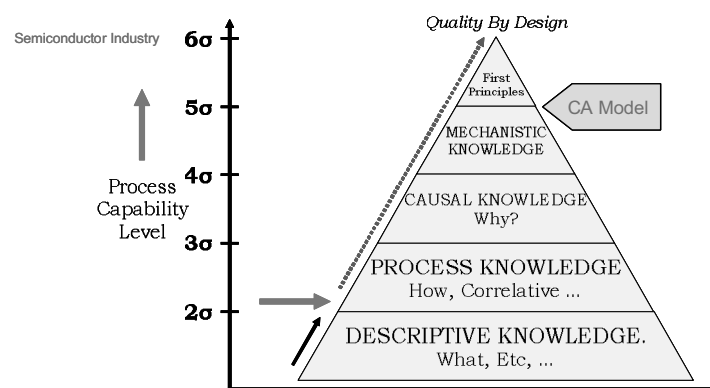


Figure 2.1: Knowledge pyramid and process capability level (2 sigma for pharmaceutical industry, 6 for semi-conductor industry).^[1]

3. Theoretical section

3.1. Solid dosage formulation design

3.1.1. Solid dosage preformulation and formulation

A. Preformulation testing

Preformulation testing is the first step in the rational development of dosage forms. It can be defined as an investigation of physical and chemical properties of a drug substance to be formulated alone or combined with excipients. The objective of preformulation testing is to gather information the formulator needs to develop stable and bioavailable dosage forms that can be produced in high quantity. The type of information needed depends on the dosage form to be developed. A recommended list of the information required in preformulation is shown in Table 3.1.

Table 3.1: Preformulation drug characterisation

Test	Method/function/characterisation
Spectroscopy	Simple UV assay
Solubility	Phase solubility, purity
aqueous	Intrinsic solubility, pH effects
pK _a	Solubility control, salt formation
salts	Solubility, hygroscopicity, stability
solvents	Vehicles, extraction
partition coeff.	Lipophilicity, structure activity
dissolution	Biopharmacy
Melting point	DSC – polymorphism, hydrates, solvates
Assay development	UV, TLC, HPLC
Stability (in solution and solid state)	Thermal, hydrolysis, oxidation, photolysis, metal ions, pH.
Microscopy	Morphology, particle size
Powder flow	Tablet and capsule formulation
bulk density	
angle of repose	
Compression properties	Tablet and capsule formulation
Excipient compatibility	Excipient choice

Independent of this pharmaceutical profiling (Table 3.1), analyst will generate data (Table 3.2) to confirm structure and purity.

Some common preformulation tests preceding the formulation of a drug into a tablet are described here.

Table 3.2: Analytical preformulation

Attribute	Test
Identity	Nuclear magnetic resonance (NMR) Infrared spectroscopy (IR) Ultraviolet spectroscopy (UV) Thin-layer chromatography (TLC) Differential scanning calorimetry (DSC) Optical rotation, where applicable
Purity	Moisture (water and solvents) Inorganic elements Heavy metals Organic impurities Differential scanning calorimetry (DSC)
Assay	Titration Ultraviolet spectroscopy (UV) High-performance liquid chromatography (HPLC)
Quality	Appearance Odor Solution color pH of slurry (saturated solution) Melting point

Particle size, shape, and surface area

Various chemical and physical properties of drug substances are affected by their particle size distribution and their shapes. The biopharmaceutical behaviour is directly affected by particle characteristics. Poorly soluble drug - showing a dissolution rate-limiting step in the absorption process - will be more readily bioavailable when administered in a finely subdivided state than as a coarse material (Wadke et al., 1989). Size also plays a role in the inhomogeneity of the final tablet. Indeed, when large differences in size exist between the active components and excipients, mutual sieving (demixing) effects can make mixing difficult. However, if materials become too fine, then undesirable properties appear. These can be electrostatic effects and other surface active properties causing stickiness and lack of flowability. Size and shape influence the flow and mixing efficiency of powders and granules too.

Several tools are commonly employed to monitor the particles size. Microscopy is a rapid technique for estimation of the range of sizes and shapes but when quantitative information is desired, the counting of a large number of particles is not suitable. For quantitative particle size

distribution analysis of materials which are larger than about 50 μm , sieving or screening is appropriate, although shape has a strong influence on the results (Wadke et al., 1989). Most pharmaceutical powders, however, range in size between 1 and 120 μm . To cover these ranges, a variety of instrumentation has been developed such as instruments based on laser scattering (Malvern). Most of these instruments measure the numbers of particles and the distributions are readily converted to weight and size distributions.

The determination of surface areas of powders has been getting increasing in recent years (Wadke et al., 1989). The techniques employed reflect the particle size, as the relationship between surface areas and particle size is an inverse one. The most common approach for determining the surface area is based on the Brunauer-Emmett-Teller (BET) theory of adsorption (Gregg et al., 1967). In short, the theory states most substances to adsorb a monomolecular layer of a gas under certain conditions of partial pressure and temperature. Knowing the monolayer capacity of an adsorbent and the area of the adsorbate molecule, the surface area can be calculated. Usually nitrogen is used as the adsorbate at a specific partial pressure determined by mixing it with an inert gas, typically helium.

Solubility and dissolution

The availability of a drug is always limited (Wells, 2001). The solubility and pK_a must be determined. In solid dosage preformulation studies, solubility dictates the ease with which formulations for oral administration are obtained. The pK_a allows determination of the appropriate pH to maintain solubility and choosing the salts is required to achieve good bioavailability to improve stability and powder properties. For tablet and capsule formulations, a solubility of less than 1 mg/ml indicates the need for a salt. In the range 1-10 mg/ml serious consideration should be given to salt formation. If the solubility of the drug cannot be manipulated in this way, then liquid filling in soft or hard gelatine capsules may be necessary. The section 3.1.3 gives more detailed information on the solubility of solids.

The dissolution rate of a drug is important when it is a rate-limiting step in the absorption process. A presentation of dissolution testing in formulation of pharmaceutical tablets is given in section 3.1.5.

Crystal properties and polymorphism

Many drug substances can exist in more than one crystalline form with different space lattice arrangements. This property is known as polymorphism. The different crystal forms are called polymorphs. Many solids may be prepared in a particular polymorphic form via appropriate manipulation of conditions of crystallisation (e.g. nature of solvent used, temperature, rate of cooling, etc.). Different polymorphic forms of a given solid differ from each

other with respect to many physical properties, such as solubility and dissolution, true density, crystal shape, compaction behaviour, flow properties, and solid-state stability. Therefore it is essential to define and monitor the solid state of a drug substance.

These crystal properties are often studied using differential thermal analysis (DTA) scanning calorimetry (DSC). DTA measures the temperature difference between the sample and a reference as a function of temperature or time when heating at a constant rate. DSC is similar to DTA, except that the instrument measures the amount of energy required to keep the sample at the same temperature as the reference, i.e. it measures the enthalpy of transition. Thus crystalline transitions, fusion, evaporation, sublimation and polymorphism are obvious changes in state which can be quantified. Furthermore, thermal analysis has been widely used as a method of purity determination and the USP includes an appendix describing the methods.

Drug and product stability

Wherever possible, commercial pharmaceutical products should have a shelf life of 3 years (Wells, 2001). The potency should not fall below 95% under the recommended storage conditions and the product should still look and perform as it did when first manufactured. By investigating the intrinsic stability of the drug it is possible to indicate types of excipients, specific protective additives and packaging which will improve the integrity of the drug and product.

Drug degradation occurs by four main processes: hydrolysis, oxidation, photolysis and trace metal catalysis. Hydrolysis and oxidation are the most common pathways, and in general light and metal ions catalyse a subsequent process.

The typical stress conditions used in preformulation stability assessment of solids are listed in Table 3.3.

Table 3.3: Stress conditions used in preformulation stability assessment for solid material.

Test	Conditions
Heat (°C)	4, 20, 30, 40, 40/75%, 50 and 75
Moisture uptake	30, 45, 60, 75 and 90% RH at RT ^{a,b}
Physical stress	Ball milling

a: RT is ambient room temperature. Can vary between 15 and 25 °C.

b: Saturated solutions of MgBr₂, KNO₂, NaBr, NaCl and KNO₃ respectively.

Powder flow properties

Flowability of a powder material can be defined as the whole of the aptitudes enabling it to flow. Flowability is one of the principal characteristics of a powder mix as it plays an essential role in many processes (mixing, filling a tableting machine during compression process, etc.). A good flowability enables a complete and regular flow without demixing or segregation (Deleuil, 1987). For compression, good flowability is a necessary but not sufficient condition for a high speed tableting in pharmaceutical production.

When limited amounts of drug are available, flowability can be evaluated by measurements of bulk density and angle of repose. Bulk density is a simple test, developed to evaluate the flowability of a powder by comparing the poured (fluff) density ($\rho_{B\min}$) and tapped density ($\rho_{B\max}$) of a powder and the rate at which it packed down. A useful empirical guide is given by Carr's compressibility index (Carr, 1965):

$$\text{Carr's index (\%)} = \frac{\text{Tapped density} - \text{Poured density}}{\text{Tapped density}} 100 \quad \text{Equation 1}$$

This index can be interpreted as in Table 3.4.

Table 3.4: Carr's index as an indication of powder flow

Carr's index (%)	Type of flow
5-15	Excellent
12-16	Good
18-21	Fair to passable
23-35	Poor
33-38	Very poor
>40	Extremely poor

A similar index has been defined by Hausner (Hausner, 1967):

$$\text{Hausner ratio} = \frac{\text{Tapped density } (\rho_{B\max})}{\text{Poured density } (\rho_{B\min})} 100 \quad \text{Equation 2}$$

Values less than 1.25 indicate good flow (= 20% Carr), whereas greater than 1.25 indicates poor flow (= 33% Carr). Between 1.25 and 1.5, added glidant normally improves flow.

The tapped density test is performed by measuring the volume of a powder column (100 g of powder placed in a transparent graduated cylinder) while this column undergoes vibrations of regular amplitude and frequency in standard conditions (described in USP). This measuring method characterises the ability of powders for rearrangement under gravity and vibrations. If a powder rearranges easily, its flowability is good. An empirical linear relationship exists

between the change in bulk density and the log number of taps in a jolting volumeter. No linearity can be found up to two taps and after 30 taps when the bed consolidates more slowly. The slope is a measure of the speed of consolidation and is useful for assessing powders or blends with similar Carr's indices and the benefit of glidants (Wells, 2001).

Angle of repose is another test used in preformulation to evaluate the flowability of a powder. A static heap of powder, with only gravity acting upon it, will tend to form a conical heap. One limitation exists: the angle to the horizontal cannot exceed a certain value, and this is known as the angle of repose (θ). If any particle temporarily lies outside this limiting angle, it will slide down the adjacent surface under the influence of gravity until the gravitational pull is balanced by the friction caused by interparticulate forces. Accordingly, there is an empirical relationship between θ and the ability of the powder to flow. However, the exact value for angle of repose does depend on the method of measurement. The angle of repose given in Table 3.5 may be used as a guide to flowability.

Table 3.5: Angle of repose as an indication of powder flow properties.

Angle of repose [°]	Type of flow
<20	Excellent
20-30	Good
30-34	Passable
>40	Very poor

Compression properties

The compression properties of most drug powders are extremely poor and usually require the addition of compression aids (see part B of this section) (Wells, 2001). This information on the compression properties of the pure drug is extremely useful. Although the tableted material should be plastic (section 3.1.2), i.e. be capable of permanent deformation, it should also exhibit a degree of brittleness (fragmentation). Thus, if the drug dose is high and it behaves plastically, the chosen excipients should fragment (e.g. lactose). If the drug is brittle or elastic, the excipients should be plastic, (e.g. microcrystalline cellulose).

Excipients compatibility

To successfully design a stable and effective solid dosage form it is essential to be careful with the excipients which are added to facilitate the administration, promote the consistent release and bioavailability of the drug and protect it from degradation. Thermal analysis can be used to investigate and predict any physicochemical interactions between components in a

formulation and can therefore be applied to the selection of suitable chemically compatible excipients.

B. Tablet formulation and design

Tablet formulation and design may be described as the process whereby the formulator insures the correct amount of drug to be delivered in the right form, at the proper time and rate as well as in the desired location, while having its chemical integrity protected to that point (Peck et al., 1989).

The design of a tablet usually involves a series of compromises the formulator has to accept, since producing the desired properties (e.g., resistance to mechanical abrasion or friability, rapid disintegration and dissolution) frequently involves competing objectives. The correct selection and balance of excipients materials for each active ingredient or ingredient combination in a tablet formulation to achieve the desired response is in practical experience not easy to achieve (Peck et al., 1989). Furthermore it is essential to develop tablet formulations and processing methods which may be validated. The cost of raw material or a particular processing step must be also considered before selecting a final tablet formulation or manufacturing process.

The first step in any tablet design or formulation activity is careful consideration of the preformulation data. The formulator should absolutely have a complete physicochemical profile of the active ingredients available before initiating the formulation development (see part A of this section). At the conclusion of the preformulation study, it may also be known which tableting process (direct compression, wet/dry granulation) will be appropriate for the drug.

Because of numerous problems related to the formulation of active ingredients, the majority of drug systems involve the use of excipients. There are six major excipients categories: diluents, binders, lubricants, disintegrants, colors and sweeteners (flavors excluded).

In order to provide guidelines for the selection of excipients, it is necessary to know their properties and how these affect the properties of the entire formulation. Figure 3.1 gives an overview of some of the important factors to be considered while choosing excipients for solid dosage forms.

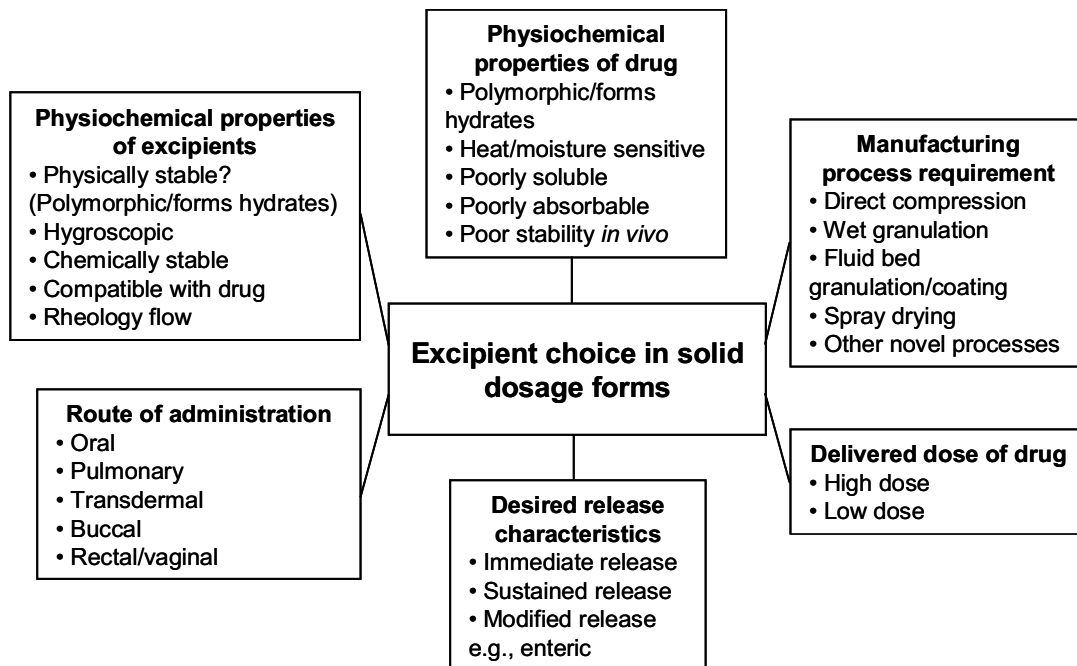


Figure 3.1: Factors to consider when choosing excipients for solid dosage forms. ^[2]

Two major classifications of additives by function include those which affect the compressibility of the tablets:

- diluents
- binders and adhesives
- lubricants, anti-tacking agents and glidants

and those which affect the biopharmaceutics, chemical and physical stability, and marketing considerations of the tablet:

- disintegrants
- colors
- flavors and sweeteners
- miscellaneous components (e.g. buffers and adsorbents).

Diluents

Diluents are fillers designed to obtain the required bulk of the tablet when the drug dosage itself is inadequate to produce this bulk.

Although diluents are normally assumed to be inert ingredients they can significantly affect the final tablet's biopharmaceutic, chemical, and physical properties. Lactose is the most widely used diluent in tablet formulation. It has no reaction with most drugs, whether it is used in the hydrous or anhydrous form. Starch is occasionally used as a tablet diluent. However the

use of starch can lead to poor flowability and bad compressibility. Starch typically has a high moisture level. Various directly compressible starches are available (e.g. StaRX 1500).

Mannitol is the most expensive sugar used as a table diluent but due to its negative heat in solution, its slow solubility and pleasant feeling in the mouth, it is widely used in chewable tablets. Sucrose and various sucrose-based diluents are employed in tablet making, but some manufacturers avoid their use in products because of diabetics. Microcrystalline cellulose, often referred to by the trade name Avicel, is a direct compression material. The flow properties of this material are generally good (Banker et al., 1986).

Binders and adhesives

Binders and adhesives are added to tablet formulations to improve cohesiveness of powders, thereby providing the necessary bonding to form granules, which under compaction form a cohesive mass or compact (Peck et al., 1989). The location of the binder within the granule can affect the granulation's quality (Seager et al., 1979). The formulation of granules helps to convert powders to granules which may flow in a more uniform manner from the hopper to the feed system. The primary criterion when choosing a binder is its compatibility with the other tablet components. Secondly, it must grant sufficient cohesion to the powders to allow for normal processing (sizing, lubrication, compression, and packaging). At the same time it should allow the tablet to disintegrate and the drug to dissolve upon ingestion, releasing the active ingredients for absorption. In a comparative study about common tablet binder ingredients the following materials to be compressed (non exhaustive list), in descending order of adhesive strength, have been analysed: acacia, cellulose derivatives, gelatine, glucose, polymethacrylates, polyvinylpyrrolidone, starch, sucrose, sorbitol, sodium alginate (Rubio, 1957).

Disintegrants

A disintegrant is added to most tablet formulations to facilitate a break-up or disintegration of the tablet when it contacts water in the gastrointestinal tract. They may perform by drawing water into the tablet, induce particle-particle repulsive forces and/or swell, causing the tablet to burst apart (see section 3.1.4). Tablet fragmentation may be critical to the drug's subsequent dissolution. A detailed description and listing of the common disintegrants is given in section 3.1.4.

Lubricants, antiadherents, and glidants

These three classes of materials are typically described together because they have overlapping functions. The differences between these terms are:

Lubricants are intended to reduce the friction during tablet ejection between the walls of the

tablet and the walls of the die cavity in which the tablet was formed. Anti-tacking agents reduce sticking or adhesion of material to the punches or to the die wall. Glidants are intended to promote flow of the granules or powder by reducing friction between the particles (Banker et al., 1986). The most common antiadherents are magnesium stearate (reduce however the compactibility of the powder mix in which it is added), talc, starch and cellulose. Common lubricants are magnesium stearate, stearic acid (pure, in salt or derivatives form), and polyethylene. Among widely used glidants there are silica derivatives, talc and magnesium stearate.

Colorants

In general colorants are incorporated into tablets for product identification (to distinguish similar-looking products within a product line or to avoid mix-ups during manufacturing) or aesthetical reasons of the tablet marketing value.

Flavors and sweeteners

They are commonly used to improve the chewable tablets' taste. Cook reviewed the area of natural and synthetic sweeteners (Cook, 1975). Flavours are incorporated as solids in the form of spray-dried beadlets and oils usually at the lubrication step, because of the sensitivity of these materials to moisture and their tendency to volatilise when heated. Sweeteners are added to chewable tablets when the commonly used carriers such as mannitol, lactose, sucrose and dextrose do not sufficiently mask the taste of the components.

Table 3.6 lists some of the most common substances used in tablet formulation for each type of excipients.

Table 3.6: Examples of substances used as excipients in tablet formulation

Type of excipient	Example of substances
Filler	Lactose Sucrose Glucose Mannitol Sorbitol Calcium phosphate Calcium carbonate Cellulose
Disintegrant	Starch Cellulose Crosslinked polyvinyl pyrrolidone Sodium starch glycolate Sodium carboxymethyl cellulose
Solution binder	Gelatin Polyvinyl pyrrolidone Cellulose derivatives Polyethylene glycol Sucrose Starch
Dry binder	Cellulose Methyl cellulose Polyvinyl pyrrolidone Polyethylene glycol
Glidant	Silica Magnesium stearate Talc
Lubricant	Magnesium stearate Stearic acid Polyethylene glycol Sodium lauryl sulphate Sodium stearyl fumarate Liquid paraffin
Antiadherent	Magnesium stearate Talc Starch Cellulose

3.1.2. Compression of pharmaceutical powder into tablets

A powder in a die can be considered as a solid dispersion in a gaseous media where the particles are however in contact in the bulk material. The idea that powders could be considered as 4th state of matter was proposed by Leuenberger (Leuenberger et al., 2002). Indeed, similarities can be found between powders and the three states of matters:

- solid: powders can be deformed reversibly

- liquid: powders are able to flow
- gas: powders are to some extent compressible

A. The compression process

Compression is the process of applying pressure to a material. In pharmaceutical tableting an appropriate volume of powder in a die cavity is compressed between an upper and a lower punch to consolidate the material into a single solid matrix. This compact is then ejected from the die cavity as an intact tablet (Parrot, 1981b).

It is important to distinguish between the terms compressibility and compactibility. The compressibility is the ability of the material to undergo a reduction in volume. The compactibility is defined as the ability of the material to produce tablets with sufficient strength under the effect of densification (Alderborn et al., 1996b; Jetzer et al., 1983). The compaction of tablets is a uniaxial compression. The free particles, which are filled into the die, get condensed by an applied force from an upper or a lower punch or both. The aim of this condensation is the formation of a compressed core with a well defined shape. According to Train the compression process can be described in four different stages which are in general the same for powders, powder-mixtures and granulate (Train, 1956). These stages were resumed (Von Orelli, 2005) as follows:

Stage I:

Before the compression process starts the particulate solid must be filled into the die. The powder bed volume corresponds to a volume between bulk and tapped density. During stage I, the punch touches the material and the particles start to overcome the friction force and rearrange themselves by slippage into an energetically convenient position. When particles are all in contact to each other, a dense packing is achieved and the bulk density corresponds approximately to the tapped density. The particle placement in the matrix depends on the powder's flowability, on the physical properties of the particles (size, surface, shape, density, etc.), on the filling protocol (speed, movement of the hopper, centrifugal forces, vibrations) and on the press type (Woodhead et al., 1983; Zou et al., 1996).

Stage II:

Due to the immobility of the particles, an increase in pressure will lead to temporary columns, struts and vaults surrounding protected voids within the bulk. Nevertheless the inherent cohesive properties of most drugs and excipients are not sufficient to form tablets with adequate strength for subsequent handling (Leuenberger et al., 1986).

Stage III:

When the stress to the material is increased, deformation (particles change of form) will occur. If the deformation disappears completely (return to the original shape) upon release of the stress, it is an elastic deformation (Figure 3.2). A deformation that does not completely recover after release of the stress is a plastic deformation (Figure 3.2). The deformation depends on the properties of the substance and is determined by the crystal characteristics of the substance. Both plastic and elastic deformations may occur although one type predominates for a given material. At first, it undergoes an elastic deformation, the forming is reversible when the pressure is released and the solid regains its natural formation. Then, when the compression pressure is increased, the linear-elastic range is exceeded, an irreversible deformation will result. The transition between reversible and irreversible deformation is called yield point. At last, when the pressure is increased further on at a certain point the material breaks. Characteristic for brittle material, however, is the fact that the plastic range is extremely small or missing; the elastic deformation is followed by a breaking of the substance.

Stage IV:

In this stage a very strong structure is formed and the behaviour of this compact under pressure depends on material properties. If the formed structure is strong, any further reduction in volume of the compact involves the normal compressibility of the solid material. In some cases a further increase in stress may result in undesirable phenomena (see Figure 3.2) such as capping and lamination (Leuenberger et al., 1986). These phenomena result from an elastic re-extension of the material when the force is taken off the system after compression.

Finally, it has to be pointed out that the course of the above described compression process depends strongly on the substance characteristics. Furthermore, the phenomena are not sequential but overlapping.

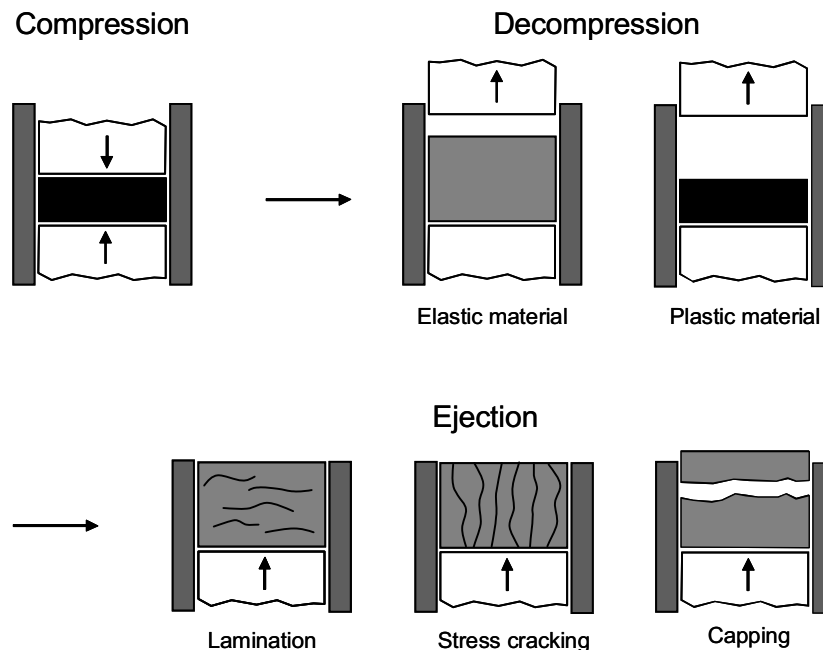


Figure 3.2: Problems appearing during compression: [3]

- lamination, the compact cleaves in several parallel plans which are normal to the compression plan
- stress cracking, if the side surface is damaged by sticking of the compact to the matrix walls
- capping: the upper part of the compact separates in a perpendicular direction to the compression axis

B. Bonding in tablets

Bonding surface area

Bonding surface area is often defined as the effective surface area taking part in the interparticulate attraction (Alderborn et al., 1996a). In the case of solid bridges (see next section), the term corresponds to the true interparticulate contact area. For intermolecular forces the term is more difficult to define but can be estimated from surface area measurements of the starting material. The internal surface area is small for dense crystalline solids (e.g. sodium chloride) but may be considerably greater than external surface area in case of porous bodies (e.g. microcrystalline cellulose). Thus the bonding surface area is a function of several secondary factors (Duberg et al., 1985) (see table Table 3.7).

Table 3.7: Factors influencing the surface area of tablet particles and the bonding surface area in tablets. ^[4]

Tablet particle surface area		Bonding surface area	
Before compaction	After compaction	During compaction	After compaction
Particle size	Particle size	Particle size	Particle size
Particle shape	Particle shape	Particle shape	Particle shape
	Fragmentation	Fragmentation	Fragmentation
		Plastic deformation	Plastic deformation
		Elastic deformation	Elastic deformation
			Elastic recovery
			Friction properties
			Bond strength

Bonding mechanisms

During densification process, points and surfaces of contact between particles enable formation of bonding which ensure cohesion of the compact. Rumpf determined five types of possible attraction (Rumpf, 1962b):

1. Solid bridges (sintering, melting, crystallisation, chemical reactions, and hardened binders)
2. Attractions between solid particles (molecular and electrostatic forces)
3. Shape-related bonding (mechanical interlocking)
4. Bonding due to movable liquids (capillary and surface tension forces)
5. Non-freely-movable binder bridges (viscous binders and adsorption layers)

This classification was widely accepted in literature but in case of compaction of dry, crystalline powders, it has been suggested that the dominating bond types adhering particles together could be restricted to three types (Fürher, 1977):

1. Solid bridges (due to, e.g. melting):

They contribute to the overall compact strength and can be defined as areas of real contact, i.e. contact at an atomic level between adjacent surfaces in the tablet. They appear when very high pressure is applied to the material during compression. Indeed, the pressure applied to a particulate system is transmitted through contact points between particles. This creates high friction zones where the temperature increases. Different types of solid bridges have been proposed in the literature, such as solid bridges due to melting, self-diffusion of atoms between surfaces, and recrystallisation of soluble materials in the compact (Ahlneck et al., 1989; Down et al., 1985; Mitchell et al., 1984; Rumpf, 1962a).

2. Distance attraction forces (intermolecular forces):

The intermolecular indicates all bonding forces that act between surfaces separated by some distance. The term includes van de Waals forces, electrostatic forces, and hydrogen bonding (Israelachvili, 1985). The dominant interaction force between solid surfaces is the van der Waals force of attraction (Derjaguin, 1960; Derjaguin et al., 1956; Israelachvili et al., 1973). Hydrogen bonding is predominantly an electrostatic interaction and may occur either intramolecularly or intermolecularly (Israelachvili, 1985). Electrostatic forces arise during mixing and compaction due to triboelectric charging.

3. Mechanical interlocking (between irregularly shaped particles):

This term is used to describe the hooking and twisting together of the packed material. This bonding mechanism depends on the shape and surface structure of the particles. The long needle-formed fibers and irregular particles have a higher tendency to hook and twist together during compaction compared with smooth spherical ones. This mechanism is not founded on atomic interaction forces and therefore plays a minor role (Shotton et al., 1976a).

C. Compression equipment

Whatever the compression equipment, tableting always follows three major steps:

- matrix filling with powder or granules
- compression by displacement of punches
- ejection of the compact out of the matrix

The quality of the tablet obtained after compression depends on different factors such as:

- the intrinsic properties of the material to be compressed
- the type of equipment used
- the compression speed
- punches displacements amplitude
- the pressure applied to the powder bed

However, it has to be pointed out that the adjustments of the compression parameters on the equipment are not sufficient to produce a robust tablet if the formulation is not optimised. Furthermore, the compression parameters used can in some cases give information on the defaults of a formulation.

Machine for compression

The production of tablets is performed using eccentric or rotary (simple or multi-stations) presses. The eccentric press produces about 40 to 120 tablets per minute. The rotary press has a multiplicity of stations arranged on a rotating table with the dies. A few or many

thousands tablets can be produced per minute. There are numerous models of presses, manufactured by a number of companies, ranging in size, speed, and capacity. As their tableting speed is rather low, eccentric presses are usually used only at the formulation step. Four phases are necessary to achieve the production of a compact with an eccentric press (see Figure 3.3):

Phase I: the filling shoe, the upper and lower punches are in starting position and the matrix is filled with powder.

Phase II: the upper punch goes down into the die and compresses the powder bed.

Phase III: the upper punch is back at his initial position, while the lower punch pushes the tablet out of the matrix

Phase IV: the filling takes off the produced tablet and at the same time fills again the matrix with powder

In the case of industrial rotary tablet press filling of the die, compression and ejection occur at the same time (Figure 3.3) and then enable the production of tablet at a much higher rate. Several punch pairs (upper and lower) are both guided by rotary trains. The vertical position of punches changes depending on the position in the rotary train. The phases of the compression process are in this case:

Phase I: filling of the matrix with powder when the upper punch goes in its lower position.

Phase II: while the lower punch is in its lower position, the upper punch starts to go down guided by the curvature of the upper train (precompression).

Phase III: the upper and lower punches are between rolls (main compaction).

Phase IV: the upper punch is in its highest position; the lower punch is guided up to eject the tablet.

The actual multi stations industrial rotary presses are usually equipped with a second pair of rolls for precompression (see Figure 3.4) which allow increasing the rotation speed of the machine while reducing the capping or laminating problems (often due to entrapped air in the die during compression).

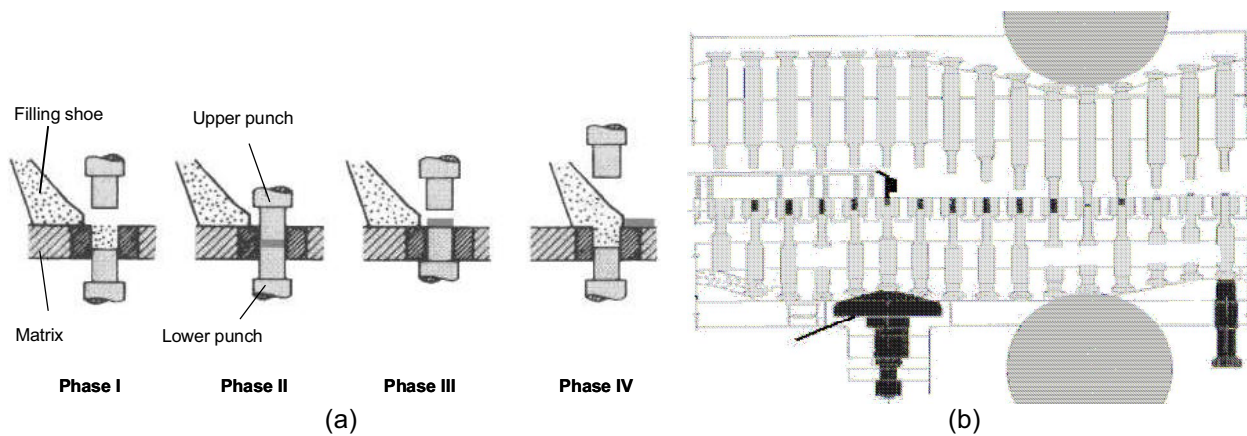


Figure 3.3: Schema of the compression process with an eccentric press (a) and a rotary tablet press (compression station only).^[5]

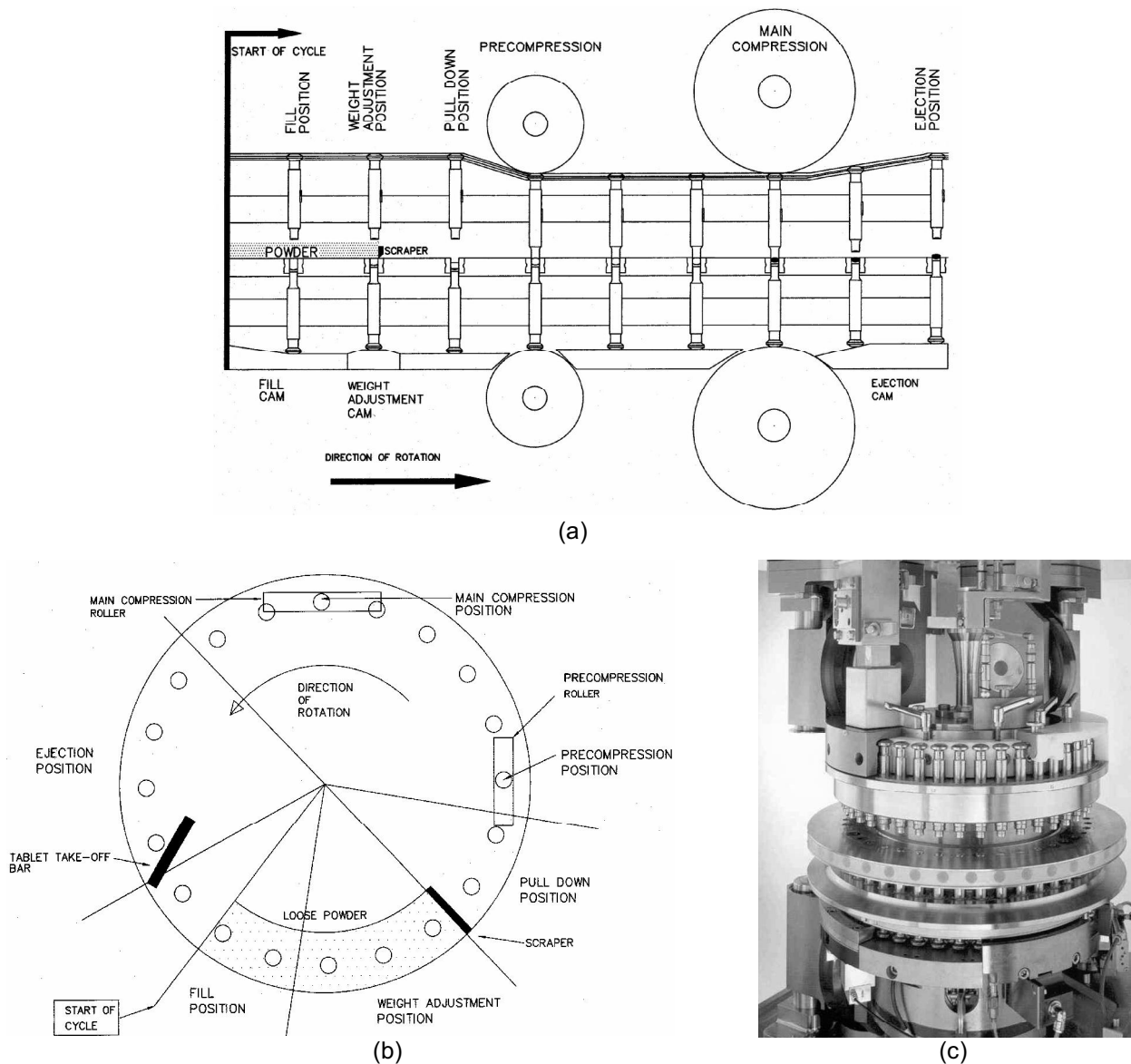


Figure 3.4: Multi stations rotary press with precompression and compression stations. (a): schematic view from side (b) schematic view from top, (c) picture of a Fette machine.^[6]

Compression simulators

Compression simulators are sophisticated tools that enable the reproduction of different compression parameters of industrial machine (ex. compression speed, compression force, etc.). The interest of these tools is to study and compare the characteristics of formulations under compression in industrial conditions. Published works (Marshall, 1989; Muller et al., 1994; Nokhodchi et al., 1996; Yang et al., 1996) encourage to use compression simulators as research tools for robust formulations. The major problem, however, is the huge expenses for such a simulator. At the Institute of Pharmaceutical Technology Basel, two kinds of simulators are in use: A Zwick[®] Universal testing Instrument, i.e. a punch and die set, and a Presster[™] compaction simulator. The Presster[™] (see Figure 3.5) is a linear-type rotary tableting machine replicator, which works with one single pair of punches and offers the possibility to simulate different rotary tableting machines by mimicking the mechanics of these machines (Picker, 2003). Presster[™] is instrumented with:

- Linear Variable Differential Transformers (LVDT) for upper and lower punch displacement measurement.
- Strain gauges for force measurement during compression and precompression.
- Strain gauges for die wall expansion measurement with instrumented die.
- Strain gauges for ejection force.
- Strain gauges for tablet take-off force.

The following set up can be installed before compression:

- Selection of an industrial machine model in a list
- Filling position of the lower punch before compression
- Minimal gap at between the punches during precompression and compression by variation of the rolls positions
- Compression speed
- Ejection angle

For a given industrial machine model and for a given compression speed, the contact time of the punch head's flat part with the compression roll (called Dwell time, see Figure 3.6) will be the same for each compression run. This is an important point.

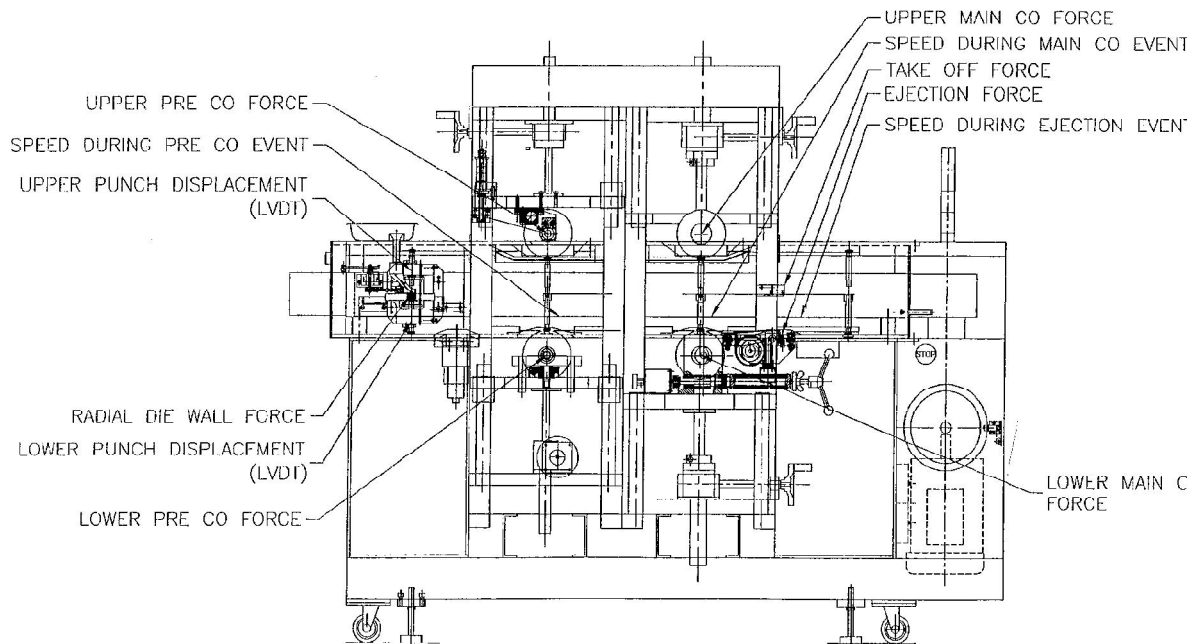


Figure 3.5: Presster™ instrumentation overview [6]

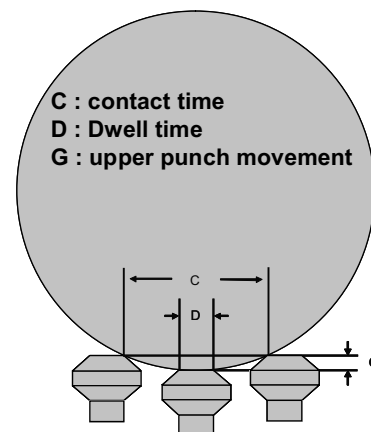


Figure 3.6: Schema of the lower punch position compared to the compression roll just before, at and just after Dwell time. [6]

D. Description of densification cycle

The punches pressure is recorded against time (Figure 3.7a) or against upper punch displacement (Figure 3.7b). According to Jones and Schmidt it is possible to distinguish four phases in a compression cycle (Schmidt et al., 1994):

1. Compression phase (t_1-t_2 or AB):

The compression is the phase when the upper and the lower punches are brought together until either the minimal distance is reached or the maximal pressure.

2. Relaxation phase (t_2-t_4)

The pressure increases when the punches are maintained at their minimal distance. This phase expresses the viscoplastic properties of the material and the bonding probability increases. It was demonstrated (Masteau et al., 1998) that raising the Dwell-time or decreasing the compression speed is favourable to the formation of solid bonds and enhances the mechanical quality of the resulting compact.

3. Decompression phase (t4-t5 or BC)

This phase corresponds to the stress release when the punches leave the matrix. Then the compact expands axially in the matrix. This expansion can eventually destroy part of the bonds formed during compression and relaxation phases.

4. Ejection (t6-t7)

Ejection phase is the terminal phase of the cycle. This phase is also very important for the mechanical properties of the compacts. The efficiency of the punches and die lubrication will influence the sticking of the tablet to the matrix induced by the frictions tablet/die wall (Velasco et al., 1997). An insufficient lubrication can also induce lamination and capping effect.

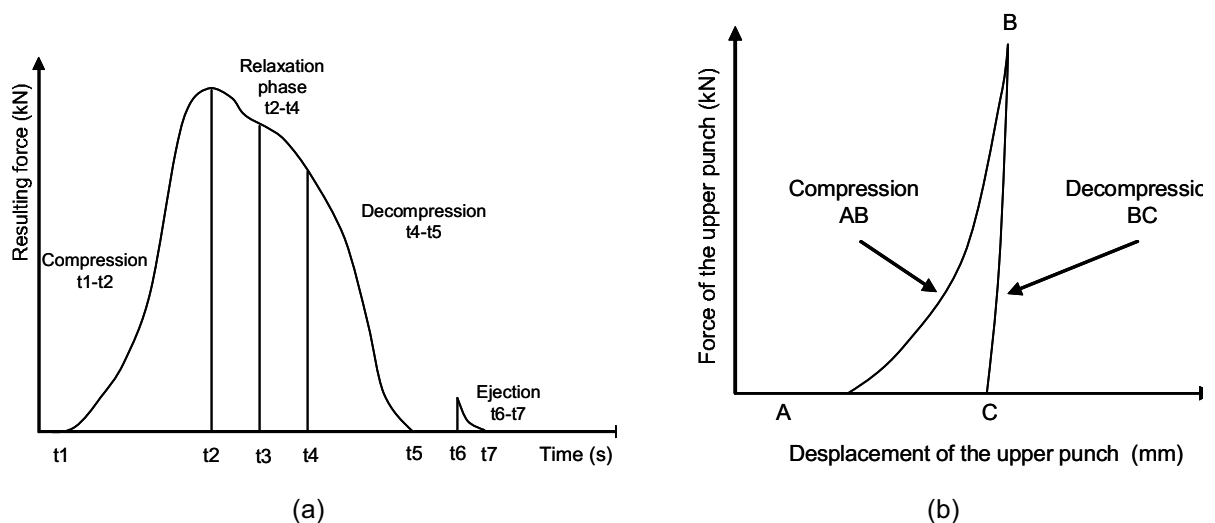


Figure 3.7: (a): curve-type of pressure against time on a rotary tablet press, (b) curve-type pressure against upper punch displacement on a testing machine. ^[3]

E. Energy and power occurring during compression

De Blaey and Polderman identified five steps consuming energy during compression (Ragnarsson, 1996). They lead to:

1. Bring the particles close together.
2. Overcome interparticular frictions.
3. Overcome particle/matrix wall and particles/punches frictions.

4. Deform and create bonds.
5. Dissipate elasticity.

Energy consumption of the steps 1 and 2 is assumed to be negligible compared to the others. If the tooling is properly lubricated, the step 3 can also be neglected. If this is not the case, the work induced by these forces should be subtracted from the total compression work as this energy does not participate to the creation of bonds. In the same way, decompression enables the release of the stresses and thus expresses the elastic property of the material. If the elastic energy is also subtracted from the total compression work, the resulting true compression work corresponds to the deformation and to the creation of bonds (Figure 3.8).

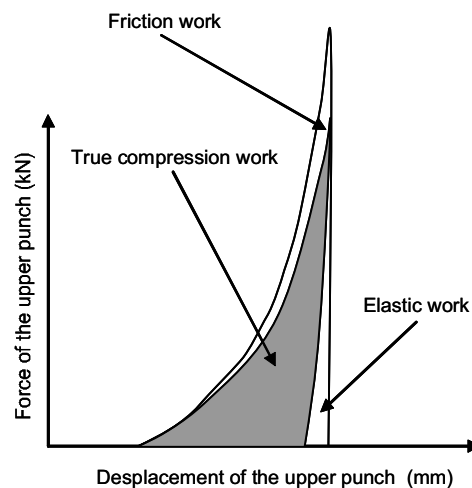


Figure 3.8: Energy occurring during compression ^[3]

F. Pressure distribution within a compact

The pressure distribution within a compact is not uniform due to the material's heterogeneity and to the conditions of the compression process: the stress applied on a particle is transmitted to the particles in its neighbourhood, passed on to the surfaces of contact creating a pressure gradient (Parrot, 1981c). These contacts are permanently modified by the particles' deformation (plastic deformation or fragmentation), the rearrangements, the particle/particle frictions and the particle/matrix wall frictions. The density distribution within the compact is then heterogeneous and the calculated density of a compact is an average value. Train identified zones of high density (HD) and lower density (LD) within the powder bed (Train, 1956), as schematized in Figure 3.9.

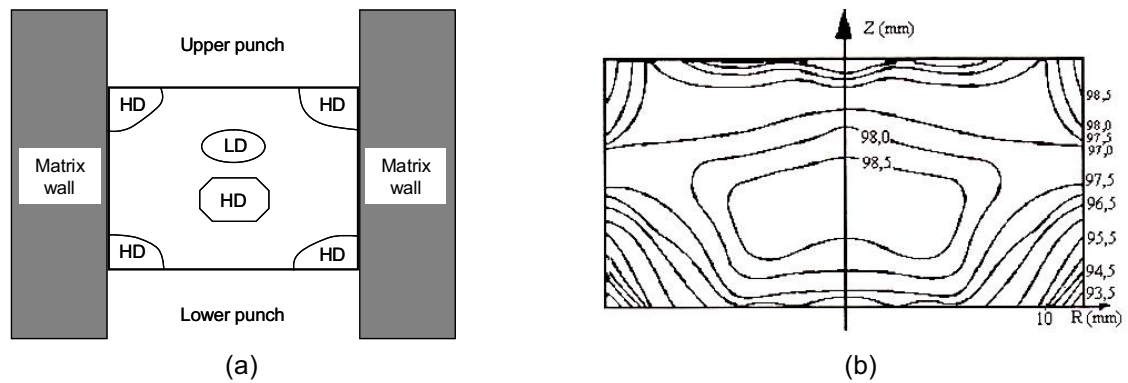


Figure 3.9: Heterogeneity of the density according to Train (a) (Train, 1956), measured in the section of a compact by Nyström (b) (Nyström et al., 1993).^[3]

G. Mathematical characterisation of the compression process

A large amount of research works were published about the development of mathematical models to describe the powder compression process. An overview of the main compression equation was proposed by Celik (Celik, 1992). These equations describe the state of compression (density, porosity, volume, etc.) to the applied pressure. The most used models are the Heckel equation (Equation 3) (Heckel, 1961a, 1961b), its modification (Equation 4) (Kuentz et al., 1999a), the equation according to Kawakita (Equation 5) (Kawakita et al., 1970/71) and the equation derived by Cooper and Eaton (Cooper et al., 1962).

Despite the large number of equations none of them were enabling a universal description of the powder compression, probably because of the numerous parameters involved.

Heckel:
$$\ln\left(\frac{1}{1-\rho_r}\right) = K\sigma + A$$
 Equation 3

modified Heckel:
$$\sigma = \frac{1}{C} \left[\rho_{rc} - \rho_r - (1 - \rho_{rc}) \ln\left(\frac{1-\rho_r}{1-\rho_{rc}}\right) \right]$$
 Equation 4

Kawakita:
$$C_k = \frac{V_0 - V}{V_0} = \frac{ab\sigma}{1 + b\sigma} \text{ with } a = \frac{V_0 - V_\infty}{V_0}$$
 Equation 5

where:

σ : compression pressure [MPa]	V_0 : initial apparent volume [cm ³]
K, C, b : constants [MPa ⁻¹]	V_∞ : apparent volume after infinite pressure [cm ³]
A, a : constants	V : apparent volume under applied pressure [cm ³]
ρ_{rc} : relative critical density	C_k : degree of volume reduction
ρ_r : relative density ($\rho_r = 1 - \varepsilon$) with ε : porosity of the tablet)	

Although it was initially established for iron powder, the Heckel equation was the most commonly used model to describe pharmaceutical powder compression. It supposes that the reduction of the powder volume under pressure follows a first order kinetic (see Equation 3) for which pores are the reactive agents; this assimilation shows only one deformation mechanism: the plasticity of materials. The deformation of pharmaceutical powders follows several mechanisms and the kinetic of porosity reduction is not of first order. The initial curve is attributed to rearrangement and fragmentation. The linear part of the curve shows the plastic deformation mechanism (see Figure 3.10).

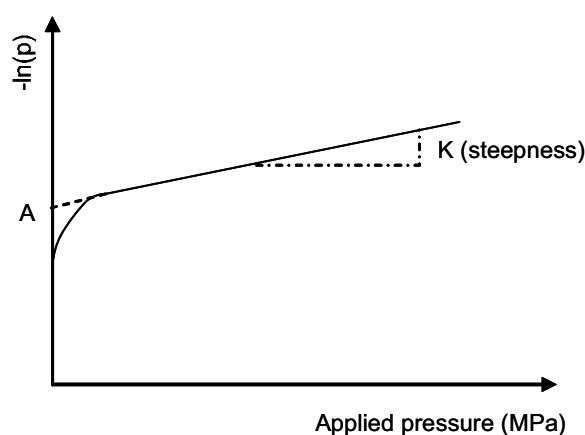


Figure 3.10: Heckel model curve ^[3]

3.1.3. Solubility of solids

A. Definition of the solubility

Solubility is a chemical property referring to the ability for a given substance, the solute, to dissolve in a solvent (Atkins et al., 2002). It is commonly expressed as a concentration, either molarity (moles of solute / litre of solvent) or molality (moles of solute / kg of solvent). Solubility is measured in terms of the maximum amount of solute dissolved in a solvent at equilibrium at a given temperature. The resulting solution is called a saturated solution. In a saturated solution in contact with undissolved solid solute, the rate at which molecules or ions leave the crystal surface is equal to the rate at which the solvated molecules or ions return to and become a part of the solid crystal. A saturated solution contains the maximum amount of solute, additional solute won't dissolve. An unsaturated solution contains less than the maximum amount of solute, additional solute will dissolve. A supersaturated solution contains more than the maximum amount of solute and is unstable, additional solute induces rapid crystallisation.

B. Solubility of drugs

The aqueous solubility of a drug is an important factor affecting its bioavailability. Solid drugs administered orally for systemic activity must dissolve in the gastro-intestinal fluids prior to their absorption. Thus, the rate of dissolution of drugs in gastrointestinal fluids could influence the rate and extent of their absorption.

USP expresses solubility in terms of millilitres of solvent required to dissolve 1g of solute; e.g., 1g of boric acid dissolves in 18 ml of water. For substances whose solubility is not definitely known, the value is described in pharmaceutical compendia by the use of certain general descriptive terms (see Table 3.8).

Table 3.8: USP XXIV descriptive terms of solubility.

Term	Parts of solvent required (ml) for one part of solute (g)
Very soluble	<1
Freely soluble	1-10
Soluble	10-30
Sparingly soluble	30-100
Slightly soluble	100-1'000
Very slightly soluble	1'000-10'000
Practically insoluble or insoluble	>10'000

C. Solvation process

The process of dissolving is called solvation, or when water is the solvent, hydration. During solvation, the solvent is first attracted to the solute and then solvent particles surround the solute particles and pull them into solution (see schema in Figure 3.11). Thus, the solubility of one substance dissolving in another is determined by the balance of intermolecular forces solvent/solute and the entropy change during the solvation. The process of dissolution involves the breaking of interionic or intermolecular bonds in the solute, the separation of the molecules of the solvent to provide space for the solute, and the interaction between the solvent and the solute.

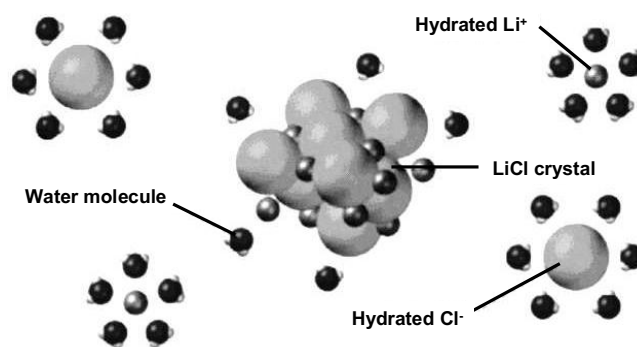


Figure 3.11: Hydration of Lithium chloride (LiCl): the negative oxygen atoms are attracted to Li^+ and the positive hydrogen atoms are attracted to Cl^- .^[7]

D. Factors influencing solubility

The solubility of a compound depends on the physical and chemical properties of the solute and the solvent, the pressure (can be neglected for solid dissolved in liquids), the pH of the solution and on the presence of other species dissolved in the solvent. Solubility of acidic or basic compounds is pH-dependent and can be altered by forming salts. The solubility of every new drug must be determined as a function of pH over the physiological pH range of 1 to 8. Just as different factors affect the amount of solute that dissolves, there are also various factors that influence how quickly a solute dissolves such as the temperature, the agitation of the dissolution medium and the surface area between solute and solvent (state of subdivision of the solute). For around 95% of solids, the solubility increases with temperature (Hill et al., 1999). At high temperatures, solvent particles move faster and solvation occurs faster. Figure 3.12 shows solubility curves for some typical inorganic solid salts. As solvation occurs at the surface between solute/solvent, solutes dissolve faster when the surface area of the solute is increased by crushing it into smaller pieces. Indeed, the greater the surface area, the more opportunities there are for the solvent to attack the solute.

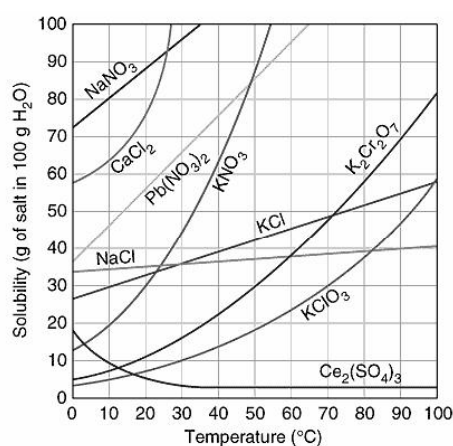


Figure 3.12: The dependence of solubility on temperature.^[8]

E. Determination of the solubility

A semi-quantitative determination of solubility can be made by adding the solute in small incremental amounts to a fix volume of solvent. After each addition, the system is shaken and examined visually for any undissolved solute particles. When some solute remains undissolved the total amount added up to that point serves as a good and rapid estimate of solubility.

Different empirical methods were developed to predict the solubility like the Hansen Solubility Parameters and the Hildebrand solubility parameters (Hancock et al., 1997), the prediction of solubility from other physical constants such as the enthalpy of fusion (Marsac et al., 2006) or from the partition coefficient (Valvani et al., 1980). Furthermore numerous computational methods have been developed for the prediction of aqueous solubility from a compound's structure (Jorgensen et al., 2002).

Hansen approach for solubility prediction

The cohesive energy holding a substance together gives a direct measure of the attraction between atoms and molecules. Cohesive energy results from Van der Waals interactions, covalent bonds, hydrogen bonds, electrostatic interactions, induced and permanent dipole interactions. Cohesive energy determines critical physico-chemical properties of a drug or excipient such as melting point, mechanical force, solubility and so on (Hancock et al., 1997). This energy can be quantified by the use of the solubility parameters (Hildebrand et al., 1950) based on the following equation:

$$\Delta H = V_T \left\{ \left(\frac{\Delta E_{v1}}{V_{m1}} \right)^{0.5} - \left(\frac{\Delta E_{v2}}{V_{m2}} \right)^{0.5} \right\}^2 \phi_1 \phi_2 \quad \text{Equation 6}$$

where ΔH is the heat of mixing, V_T the total volume, ΔE_v the energy of vaporisation, V_m the molar volume, ϕ the volume fraction, and 1 and 2 refer to the solvent and solutes components, respectively.

The Hildebrand solubility parameter δ of each component is defined as follows:

$$\delta = \left(\frac{\Delta E_v}{V_m} \right)^{0.5} \quad \text{Equation 7}$$

When the solubility parameters of two materials are similar, they will be mutually soluble. Hansen has subdivided the total solubility parameter into partial parameters (Hansen, 1967a, 1967b) in this manner:

$$\delta^2 = \delta_d^2 + \delta_p^2 + \delta_h^2 \quad \text{Equation 8}$$

where δ_d , δ_p and δ_h are the partial parameters for dispersion, for polar interaction and for hydrogen bond interaction, respectively. The partial solubility parameters express the interatomic/intermolecular forces (Barton, 2000).

The partial solubility parameters can be calculated on the basis of the molecular structure of the compound. Several group contribution methods have been developed for calculating solubility parameters (Rowe, 1988; Van Krevelen et al., 1976). This approach can especially be useful in the preformulation process for a first characterisation of the material, if this one is not available in sufficient quantity for experimental determinations (Hancock et al., 1997).

Solubility prediction from the partition coefficient

The partition coefficient gives a measure of the differential solubility of a compound in a hydrophobic solvent (octanol) and a hydrophilic solvent (water) as follows:

$$\text{Log}P_{O/W} = \text{Log} \frac{C_o}{C_w} \quad \text{Equation 9}$$

where $\text{Log}P_{O/W}$ is the octanol/water partition coefficient, C_o is concentration of the compound in an aqueous phase and C_w is the concentration in the immiscible solvent. The following equation gives an estimation of the aqueous solubility S_{aq} of a drug:

$$\text{Log}S_{aq} = -\text{Log}P_{O/W} - 0.01MP + 1.05 \quad \text{Equation 10}$$

where MP is the melting point. As this is an empirical equation it may work well for certain compounds but not for all.

3.1.4. Disintegration of pharmaceutical tablets

A. Importance of the disintegration process in drug absorption

Bioavailability of a drug depends of its absorption into the bloodstream occurring in stomach and intestine. Absorption of an active ingredient affects its solubility in gastrointestinal fluid and its permeability across gastrointestinal membrane. Solubility of a drug mainly depends on its physical and chemical characteristics.

However, drug dissolution rate is greatly influenced by the breakdown (or disintegration) of compacts into smaller fragments. Disintegration increases surface of contact between formulated drug and liquid what thereby facilitates drug dissolution. In pharmaceutical science, disintegration usually means the process by which a solid dosage form breaks up when it comes into contact with an aqueous medium (Guyot-Hermann, 1992).

Disintegration represents a limiting factor of dissolution, especially for low soluble drugs in water or in biological fluids. Thus disintegration times are often directly correlated to dissolution

rate constants (Carstensen, 1995; Carstensen et al., 1980a; Carstensen et al., 1978; Carstensen et al., 1980b). Figure 3.13 illustrates the ways in which drugs formulated into tablets become available to the body.

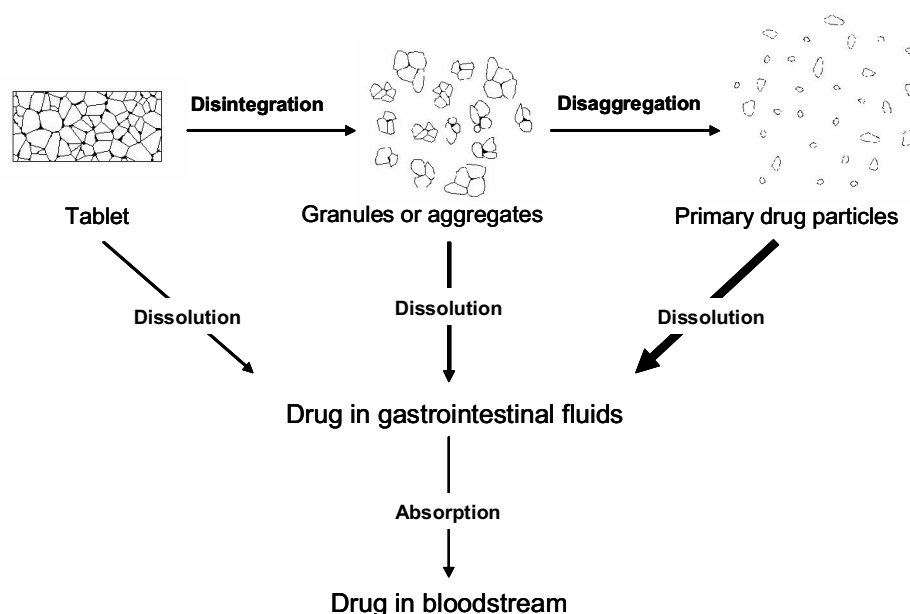


Figure 3.13: Liberation process of a drug formulated into a tablet. In aqueous media (in vivo or in vitro) tablets first disintegrate into aggregates (or granules if granulation was processed before compression). Large released fragments are then disaggregating into smaller fragments or primary particles. Drug dissolution occurs before, during and after disaggregation but optimum dissolution is reached with small particles only (large surface of contact between drug and liquid). When dissolved drug is absorbed through gastrointestinal membrane and can reach the bloodstream to be distributed to the body tissues.

B. Mechanisms of disintegration

A properly formulated tablet will disintegrate in only a few minutes. Drug dissolution will occur at each stage of the disintegration process (see Figure 3.13). However, most of the drugs are poorly water-soluble and only the dissolution of primary drug particles at the last stage is significant. To understand the reason why a tablet breaks up when it is soaked in water, it is essential to know how particles cohere in a compact. Cohesion mechanisms in a pharmaceutical tablet (Guyot-Hermann, 1992; List et al., 1979; Rumpf, 1962a) are listed below:

- mechanical interlocking of particles
- capillary binding (liquid bridges)
- intermolecular bonding (Van de Waal's forces, hydrogen bonds and electrostatic forces)
- interparticle welding (solid bridges) by partial dissolution, partial melting and by molecular diffusion (Carstensen, 1973; Gray, 1968; Parrot, 1981a).

Mechanical interlocking is believed to play a minor role in pharmaceutical tablets. Capillary bonding and some of the intermolecular bondings are overcome by the presence of water. Interparticle welding is very harmful for fast disintegration. It is possible to avoid these unpropitious bondings by adequate formulations (Guyot-Hermann, 1992).

Water is thus an essential factor in disintegration and it is necessary to introduce liquid quickly into the tablet structure for fast disintegration. Disintegration time can be reduced by including disintegrating agents (called disintegrants) in tablet formulations. Insertion of hydrophilic and insoluble disintegrant particles among the drug particles promotes moisture penetration in the tablet and breaking up of the solid dosage form. Primary drug particles will be then exposed to the dissolution liquids and dissolution rate will be increased (Augsburger, 2007). If robust tablet formulation is performed, water is up-taken rapidly by the compact.

Different mechanisms of disintegration and disintegrant action follow penetration of water into a tablet. The speed and degree of tablet disintegration is determined primarily by the quantity and intrinsic properties of the disintegrant used.

A number of theories to explain the disintegration process of pharmaceutical tablets have been developed in the past (Bolhuis et al., 1982; Caramella et al., 1984; Guyot-Hermann, 1992; Guyot-Hermann et al., 1981; Kanig et al., 1984; Lowenthal, 1972a, 1973; Shangraw et al., 1980). Every hypothesis has been verified for certain solid dosage formulations but was not confirmed for some other. Consequently there is no one unique and universal theory explaining disintegration phenomenon. It is assumed that disintegration is rather a combination of several different mechanisms (Kanig et al., 1984). However the central role of water in tablet disintegration remains uncontested.

The four main mechanisms accepted for disintegration process are:

- Diffusion of water within tablets by capillary action (wicking).
- Break-up of particle-particle bondings (repulsion).
- Swelling of disintegrant particles in contact with water.
- Initial shape recovery by disintegrant particles that were deformed during tableting (deformation).

Capillary action or wicking

When a tablet is put into an aqueous medium, the liquid is uptaken through porous structures of the compact by capillary action. Water replaces the air adsorbed on the particles, which weakens the intermolecular bonds (see next paragraph) (Kanig et al., 1984; Lowenthal, 1972a, 1973). Water uptake depends of hydrophilicity of the drug-exciipient mix and on tableting conditions (porosity). Indeed, low interfacial tension towards aqueous fluid helps disintegration by creating a hydrophilic network around the drug particles. In other words, if

pore walls are constituted of hydrophilic particles, water can penetrate. Furthermore, sufficient porosity is necessary for rapid uptake. Porosity of a compact can be controlled by appropriate compression force during tableting (Higushi et al., 1953; Lowenthal et al., 1971; Ringard et al., 1988). When a formulation is low hydrophilic, disintegrants working by 'wicking' action can be added to force water to diffuse in capillary network. Moisture follows the path formed by disintegrant particle. Hydrophilic disintegrants with fibrous structure are the most relevant in this case (ex: croscarmellose sodium) (a schematic view of the 'wicking' action by fibrous disintegrants is shown in Figure 3.15c).

Particle-particle repulsive forces

This mechanism based on particle repulsion was proposed to explain disintegration of a tablet made with 'non-swelling' disintegrants (Guyot-Hermann et al., 1981) (see paragraph on swelling mechanism). Researchers found that repulsion is secondary to wicking. When water is drawn into pores by capillary action, particles start to repulse each other due to the resulting electrical force (see schema in Figure 3.15d).

Swelling of disintegrant particles

Swelling disintegrants have the capacity to increase in volume when they are in contact with water. By swelling, the bonding of other ingredients in a tablet may be overcome causing the tablet to fall apart (see Figure 3.15a). Although not all effective disintegrants can swell, this mechanism is believed to explain the action of certain disintegrating agents (e.g. starch) (Carter, 2007).

Swelling was the first mechanism of disintegration to be proposed. Indeed, during a long period of time starch (from potato and corn) and its derivatives were the main components added in pharmaceutical tablets. Studies about swelling capacity of different starches abound in literature (Hellman et al., 1952; Modrzejewski et al., 1965; Patel et al., 1966).

Swelling disintegrants are very hygroscopic making possible the diffusion of water through the grains. It was proved that a rapid rate of swelling or water transport is crucial for successful disintegration (Van Kamp et al., 1986). Moreover, it was shown that the rupture tablet's surface employing starch as disintegrant occurs where starch agglomerates were found (Lowenthal, 1972a, 1973; Lowenthal et al., 1971). It is assumed that to swell rapidly the entire tablet, sufficient amount of starch must be provided. At an optimum concentration disintegrant grains form channels through the whole compact (Bolzolakis et al., 1984; Bolzolakis et al., 1982; Caramella et al., 1984; Fassihi, 1986). Above optimum concentration of swelling ingredient it will be difficult to compress a tablet.

Some researchers showed a relationship between disintegration efficiency and the porosity of the tablets (Berry et al., 1950; Couvreur et al., 1974). If the pore diameters are smaller than the increase in the diameter of swollen disintegrant particles, these may exert their disintegration action. According to these authors, if the pore diameters are greater than the diameter of swollen disintegrant particles, no disintegration will take place (see Figure 3.14). Porosity is correlated in particular to the compression force; this latter may influence disintegration time. Thus, when compression force is increased, disintegration time may decrease to a minimum. Beyond this critical compression force, the disintegration time often increases (Colombo et al., 1980; Couvreur et al., 1974).

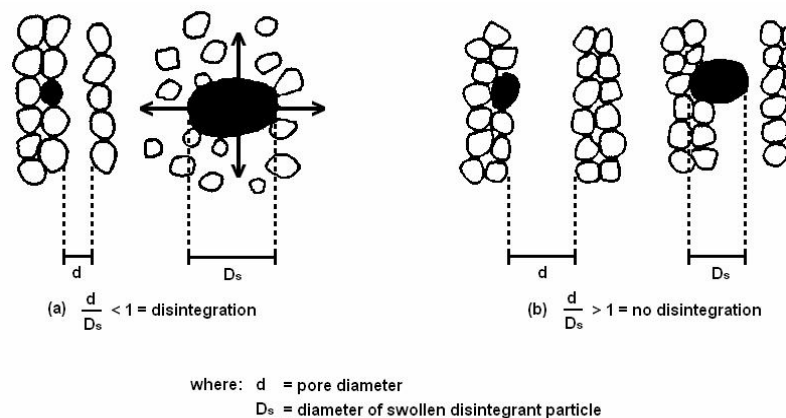


Figure 3.14: Disintegration as a function of the ratio pore diameter / swollen disintegrant particle diameter.^[9]

In the same sense, starch grains are assumed to swell back to their original uncompressed size (see next mechanism of disintegration) acting like loaded springs (Ingram et al., 1966). Thus the degree of swelling may be enhanced by sufficient compression of the tablets (low porosity) (Nogami et al., 1969). Tablets with high porosity show poor disintegration due to lack of adequate swelling force (insufficient compression of the starch grains). For very porous powder plug (like capsules) a higher content of a strong sweller (as it must fill void spaces before expanding further), (Caramella et al., 1984). However, if porosity is too low, fluid is unable to penetrate in the tablet and disintegration will be slow.

Several authors contested the dominance of swelling in disintegration process (List et al., 1979). One argument among other is that the porosity of most tablets is greater than the expansion of the starch grains (Guyot-Herman et al., 1981; Ingram et al., 1966). Other controversial arguments are the slowness of the swelling process versus the quickness of certain disintegrations, the small volume increase of some effective disintegrants, and the lack of energy release. By confuting these three arguments, authors conclude that the volume

expansion is not necessary for an effective disintegration as long as the disintegrant possesses enough swelling force.

By measuring the force resulting of the increase in volume of disintegrating tablets, the swelling pressure has been found with respect to the rapidity and the efficiency of the disintegration process (Caramella et al., 1984; Caramella et al., 1990; Colombo et al., 1981; Colombo et al., 1984; Colombo et al., 1980; List et al., 1979; Muazzam, 1979). The authors found an indisputable relationship between the swelling pressure of the tablet and its disintegration time. However not all substances that develop a swelling pressure when in contact with water are able to act as disintegrant agents (e.g. mucilaginous and gel-forming substances) as their viscosity hinders the advancing movement of water into the tablet structure. It was shown that the swelling pressure increases, and consequently the disintegration time decreases, as the particle size of the disintegrant increases for a given disintegrant (List et al., 1979). Porosity was not taken into account for this study.

The dynamic aspect of the disintegration process was analysed using different mathematical approaches. Thus, swelling pressure development was found to be directly related to water penetration (Colombo et al., 1980).

New generation of starches were developed which further decrease disintegration time. Modified starches act predominantly by massive and rapid swelling (see part C of this section).

Deformation of disintegrant particles

It was proved that during tablet compression, disintegrant particles get deformed and that they tend to recover their initial structure in contact with water which produces a break up of the tablet (Guyot-Hermann et al., 1981; Hess, 1978), see Figure 3.15b. The swelling capacity of starch was improved when grains were extensively deformed during compression.

It has to be reminded that if disintegration mechanisms were often discovered and described at different periods of time it is not correct to consider them as individual mechanisms. They are assumed to participate all together up to a certain level in the disintegration process. Disintegration is the result of inter-relationships between these major mechanisms.

Furthermore some mechanisms have not been always clearly identified. Indeed, uptake of water by capillary action is usually followed by disruption of bonding forces between particles (repulsion) upon exposure to moisture. Moreover recovery of initial shape of deformed disintegrant grains can be interpreted as moderate swelling.

To resume, when a tablet is put in a dissolution medium, the liquid enters the tablet through a combined capillary-disintegrant network. When the drug is very low water-soluble, addition of hydrophilic disintegrant is the only way to force diffusion of water through a compact.

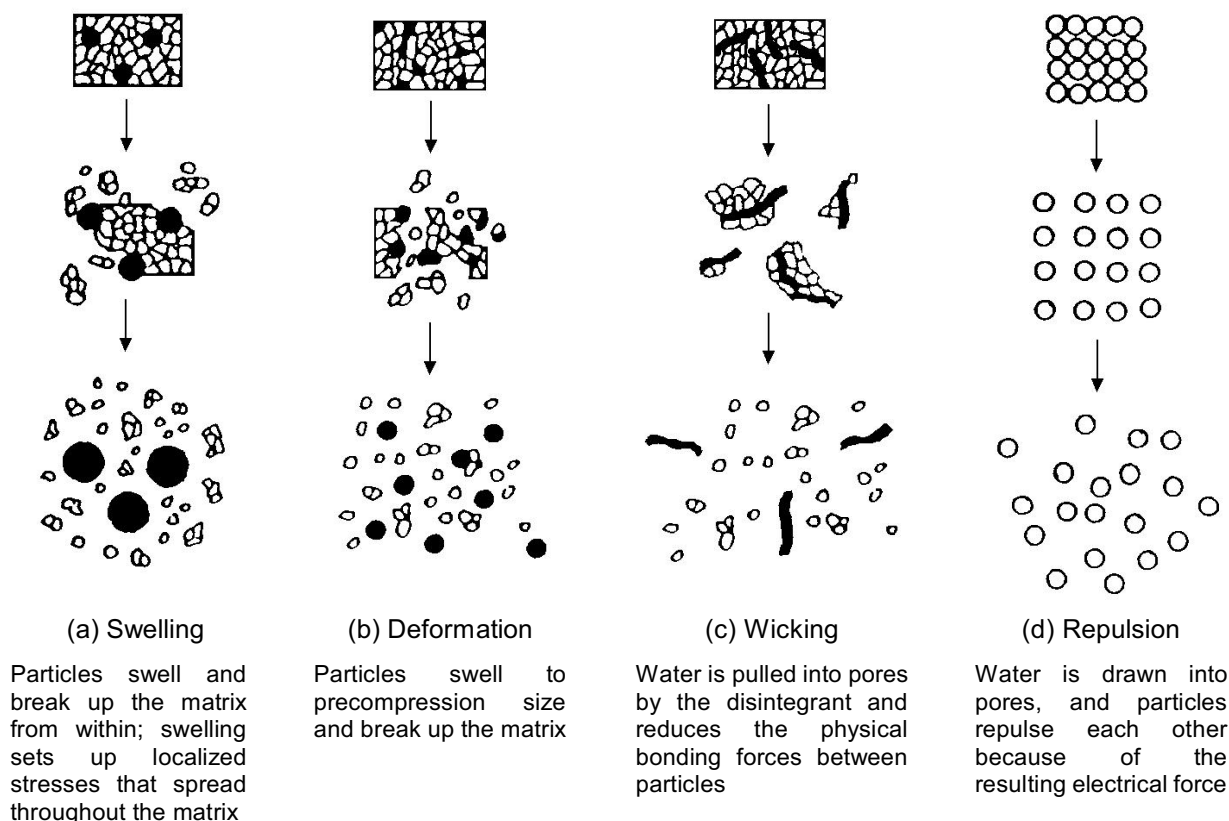


Figure 3.15: Schema of the principle mechanisms proposed to explain disintegration of tablet (Kanig et al., 1984; Luginbuehl, 1994): swelling (a), deformation (b), capillary action (c) and repulsion (d).^[10]

The entrance of water tends to break particle-particle bonding forces and induce repulsion forces. By swelling in contact with water, some types of disintegrants (e.g. normal starch) recover their initial shape and size. Some other types swell much over their initial volume (e.g. modified starch).

Other mechanisms of disintegration can be involved in special cases. For example effervescent tablets disintegrate mainly by release of gases. Interaction between bicarbonate and carbonate with citric acid or tartaric acid causes release of carbon dioxide. In this case, disintegration is due to generation of pressure within the tablet. These disintegrants are highly sensitive to small changes in humidity level and temperature and a strict control of environment is required during manufacturing of the tablets. The effervescent blend is either added immediately before tableting or can be added in to two separate fraction of formulation.

Enzymes present in the body can act as disintegrants as well by destroying the binding action of binder included in formulation.

When disintegrants with exothermic properties get wet, localised stress is generated due to capillary air expansion, which helps in tablet disintegration. This heat of wetting (air expansion) is however limited to only a few types of disintegrants and cannot describe the action of most modern disintegrating agents.

It has to be mentioned that the presence in a tablet formulation of other excipients like fillers, binders or lubricants may cause problems for disintegration. The solubility and compression characteristics of fillers affect rate and mechanism of disintegration. Soluble fillers may increase the viscosity of water entering the capillary system and thus reduce effectiveness of strongly swelling disintegrating agents. Furthermore, disintegrating time of tablet increases with growing binding capacity of the binders. In the majority of cases lubricants are hydrophobic and they are usually used in small quantities. During mixing lubricant particles may adhere to the surface of the other particles. This hydrophobic coating inhibits water uptake by capillary action and affect tablet disintegration (sodium starch glycolate remains however unaffected in the presence of hydrophobic lubricants unlike other disintegrants).

C. Types of disintegrants

Starch

Until recently it was the only excipient used to improve tablet disintegration. Starch is still widely used due to its low price. However it requires considerable expertise and careful control of the tablet manufacturing process to be effective (Melia et al., 1989). Starch acts mainly by wicking and restoration of deformed particles. Upon exposure to water starch grains release a certain amount of stress (moderate swelling) coming from the disruption of hydrogen bonding formed during compression. Unmodified starch grains exhibit natural variation in swelling properties as it depends of the amount of stress loaded in grains during deformation under pressure. Native starches have certain limitations and have been replaced by pregelatinised and modified starches with new interesting characteristics.

Pregelatinised Starch

Pregelatinised starch is a directly compressible form of starch consisting of intact and partially hydrolysed and ruptured starch grains (e.g. Starch 1500®). It has multiple uses in formulations as a binder, filler and disintegrant. The main mechanism of action is through swelling. However, pregelatinised starch may become sticky when it swells and holds the tablet fragments together after disintegration.

Microcrystalline Cellulose (MCC)

Microcrystalline Cellulose is basically cellulose derived from high quality wood pulp (e.g. Avicel[®]). When added in enough quantity to formulations it is an effective tablet disintegrant. It is also widely used in formulations because of its excellent flow and binding properties. The wicking action of this substance is due to the breaking of hydrogen bonding between adjacent bundles of MCC under the influence of moisture.

To reach even faster dissolution a new generation of 'superdisintegrants' were developed (Gould et al., 1986; Shangraw et al., 1980). Superdisintegrants are usually chemically modified starch or cellulose, with introduced carboxyl groups. Moreover, inter-chain crosslinks make them non-sticky on swelling. These modifications increase greatly uptake of water and swelling capacity. As a consequence a reduced amount is required in formulations.

Modified Starch

This type of starch exhibits high swelling properties and decreases considerably disintegration time. Modified starch is produced by carboxymethylation of native starch followed by cross linking (cross linked starch). One type of modified starch is sodium starch glycolate. Low substituted carboxymethyl starches are also marketed (ex: Explotab[®], Primojel[®]). These types of starches act by rapid and extensive swelling with minimum gelling. Consequently modified starches are highly efficient at low concentration. However if it goes beyond its limit, it can produce a viscous and gelatinous mass, which increases the disintegration time by resisting the breakup of tablet.

Cross-linked polyvinylpyrrolidone (crospovidone)

This disintegrant is water insoluble (because of cross-links) and strongly hydrophilic. (e.g. Polyplasdone XL[®], Kollidon CL[®]). Crospovidone acts by wicking, swelling and possibly by some deformation recovery.

Modified Cellulose (croscarmellose sodium)

Modified cellulose is sodium carboxymethyl cellulose which has been crosslinked to render it insoluble (e.g. AcDiSol[®]). Disintegration is caused by wicking action (fibrous structure) and by swelling with minimal gelling (see photos of a disintegrating tablet containing AcDiSol[®] in Figure 3.16).

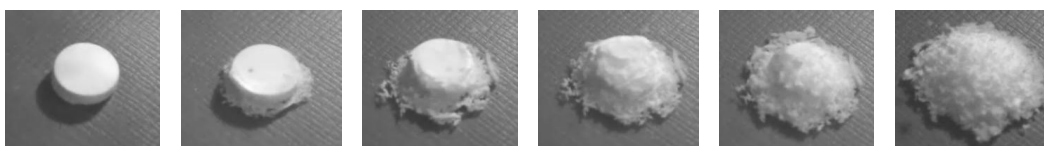


Figure 3.16: Photos at different interval of time of disintegrating dicalcium phosphate tablets with 1% superdisintegrant (AcDiSol[®]) in purified water at zero degree of agitation. Disintegration time measured according to pharmacopoeia for this formulation was 15 seconds. ^[11]

Superdisintegrants have many advantages: they are more effective in lower concentrations than classical disintegrants, they have less effect on compressibility and on flowability and are intragranularly more effective. However their high hygroscopicity may cause incompatibility with moisture sensitive drugs and their price is higher than classical disintegrants.

Disintegrants in common use are given in Table 3.9. Optimum %(w/w) for direct compression and mechanisms of action are listed for each type of disintegrant.

Table 3.9: Most common used disintegrant with example of industrial forms, respective advised %(w/w) for direct compression and principal mechanism of action.

Disintegrant	Examples	%(w/w)	Mechanism
Native starch	-	-	Wicking, deformation
Pre-gelatinised starch	StaRX 1500 [®]	5-10 %.	Swelling
Modified starch	Explotab [®] , Primojel [®]	4-6 %.	Swelling
Microcrystalline cellulose	Avicel [®]	10-20 %	Wicking
Cross-linked sodium carboxymethylcellulose (Croscarmellose)	AcDiSol [®]	1-3 %	Wicking and swelling
Cross-linked polyvinylpyrrolidone (Crospovidone)	Polyplasdone XL Kollidon CL	2-4 %	Wicking, swelling and possibly deformation

D. Method of addition of disintegrants

The method of addition of disintegrants is also a crucial part. If disintegration is necessary, disintegrating agent can be added prior to granulation (intragranular), prior to compression (extragranular) or at the both processing steps. Extragranular fraction of disintegrant facilitates break-up of tablets to granules and the intragranular addition of disintegrants produces further erosion of the granules to fine particles.

E. Mathematical description of disintegration

From a mathematical point of view, several approaches have been taken to describe the disintegration process (Bolhuis et al., 1982), including a description of the tablet dissolution in terms of its weight as a function of time (Carstensen et al., 1980a) and to analyse the force of disintegration as a function of time (Caramella et al., 1988; Caramella et al., 1986; Colombo et al., 1984). Important addition to mathematical approach describing the mechanism of disintegration was done by taking into account the stochastic nature of disintegration and water up-take (Luginbuehl et al., 1994). Important relations between the event of disintegration and the water up-take kinetics were developed (Caramella et al., 1986).

F. In vitro disintegration test

The official material and method to determine *in vitro* disintegration time of pharmaceutical tablets is assessed by official test methods laid down in National and International Pharmacopoeias. A disintegration test apparatus of the type described in the USP is schematized in Figure 3.17.

The dosage form is moved automatically up and down in medium of water (or simulated gastric juice) kept at 37 at a speed of 30 rounds per minute. The time taken for the constituent particles to fall through the mesh of standard size is recorded. To pass the test, the tablet must disintegrate within a specified period.

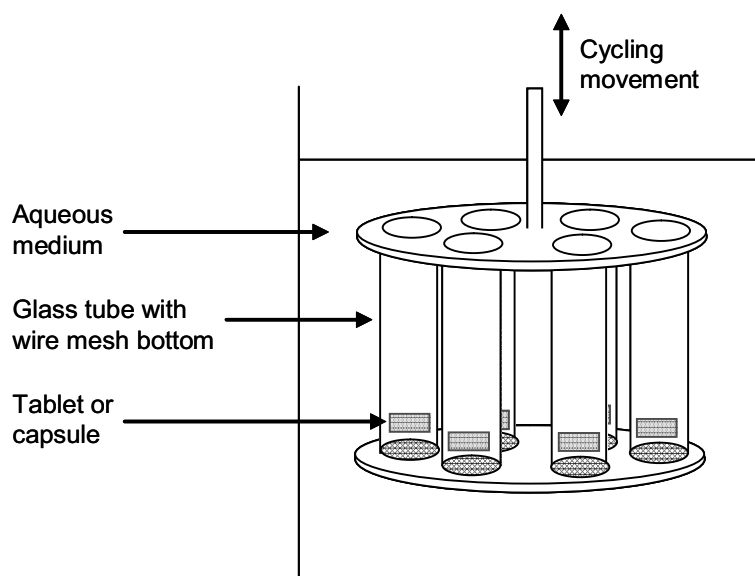


Figure 3.17: In vitro disintegration test apparatus^[12]

G. The role of water uptake in the disintegration process

The two main mechanisms of disintegration are the swelling theory and the annihilation of the interparticle cohesion forces in the presence of water (Guyot-Hermann, 1992). As it is depicted in Figure 3.18, capillarity governs the first step of these two processes. In the latter, the repulsion force may proceed from all the mechanisms:

- A:** Water penetration \longrightarrow Swelling of disintegrant \longrightarrow Force development \longrightarrow Disintegration
- B:** Water penetration \longrightarrow Annihilation of cohesion forces between particles \longrightarrow Repulsion force \longrightarrow Disintegration

Figure 3.18: Two main processes causing the disintegration of a pharmaceutical tablet.

A: Scheme of the swelling mechanism of tablet disintegration. The disintegrant particles causes tablet destruction when in contact with water (Caramella et al., 1987b).

B: Scheme of the annihilation of interparticle cohesion forces in the presence of water causes tablet disintegration (Guyot-Hermann, 1992).

According to Van Kamp the necessity for the fast conduction of water inside the whole tablet structure makes it probable that disintegration is essentially a problem of porous structure wetting, whatever the disintegration theory (Van Kamp et al., 1986).

The penetration of a liquid into a porous structure depends on the balance between several forces such as capillary and viscous forces. In lactose/starch tablets, water tends to wet the starch first and then moves forward into the tablet by the starch grain chains or agglomerates (Guyot-Hermann, 1992). The same phenomenon was observed in Emcompress[®]/starch tablets (Couvreur et al., 1974).

Usually, the liquid volume uptake with respect to time is expressed by the Washburn equation as follow (Washburn, 1921):

$$v^2 = \frac{2 m \gamma \cos \theta}{k_o \eta} \quad \text{Equation 11}$$

where: m is the hydraulic pore radius, γ is the surface tension of the penetration liquid, θ is the contact angle between the liquid and the pore wall, η is the liquid viscosity, k_o is a constant depending on the pore shape.

The former equation is usually applied by pharmaceutical researchers (Couvreur et al., 1976; Stamm et al., 1984) in the form:

$$L^2 = \frac{R \gamma \cos \theta}{2 \eta} \quad \text{Equation 12}$$

in which L is the length of liquid penetration.

In the pharmaceutical field this equation was applied to various substances (Nogami et al., 1966; Stamm et al., 1984; Van Kamp et al., 1986).

According to Nogami, “the wetting of powder with liquid depends essentially on various conditions of powder surface such as surface moisture content, crystal structure and crystallinity” (Nogami et al., 1966).

From the Washburn equation, it can be concluded that the penetration of water into a powder bed depends on the average diameter of the void spaces (assimilated to cylindrical pores), and on the contact angle, i.e. the wettability of the solid by water.

Couvreur and some other researchers show a certain correlation between the length of water penetration and disintegration time (Couvreur, 1975).

However, the Washburn equation is not always confirmed by experiments, for example in the case of tablets containing highly-soluble excipients or in the case of microcrystalline cellulose tablets (Van Kamp et al., 1986).

Several reasons were identified to explain discrepancies in the application of Washburn equation to pharmaceutical tablets (Stamm et al., 1984):

- The form of Washburn equation used corresponds to a capillary model with cylindrical pores of regular diameter; however, tablets pores are irregular and tortuous.
- The equation is only applicable to homogeneous system, not to multi-components tablets. Indeed, each component can present a different wettability and then $\cos \theta$ varies.
- The Washburn equation is only verified when the compacted powder structure can be kept during the liquid uptake. However, the tablet volume and shape can change due to localized disintegration and dissolution.
- The composition of the penetrating liquid may vary during its movement forward into the tablet by the dissolution of some of its components. Consequently the surface tension and the viscosity of the liquid may change during the uptake time.

If the different parameters of the equation are well accepted, a strict mathematical interpretation must be applied with precaution.

H. Rules to design fast disintegrating tablets

Guyot-Hermann listed four main rules for the design of robust, quickly disintegrating tablets with respect to the water uptake improvement (Guyot-Hermann, 1992):

- First rule: set up of a continuous hydrophilic network inside the compact
- Second rule: reduce the viscosity inside the tablet
- Third rule: decrease the hydrophobicity of the mixture for compression
- Fourth rule: set up a propitious hydrophilic porosity

First rule: set up of a continuous hydrophilic network inside the compact

It can be seen in many publications that a critical concentration of disintegrant is evident when increasing the amount of disintegrant in a given formulation of tablet. Below this critical concentration, the disintegration time is high. At the critical concentration, the disintegration time decreases often dramatically. Above this critical concentration, the disintegration time may continue to decrease or increase again in case of swelling disintegrants like starch.

Some authors determined or listed the critical concentration for various formulations (Fukuzawa et al., 1967; Nakai et al., 1977; Patel et al., 1966; Yuasa et al., 1986).

Leuenberger proposed a general model based on percolation theory (Leuenberger et al., 1987b) to explain the critical concentration and extend it to other tablet properties such as compression (see further section). Application of percolation theory could be used to estimate the critical concentration without experimental work.

Ringard and Guyot-Hermann have shown that the critical concentration corresponds to a very great increase in the water uptake of the tablet (Ringard et al., 1977). Consequently, it was suggested that a critical amount of disintegrant corresponding to a continuous hydrophilic structure or continuous network allows a fast progression of water into the whole tablet. For example the role of starch grains distribution in the tablet disintegration was shown using scanning electron microscopy (Hess, 1978).

Two methods exist for the determination of the critical amount of disintegrant allowing for a fast penetration of water: the empirical method and the calculation method. The empirical method has been detailed by Ringard and Guyot-Hermann and used by Surleve. The method is based on the determination of the most hydrophilic mixture, supposing that with increasing hydrophilicity of the mixture, the disintegration time is becoming shorter (Ringard et al., 1982; Surleve, 1981).

The calculation method can only be applied when the disintegrant is constituted of rounded particles (e.g. starch and cross-linked PVP). Several authors have pointed out that the critical disintegrant concentration allowing for fast disintegration seems to be dependent on the particle size of the associated drug (Caramella et al., 1987a; Commons et al., 1968; Patel et al., 1966; Ringard et al., 1978). Ringard and Guyot-Hermann applied the coordination concept as an attempt at a calculation in order to achieve a continuous network of hydrophilic particles in a tablet (Ringard et al., 1988). The principle of the calculation is as follows: in a binary mixture of two-dimensional spheres, the "contact coordination" is the number of small spherical particles which can be close to a larger one (Ben Aim et al., 1968-1969). For practical reasons, the weight of disintegrant has been substituted for the number of particles. The general equation to calculate the most effective concentration of disintegrant presenting a rounded form is:

$$M = 0.32 \frac{d_1}{d_2} \left[\left(\frac{D_1}{D_2} + 1 \right)^3 - 1 \right] \frac{D_1}{D_{1s}} \quad \text{Equation 13}$$

where M is the mass of disintegrant (g) needed by 1g of drug or diluent, d_1 and d_2 are the real densities of the disintegrant and the drug or diluent, respectively (air comparison pycnometer). D_1 and D_2 are the average diameters determined by microscopy (Ferret's diameter). D_{1s} is the disintegrant diameter in the disintegration medium. Many applications of the equation were carried out in practice (Bollaert et al., 1984; Ponchel et al., 1990; Ringard et al., 1982). However the disintegrant concentration needed for the setting up of the continuous network in the tablet is not always the best concentration as it can sometimes affect mechanical properties of the compact, for example the compressibility or the compactibility.

The limits of the application of the equation are the following:

- The diameter ratio D_1/D_2 must be at most 0.3 for a correct coating of a big particle by smaller ones.
- The lower limit of D_1/D_2 is theoretically conditioned by the void space between disintegrant particles (see Figure 3.19a). If drug particles are very fine, they form aggregates, and the network of disintegrant particles encloses these aggregates in its meshes (see Figure 3.19b).
- The shape of particles must not differ too much from the spherical form ($D_1/D_2 \leq 0.3$).
- The setting up of the continuous network in the whole tablet structure needs to take into account, for the calculation of the starch amount, not only the drug particles, but also the excipients particles.

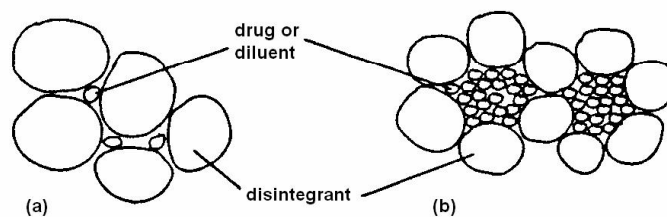


Figure 3.19: Particle arrangements when drug or diluent particles are very fine^[13]

Furthermore another important aspect of disintegrating tablet formulation is the way of introducing the disintegrant in a tablet formulated from granules. This depends on the type of drug release (fast or slow) desired and on the place in GIT where the drug must be dissolved. In case of fast release tablets, the best way to obtain a fast disintegrating tablet is to incorporate disintegrant inside the granules (intragranular) and between the granules within the compact (extragranular) (Lowenthal, 1972a, 1972b; Shotton et al., 1976b). In both cases the continuous network hydrophilic network must be set up (see Figure 3.20).

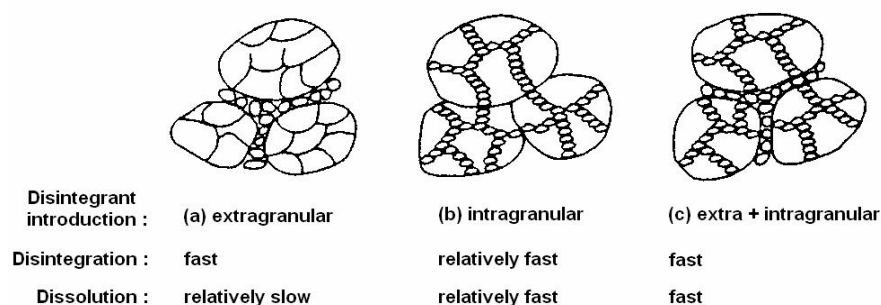


Figure 3.20: Theoretical distribution of disintegrant and consequent disintegration and dissolution.^[13]

Second rule: the viscosity inside the tablet must be low

The viscosity of the penetrating liquid has a direct influence on the disintegration of a tablet. Indeed, the higher the viscosity of the liquid, the slower will be its penetration and then disintegration. It should be kept in mind that when water penetrates the compact, it may develop a viscosity in contact with the components of the tablet. Granulating agents are the most likely to cause high viscosity.

Third rule: to decrease the hydrophobicity of the mixture for compression

Hydrophobic lubricants such as magnesium stearate are often used in formulation of tablets. The studies of the influence of magnesium stearate on disintegration time show that disintegration time increases with increasing amount of lubricant and when increasing the mixing time (Bolhuis et al., 1981; Van Kamp et al., 1986). Indeed, when mixing the formulation the very small particles of lubricant adhere to the surface of the other particles (drug, disintegrant) and create a hydrophobic coating, hindering the wetting and the penetration of water in the tablet (see Figure 3.21).

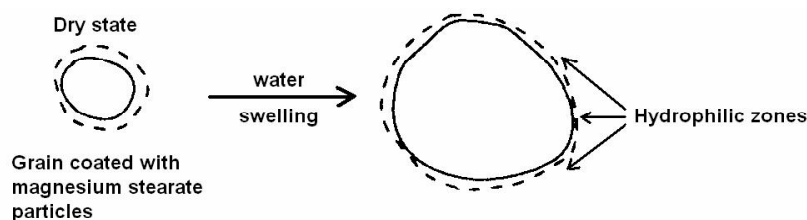


Figure 3.21 Behaviour of a starch grain coated with magnesium stearate when in contact with water. [13]

Fourth rule: set up a propitious hydrophilic porosity

One of the major factors contributing to water penetration is the porosity of the tablet and whether the pore walls are wettable (hydrophilic particles). According to some authors, pores should not be too large in order to allow either for the effect of the swelling (see Figure 3.14) or for a longer penetration length according to other authors.

Hüttenrauch pointed out the main properties for a good disintegrant (Huettenrauch et al., 1973). With regard to the previous rules listed, a direct correlation with the following optimal disintegrant properties is obvious:

- Strong hydrophilicity: for the suction of water inside the tablet (ex: modified starches, cross-linked polyvinylpyrrolidone as Polyplasdone XL[®], cellulose, modified celluloses as Avicel[®] or AcDiSol[®]).

- Weak hydrosolubility: to avoid the increase in viscosity of the penetrating liquid (ex: carboxymethyl starches as Explotab[®], sodium carboxy methylcellulose as AcDiSol[®]).
- Weak mucilaginous behaviour in contact with water.
- High binding power capacity for plastic deformation and hydrogen bond formation.
- Good flowability and good compressibility.

3.1.5. Dissolution of pharmaceutical compacts

A. Importance of the dissolution process in drug absorption

Dissolution is defined as the process by which a solid substance enters the solvent to yield a solution. The process by which a solid substance dissolves is controlled by the affinity between the solid substance and the solvent.

Drug absorption into systemic circulation from a solid dosage form after oral administration depends on the release of the drug substance, the drug's dissolution or solubilisation under physiological conditions, and the permeability across the gastrointestinal tract.

The dissolution characteristics of drugs can be influenced by different factors such as the physical characteristics of the dosage form, the wettability of the dosage unit, the penetration ability of the dissolution medium, the disintegration, disaggregation and swelling process of the dosage form. A pharmaceutical tablet disintegrates into granules, and these granules disaggregate in turn into fine particles (see Figure 3.13). Disintegration, disaggregation, and dissolution may occur simultaneously with the release of a drug from its delivery form. The effectiveness of a tablet in releasing its drug depends then somewhat on the rate of disintegration of the dosage forms and disaggregation of the granules. Yet the solid drug's dissolution rate is usually more important. Most of the time, dissolution is the limiting or rate-controlling step in bioabsorption because of the poor solubility of the majority of the drugs. However, high water-soluble drugs will tend to dissolve rapidly, making the passive diffusion of drug and/or the active transport of drug the rate-limiting step for absorption. Intermediate cases exist for which the absorption rate is affected by both steps and none of them is rate-limiting.

B. Surface area

It is obvious that the surface area of a solid dosage form will change during the dissolution process. The change in surface area will alter the fluid-flow dynamics involved in the dissolution constant (see equations of dissolution rate in part D of this section).

Such an effect is more pronounced in disintegrating dosage forms than in non-disintegrating forms. Non-disintegrating dosage forms gradually reduce their surface area during the process. Disintegrating forms, however, release particles of various sizes and density during disintegration and disaggregation process.

The several paths of the total dissolution process are shown in Figure 3.22. The illustration shows that in case of non-disintegrating solids the reduction in surface area, S , starts from the beginning of the test. For disintegrating solids surface area increases through much more significant and discrete steps during the total dissolution test (Hanson et al., 2004).

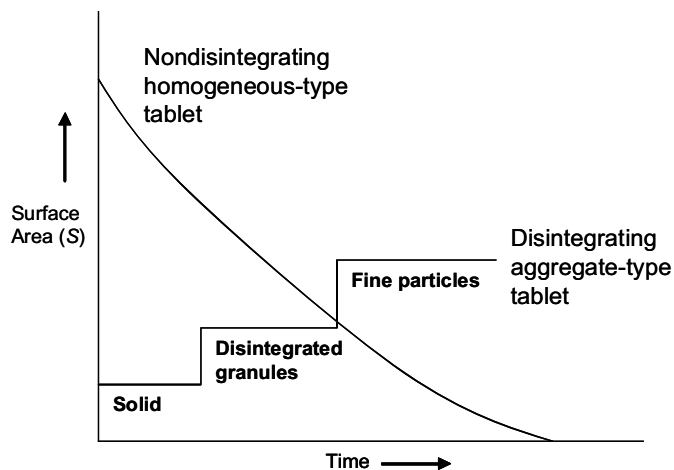


Figure 3.22: Surface area vs. time in the process of dissolution. ^[14]

The changes described above may explain the typical dissolution-curve profiles shown in Figure 3.23. Disintegration, disaggregation and dissolution processes may vary with time. In some cases, one or the other may be rate limiting and may take greater importance in the total dissolution process. Common experience indicates that the dissolution rate increases as the particles size decreases (Figure 3.23). However, that correlation is not always true. As particle size is reduced and surface area increased there may be mutual interference in the motion of particles, changes in electrical potential among particles, molecular layers of solvent tightly bound around particles, and other retarding influences, including a greater influence of hydrophobic properties imparted to the liquid-solid interface by various means. The solid-liquid interface may also be influenced by tablet lubricants, such as magnesium stearate, and by adsorption of gases onto the surface of the particles (Hanson et al., 2004).

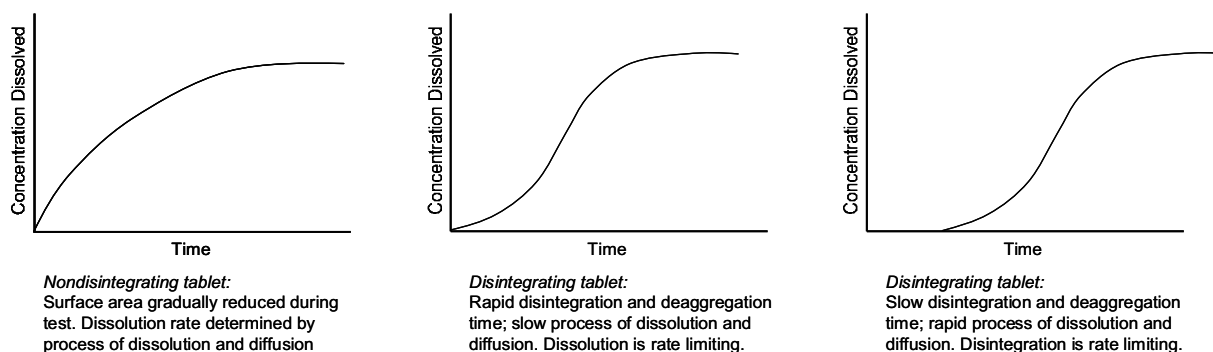


Figure 3.23: Typical dissolution profile curves observed with various solids of non-disintegrating and disintegrating aggregate types. ^[14]

C. Dissolution process

The basic step in drug dissolution is the reaction of the solid drug with dissolution medium. This reaction takes place at the solid-liquid interface. The dissolution kinetics are depending on three factors, namely the flow rate of the dissolution medium toward the solid-liquid interface, the reaction rate at the interface, and the molecular diffusion of the dissolved drug molecules from the interface toward the bulk solution, Figure 3.24 (Macheras et al., 2006).

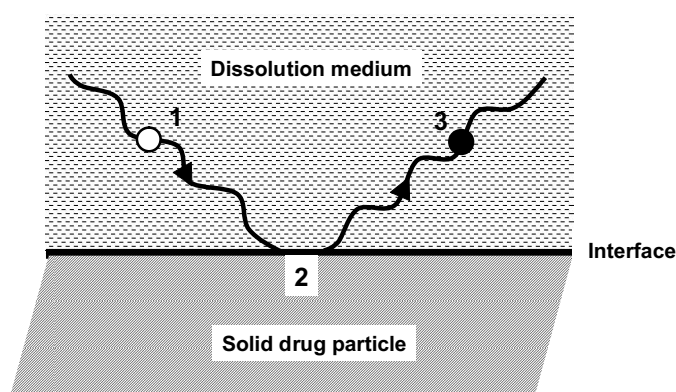


Figure 3.24: The basic steps in the drug dissolution mechanism. (1) The molecules (\circ) of solvent and/or the components of the dissolution medium are moving toward the interface; (2) adsorption-reaction takes place at the liquid-solid interface; (3) the dissolved drug molecules (\bullet) move toward the bulk solution. ^[15]

Dissolution process can be either limited diffusion or by reaction, depending on which is the slower step. The relative importance of the interfacial reaction and molecular diffusion (step 2 and 3 in Figure 3.24, respectively) can vary depending on the hydrodynamic conditions prevailing in the microenvironment of the solid. Indeed, both steps 2 and 3 are strongly depending on the agitation conditions. Besides, the reactions at the interface (step 2) and drug diffusion (step 3) are dependent on the composition of the dissolution medium. The relative importance can vary according to the drug properties and the specific composition of the medium.

Early studies formulated two main models for the interpretation of the dissolution mechanism: the diffusion layer and the interfacial barrier model. Both models assume that there is a stagnant liquid layer in contact with the solid (see Figure 3.25).

According to the diffusion layer model (Figure 3.25A), the step that limits the rate at which the dissolution process occurs is the rate of diffusion of the dissolved drug molecules through the stagnant liquid layer rather than the reaction at the solid-liquid interface. For the interfacial barrier model (Figure 3.25B), the rate-limiting step of the dissolution process is the initial transfer of drug from the solid phase to the solution, i.e., the reaction at the solid-liquid interface (Macheras et al., 2006).

Although the diffusion layer model is the most commonly used, various alterations have been proposed like, for example, the convection-diffusion model (Levich, 1962). The current views of the diffusion layer model are based on the so-called *effective diffusion boundary layer*, the structure of which is heavily dependent on the hydrodynamic conditions (stirring).

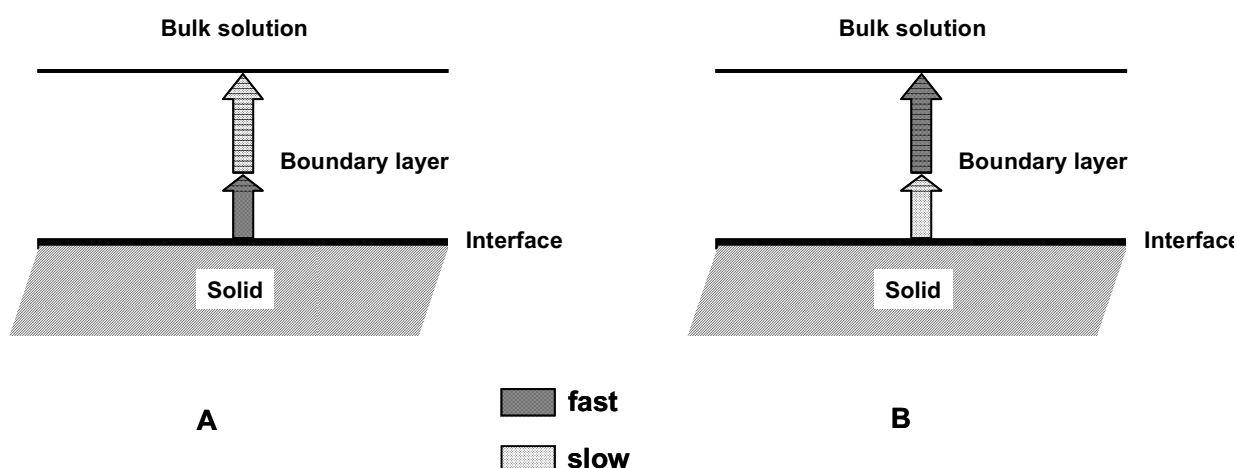


Figure 3.25: Schematic representation of the dissolution mechanisms according to: (A) the diffusion layer model, and (B) the interfacial barrier model. ^[15]

D. Mathematical description of the dissolution process

As it will be detailed further in part E, in-vitro dissolution tests are performed to determine the release rate of drug products. Indeed, drug dissolution studies are useful in the early stage of drug development and formulation to optimise drug and dosage-form characteristics that will influence the bioavailability. The quantitative analysis of the values obtained in dissolution/release tests is easier when using mathematical formulas expressing the dissolution results as a function of some of the dosage forms characteristics. In some cases, the mathematical models are derived from the theoretical analysis of the occurring process. In most of the cases the theoretical concept does not exist and some empirical equations have proved to be more appropriate.

As the diffusion layer model is the most commonly used, the mathematical descriptions of the dissolution process presented here concern only this model and follow mainly the excellent reviews of Costa on modeling and comparing dissolution profiles (Costa et al., 2001) and of Dokoumetzidis on the historical evolution in dissolution research (Dokoumetzidis et al., 2006).

Zero order kinetics

Drug dissolution from pharmaceutical dosage forms that do not disaggregate and release the drug slowly (assuming that area does not change and no equilibrium conditions are obtained) can be represented by the following equation:

$$W_0 - W_t = Kt \quad \text{Equation 14}$$

where W_0 is the initial amount of drug in the pharmaceutical dosage form, W_t is the amount of drug in the pharmaceutical dosage form at time t and K is a proportionality constant. Dividing this equation by W_0 and simplifying:

$$f_t = K_0 t \quad \text{Equation 15}$$

where $f_t = 1 - (W_t / W_0)$ and f_t represents the fraction of the drug dissolved in time t and K_0 the apparent dissolution rate constant or zero order release constant.

This model can be also expressed as follows:

$$Q_t = Q_0 + K_0 t \quad \text{Equation 16}$$

where Q_t is the amount of drug dissolved in time t , Q_0 is the initial amount of drug in the solution (most times, $Q_0 = 0$) and K_0 is the zero order release constant.

In this way, a graphic of the amount of drug dissolved versus time will be linear if the previously established conditions were fulfilled. This relation can be used to describe the drug dissolution of modified release dosage forms as matrix tablets with low soluble drugs (Varelas et al., 1995). The pharmaceutical dosage forms following this profile release the same amount of drug by unit of time and it is the ideal method of drug release in order to achieve a pharmacological prolonged action.

First order kinetic

The rate at which a solid dissolves in a solvent was proposed in quantitative terms by Noyes and Whitney in 1897 and elaborated subsequently by other workers (Gibaldi et al., 1967; Kitazawa et al., 1975; Kitazawa et al., 1977; Wagner, 1969). The dissolution phenomena of a solid particle in a liquid media imply a surface action, as it can be seen by the Noyes-Whitney equation:

$$\frac{dC}{dt} = K(C_s - C) \quad \text{Equation 17}$$

where C is the concentration of the solute in time t , C_s is the solubility in the equilibrium at experience temperature and K is a first order proportionality constant.

The exponential behaviour of the dissolution phenomena can be seen by the integrated form of Noyes-Whitney equation is:

$$\ln \frac{C_s}{(C_s - C)} = Kt \quad \text{Equation 18}$$

Equation 17 was altered (Brunner et al., 1900) to incorporate surface area S accessible to dissolution and by letting $K = K_1 S$, getting:

$$\frac{dC}{dt} = K_1 S (C_s - C) \quad \text{Equation 19}$$

where K_1 is a new proportionality constant. It was shown that the rate of dissolution depends on the exposed surface, the rate of stirring, temperature, the structure of the surface, and the arrangement of the apparatus.

Using the diffusion layer concept and Fick's second law the following equation, known as the Nernst-Brunner equation, was derived (Brunner, 1904; Nernst, 1904) by letting $K_1 = D/(Vh)$:

$$\frac{dC}{dt} = \frac{DS}{Vh} (C_s - C) \quad \text{Equation 20}$$

where D is the diffusion coefficient, h the thickness of the diffusion layer and V is the volume of the dissolution medium.

In diffusion layer concept or film theory it is assumed that an aqueous diffusion layer or stagnant liquid film of thickness h exists at the surface of a solid undergoing dissolution, as observed in Figure 3.26. This thickness h represents a stationary layer of solvent in which the solute molecules exist in concentrations from C_s , the saturation concentration at the solid's surface ($x=0$), to C , the concentration of the dissolved solid in the agitated dissolution media. Beyond the static diffusion layer, at x greater than h , mixing occurs in the solution, and the drug is found at a uniform concentration C throughout the bulk phase.

At the solid surface-diffusion layer interface, the drug in the solid is in equilibrium with the drug in the diffusion layer. The gradient, or change in concentration with distance across the diffusion layer, is constant, as shown by the straight downward-sloping line (Figure 3.26). This is the gradient represented in Equation 20 by the term $(C_s - C)/h$ (Martin et al., 1993).

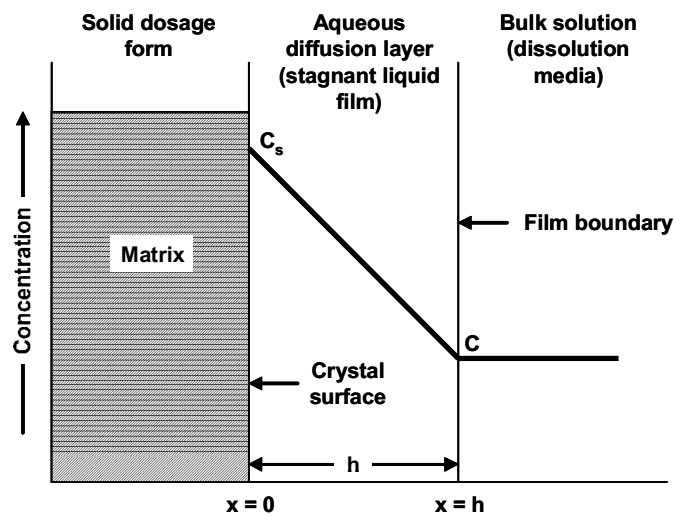


Figure 3.26: Dissolution of a drug from a solid matrix, showing the stagnant diffusion layer between the dosage form surface and bulk solution. ^[16]

Equation 19 was adapted by Hixson and Crowell in the following manner by multiplying both terms of equation by V :

$$\frac{dW}{dt} = KS(C_s - C) \quad \text{Equation 21}$$

where W is the amount of solute in solution at time t , dW/dt is the passage rate of the solute into solution in time t and $K = K_1V = D/h$ is a constant.

Equation 21 can be rewritten as:

$$\frac{dW}{dt} = \frac{KS}{V}(VC_s - W) = k(VC_s - W) \quad \text{Equation 22}$$

where $K = K_1S$. If one pharmaceutical dosage form with constant area is studied in ideal conditions (sink conditions), it is possible to use this last equation that, after integration, will become:

$$W = VC_s(1 - e^{-kt}) \quad \text{Equation 23}$$

This equation can be transformed, applying decimal logarithms in both terms, into:

$$\log(VC_s - W) = \log VC_s - \frac{kt}{2.303} \quad \text{Equation 24}$$

The following relation can also express this model:

$$Q_t = Q_0 e^{-K_1 t} \quad \text{Equation 25}$$

or in decimal logarithms:

$$\log Q_t = \log Q_0 + \frac{K_1 t}{2.303} \quad \text{Equation 26}$$

where Q_t is the amount of drug released in time t , Q_0 is the initial amount of drug in the solution and K_1 is the first order release constant. In this way a graphic of the decimal logarithm of the released amount of drug versus time will be linear. The pharmaceutical dosage forms following this dissolution profile, such as those containing water-soluble drugs in porous matrices (Mulye et al., 1995) release the drug in a way that is proportional to the amount of drug remaining in its interior, in such way, that the amount of drug released by unit of time diminishes.

In the previous equations, it was assumed that h and S were constant, but this is not the case. The static diffusion layer thickness h is altered by the force of agitation at the surface of the dissolving tablet. The surface area S obviously does not remain constant as a powder, granule, or tablet dissolves, and it is difficult to obtain an accurate measure of S as the process continues. In experimental studies of dissolution, the surface may be controlled by placing a solid (for example a tablet or a pellet) in a holder that exposes a surface of constant area (intrinsic dissolution). Although this ensures better adherence to the requirements of previous equations and provides valuable information on the drug, it does not simulate the actual dissolution of the material in practice (Martin et al., 1993).

Weibull model

A general empirical equation described by Weibull (Weibull, 1951) was adapted to the dissolution/release process (Langenbucher, 1972). This equation can be successfully applied to almost all kinds of dissolution curves and is commonly used in these studies (Goldsmith et al., 1978; Romero et al., 1991; Vudathala et al., 1992). When applied to drug dissolution or release from pharmaceutical dosage forms, the Weibull equation expresses the accumulated fraction of the drug, m , in solution at time, t , by:

$$m = 1 - \exp\left[\frac{-(t - T_i)^b}{a}\right] \quad \text{Equation 27}$$

In this equation $m = M / M_0$ with M is the amount of drug dissolved as a function of time t and M_0 is total amount of drug being released. The scale parameter, a , defines the time scale of the process. The location parameter, T_i , represents the lag time before the onset of the dissolution or release process and in most cases will be zero. The shape parameter, b , characterises the curve (see Figure 3.27) as either exponential ($b = 1$) (Case 1), sigmoid, S-

shaped, with upward curvature followed by a turning point ($b > 1$) (Case 2), or parabolic, with the exponential ($b < 1$) (Case 3).

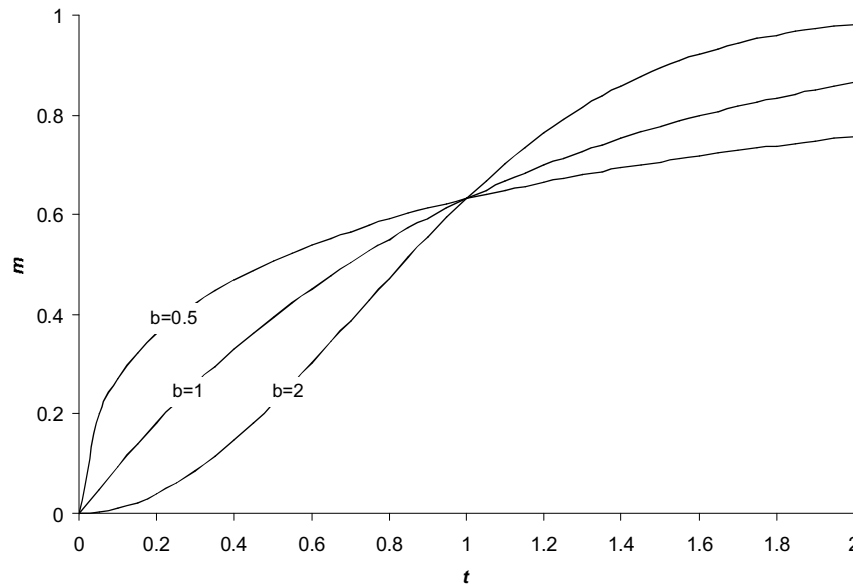


Figure 3.27: Accumulated fraction of drug dissolved, m , as a function of t to the Weibull distribution function ($T_i = 0$, $a = 0$).^[15]

This equation may be rearranged into:

$$\log[-\ln(1-m)] = b \log(t - T_i) - \log a \quad \text{Equation 28}$$

From this equation a linear relation can be obtained for a log-log plot of $-\ln(1-m)$ versus time, t . The shape parameter, b , is obtained from the slope of the line and the scale parameter, a , is estimated from the ordinate value ($1/a$) at time $t = 1$.

Because this is an empiric model, not deduced from any kinetic fundament, it presents some deficiencies and has been the subject of some criticism (Christensen et al., 1980; Pedersen et al., 1978), such as:

- There is not any kinetic fundament and could only describe, but does not adequately characterise, the dissolution of the drug.
- There is not any single parameter related with the intrinsic dissolution rate of the drug.
- It is of limited use for establishing in vivo/in vitro correlations.

Hixson-Crowell model (cubic root law)

Hixson and Crowell (1931) recognizing that the particle regular area is proportional to the cubic root of its volume (Hixson et al., 1931), derived an equation that can be described in the following manner:

$$W_0^{1/3} - W_t^{1/3} = Kt \quad \text{Equation 29}$$

where W_0 is the initial amount of drug, M_0 , in the pharmaceutical dosage form, W_t is the remaining amount of drug in the pharmaceutical dosage form at time t (difference of the initial mass M_0 and the dissolved mass M). K is a constant incorporating the surface-volume relation and including different parameters such as density of the solid, diffusion coefficient, particle number, geometry of the particles and so on. This expression applies to pharmaceutical dosage form such as tablets, where the dissolution occurs in planes that are parallel to the drug surface if the tablet dimensions diminish proportionally, in such a manner that the initial geometrical form keeps constant all the time. The Equation 29 can be formulated as follows:

$$M = M_0 - (M_0^{1/3} - Kt) \quad \text{Equation 30}$$

The Cube Root law can be applied for solids with a defined surface area. It concerns regular geometric solid bodies and bulks of powder, which could be also multiparticulate but with a regular particle size distribution. The Cube Root law in its original form cannot be applied anymore if the solid change its characteristic dimension during dissolution. This is the case when the dosage form consists of material with different dissolution characteristics or if the particle size distribution is irregular. Thus, a lot of attempts have been done to modify the equation according to the different dissolution scenarios. Niederball modified the Hixson-Crowell equation by introducing a factor considering the number of particles (Niebergall et al., 1963) in this manner:

$$W_0^{1/3} - W^{1/3} = KN^{1/3}t \quad \text{Equation 31}$$

where N is the number of particles. This model has been used to describe the release profile keeping in mind the diminishing surface of the drug particles during the dissolution (Niebergall et al., 1963; Prista et al., 1995).

This equation, however, did not correlate very well with the measurements and the experimental data were described in a better way with a square root equation:

$$W_0^{1/2} - W^{1/2} = KN^{1/2}t \quad \text{Equation 32}$$

Higuchi derived another, modified equation for the dissolution of log normal variable powders (Higuchi et al., 1963a; Higuchi et al., 1963b). In its simplest form the equation can be written as follows:

$$W_0^{1/2} - W^{1/2} = Kt^3 \quad \text{Equation 33}$$

Higuchi model

Higuchi developed several models to study the release of either soluble and low soluble drugs incorporated in semi-solid and/or solid matrixes. Mathematical expressions were obtained for drug particles dispersed in a uniform matrix behaving as the diffusion media. In a general way it is possible to resume the Higuchi model to the following expression (generally known as the simplified Higuchi model):

$$M = K_H \sqrt{t} \quad \text{Equation 34}$$

where K_H is the Higuchi dissolution constant treated sometimes in a different manner by different authors and theories. Higuchi describes drug release as a diffusion process based in the Fick's law, square root time dependent. This relation can be used to describe the drug dissolution from several types of modified release pharmaceutical dosage forms, as in the case of matrix tablets with water-soluble drugs (Desai et al., 1966a, 1966b; Schwartz et al., 1968a, 1968b).

Other models

A lot of other mathematical models describe the drug release under different conditions like the Korsmeyer-Peppas model (Korsmeyer et al., 1983), which relates exponentially the drug release to elapsed time, the Baker-Lonsdale model (Baker et al., 1974) which describes the drug controlled release from a spherical matrix or the Hopfenberg model (Hopfenberg, 1976), describing the drug release from slabs, spheres and infinite cylinders displaying heterogeneous erosion. An overview of other existing models for mathematical description of drug release can be found in the review of Costa (Costa et al., 2001).

Although the traditional mathematical expression for the dissolution rate is the Noyes-Whitney equation, the release models with major appliance and best describing drug release phenomena are, in general, the Higuchi model, zero order model, Weibull model and Korshmeyer-Peppas model. The Higuchi and zero order models represent two limit cases in the transport and drug release phenomena, and the Korsmeyer-Peppas model can be a decision parameter between these two cases. While the Higuchi model has a large application in polymeric matrix systems, the zero order model becomes ideal to describe coated dosage forms or membrane controlled dosage forms.

The criteria to choose the “best model” to study drug dissolution/release phenomena can be the coefficient of determination R^2 , to assess the “fit” of a model equation. The value tends to get greater with the addition of more model parameters. When comparing models with different parameters, the adjusted coefficient of determination R^2 adjusted is more meaningful (Costa et al., 2001).

Release profile comparison

Some methods to compare drug release profiles were recently proposed (Chow et al., 1997; Costa et al., 2001; Tson et al., 1996). Those methods were classified, such as:

- Statistical methods based on the analysis of variance or on *t*-student tests (single time point dissolution and multiple time point dissolution)
- Model-independent methods
- Model- dependent methods, using for example the previously described models

E. Dissolution testing methodology

Many schemes have been reported for the determination of dissolution rate. All methods involve providing a renewable solid-liquid interface between the dosage form and the dissolution fluid, ensuring that this can be defined, controlled and is thus repeatable. The controlled flow of fluid over a solid introduces requirements of maintaining the surface of the solid in a position exposed to a non-accelerating flow. Most of the variations in dissolution methods have been devised to bring such variables under control (Hanson et al., 2004). Unfortunately, some of the methods are applicable only to unique dosage forms and become unsatisfactory with others. The methods of solid-dosage dissolution testing presented here are those that are already established in the compendia as official methods. An official description of a dissolution apparatuses can be found in USP XXIV as well as in the Ph. Eur. 2002 with the exact specifications.

Basket method:

Originally proposed by Pernarowski and modified to become the first official method in USP in 1970 (Pernarowski et al., 1968), and were extensively used for the testing of numerous dosage forms. It has been modified, and the official method (Apparatus 1) is schematized in Figure 3.28. The basket method represents an attempt to constrain the position of the dosage form in order to provide the maximum probability of a consistent solid-liquid interface. This method has several disadvantages: a tendency for gummy substances to clog the basket screen, extreme sensitivity to dissolved gases in the dissolution fluid, inadequate flow rates when particles leave the basket and float in the medium, and construction difficulties when automated methods are attempted (Hanson et al., 2004).

Paddle method

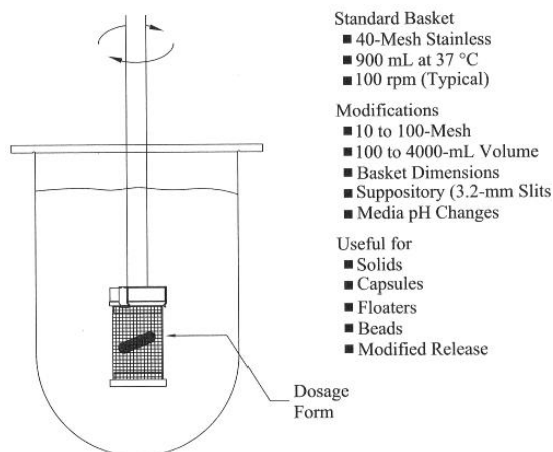
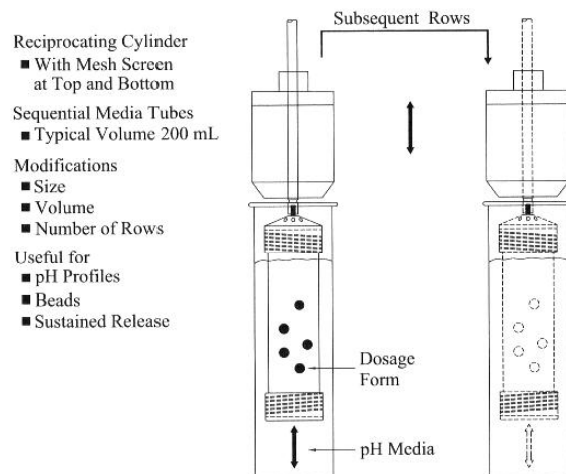
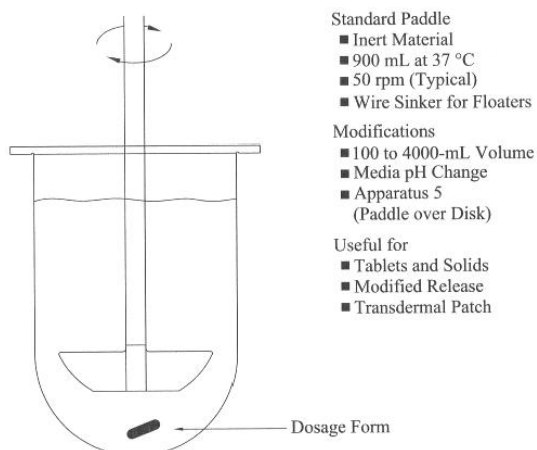
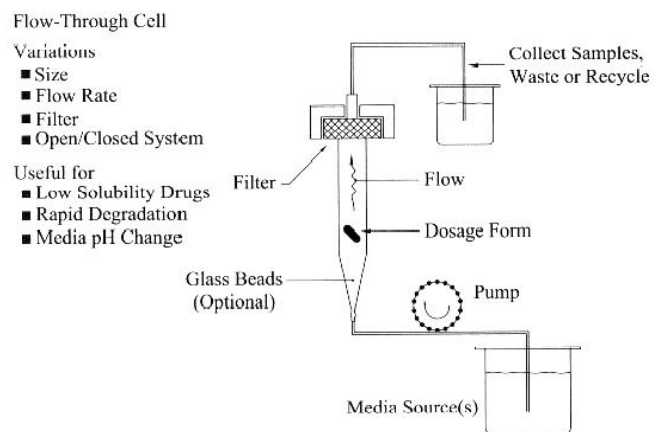
Originally developed by Poole, the paddle method (Poole, 1969) was modified through the work of scientist at US FDA. It consists essentially of a rotating paddle with a blade of specific dimensions conforming to the inside radius of a round-bottomed flask (see Figure 3.30). This method (Apparatus 2) overcomes many of the disadvantages of the rotating basket, but it requires careful precision in the geometry of the paddle and flask and suffers from unacceptable variations in dissolution data following even minor changes in paddle orientation. Its convenience for automated systems, however, is its strong point (Hanson et al., 2004).

Flow-Through methods

Proposed by many but most extensively studied by Langenbucher, flow-through methods involve constraining the dosage form in a cell and pumping dissolution fluid through that cell (Langenbucher, 1969). This system is advantageous in maintaining sink conditions for drugs with low solubility, but high dosage amounts, which saturate in volumes more than 25% of specific media volume. This method also has the added advantage of inherent adaptability to automated sampling techniques. The flow-through method is now official in the US (Apparatus 4) and European Pharmacopoeia (see schema in Figure 3.31) and may be considered for drugs that impose saturation problems with basket or paddle methods (Hanson et al., 2004).

Reciprocating cylinder apparatus

The reciprocating cylinder is now listed in USP as Apparatus 3 (Figure 3.29) for extended-release dosage forms. This is a unique system that “floats” disaggregated particles in a reciprocating stream. It has advantages of lower volume of solvent; ease of pH change; reduce dwell time to avoid degradation; ease of automated sampling; correlation with the database from the now-discarded rotating bottle apparatus; and impressive correlations with bioavailability data (Borst et al., 1997; Hanson et al., 2004).

Figure 3.28: USP Apparatus 1, Basket ^[17]Figure 3.29: USP Apparatus 3, reciprocating cylinder ^[17]Figure 3.30 USP Apparatus 2, paddle ^[17]Figure 3.31 USP Apparatus 4, flow-through cell ^[17]

F. Setting for *in vitro* dissolution measurements

In any dissolution test protocol, reproducibility must be ensured. There are number of experimental factors influencing the drug release of solid dosage forms.

One important point is that volume of the dissolution medium should be adapted to the gastro intestinal tract (GIT) and should not exceed 1L (Koch, 1984). Furthermore, concentration of the model drugs dissolved should not be significantly higher than 10% of their saturated concentration (Gibaldi et al., 1967). Koch however estimated that a solution with a drug concentration up to 25% of its saturated concentration is still acceptable to conduct a dissolution experiment (Koch, 1984). An alternative to the use of a large volume of dissolution medium at once is to carry out the drug release by giving to the media a constant supply of fresh liquid (Von Orelli, 2005). However, GIT does not extract the drug in the same manner (Koch, 1982).

The main challenge with *in vitro* dissolution testing is to maintain physiological conditions and performing sink conditions at the same time.

The pH of the dissolution media has a significant influence on the drug release. Indeed, as majority of the drugs are compounds with acidic or alkaline character, their pKa-values and the pH of the dissolution media determine their ionisation and thereby their apparent solubility. An overview of the different pH values in the body is given in Table 3.10. It is important that the pH-value at which the dissolution test is carried out correspond to the place of application of the dosage form. USP XXIV suggests a range of pH from 1.0 up to 8.0 for dissolution media. Co-solvents such as alcohol may be used to improve the dissolution and non mixable organic phase may be added to aqueous phase (Gibaldi et al., 1967) to imitate the drug permeation through the intestine wall. To simulate the surface active substances present in the physiological environment (enzymes like pepsine and pancreatine, ions, bile salts), synthetic and natural wetting agents (polysorbate 20 or 80, sodiumlaurylsulfate, dicolytesodiumsulfosuccinate, lysolecithine, bile acids) can be added in the dissolution media (Von Orelli, 2005).

Furthermore, the dissolution media should be maintained at 37°C to respect the human body temperature.

Another very important parameter, especially for the paddle method, is the speed of agitation of the dissolution medium. Indeed, the same concentration of drug should be present at each time in every part of the container and this is performed by stirring the dissolution media. In order to respect the very smooth and slow natural peristaltic movement (Levy, 1963) the most appropriate stirring speed is of 50rpm in a 500ml vessel. A compromise should be done between an insufficient stirring speed, which would not allow homogeneous concentration in the vessel and an excessive speed, which could cause turbulences in the dissolution medium. Furthermore, as the stirring speed has an important influence on the release of a solid dosage form, the same speed should be maintained for all experiments to be compared.

Table 3.10: pH-values in different sections of the GIT.

Body fluid	pH
Saliva	5.7-7.3
Gastric juice	0.9-3.2
Duodenum	6.5-7.6
Jejunum	6.3-7.3
Ileum	7.6
Colon	7.9-8.0

G. Biopharmaceutical Classification System (BCS)

In-vitro dissolution testing is a first important step to assess the quality of a certain compound and to guide development of new formulations and may be relevant, under certain conditions, to the prediction of in vivo performance of a drug (Munday et al., 1995). However, there are a number of examples of unsuccessful correlation of dissolution characteristics to bioavailability (Meyer et al., 1998). These cases can be explained on the basis of the Biopharmaceutical Classification System (BCS) (Löbenberg et al., 2000).

The Biopharmaceutics Classification System (BCS) is a drug development tool that allows estimation of the contributions of three major factors, dissolution, solubility, and intestinal permeability, that effect oral drug absorption from immediate release (IR) solid oral products (Hussain et al., 1999).

According to the BCS, drug substances are classified as reported in Table 3.11.

Table 3.11: Biopharmaceutical Classification System (BCS)

Class I	High Solubility - High Permeability
Class II	Low Solubility - High Permeability
Class III	High Solubility - Low Permeability
Class IV	Low Solubility - Low Permeability

The solubility for a classification in the BCS is defined as follows (FDA, 2000): A drug substance is considered highly soluble when the highest dose strength is soluble in 250 ml or less of an aqueous media over a pH-range of 1-7.5.

A substance is considered highly permeable when the extent of absorption is determined to be 90% or more of an administered dose based on a mass balance determination or in comparison to an intravenous dose.

According to the FDA, the permeability class can be determined across humans, across animal models (e.g. rat), across in-vitro permeation studies with human or animal excised tissue or by the use of cultured cell models (e.g. Caco-II-cells = adeno carcinoma cells).

3.2. Expert systems and solid dosage formulation design

3.2.1. General knowledge

There is a wide range of definition for expert systems. Some of them are given below:

- "Knowledge-based system that emulates expert thought to solve significant problems in a particular domain of expertise" (Sell, 1985).

- “Computer program that draws upon the knowledge of human experts captured in a knowledge base to solve problems that normally require human expertise” (Partridge et al., 1994).
- “Also known as a knowledge based system, it is a computer program that contains some of the subject-specific knowledge, and contains the knowledge and analytical skills of one or more human experts” (Wikipedia, 2007).
- “Collection of bits of know-how (fragmentary, judgmental, heuristic) in a knowledge base used to reason about a specific problem” (Bergler, 2007).
- “An intelligent computer program that uses knowledge and inference procedures to solve problems that are difficult enough to require significant human expertise for their solutions” (Feigenbaum, E.).

Expert systems are used in a wide range of scientific fields such as medical diagnosis, computer configuration, chemical data interpretation and structure elucidation, speech recognition, pattern recognition, financial decision making, mineral exploration, or military intelligence and planning. This class of program was first developed by researchers in artificial intelligence during the 1960s and 1970s and applied commercially throughout the 1980s. Because of their emphasis on knowledge, the terms ‘expert system’ and ‘knowledge-based systems’ are often used interchangeably. If any difference does exist, it is in how their input knowledge is acquired. In expert systems, input knowledge is usually acquired from human experts, whereas in knowledge-based systems it is usual for input knowledge to be acquired through non-human interaction, such as through information systems and databases.

In their simplest form, both systems have three major components: an interface, monitor and keyboard allowing two-way communication between the user and the system; a knowledge base in which all the knowledge pertaining to the domain is stored; and an inference engine in which the knowledge is extracted and manipulated to solve the relevant problem. Inferencing strategies may be either forward chaining, which involves the system reasoning from data and information obtained by consultation with the user to form a hypothesis, or backward chaining, which involves the system starting with a hypothesis and then attempting to find data and information to prove or disprove the hypothesis. Both strategies are included in most expert systems (Rowe et al., 1998).

In any kind of domain, knowledge takes the form of facts and heuristics. Facts knowledge are valid, true and justifiable by rigorous arguments, Heuristics knowledge (or ‘rules of thumb’) are the expert’s best judgment in any particular circumstance and hence justifiable only by example. Associate with these are the terms ‘data’ and ‘information’, the former referring to facts and figures, the latter being data transferred by processing such that it is meaningful to

the recipient. Knowledge can therefore be regarded as information combined with heuristic and rules. There are many levels of knowledge (see Table 3.12) which must be acquired and organised into a computer-readable format. Knowledge-based systems encode an extensive body of knowledge (general or expert) in a knowledge base (see Figure 3.32a).

Knowledge acquisition is one of the most difficult stages in the development of an expert system as it is both time-consuming, tedious, expensive and often difficult to manage. However it is a necessary element in the building of an expert system, and if done well, will lead to systems of potential use. The knowledge must be acquired not only by the expert(s) but also by all the other sources such as written documents (research reports, reference manuals, operating procedures policy statements) and consultants, users and managers.

The requirements for an Expert System are usually a high performance, an adequate response time, a good reliability, the system must be very transparent and as understandable as possible and must offer a certain flexibility.

A technique that is often used in the acquisition process is the rapid prototyping approach. In this approach, the knowledge engineer builds a small prototype system as early as possible and this is shown to both the expert and user, who can then suggest modification and additions. This system grows incrementally as more information and knowledge is gained. Acquired knowledge can be represented in the knowledge database in different ways: production rules, frames, semantic networks, decision tables, decision trees or objects. It is probable that the most common methodology is the production of rules expressing the relationship between several pieces of information by way of conditioned statements which specify sections under certain sets of conditions:

- IF (Condition 1)
- AND (Condition 2)
- OR (Condition 3)
- THEN (Action)
- UNLESS (Exception)
- BECAUSE (Reason)

Each rule implements an autonomous piece of knowledge and is easy to understand. Unfortunately, complex knowledge can require large numbers of rules, causing the system to become difficult to manage. The decision about which method of knowledge representation should be adopted depends primarily on the complexity of the domain.

Table 3.12: Levels and categories of knowledge

Shallow	Surface-level, specific, heuristic
Deep	Complete, integrated, conceptual
Explicit	Conscious, able to be articulated
Tacit	Implicit in expert's ability to solve problems
Declarative	Descriptive representation of facts
Procedural	Detailed set of rules
Meta	Knowledge about knowledge

The expert systems architecture combines a knowledge base that describes a problem domain as extensively as possible with a domain independent inference engine that combines input data and the encoded knowledge to infer 'expert advice' (see Figure 3.32b).

Expert systems can be developed using either conventional computer languages, special purpose languages or with the assistance of development shells or toolkits. Conventional languages such as PASCAL and C have the advantages of wide applicability and full flexibility to create the control and inferencing strategies required. They are also well supported and easy to customise. However, considerable amounts of time and effort are needed to create the basic facilities. Specialised languages such as LISP (a recursive language and the primary one for artificial intelligence research), PROLOG (a language based on first order predicate logic) and SMALLTALK (an object-orientated language) have been used extensively in the development of expert systems because they share the advantages of applicability and flexibility of the conventional languages but are also faster to implement.

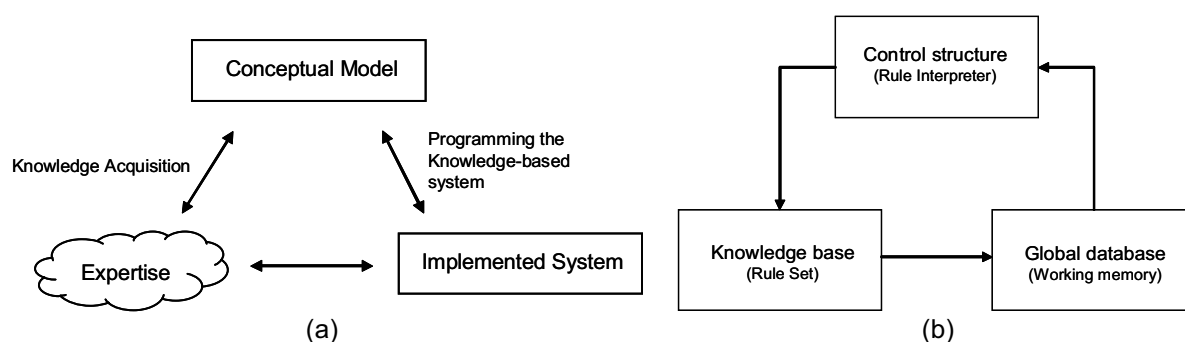


Figure 3.32: Schema of the Knowledge-based Expert Systems implementation (a) and the usual Expert Systems architecture (b).^[18]

3.2.2. Application of expert systems in pharmaceutical formulation

The first publication about expert systems in pharmaceutical product formulation was by Bradshaw on 27 April 1989 in the London Financial Times (Bradshaw, 1989); this was followed

by an article in the same year by Walk (Walko, 1989). Both refer to the work performed at ICI (now Zeneca) Pharmaceuticals UK and Logica UK, to develop an expert system for formulating pharmaceuticals using PFES. Since that time, several companies and academic institutions have reported their experiences in this area (see Table 3.13). Some examples are presented here. Further details can be found in the excellent review paper of Rowe on the use of knowledge-based and expert systems for product formulation (Rowe et al., 1998).

Cadila System

This system was developed at Cadila Laboratories (Ahmedabad, India) and has been designed to formulate tablets for active drugs based on their physical (e.g. solubility, hydroscopicity), chemical (e.g. functional groups) and biologically inter-related (e.g. dissolution rate) properties (Ramani et al., 1992). The system first identifies the desirable properties for optimum compatibility with the drug, selects those excipients that have the required properties and then recommends proportions based on the assumption that all tablet formulations comprise at least one binder, one disintegrant and one lubricant. Other excipients such as fillers or glidants are then added as required. Knowledge acquired through active collaboration with expert formulations is structured as decision tables with derived production rules. The system written in PROLOG is menu-driven and interactive with the user who is prompted to enter all the known properties of the new active drug.

Galenical Development System, Heidelberg

This system, developed in the Departments of Pharmaceutics and Biopharmaceutics and of Medical Informatics at the University of Heidelberg (Germany), has been designed to provide assistance in the development of a range of formulations (e.g. aerosols, tablets, capsules, intravenous injections), starting from the chemical and physical properties of an active drug. The project was initiated in 1990 and extensively revised and enhanced in the interim (Stricker, 1991, 1994). Originally implemented in C, the system has recently been upgraded using SMALLTALK. Knowledge representation is by means of objects, frames and production rules. Because of the complexity of the overall process, the developers have adopted an approach whereby the system focuses on one problem and its associated subset of specification and constraints at a time. These distinct development steps are worked through in succession, care being taken that any solution should not violate any constraints from previous steps. The output of the system is a formulation together with production method, recommended packaging and, where appropriate, predicted product properties.

University of London/Capsugel System

This system, developed at the School of Pharmacy, University of London (UK), supported by Capsugel together with the Universities of Kyoto (Japan) and Maryland (USA) has been designed to aid the formulation of hard gelatin capsules (Lai, 1996). The system, implemented in C, uses decision trees and production rules for knowledge representation. The system is fully interactive with the user and has a questionnaire to assist in collecting all necessary input data. From these data the system uses a variety of methods to predict properties of mixtures of the new drug and various excipients and recommends a formulation with any necessary powder processing and filling conditions. In addition, the system provides a statistical design to optimise the formulation quantitatively, the specification of the excipients used, recommended tests to validate the formulation and a complete documentation of the decision process. The system is unique concerning the broadness of its knowledge base. It contains information on a large number of excipients, a database of marketed formulations from Germany, Italy, Belgium, France and the USA, a database on literature references associated with the formulation of hard gelatin capsules, experience and non-proprietary knowledge from a group of international experts and the results from statistically designed experiments on capsule formulation. The data is frequently updated and the system has a semi-automatic learning tool that monitors users' habits regarding the use of excipients.

Sanofi System

This system, developed by personnel at the Sanofi Research Division, has been designed to formulate hard gelatin capsules based on specific preformulation data on the active drug (Bateman, 1996). The system, implemented using PFES, generates one first-pass capsule formulation with as many subsequent formulations as desired to accommodate an experimental design. Knowledge acquisition was by interview and structured using objects, frames and production rules. The user is first prompted to enter specified preformulation data on the active drug and the system recommends a formulation with relevant capsule size and production information. An explanation log, providing details of the decisions and reasoning used by the system, are also recorded.

Zeneca systems

Since April 1988, three systems have been developed at Zeneca Pharmaceuticals (Rowe, 1993, 1995; Rowe et al., (in press)). These systems, designed to formulate tablets, parenterals and film coatings, respectively, have all been implemented using PFES. Each was developed using two experts, one with extensive heuristic knowledge, the other with extensive research knowledge, and structured using objects, frames and production rules by specialised

consultancy support. Each system is fully interactive with the user, requiring specified input data on the active drug. The systems then recommend formulations with predicted properties (e.g. compaction properties for tablets, tonicity and storage life for parenterals, opacity and cracking potential for film coatings). Each system contains 'Help' routines providing both on-line help in the use of the system and the rationale behind the adoption of the specified rules/formulae used. The user is able to browse the knowledge trees at will but is unable to edit them without privileged access. Explanations for any recommendations made by the systems can be accessed easily if required. The tablet formulation system is the most frequently used expert system and is now an integrated part of the development strategy in this domain.

Boots System

Although not strictly developed for pharmaceutical formulation, this system has been included since it is the only one known for formulating topicals. Developed in 1990 at the Boots Company, the system won second prize in the UK Department of Trade and Industry Manufacturing Intelligence Awards in 1991 (Wood, 1991). The system was developed in the first instance to assist in the formulation of sun oils but has been rapidly extended to cover creams and lotions. Knowledge was acquired from senior formulators using interviews and structured as objects, frames and production rules. Implemented in PFES, this is the only system in which the developers have given details of costings and quantitative benefits.

Table 3.13: Published applications of pharmaceutical product formulation expert system ^[19]

Company/Institution	Domain	Development tool
Cadila Laboratories (India)	Tablets	PROLOG
University of Heidelberg	Aerosols	C/SMALLTALK
	Tablets	
	Capsules	
	IV injections	
University of London/Capsugel	Capsules	C
Sanofi Research	Capsules	PFES
Zeneca Pharmaceuticals	Tablets	PFES
	Parenterals	
	Film coatings	
Boots Company	Topicals	PFES

Benefits of expert system applications on products formulation

As relatively high investments of time and resources are often needed for the development of such systems, it is imperative to identify and objectify their benefits. In a large survey in 1989 involving nearly 450 responses from a wide variety of organisations and types of users, several key benefits were identified (Deware, 1989). The most important reported benefits concerned the accuracy of the decision making, the improvement of problem solving and the quality/accuracy of work (see Figure 3.33). The least important benefits were those concerned with the reduction in staff numbers or using less skilled staff. Thomas identified the overall business impact of expert studies in terms of quality availability and consistency of expertise available (Thomas, 1991). Expert systems should enable managers to begin to manage expertise as a corporate asset leading to an increased competitive edge, improved risk management, increased revenue, decreased costs and increased profitability.

The most pertinent benefits found by the users of systems in pharmaceutical formulation are discussed below:

- Knowledge availability and protection:

Some of the benefits reported are the ability to use knowledge from a broad base (Lai, 1996), the rapid access to physical and chemical data of both drugs and excipients (reducing the time spent searching literature) (Bateman, 1996; Ramani et al., 1992) as well as the existence of a coherent durable knowledge base which is not affected by staff turnover (Rowe, 1995).

- Consistency:

All systems generated robust formulations with increased certainty and consistency.

- Training:

All systems have been used to provide training for both novices and experienced formulators or to enable experienced formulators to experience unfamiliar new excipient combinations (Wood, 1991).

- Speed of development:

A reduction in the duration of the formulation process has been widely reported (Ramani et al., 1992; Rowe, 1993; Wood, 1991). Formulators working in the topical domain can now produce a formulation in 20 minutes that might otherwise have taken two days to achieve (Wood, 1991). A 35% reduction in the total time needed to develop a new tablet formulation has also been reported (Ramani et al., 1992).

- Cost savings:

Cost savings can be achieved by not only reducing the development time but also by the more effective use of materials. Several users have reported a benefit in being able to plan the

purchase and stocking of excipients and to reduce the size of raw material inventories (Ramani et al., 1992; Wood, 1991).

- Freeing experts:

The implementation of expert systems in product formulation has allowed expert formulators to devote more time to innovation (Bateman, 1996; Ramani et al., 1992; Wood, 1991). In topical formulation it has been reported that the use of an expert system has released approximately 30 days of formulating time per year per formulation (Wood, 1991).

- Improved communication

Several users have reported that expert systems promote communication and discussion amongst not only experts but also managers, enabling them to identify critical areas requiring research and/or rationalisation (Bateman, 1996; Ramani et al., 1992; Wood, 1991).

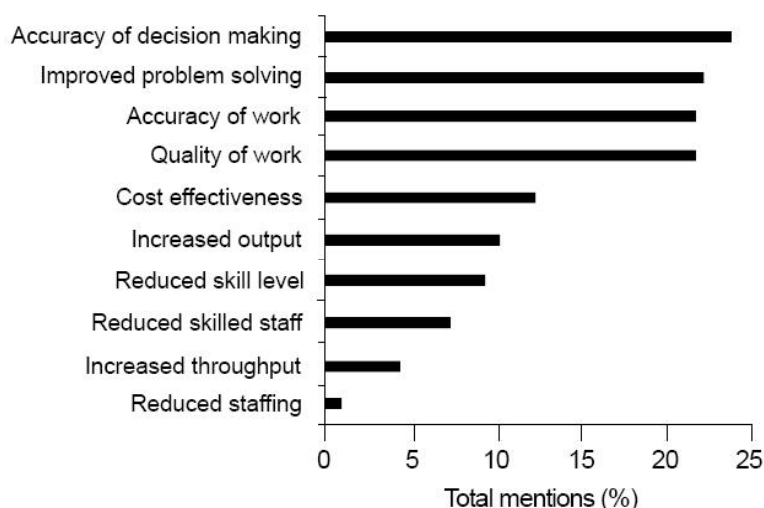


Figure 3.33: A survey of key benefits for expert systems as reported by Dewar^[19]

3.3. Main theories and models considered to develop a general (or non biased) expert system

3.3.1. Percolation theory

A. Main concepts of percolation theory

Historical background

Percolation theory is general mathematical theory of connectivity and transport in geometrically complex systems (King et al.). It is used to describe transitions in a system happening at a critical concentration ratio of the components where one or more component is spanning the whole system.

The concept was first introduced by Flory and Stockmayer (Flory, 1941; Stockmayer, 1943) to describe how the polymerisation process may lead to form a network if chemical bonds through a whole system (gelation). The terminology of percolation theory is usually associated with a publication of Broadbent and Hammersley (Broadbent et al., 1957) which propose a stochastic way of modeling the flow of a fluid or gas through a porous medium. Since the 1970s, application of percolation theory led to a large amount of publications in such diverse fields as hydrology, biology, medicine as well as materials science. The first applications to pharmaceutical technology started in the late eighties by Leuenberger (Leuenberger et al., 1987a).

Probability of occupation and occupied fraction in a system

Only the essential concepts of the percolation theory which were applied in this work are explained here. For a deeper understanding and for more mathematical details it is recommended to read “Introduction to percolation theory” (Stauffer et al., 1994) “Percolation theory” (Essam, 1980), (Gould et al., 2006) and (Bunde et al., 2005).

To introduce the basic concepts of percolation it is convenient to study the following simple example. One considers a discrete system constituted by a square lattice composed of a number N of individual square sites. Each site of the lattice can be either empty or occupied by a dot (see examples Figure 3.34).

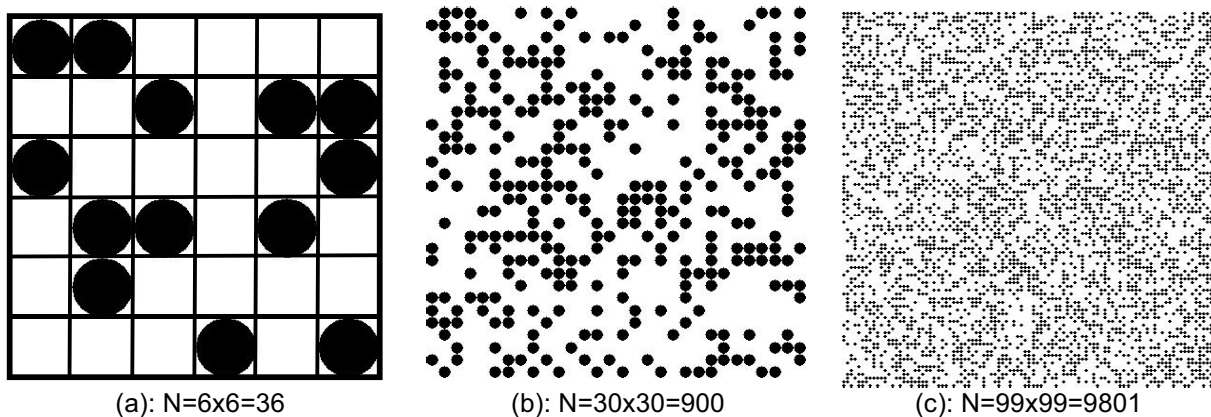


Figure 3.34: Square lattices of different sizes (with N number of sites) filled at random with dots. The square grid is drawn only for (a).^[20]

Let p be the probability for a site to be occupied (respectively $1-p$ to be empty). Then in a very large system (large N), pN will give the number of occupied sites in the system (Stauffer et al., 1994). In this case only the probability p represents with precision the occupied fraction of the system. Indeed, filling the system with dots can be considered as individual experiences: each site of the square lattice is considered one by one and a dot is placed inside with a

probability p . As the theoretical value of a probability is relevant only for a large number of repetitions of the same experience, larger will be the system, more precisely p will represent the occupied fraction or concentration of the system. Table 3.14 resumes several experiences of filling square lattices of different size with a probability p and shows an evident influence of the lattice size on the precision with which p represents the occupied fraction of the system.

Table 3.14: Influence of lattice size on the relevance for p , the probability for a single site to be occupied, to represent the real fraction of occupied sites in the total lattice.

Number of sites in the system (N)	Experiences	Number of occupied sites	Calculated fraction of occupied sites
16 (4x4)	1	4	0.25
	2	7	0.44
	3	3	0.19
9801(99x99)	1	3019	0.31
	2	2949	0.30
	3	2998	0.31

Two lattices of different sizes ($N=16$ and 9801) were computer-generated (Gonsalves R.J.). For each lattice, empty sites are considered one by one and changed into occupied state with a probability $p=0.3$. The fraction of occupied sites over total sites of the lattice was calculated. For each lattice size the experience where repeated 3 times. It is obvious that only for the large lattices of ($N=9801$), calculated fraction of occupied sites is near p .

Critical fraction or percolation threshold

In a square lattice partially filled with dots, one can observe groups of neighbouring occupied sites (see example shown in Figure 3.35). Such groups are named *clusters* in percolation theory.

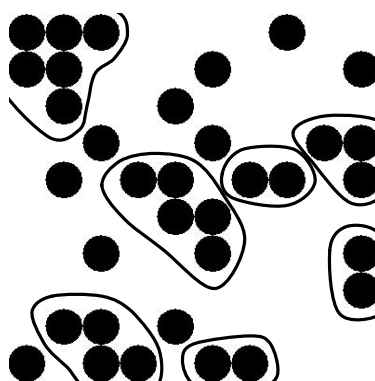


Figure 3.35: Square lattice ($N=100$, $p=0.4$) with encircled groups of neighbouring occupied squares (clusters).^[20]

Figure 3.36 shows a 99×99 lattice with different occupied fraction p increasing from 0.1 to 0.7 (or from 10% to 70%). From $p=0.1$ to $p=0.59$ (Figure 3.36a-d), only isolated cluster can be

observed in the lattice. At $p=0.6$ (Figure 3.36e), the system percolates as a spanning cluster extends from top to bottom and from left to right of the system (coloured in grey).

When p increases again the spanning cluster *strength* increases in width and height as well (Figure 3.36f-i). It is important to notice that the spanning cluster appears suddenly after an increase of p of only of 0.01 (Figure 3.36d-e). It let think that the critical value of p for which one the system percolates is probably in the range $[0.59-0.6]$.

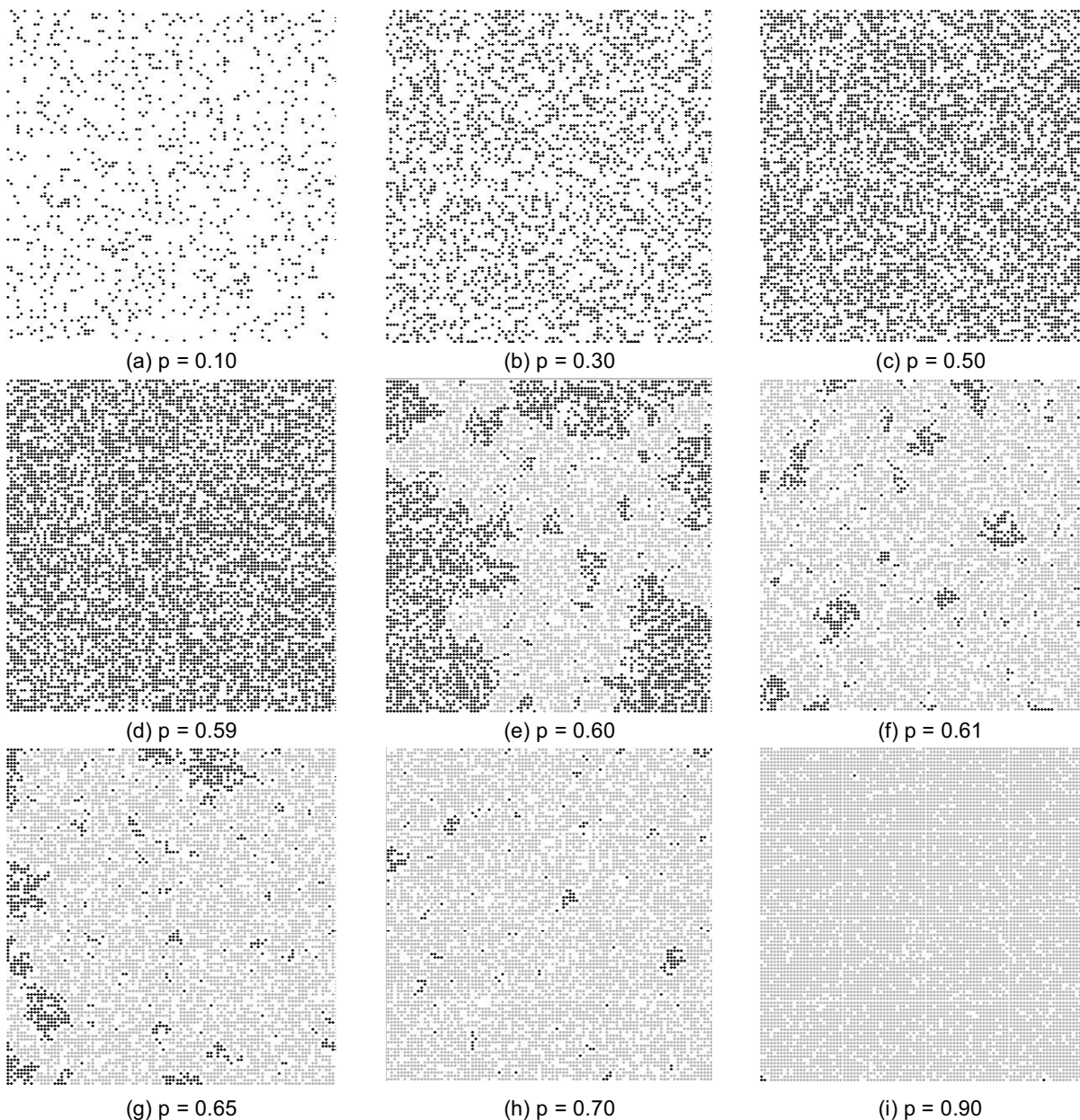


Figure 3.36: Different aspect of a 99x99 square lattice with increasing values of p . For $p=0.10$ to 0.59 the system is composed of isolated clusters of neighbour occupied sites (in black). At $p=0.60$ a spanning cluster (in light grey) appears in the system. Remaining isolated clusters are progressively integrated to the spanning cluster when p increases after 0.60 .^[20]

The critical fraction or probability for which a spanning cluster appears in a system is named *percolation threshold* p_c . The ideal value of the probability p_c is the exact one for an ideal system or *infinite system*. In such a system this spanning cluster is named *infinite cluster*.

The larger a system of size L is, the higher is the probability π that it will percolate at the exact value of p_c . Figure 3.37 shows schematically the variation of the probability π for finite ($L < \infty$) and for infinite ($L = \infty$) systems. One sees that an infinite system will percolate at the exact value of p_c , whereas in a finite system the percolation has a certain probability to happen in a range near p_c . By increasing the size of the system the difference in shape of π function for finite and infinite system reduces.

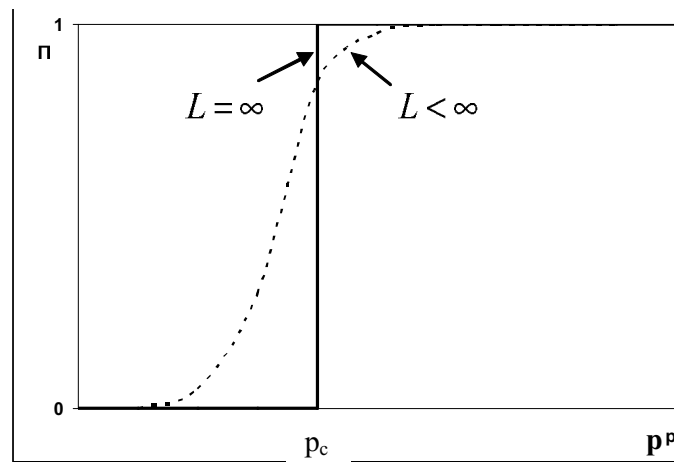


Figure 3.37: Variation of the probability π that a cluster is spanning the whole system, for finite (dashed line) and infinite (solid line) systems. ^[21]

Lattices and percolation types

The previous example of percolation was in a 2 dimensional square lattice. However, the concepts of percolation theory can be applied in other types of lattices of 2, 3 or higher dimensions. The choice of the lattice type and dimension depends on geometry of the real system to model. Figure 3.38 shows examples of 2D and 3D lattices commonly used in percolation theory.

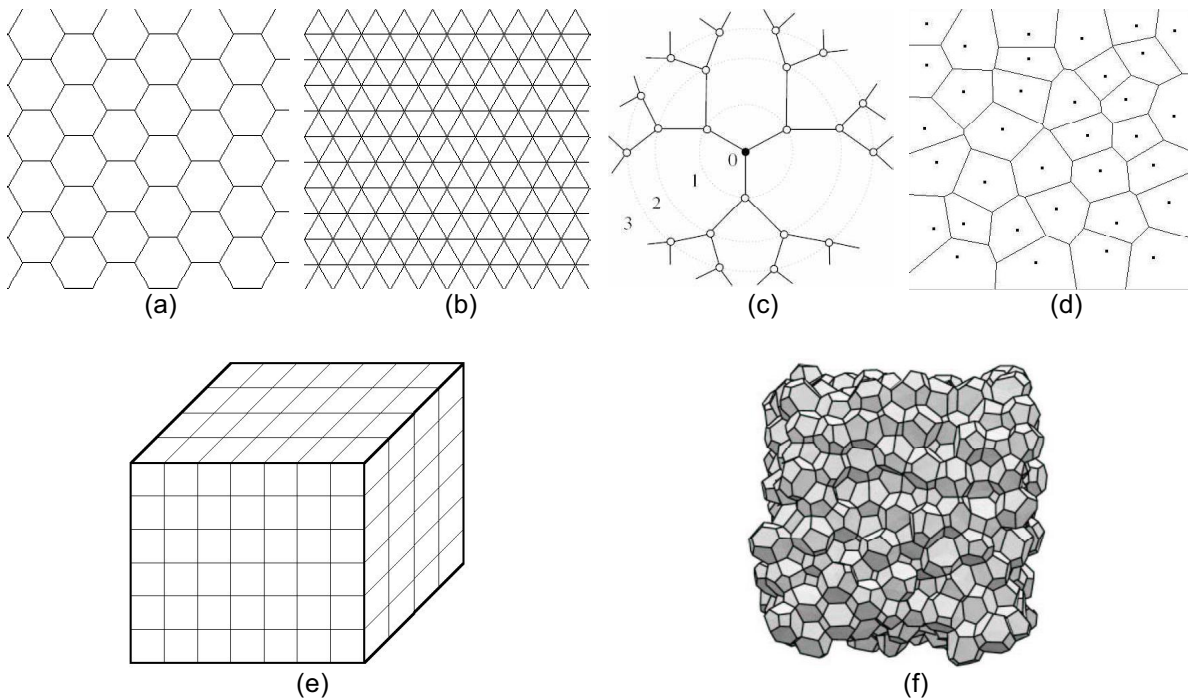


Figure 3.38: Examples of 2D (a-d) and 3D (e,f) lattices. (a) Honeycomb ^[22], (b) Triangular ^[22], (c) Bethe (coordination number $z=3$) ^[23], (d) Voronoi ^[24], (e) Cubic ^[25], (f) 3D Voronoi ^[26].

Furthermore in the example studied before, the system was percolating through occupied sites of the system. However other types of percolation exist. The four main types are site percolation, bond percolation, site-bond percolation (see previous examples) and continuous percolation.

Site percolation considers the occupied sites or the lattice vertices as relevant entities (example in Figure 3.39a), whereas bond percolation considers the connections between sites or the lattice edges as the relevant entities (example shown in Figure 3.39b). Site-bond percolation is an intermediary percolation to the two previous ones and considers the connections between occupied sites only (example in Figure 3.39c). In continuum percolation one considers elements placed randomly in a non-discrete lattice in which they can overlap each other (see example with discs in Figure 3.39d). The system percolates through the filled fraction of the lattice.

The value of the percolation threshold p_c depends on the percolation type, on the lattice type and on the dimension of it. In a one-dimensional system (line of size L divided in N sites) the exact solution is $p_c=1$ for bond or site percolation as all sites or bonds need to be occupied to form a continuous cluster through the system. Mathematical methods to calculate thresholds exactly are restricted so far to two-dimensional systems.

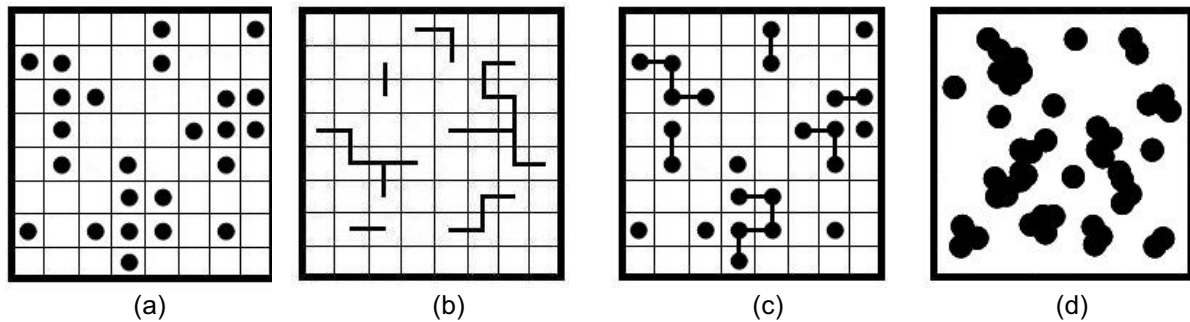


Figure 3.39: Different types of percolation in 2D systems: (a) site percolation, (b) bond percolation, (c) site-bond percolation and (d) continuum percolation.

For three- or higher dimensional systems, percolation thresholds generally cannot be derived mathematically but have to be estimated experimentally by computer simulation.

Some exceptions exist, for example Bethe lattice (Figure 3.38c), for which the exact solution can be calculated mathematically and depends only on the coordination number z . Table 3.15 gives the known site and bond percolation thresholds for most common 2D and 3D lattices. Except percolation threshold other quantities are characterising percolation (see next paragraph).

Table 3.15: Site and bond percolation thresholds for different lattices (Leuenerger, 1999; Stauffer et al., 1994).

Dimension	Lattice	Site	Bond	Coordination number z
2D	Honeycomb	0.6962	0.65271	3
	Square	0.592746	0.50000	4
	Triangular	0.500000	0.34729	6
	Diamond	0.43	0.388	4
3D	Simple cubic	0.3116	0.2488	6
	Body Centred Cubic (BCC)	0.246	0.1803	8
	Face Centred Cubic (FCC)	0.198	0.119	12
> 3D	Bethe	$1/(z-1)$	$1/(z-1)$	z
	d=4 hypercubic	0.197	0.1601	8
	d=5 hypercubic	0.141	0.1182	10
	d=6 hypercubic	0.107	0.0942	12
	d=7 hypercubic	0.089	0.0787	14

Quantities characterising percolation

As it was explained previously, the percolation threshold is a quantity for a system depending on the lattice type, the dimension of the system and on the type of percolation. Other quantities characterise percolation and some of them are presented here.

In a percolating system not all occupied sites are in the spanning cluster. Let $P(p)$ be the fraction of occupied sites belonging to the percolating cluster:

$$P(p) = \frac{\text{number of sites in the spanning cluster}}{\text{total number of sites}} \quad \text{Equation 35}$$

In a very large system it is equivalent to say that $P(p)$ is the probability that an occupied site is in this spanning cluster at p . $P(p)$ gives then an indication of the *strength* of the infinite cluster.

Another quantity is the mean cluster size distribution $n_s(p)$ defined by:

$$n_s(p) = \frac{\text{average number of clusters of size } s}{\text{total number of lattice sites } N} \quad \text{Equation 36}$$

For $p \geq p_c$, the spanning cluster is excluded from n_s . For historical reasons, the size of a cluster refers to the number of sites in the cluster rather than to its spatial extent.

Because $N \sum_s s n_s$ is the total number of occupied sites and $N s n_s$ is the number of occupied sites in clusters of size s , the quantity:

$$w_s = \frac{s n_s}{\sum_s s n_s} \quad \text{Equation 37}$$

is the probability that an occupied site chosen at random is part of an s -site cluster. Hence, the mean cluster size S is given by:

$$S = \sum_s s w_s = \frac{\sum_s s^2 n_s}{\sum_s s n_s} \quad \text{Equation 38}$$

This sum in Equation 38 is over the finite clusters only.

It is convenient to associate a characteristic linear dimension or connectedness length or correlation length $\xi(p)$ with the cluster. One way to do is to define the radius of gyration R_s of a single cluster of s sites as

$$R_s^2 = \frac{1}{s} \sum_{i=1}^s (r_i - \bar{r})^2 \quad \text{Equation 39}$$

where

$$\bar{r} = \frac{1}{s} \sum_{i=1}^s r_i \quad \text{Equation 40}$$

and r_i is the position of the i th site in the same cluster. The quantity \bar{r} is the familiar definition of the centre of mass of the cluster. From Equation 39, we see that R_s^2 is the root mean

square radius of the cluster measured from its centre of mass. The connectedness length ξ can be defined as an average over the radii of gyration of all the finite clusters. If we consider a site on a cluster of s sites, the site is connected to $s-1$ other sites and the average square distance to these sites is R_s^2 . The probability that a site belongs to a cluster of site s is $w_s = sn_s$. According to this, one definition of ξ is:

$$\xi^2 = \frac{\sum_s (s-1)w_s R_s^2}{\sum_s (s-1)w_s} = \frac{\sum_s s^2 n_s R_s^2}{\sum_s s^2 n_s} \quad \text{Equation 41}$$

Power scaling laws in percolation theory

It was seen before that percolation in a system is a sudden event and is characterised by a change in the geometry of the system (percolating cluster). Except percolation threshold, other quantities or properties of the system exhibit a sharp transition near p_c and can be characterised by power laws in this area.

Since there is no spanning cluster for an occupancy probability below the percolation threshold then $P(p)$ must be zero for $p < p_c$. For $p \geq p_c$ there is an infinite cluster and it can be shown (Stauffer et al., 1994) that close to the percolation threshold $P(p)$ follow the power law below (see profile Figure 3.40):

$$P(p) \propto (p - p_c)^\beta \quad \text{with } p \geq p_c \quad \text{Equation 42}$$

where β is a critical exponent. β , as the other exponent described in the next power laws of percolation theory, is entirely independent of the kind of lattice being studied or whether it is bond or site percolation. It only depends on the dimensionality of space (i.e. 2D, 3D and so on). This is known as universality and is an important aspect of percolation theory. However it has to be remembered that the percolation threshold is not universal (see above). In two dimensions it is often possible to determine exact values for the exponents, whereas in three dimensions there are only approximate results or numerical estimates.

In the same way $\xi(p)$ can also be described with a power law in this manner:

$$\xi(p) \propto (p - p_c)^{-\nu} \quad \text{Equation 43}$$

whith ν is the critical exponent.

As it is shown in Figure 3.41, $\xi(p)$ is an increasing function of p for $p < p_c$ and decreasing function of p when $p > p_c$. Moreover, at $\xi(p = p_c)$ is approximately equal to the linear dimension L of the system and hence diverges as $L \rightarrow \infty$. Indeed, as p approaches

p_c , the probability that two occupied sites are in the same cluster increases. In the limit of $L \rightarrow \infty$, $\xi(p)$ grows rapidly in the critical region, $|p - p_c| \ll 1$.

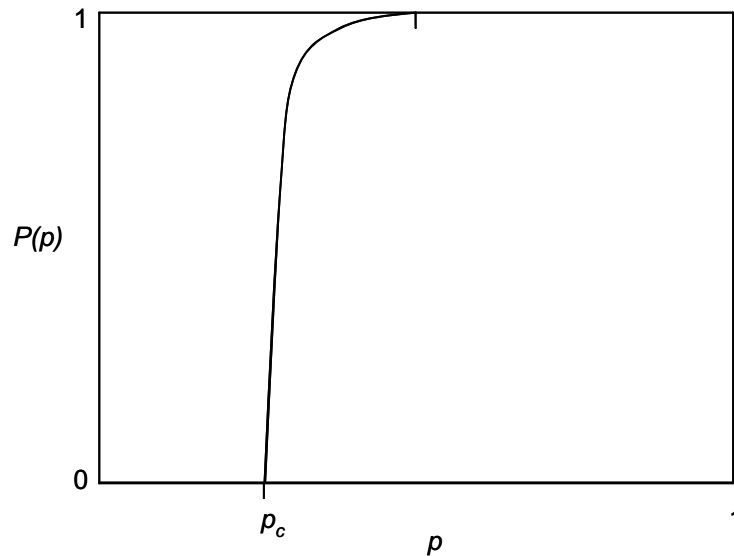


Figure 3.40: Qualitative p -dependence of the probability $P(p)$ that an occupied site is in the spanning cluster. ^[27]

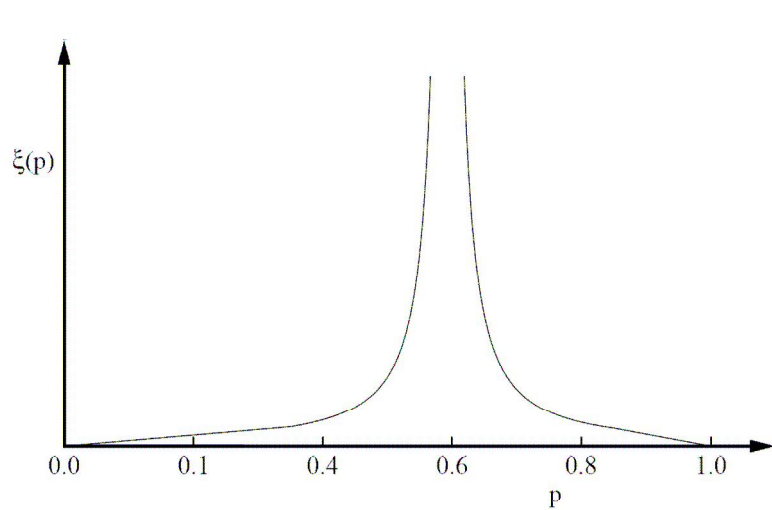


Figure 3.41: Qualitative p -dependence of the connectedness length $\xi(p)$ ($p_c = 0.6$). The divergent behaviour of $\xi(p)$ in the critical region is characterised by the exponent ν . ^[28]

The mean number of sites in the infinite clusters $S(p)$ also diverges in the critical region. Its behaviour is written as:

$$S(p) \propto (p - p_c)^{-\gamma} \quad \text{Equation 44}$$

where γ is the critical exponent.

The most common critical exponents for percolation are summarised in Table 3.16. It can be seen that the critical exponent only depends of the dimension of the system but neither on lattice type nor on percolation type (universality).

Table 3.16: Several of the critical exponents for the percolation in $d = 2$ and $d = 3$ dimensions. Ratios of integers correspond to known exact results.

Quantity	Functional form	Exponent	d=2	d=3
Order parameter	$P_\infty(p) \sim (p - p_c)^\beta$	β	5/36	0.4
Mean size of finite clusters	$S(p) \sim p - p_c ^{-\gamma}$	γ	43/18	1.8
Correlation length	$\xi(p) \sim p - p_c ^{-\nu}$	ν	4/3	0.9
Cluster numbers	$n_s \sim s^{-\tau} \quad p = p_c$	τ	187/91	2.2

Because it is possible to simulate only finite lattices, a direct fit of measured quantities ξ , P_∞ and $S(p)$ to their assumed critical behaviour for infinite lattice would not yield good estimates for the corresponding exponents ν , β and γ . Indeed, if p is close to p_c , the extent of the largest cluster becomes comparable to L , and the nature of the cluster distribution is affected by the finite size of the system (ξ is comparable to L). A finite system cannot exhibit a true phase transition characterised by divergent physical quantities. ξ and S reach a finite maximum at $p = p_c(L)$. The effect of finite size scaling can be however exploited to determine the critical exponent by the *finite size scaling* analysis (Gould et al., 2006)

Another important point is that a relation or scaling law between the critical exponents exists:

$$2\beta + \gamma = \nu d \quad \text{Equation 45}$$

where d is the spatial dimension of the lattice. This scaling law indicates that the universality class depends on the spatial dimension.

In a real physical system, if transitions in the property of the system happen at a critical concentration ratio of the components, it is assumed that percolation theory can be used to describe and characterise the transition in the system.

Geometry of a system will change abruptly near (real finite system) or at (ideal infinite system) the percolation threshold p_c . Near the percolation threshold the system property X which is related to percolation effect can be thus described with the basic power law of percolation theory:

$$X = S(p - p_c)^q \quad \text{Equation 46}$$

with: X : system property
 S : scaling factor
 p : occupation probability in the system
 p_c : percolation threshold
 q : critical exponent

In order to use properly the percolation equation it is prerequisite to determine unambiguously the values of the percolation threshold p_c , and of the critical exponent q . If both parameters are unknown, it has to be kept in mind that in a statistical analysis of the data (e.g., by non-linear regression analysis) the estimates of p_c and q are interrelated (Leuenberger, 2000).

p_c is directly related to the lattice type, the percolation nature (bond, site, continuum, etc.) and the dimension involved. The value of the critical exponent q depends on the process involved. In some cases, rather precise values are known (see Table 3.16). It has to be kept in mind that the critical exponents do not depend on the type of lattice but on the dimension of the lattice. The critical exponent can also be a function of a fractal dimension (see next section about fractals) involved in a process (Ehrburger et al., 1990).

B. Fractals

Definitions and generalities

As mentioned previously, the critical exponent of the power law of percolation theory depends also on fractal dimension. The basic concepts of fractals are presented here.

Our understanding of the nature has been based on the description of object in Euclidean (or topologic) systems of dimension one, two or three. Each object has a unique value for its characteristics (length, area, or volume). When these objects are viewed at higher magnification they do not reveal any new features (a line is a line independently of the scale at which one it is observed) (Macheras et al., 2005).

In the real world, however, objects are irregular and continue to exhibit detailed structure over a large range of scale (clouds, mountains, coastlines, lungs, etc.). Mandelbrot was the first to model this irregularity mathematically (Mandelbrot, 1977). He named *fractal* structures in space that cannot be characterised by a single spatial scale. Fractal geometry allows scientists to formulate alternative hypotheses for experimental observations, which lead to more realistic explanations compared to the traditional approaches (Macheras et al., 2005).

To understand the importance of fractal geometry on the characterisation of real objects, one can imagine measuring a coastline. If one takes a ruler of a certain size and uses it to measure the same coastline but on maps with different scales, the measured length will increase as the scale of the map decreases. Indeed lower will be the scale of the map (higher will be the magnification) more details of the coastline are revealed. The same phenomena will be observed when measuring a coastline with one single map but using decreasing ruler sizes (see example in Figure 3.42). General property of fractal objects (like a coastline) is that their characteristics (length in the previous example) are said to “scale” with the measurement resolution (previously the ruler size). This would not be the case in a Euclidian system. Indeed, the length of a mathematical line (like the edge of a square) stays the same independent of the size of the ruler used to measure it.



Figure 3.42: Example of fractal problem in nature: how long is the coast of Britain? Three different measurement of the same map with three different ruler sizes are shown. ^[29]

According to Mandelbrot, a fractal can be defined as a “rough or fragmented geometric shape that can be subdivided in parts, each of which is (at least approximately) a reduced-size copy of the whole” (Mandelbrot, 1982). In other words it means that parts of a fractal object are smaller exact copies of the whole object (Macheras et al., 2005). The most interesting property of fractals is this geometric self-similarity. The consequence is that they cannot be represented by classical geometry. Figure 3.43 shows three examples of fractal structures. The geometric self-similarity of fractal object is ensured by replacement rules. For example, the Koch curve

(Figure 3.43a) is constructed at each step by dividing each line into three segments, removing the middle segment and replacing it by two segments of the same length. To construct a Sierpinski triangle one removes an equilateral triangle with area equal to one-quarter of a remaining triangle (Figure 3.43b). For the Menger sponge, at each step one-third of the length of the side of each cube is removed taking care to apply this rule in 3 dimensions and avoiding the removal of corner cubes (Figure 3.43c).

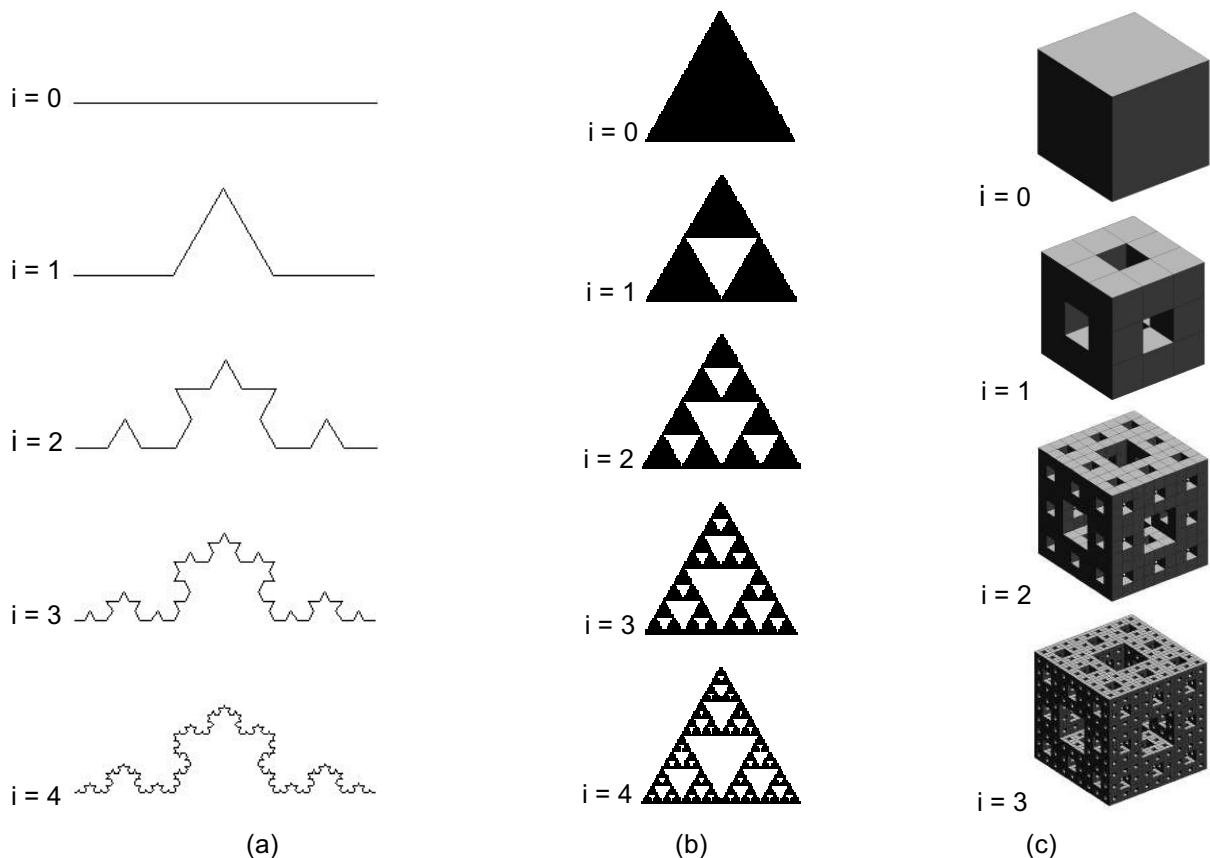


Figure 3.43: Generation of (a) Koch curve (first four iterations) ^[30], (b) Sierpinski triangle (first four iterations) ^[31] and (c) Menger sponge (first three iterations) ^[32].

The replacement rules enable to see the detail structure of fractal object after a resolution change. Figure 3.44 shows how the level of detail for the generation $i=4$ of the Koch curve becomes similar to the one of generation $i=3$ when the scale length is reduced of a factor 3.

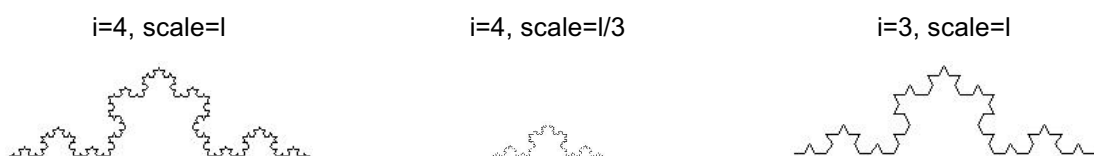


Figure 3.44: By reducing the generations $i=4$ of the Koch curve by a factor 3, only the details of generation $i=3$ are visible. ^[30]

However, the fractal objects in nature are not generated by exact mathematical rules or scaling law. They are said to be statistically similar since portions of natural fractal objects resemble the whole object instead of being exact copies of the whole. They are designed as *random fractal* to underline their statistical character. Clusters of occupied sites or bonds in percolation theory exhibit such a random fractal character.

The scaling relationship between the characteristic $\theta(\omega)$ of a fractal object measurement resolution or scale ω has the form of the following scaling power law:

$$\theta(\omega) = \beta \omega^\alpha \quad \text{Equation 47}$$

where β and α are constants for the given fractal object studied. α can be an integer or a fraction.

Equation 47 can be written in this manner:

$$\ln \theta(\omega) = \ln \beta + \alpha \ln \omega \quad \text{Equation 48}$$

This equation reveals linearity between the measured characteristic $\theta(\omega)$ and the scale ω . Such power laws are one of the most abundant sources of self-similarity characterising heterogeneous media (Macheras et al., 2005).

Because of the previously mentioned properties, fractal objects have no integer dimensions like the usual geometric forms. Several dimensions for the same object can be defined. The topologic dimension d_t is the "normal" idea of the dimension of an object. The embedding dimension d_e is the dimension of the Euclidean space that contains the object under study. d_t and d_e are the same for Euclidean objects but for fractal objects they have the following relationship between the different dimensions definitions: $d_t \leq d_f \leq d_e$. A coastline, for example, will have a d_f lying between a $d_t = 1$ and $d_e = 2$.

Thus it is possible to calculate the fractal dimension d_f using the concept of self-similarity if the replacement rule of the fractal object is known. Let m be the number of exact copies of the entire geometric fractal that are observed when the resolution of scale is changed by a factor r . The value of d_f is calculated as follows:

$$d_f = \frac{\ln m}{\ln r} \quad \text{Equation 49}$$

after algorithm transformation:

$$m = r^{d_f} \quad \text{Equation 50}$$

In a Koch curve, for instance, each segment is divided into three new segments ($r=3$) and the new segment in the centre is replaced by two new segments which leads to 4 new segments ($m=4$): $d_f = \frac{\ln 4}{\ln 3} \approx 1.2619$. If we look at the generation $i=2$ of Koch curve (Figure 3.43a) we see 4 times the generation $i=1$ at smaller scale reduced of $1/3$. With a fractal dimension of 1.2619, the Koch curve is neither a line ($d=1$) nor an area ($d=2$). With a fractal dimension $d_f = \frac{\ln 3}{\ln 2} = 1.5815$ Sierpinski triangle (Figure 3.43b) lies between 1 and 2 dimensions. Menger sponge (Figure 3.43c) has $d_f = \frac{\ln 20}{\ln 3} = 2.727$ and lies between 2 and 3 dimensions.

The fractal dimension increases as the relief of the fractal increases. Figure 3.45 shows the evolution of the fractal dimension of the Koch curve with increasing the indentation angle α .

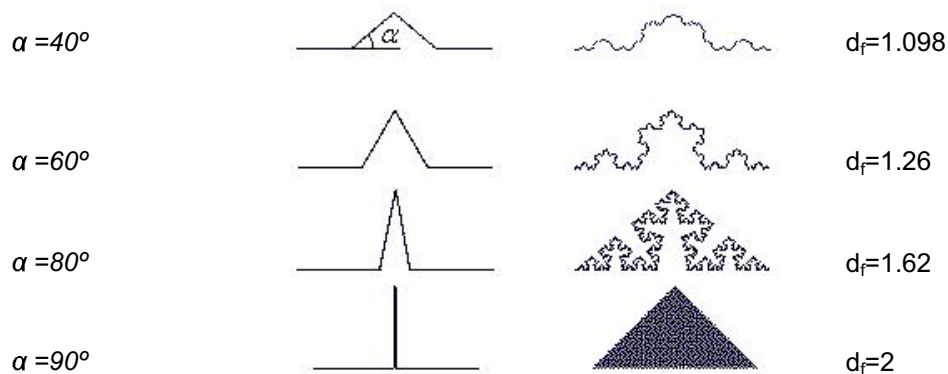


Figure 3.45: Koch curve profiles for different indentation angle α . The fractal dimension d_f is given for each profile ^[33].

For objects with irregular shape (real objects, see example in Figure 3.46) self-similarity principles cannot be applied in this case. The investigator has to estimate d_f from the experimental data. One of the approaches is to use the power-law scaling method and derive the following relationship between the measured characteristic θ and the function of the dimension $g(d_f)$:

$$\theta \propto \omega^{g(d_f)} \quad \text{Equation 51}$$

where ω represents the various resolutions used.

Then, the exponents of Equation 47 and Equation 51 are the same:

$$g(d_f) = \alpha \quad \text{Equation 52}$$

The form of $g(d_f)$ depends of the measured characteristic θ :

- When the characteristic is the mass of the fractal object, $d_f = \alpha$.
- When the characteristic is the average density of the fractal object, $d_f = d_e + \alpha$, where d_e is the embedding dimension
- For measurements regarding lengths, area, or volumes of objects: $d_f = d_e - \alpha$. d_f can be estimated form many other characteristics of fractal objects by finding the appropriate relationship between d_f and α .

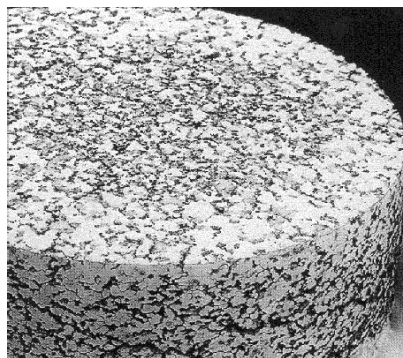


Figure 3.46: Apparent fractal structure in a compact.

The fractal structure of percolation clusters near percolation threshold

Near p_c , on length scales smaller than ξ both infinite and finite clusters are self-similar, i.e. if we cut a small part out of a large cluster, magnify it to the original cluster size and compare it with the original, we cannot tell the difference: both “look” the same (Bunde et al., 2005). This feature is illustrated in Figure 3.47, where a larger cluster at p_c is shown in four different magnifications.

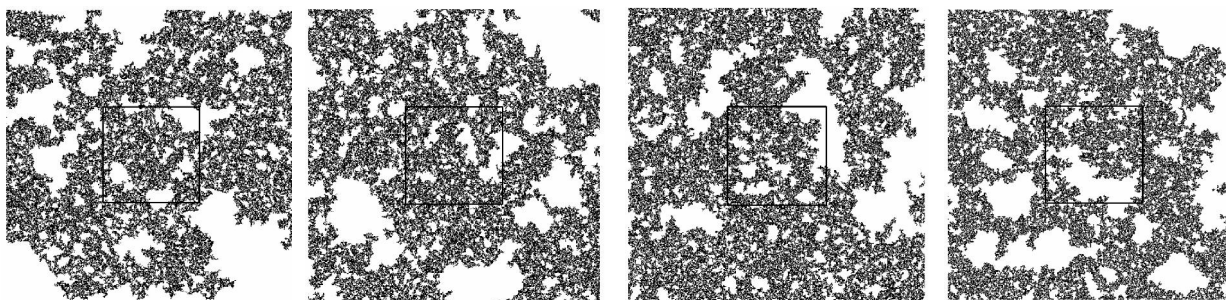


Figure 3.47: Four successive magnifications of the incipient infinite cluster that forms at the percolation threshold on the square lattice. Three of the panels are magnifications of the centre squares marked by black lines. In the figure that you see, however, the labels of the four panels have been removed and the panels have been scrambled. ^[34]

The fractal dimension d_f of a cluster is smaller than the dimension d_e of the embedding lattice (see previously). The mean mass $M(r)$ of the cluster within a radius r increases with r as:

$$M(r) \propto r^{d_f}, \quad r \ll \xi \quad \text{Equation 53}$$

Above p_c on length scales larger than ξ the infinite cluster can be regarded as an homogeneous system which is composed of many cells of size ξ . Mathematically, this can be summarised as:

$$M(r) \propto \begin{cases} r^{d_f}, & \text{if } r \ll \xi \\ r^d, & \text{if } r \gg \xi \end{cases} \quad \text{Equation 54}$$

Figure 3.48 shows part of the infinite cluster above p_c ($p = 1.003p_c$) on different length scales. At large length scale ($r \gg \xi$, first picture in Figure 3.48) the cluster appears homogeneous, while on lower length scales ($r \ll \xi$, last three pictures in Figure 3.48) the cluster is self-similar.

The fractal dimension d_f can be related to the critical exponent β and ν in the following way: above p_c , the mass M_∞ of the infinite cluster in a large lattice of size L^d is proportional to $L^d P_\infty$. On the other hand, this mass is also proportional to the number of unit cells of size ξ , $(L/\xi)^d$, multiplied by the mass of each cell which is proportional to ξ^{d_f} . This yields (Equation 42, Equation 43):

$$M_\infty \propto L^d P_\infty \propto L^d (p - p_c)^\beta \propto (L/\xi)^d \xi^{d_f} \propto L^d (p - p_c)^{\nu d - \nu d_f} \quad \text{Equation 55}$$

and hence, comparing the exponents of $(p - p_c)$,

$$d_f = d - \frac{\beta}{\nu} \quad \text{Equation 56}$$

Since β and ν are universal, d_f is also universal.

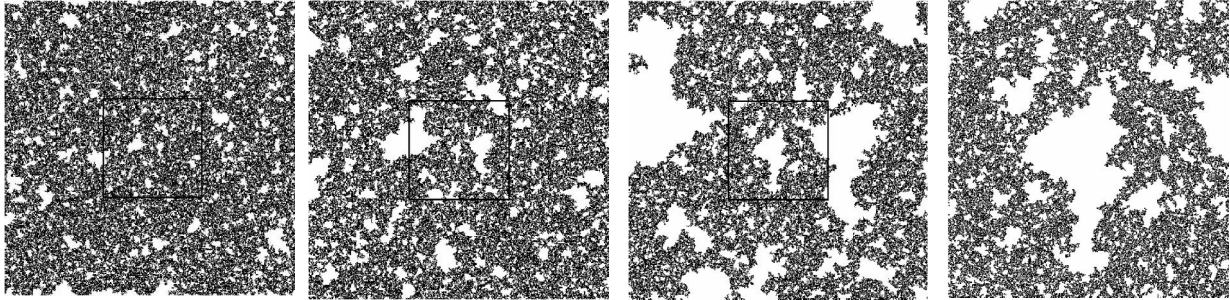


Figure 3.48: The same system as Figure 3.47 except that now it is slightly above the percolation threshold (0.3%) and the panels is not scrambled. The first picture shows the original and the other pictures are magnifications of the centre squares marked by black lines. The correlation length ξ is approximately equal to the linear size of the third (lower left) picture. When comparing the two lower pictures, the self-similarity at small length scales below ξ is easy to recognize. ^[34]

C. The renormalisation group

One of the main interests of renormalisation theory is the renormalisation group method to examine physical quantities near the critical point on different scales. It is probably the most important new method developed in theoretical physics during the past twenty-five years. Kenneth Wilson was honoured in 1981 with the Nobel Prize in physics for his contribution to the development of the renormalisation group method. This method can be used in particular to calculate the percolation threshold p_c and the critical exponent ν (Gould et al., 2006).

To introduce renormalisation, let's consider a photograph of a percolation configuration generated at $p = p_0 < p_c$. When the photograph is seen for far away, it is not possible to distinguish anymore neither occupied sites adjacent to each other nor single site clusters. Furthermore, branches emanating from larger clusters and narrow bridges connecting large "blobs" are lost in the distance view of the photograph. Hence, for $p_0 < p_c$, the distant photograph looks like a percolation configuration generated at a value of $p = p_1$ less than p_0 . In addition, the connectedness length $\xi(p_1)$ of the remaining clusters is smaller than $\xi(p_0)$. If the photograph is observed from even further away, the new cluster look even smaller with a value $p = p_2$ less than p_1 . Eventually it will not be possible to distinguish any cluster and the photograph will appear as if it were at $p = 0$.

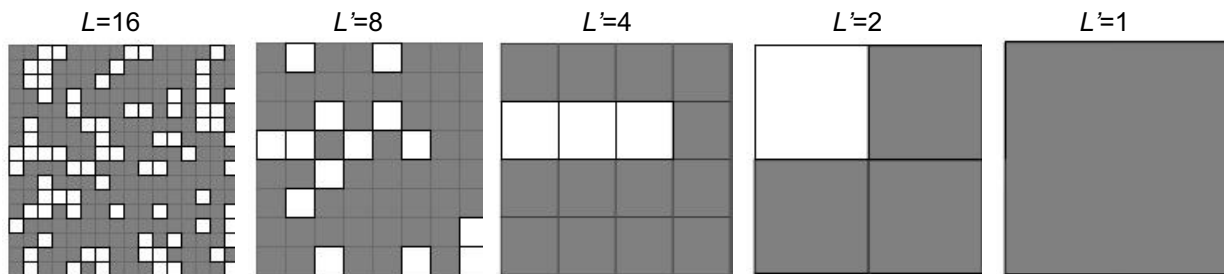
In the same way, if a photograph of a percolation configuration at $p_0 > p_c$ is observed far away, the region of unoccupied sites will become less discernible. The photograph will look like

a configuration generated at $p = p_1$ greater than p_0 with $\xi(p_1) < \xi(p_0)$. Even more far away, the photograph will eventually appear to be at $p = 1$.

At $p = p_c$, all length scales are present and it does not matter which length scale is used to observe the system. Hence, the photograph will appear the same (although smaller overall) regardless the distance at which the system is seen.

In order to better understand the mechanism of renormalisation, the following example is described. A square lattice is renormalised by merging four sites of the lattice into one supersite (see Figure 3.49) for two cases; with p below and p above p_c . In this example, it is considered that a group of four sites is transformed into an occupied site if there is a vertical spanning cluster. If this is not the case, the four sites system is transformed into an unoccupied site. It can be seen that the renormalisation conserves the percolating characteristics of the system. Indeed if $p > p_c$ renormalisation leads to one single occupied site (percolation through the single site). If $p < p_c$, the final site obtained is not occupied (no percolation through the single site).

$p=0.7$



$p=0.5$

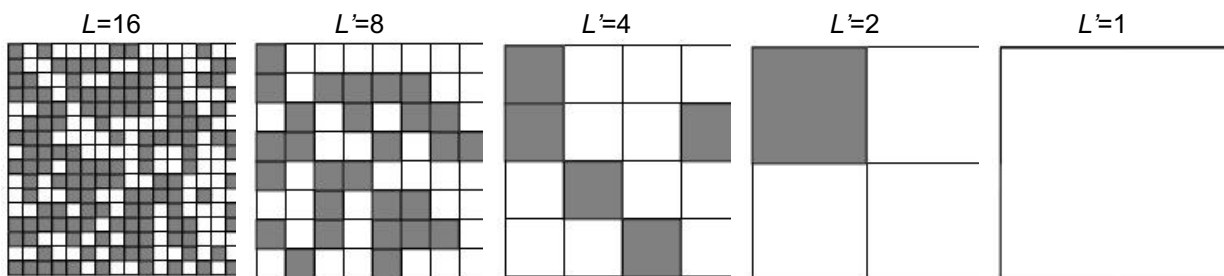


Figure 3.49: Percolation configurations generated at $p=0.7$ and $p=0.5$. The original configurations were renormalised three times by transforming cells of four sites into one new supersite. ^[35]

In the example depicted in Figure 3.49, the replacement of cells by sites gives the same symmetry. However, renormalisation has to be considered as a change of scale. After

renormalisation, all distances are smaller by a factor b , where b is the linear dimension of the cell. Hence, the connectedness length for the renormalised lattice is rescaled by a factor b .

If the sites are occupied with a probability p , then the cells obtained after one renormalisation step are occupied with a probability p' , where p' is given by a renormalisation transformation or a recursion relation of the form:

$$p' = R(p) \quad \text{Equation 57}$$

The quantity $R(p)$ is the total probability that the sites form a spanning path:

$$p' = R(p) = p^4 + 4p^3(1-p) + 2p^2(1-p)^2 \quad \text{Equation 58}$$

The case presented in Figure 3.49 $R(p)$ calculation (see Equation 58) is, for instance, performed by considering the seven vertically spanning site configurations for a $b=2$ cell (see Figure 3.50).

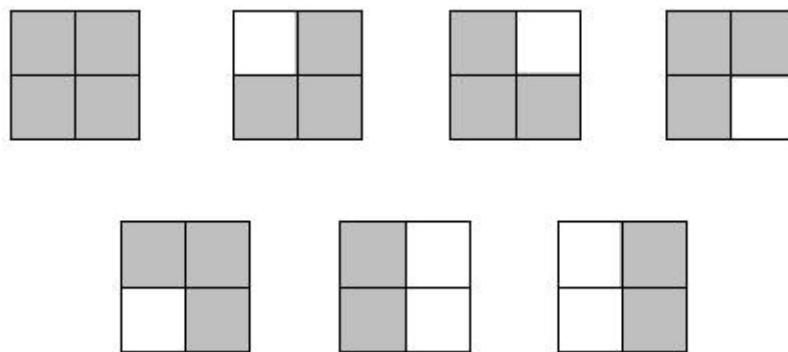


Figure 3.50: The seven (vertically) spanning configurations on a $b = 2$ cell. ^[35]

D. Applications in pharmaceutical technology

Percolation theory was used successfully to describe various tablet properties. The application of the percolation theory in powder technology was reviewed in an excellent paper by Leuenberger (Leuenberger, 1999).

It is well known that heterogeneous ensembles like pharmaceutical formulations for solid dosage forms represent disordered particulate systems where it is necessary to take into account a geometrical description (Ringard et al., 1988), i.e. a topological modeling. Powder systems, compacted or not, consist of particles and void space. Thus, underlying a lattice, the occupied sites correspond to material whereas the unoccupied sites correspond to void space (pores). Applying the percolation theory in powder technology, the probability p of the occupied sites is usually replaced by the analogous relative density p_r (Lanz, 2006).

In percolation theory, geometrical phase transitions are independent of physical and chemical properties of the components, which facilitate the modeling. The theory is, in fact, the most suitable tool to predict and simulate the geometrical phase transitions in a complex multi-particulate system and allows finding the regions where the system undergoes transitional changes in its properties.

In terms of solid dosage form design, such regions usually are linked to extreme values of drug dissolution rate, tablet disintegration time, tablet water uptake, etc. (Kimura et al., 2007; Leuenberger, 1999; Leuenberger et al., 1987b; Ringard et al., 1988; Stauffer et al., 1994).

In recently published works, the application of percolation theory was expanded to investigations of pharmaceutical compacts' key properties.

Caraballo applied the theory to explain the release profiles from inert matrix compressed tablets (Caraballo et al., 1993), to design controlled release of such systems (Caraballo et al., 1999) and to study the relationship between drug percolation threshold and particle size in matrix tablets (Caraballo et al., 1996; Millan et al., 1998). The effect of percolation on drug dissolution kinetics, and the relation between tablets fractal dimensions and dissolution kinetics of inert non-swelling insoluble matrices were studied by Bonny and Leuenberger using ethylcellulose (Bonny, 1992; Bonny et al., 1993a, 1993b, 1993c). The influence of particle size on the excipient percolation thresholds, the release and the hydration rate in case of HPMC hydrophilic matrix tablets were recently studied by Miranda, Millan, Caraballo and Fuertes (Fuertes et al., 2006; Miranda et al., 2006a, 2006b, 2007). Percolation theory was applied as well to model the diffusion of aqueous medium in porous compacts (Ellis et al., 2006; Hastedt et al., 1990).

The theory was also used to interpret water uptake, disintegration time and intrinsic dissolution rate of tablets (Kimura et al., 2007; Luginbuehl, 1994; Luginbuehl et al., 1994). In the case of disintegration, they found that a critical concentration of disintegrant exists for which one the disintegration time (DT) reaches a minimum. In case of swelling disintegrant, DT decreases with increasing the disintegrant volumetric percentage (% v/v) of the mix until a critical value (percolation threshold). After this critical amount of disintegrant, DT increases again with increasing disintegrant percentage, giving a typical V-shape curve while plotting DT versus disintegrant volumetric percentage. The increase of DT after the critical value of disintegrant amount was interpreted as follows:

- After threshold, the excess of swollen disintegrant starts retarding the penetration of water by blocking pores within the compact (Kimura et al., 2007).
- After the percolation threshold, the continuous cluster of material conducting water (composed of disintegrant particles and pores) starts to extend by forming dead-end arms

(excess of disintegrant). The increased complexity of the network retards the penetration of water within the tablet in comparison to the continuous cluster at the percolation threshold (Krausbauer et al., 2007).

Figure 3.51 summarises in a schema the hypothesis mentioned above explaining the typical profile of DT against $\%(v/v)$ of swelling disintegrant in a tablet.

Percolation theory was also applied to the tensile strength, which was already intensively investigated by Kuentz and Leuenberger (Kuentz et al., 2000; Kuentz et al., 1999b). Based on the percolation theory, they proposed a power law, which proved superior relevance compared to the well-known equation of Ryshkewitch and Duckworth (Ryshkewitch, 1953).

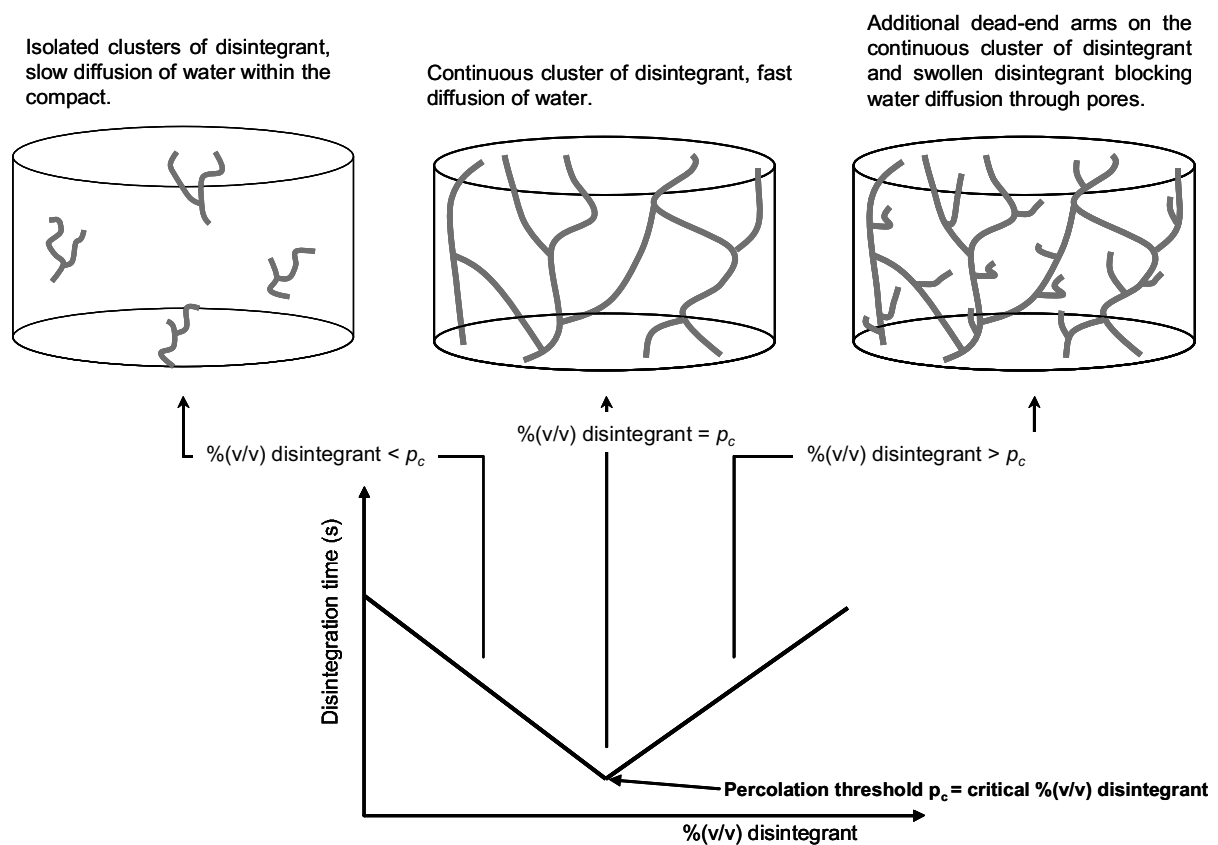


Figure 3.51: Percolation theory and disintegration time of a tablet containing swelling disintegrant.

3.3.2. Cellular automata

A. What are cellular automata?

Definition

A definition of cellular automata is given below: "Cellular automata (often termed CA) are an idealisation of a physical system in which space and time are discrete, and the physical

quantities take only a finite set of values” (Chopard et al., 1998). In other words, a cellular automaton is a discrete model consisting of a regular grid of cells (in any finite number of dimensions). Each cell is in one of a finite number of states (each cell type has a finite number of possible states). Time is also discrete, and the state of a cell at time t is a function of the states of a finite number of cells (called its neighbourhood) at time $t-1$. Every cell type has the same rule for updating, based on the values in this neighbourhood. Each time the rules are applied to the whole grid a new generation is created.

However, the best way to understand easily CA modeling is to go through simple examples, as it is proposed further on.

Historical background

The following chapter gives an overview of the history and the development of CA in order to understand how this modeling technique became useful in applied sciences. For a more detailed historical background it is recommended to refer to the excellent book of Chopard (Chopard et al., 1998).

The concept of CA appeared in the late 1940s. During the following fifty years, CA have been developed and used in many different fields of science (biology, physics, etc.). A vast number of conference proceedings (Doolen, 1990; I.S.I, 1989; Livi et al., 1988; Manneville et al., 1989; Perdang, 1993; Pires et al., 1990), special journal issues (Boon, 1992; Toffoli et al., 1984) and articles were related to these topics.

John von Neumann is certainly the pioneer in CA modeling. He was thinking of imitating the behaviour of a human brain in order to build a machine able to solve very complex problems. He thought that such a machine should also contain self-control and self-repair mechanisms. He actually wanted to get rid of the difference which exists between processors and the data, by considering them on the same footing. He considered the problem from a formal viewpoint and proposed the properties such a system should have to be self-replicating. He tried to find a logical abstraction of the self-reproduction mechanism, without reference to the biological processes involved. Following the suggestions of Ulam (Ulam, 1952), von Neumann used a fully discrete mad up of cells universe to solve his problem. Each cell is characterised by an internal state, which typically consists of a finite number of information bits. Von Neumann suggested that this system of cells evolves, in discrete time steps, like simple automata which only know of a simple recipe to compute their new internal state. The rule determining the evolution of this system is the same for all cells and is a function of the states of the neighbour cells. The same clock drives the evolution of each cell and the updating of the internal state of each cell occurs synchronously. Nowadays what is named cellular automata refers directly to the fully discrete dynamical systems (cellular space) invented by von Neumann. Due to its

complexity, the von Neumann rule (Burks, 1970) has only been partially implemented on a computer (Pesavento, 1995) but he succeeded in finding a discrete structure of cells bearing in themselves the information to generate new identical individuals. By creating a self-replicating CA, von Neumann obtained a “machine” able to create new machines of identical complexity and capabilities. Furthermore, the von Neumann rule has the property of universal computation, which means that the initial configuration of the CA can lead to the solution of any computer algorithm (any computer circuit can be simulated by the rule of the automaton).

Other works followed the one of von Neumann and this line of research is still of interest (Reggia et al., 1993). Codd, Langton and Bly proposed much simpler CA rules capable of self-replicating (Bly, 1989; Codd, 1968; Langton, 1984). By simplification, the property of computational universality was lost, but the idea of a spatially distributed sequence of instructions which can create a new structure containing the same instructions is conserved (a kind of DNA). CA were an early attempt in the direction of artificial life and are still in progress (Langton, 1994; Langton et al., 1992).

A simple ecological model brought the concept of CA to the attention of wide audience. In 1970, the mathematician John Conway proposed the *game of life* (Gardner, 1970). His goal with this two-dimensional CA was to find a simple rule leading to complex behaviours. The *game of life* revealed an unexpectedly rich behaviour. Complex structures emerge out of a primitive “soup” and evolve so as to develop some skills. CA were also used in 1950s for image processing (Preston et al., 1984). Pixels of an image can be treated simultaneously, using simple local operations. At the beginning of the 1980s, Wolfram studied in detail a family of simple one-dimensional CA rules, known as Wolfram rules (Wolfram, 1986, 1994). He noticed that CA are discrete dynamical system that exhibit many of the behaviours encountered in a continuous system but in a much simpler framework.

An important step was accomplished in the 1980s with the work of Hardy, Pomeau and Pazzis. They develop lattice gas model, which appeared to be CA. This model consists of a simple and fully discrete dynamics of particles moving and colliding on a two-dimensional square lattice, in such a way as to conserve momentum and particle number.

B. Fundamental properties of CA

As it was defined previously, a cellular automaton is a discrete model with interactions that are uniform in structure. Cellular automata are characterised by the following fundamental properties:

- They consist of a regular grid of *cells*. The grid can be in any finite number of dimensions.
- Each cell is of a specific type and each cells type is characterised by a state taken from a finite set of states.

- The evolution takes place in discrete time steps: time is discrete, and the state of a cell at time t is a function of the states of a finite number of cells (called its *neighbourhood*) at time $t-1$.
- Each cell evolves according to the same rule which depends only on the state of the cell and of the state of neighbouring cells.
- The neighbourhood type and range of nearby cells is defined in the same way for each cell (examples of neighbourhood ranges for two different neighbourhood types in Figure 3.52), i.e. the neighbourhood relation is local and uniform.
- Every cell has the same rule for updating, based on the values in this neighbourhood. Each time the rules are applied to the whole grid a new *generation* is created, i.e. the system is updated.

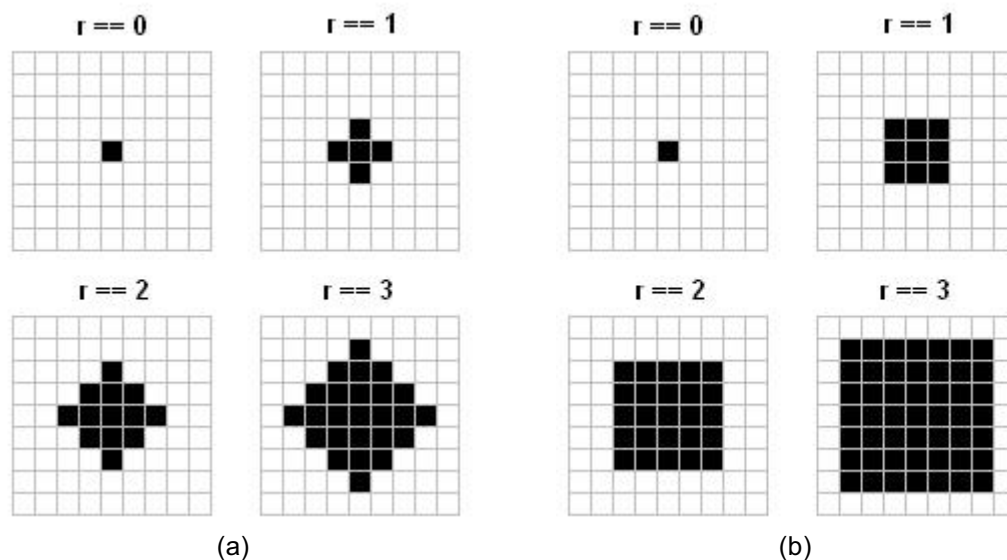


Figure 3.52: Two examples of neighbourhoods for range $r = 0, 1, 2,$ and 3 :

(a) von Neumann neighbourhood: only orthogonal neighbour cells are concerned. ^[36]

(b) Moore neighbourhood: orthogonal and diagonal neighbour cells are concerned. ^[37]

r gives the lattice range where the neighbourhood is defined. The state of the neighbouring cells will determine, according to the rule set, the state of the central cell after update at time $t+1$.

C. Two simple examples

One dimensional example: the rule 30 CA

The simplest nontrivial CA would be one dimensional, with two possible states per cell (black or white), and a cell's neighbours defined to be the adjacent cells on either side of it. A cell and its two neighbours form a neighbourhood of 3 cells, so there are $2^3=8$ possible patterns for a neighbourhood. There are then $2^8=256$ possible rules to update the change the

state of a cell according to its neighbourhood. These 256 CAs are generally referred to using Wolfram notation (Wolfram, 2002), a standard naming convention invented by Wolfram. The name of a CA is the decimal number which, in binary, gives the rule table, with the eight possible neighbourhoods listed in reverse counting order (1='black', 0='white'). For example, Table 3.17 defines the "rule 30" and the "rule 110" (in binary, 30 and 110 are written 11110 and 1101110, respectively).

Table 3.17: Two rules, 30 and 110, used to change the state of a cell (in black) at time $t+1$ according to the state of its two adjacent cells (in grey).

current pattern	111	110	101	100	011	010	001	000
new state for centre cell								
Rule 30:	0	0	0	1	1	1	1	0
Rule 110:	0	1	1	0	1	1	1	0

Figure 3.53a and Figure 3.53b show graphically the rule 30 and the two first updates of the one-dimensional CA at units of time $t=1$ and $t=2$, starting with at $t=0$ with CA having all cells at state 0 (white) except the central cell at state 1 (black). Figure 3.53c shows the 16 updates of the system one below the other (from $t=0$ to $t=15$). In Figure 3.53d the system updates are shown for the 200 first updates. A picture of a seashell is shown beside as comparison between CA and natural patterns. Indeed, some living beings use naturally occurring cellular automata in their functioning. Patterns of some seashells, like the ones in *Conus* genus (see Figure 3.53d), are generated by natural CA. The pigment cells reside in a narrow band along the shell's lip. Each cell secretes pigments according to the activating and inhibiting activity of its neighbour pigment cells, obeying a natural version of a mathematical rule. The cell band leaves the colored pattern on the shell as it grows slowly. For example, the widespread species *Conus textile* bears a pattern resembling the Rule 30 CA described above. Many other examples of similarity between CA and nature behaviour were identified and presented by Wolfram (Wolfram, 2002).

This is a very interesting aspect of CA: from very simple rules and system, it is possible to imitate natural phenomena, which could not, or hardly, be described by mathematical description. The advantage and the potential of CA modeling is so, that by imitating simple rules of nature, it is possible to obtain global natural phenomena of high complexity.

Two-dimensional example: Conway's game of life

The Game of Life is a CA invented by the mathematician John Conway in 1970 and is probably the most often programmed computer game in existence. This game became widely known when it was mentioned in an article published by Scientific American in 1970. It consists

of a collection of cells which, based on a few mathematical rules, can live, die or multiply. Depending on the initial conditions, the cells form various patterns throughout the course of the game (see Figure 3.55).

- Origins of the CA:

Conway was interested by the problem, presented by von Neumann, to find a hypothetical machine that could build copies of itself. Von Neumann found a mathematical model for such a machine with very complicated rules on a rectangular grid. Conway tried to simplify von Neumann's ideas and eventually succeeded. By coupling his previous success with Leech's problem in group theory with his interest in von Neumann's ideas concerning self-replicating machines, Conway devised the Game of Life.

It made its first public appearance in the October 1970 issue of *Scientific American*, in Martin Gardner's "Mathematical Games" column. From a theoretical point of view, Conway's CA is interesting because it has the power of a universal Turing machine: that is, anything that can be computed algorithmically can be computed within Conway's Game of Life.

Ever since its publication, Conway's Game of Life has attracted much interest because of the surprising ways in which the patterns can evolve. Life is an example of emergence and self-organisation. It is interesting for physicists, biologists, economists, mathematicians, philosophers, generative scientists and others to observe the way that complex patterns can emerge from the implementation of very simple rules. The game can also serve as a didactic analogy, used to convey the somewhat counterintuitive notion that "design" and "organisation" can spontaneously emerge in the absence of a designer.

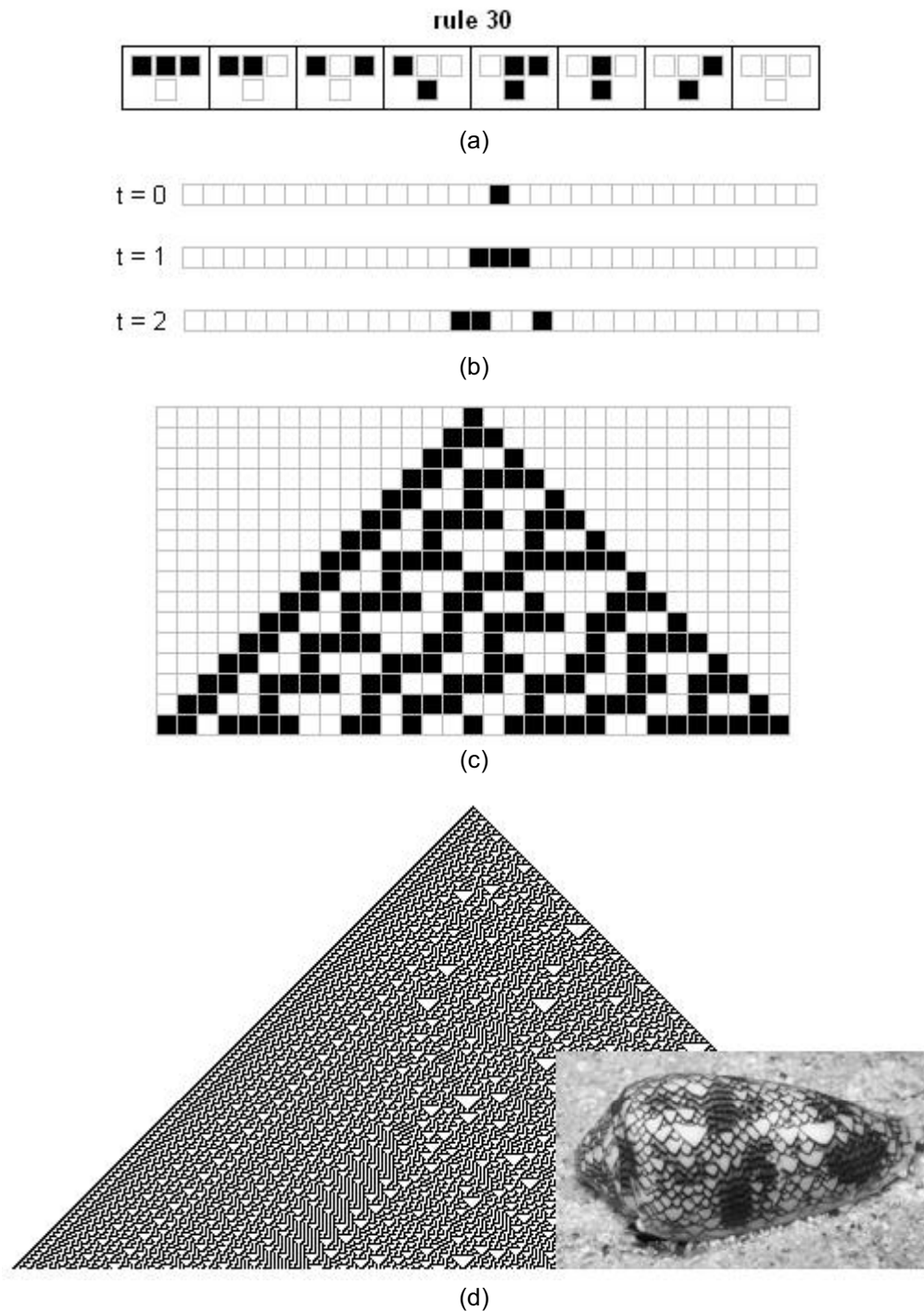


Figure 3.53: The rule 30 CA: (a) graphical representation of the Rule 30, (b) CA pattern a unit time $t=0, 1$ and 2 , (c) 15 first updates of the rule 30 CA, (d) 200 first updates of the rule 30 CA with a picture of the seashell *Conus* genus pattern. ^[38]

- Rules of the CA:

The universe of the Game of Life is an infinite two-dimensional orthogonal grid of square cells, each of which is in one of two possible states, live or dead. Every cell

interacts with its eight neighbours, which are the cells that are directly horizontally, vertically, or diagonally adjacent. At each step in time, the following transitions occur (see graphical representation Figure 3.54):

- Any live cell with fewer than two live neighbours dies, as if by loneliness.
- Any live cell with more than three live neighbours dies, as if by overcrowding.
- Any live cell with two or three live neighbours lives, unchanged, to the next generation.
- Any dead cell with exactly three live neighbours comes to life.

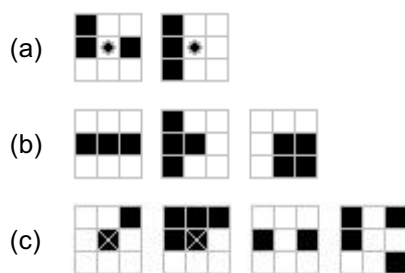


Figure 3.54: Rules of the Game of Life:

(a) dead cell with exactly three live neighbours becomes a live cell (birth).

(b) a live cell with two or three live neighbours stays alive (survival).

(c) in all other cases, a cell dies or remains dead (overcrowding or loneliness).^[39]

The initial pattern constitutes the 'seed' of the system. The first generation is created by applying the above rules simultaneously to every cell in the seed. Births and deaths happen simultaneously, and the discrete moment at which this happens is sometimes called a *tick*. (In other words, each generation is a pure function of the one before.) The rules continue to be applied repeatedly to create further generations.

In addition to the original rules, Life can be played on other kinds of grids with more complex patterns. There are rules for playing on hexagons arranged in a honeycomb pattern, and games where cells can have more than two states (imagine live cells with different colors).

The Game of Life is one of the simplest examples of what is sometimes called "emergent complexity" or "self-organizing systems." This subject area has captured the attention of scientists and mathematicians in diverse fields. It is the study of how elaborate patterns and behaviours can emerge from very simple rules. It helps us understand, for example, how the petals on a rose or the stripes on a zebra can arise from a tissue of living cells growing together (see also previous example with 1 dimensional CA). It can even help us understand the diversity of life that has evolved on earth.

In Life, as in nature, we observe many fascinating phenomena. Nature, however, is complicated and we are not sure of all the rules. The game of Life lets us observe a system where we know all the rules.

- Emerging objects:

Many different types of patterns occur in the Game of Life, including static patterns ("still lifes"), repeating patterns ("oscillators" - a superset of *still lifes* which repeats successively several patterns), and patterns that translate themselves across the board ("spaceships"). Common examples of these three classes are shown below (Figure 3.55) with live cells shown in black and dead cells shown in white.

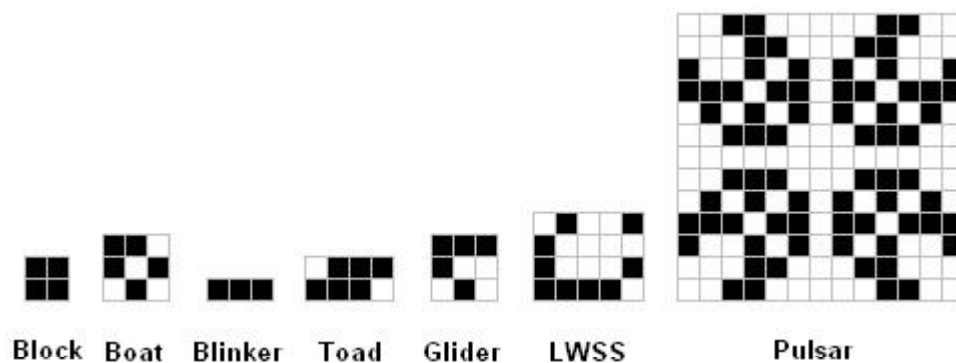


Figure 3.55: Examples of emerging objects in Game of Life

The "block" and "boat" are *still lifes*, the "blinker" and "toad" are *two-phase oscillators*, and the "glider" and "lightweight spaceship" ("LWSS") are *spaceships* which steadily march their way across the grid as time goes on. The "pulsar" is the most common period 3 *oscillator*.^[40]

An example of Game of Life is shown in Figure 3.56. The game starts with the "Gosper Glider Gun" (Figure 3.56a), a pattern discovered in 1970 by Bill Gosper. This interesting pattern produces new gliders every 30th generation when the two main patterns meet during their regular back and forth passes. The produced gliders move in the direction of the bottom right corner of the system (see Figure 3.56b, c, d, e, f).

Studying the patterns of Life can result in discoveries in other areas of math and science.

The behaviour of cells or animals can be better understood using simple rules. A behaviour that seems intelligent, such as we see in ant colonies, might just be simple rules that we don't understand yet. Traffic problems might be solved by analysing them with the mathematical tools learned from these types of simulations. Computer viruses are also examples of cellular automata. Finding the cure for computer viruses could be hidden in the patterns of this simple game. Human diseases might be cured if we could better understand why cells live and die. (Callahan, 2007)

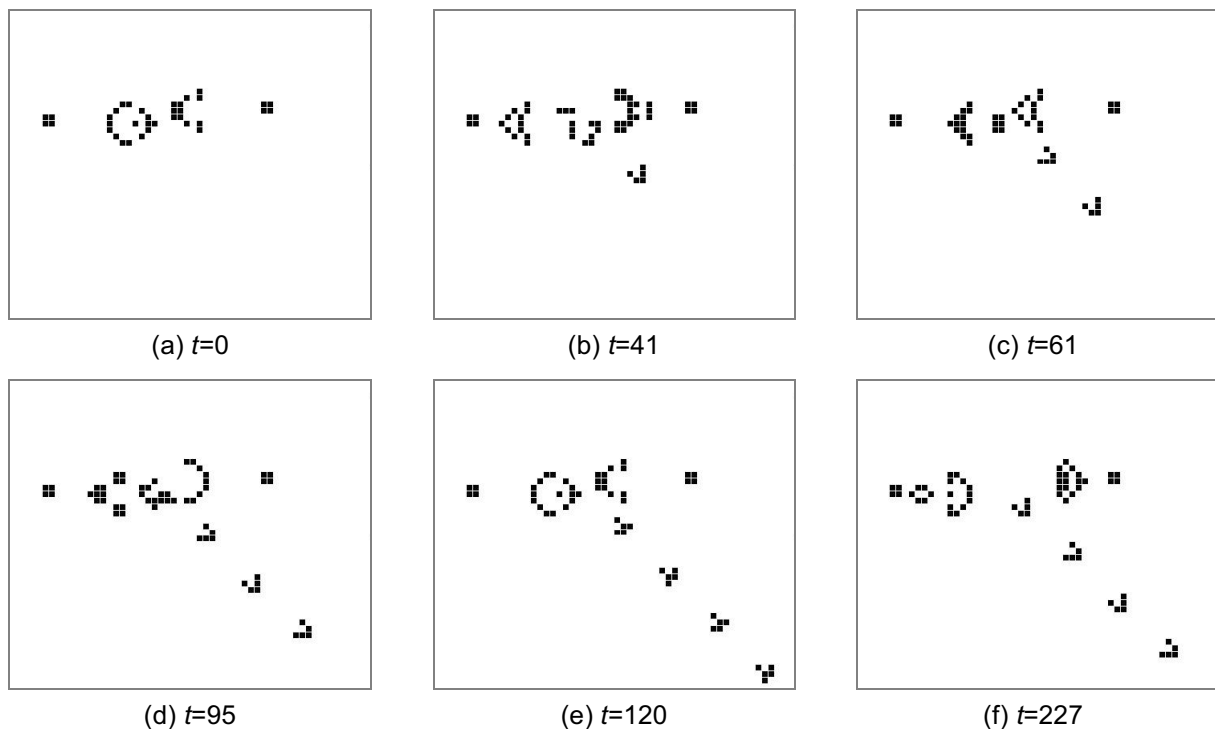


Figure 3.56: Example of Game of Life: the "Gosper gun". Screenshots of several updates are shown. The value of t give the update of the system according to the rules of the Game of Life. It corresponds to the unit of time and the a new generation of cell in the system. ^[41]

D. CA for modeling physical systems

Cellular automata represent for physicists an alternative to differential equations in modeling laws of physics (Omohundro, 1984; Toffoli, 1984). This has resulted in investigation of CA models for physical systems such as models for pattern formation in reaction-diffusion systems (Madore et al., 1983; Oono et al., 1985; Winfree et al., 1985) or the modeling of hydrodynamical systems (Frisch et al., 1986). Cellular automata have been also used to model different chemical processes like the absorption-desorption phenomenon (Chopard et al., 1989). The Lattice Gas Automaton (LGA) has been the central model for simulating hydrodynamics and reaction-diffusion processes (Dupuis et al., 2000). Despite the discrete dynamics which a LGA generates, it is able to follow the behaviour prescribed by Navier-Stokes equations of hydrodynamics. Application of CA modeling in physical system were reviewed in more detailed (Chopard et al., 1998; Ganguly et al., in press; Vichniac, 1984).

CA have been sometimes applied in the modeling of pharmaceutical systems or in systems close to these latter and easily applicable in the pharmaceutical field.

For example, a CA model Katsura published a simulation method for the flow behaviour of granular materials using cellular automaton (Katsura et al., 2005). The automaton rule consists

of the transition rule of constituent particles and interaction rule between particles. The validity of the method was confirmed by comparison of the simulated flow pattern of discharging flow from a hopper with experimental one (see Figure 3.57).

Barat recently reviewed models for drug dissolutions including cellular automata approach (Barat et al., 2006) of Zygourakis and Markenscoff who invented a new type of CA method to simulate the release from bio-erodible devices, in order to design formulations with optimal release characteristics (Zygourakis et al., 1996). In this model the DDS can be of any shape and the liquid around it is represented as a computational 2D grid, which is designed as a dynamic system with transient behaviour. To bring to the reader a first view of how drug dissolution can be simulated using CA modeling, the approach of Barat is briefly detailed here. Figure 3.58 shows a graphical representation of some steps in the *in silico* erosion process.

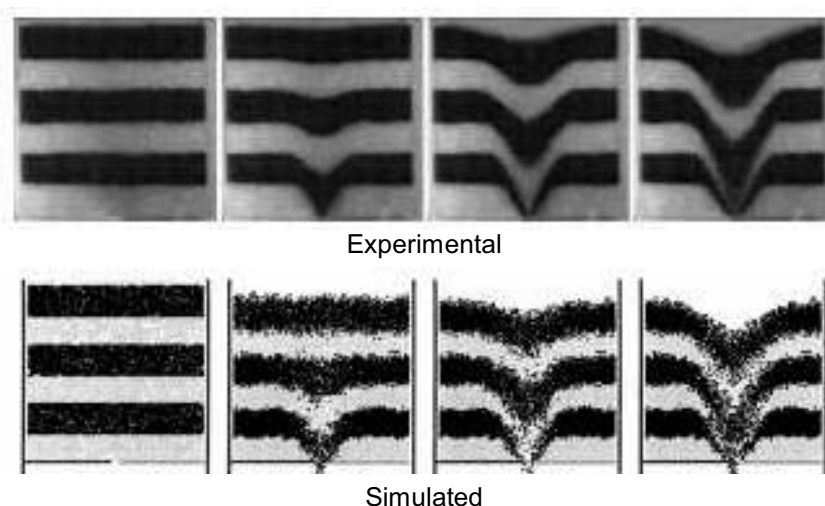


Figure 3.57: Comparison of flow behaviour of particles discharging from a hopper. ^[42]

The microscopic mechanisms of the dissolution phenomena are defined in terms of local relations between the sites. Each cell represents a small volume of either a solid component or solvent. The initial state $x_k(0)$ of an arbitrary computational cell is defined as 0 if the cell k is filled with solvent or U_i if the cell k belongs to solid component i , where U_i , $i=1, 2, \dots, M$ are suitably chosen numbers. Since the solid phases dissolve at different rates, the cells belonging to each phase will have different life expectations (a long life expectation corresponds to slow dissolution rate). As the solvent progressively dissolves the various solid phases, the solid concentration in each cell decreases until all the solid completely disappears. The following rules for updating the state of each computational cell were adopted:

- If the computational cell k is occupied by solid phase i , its initial state is set to U_i (at $t=0$).

- When the computational cell k becomes exposed to solvent, its state starts to decrease, until it reaches the dissolution threshold D_i . The rate at which the state decreases depends on the number of neighbouring cells that are completely filled with solvent.
- When the state of the computational cell k falls below the dissolution threshold D_i , then x_k is set to zero to denote that the solid in this cell has been completely dissolved and the previously solid cell is now completely filled with solvent.

The model handles the different dissolution rates of the solid component by assigning different lifetimes L_i to each of the M components. That is, $L_i = U_i - D_i$ for $i=1,2,\dots,M$.

Possible porosity of the device, with various sizes of the pores is taken into account. The simulation results were analysed to show how the overall release rates are affected by the intrinsic dissolution rate, drug loading, porosity and the dispersion of the drug in the bioerodible matrix. The article suggests that drug design approach which combines computer simulations and laboratory experimentation is likely to significantly reduce laboratory experimentation and the associated time and costs.

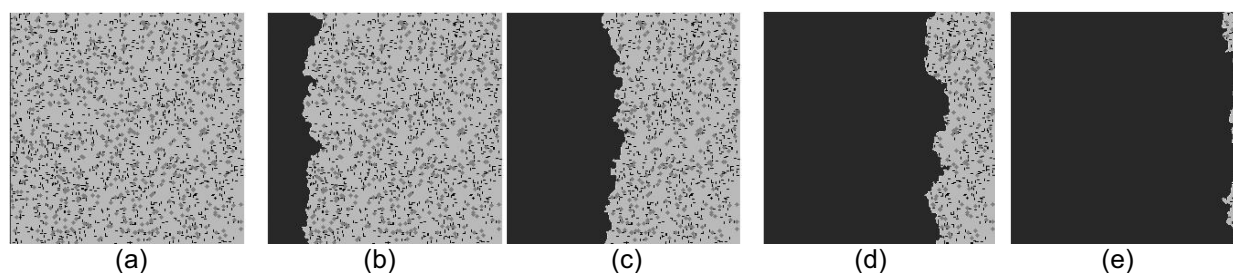


Figure 3.58: Sequence of images from a run of the Zygourakis CA simulating the erosion of a porous device loaded with 5% of another solid that dissolves rapidly. In light grey, the polymer matrix, in grey, the dissolving solid (drug), the black seed represents the macropores in multicomponent device and the homogeneous black phase represents the solvent (aqueous phase).^[43]

The cellular automata proposed by Zygourakis and Markenscoff have shown a good potential to become a valuable computational tool for designing bioerodible devices with optimal release characteristics. However, the model is two-dimensional and does not offer yet all possibilities necessary to become a general tool for solid dosage dissolution testing and design.

4. Conception and implementation of the expert system

4.1. General conception

4.1.1. Reasons to develop an new innovative expert system for pharmaceutical solid dosage formulation design

The aim of this expert system is to propose an ultimate tool to help in the formulation design of pharmaceutical solid dosage forms. It does not pretend, of course, to be able to replace experience and expertise of professional formulators. Whereas, this tool is developed to provide an efficient software platform to make formulators task easier by narrowing the search for an optimal formulation.

As it was presented in section 3.2.2, the most important benefits of expert system applications on products formulation concerned the accuracy of the decision-making, the improvement of problem solving and the quality/accuracy of work. Reduction of skilled staff or in staff numbers was identified as the least benefits of such tools. Indeed, users of previous systems reported the following important benefits: knowledge availability, consistency in designing right first time formulations, training staff, speed of development, freeing experts for more innovation tasks and of course in cost savings.

Furthermore, a clear need for new innovative expert systems was confirmed by a recent publication, which measured the return on investment on modeling and simulation tools in pharmaceutical development: "Based on in-depth interviews with research scientists in pharmaceutical development, Health Industry Insights (HII) concludes that there is a significant return on investment (ROI) to be realised from the use of modeling and simulation software tools. HII's ROI model is derived from conversations with researchers at major pharmaceutical companies and academia. The results of the model suggest a cumulative ROI on the order of \$3.10 for every \$1 invested in these tools. The ROI varies based on type of users (occasional or power)." (Louie et al., 2007).

4.1.2. Non-biased expert system: a ES backbone based on general mathematical and physical models

Some already existing ES propose to design new formulations by performing *in silico* treatment of experimental data sets (e.g. Artificial Neural Networks). These approaches are often efficient for designing new formulations with properties and components similar to

formulations providing the data. However, the design of a very different formulation may be biased by these experimental data.

It was then decided to develop an ES backbone, which could represent a general non-biased formulation design tool. ES backbone is thus based on mathematical and physical models only and does not need experimental data for modeling. Whereas it uses robust models, which are independent of specific dosage forms parameters.

4.1.3. Modular architecture: a toolbox for solid dosage formulation design

It was decided to build ES on a modular architecture. Each module of ES is developed to optimise a certain property of the formulation. A general algorithm of optimisation has to evaluate *in silico* results from each module and determines best compromises for the final formulation. Evaluation method is detailed in next section.

Different reasons motivated the choice for modular architecture of ES:

- With such architecture, ES is similar to a toolbox or “Swiss knife” for formulation design. Users can work on all properties of the future formulation by using all modules together (global formulation design). If formulators need to solve only one specific problem of the formulation (e.g. disintegration optimisation), a module can be then used individually.
- It is possible to switch on and off certain modules of the system during global formulation design. In this case, quality evaluation algorithm will take into account only the activated modules.
- Modular architecture is more convenient for development, maintenance and further improvements of the system. It is possible to work on new modules separately and to add them easily into ES for increasing formulation options offered by the tool. Furthermore, if modifications are done on one single module, it will not change the results obtained individually with the other modules but will influence final formulation only.
- It is possible to develop further on new modules without having to change the global evaluation algorithm. It will be necessary, however, to include the modeling results from added module into the inputs of the quality evaluation unit.

Figure 4.1 gives an overview of already implemented modules and of modules planned for further development of ES.

A full description of “Disintegration optimisation” module is given in section 4.3.1. “Dissolution simulation” module is presented in section 4.3.2. “Tablet designer” and “Database” modules are described in the same section, as they must be used together with “Dissolution simulation” module.

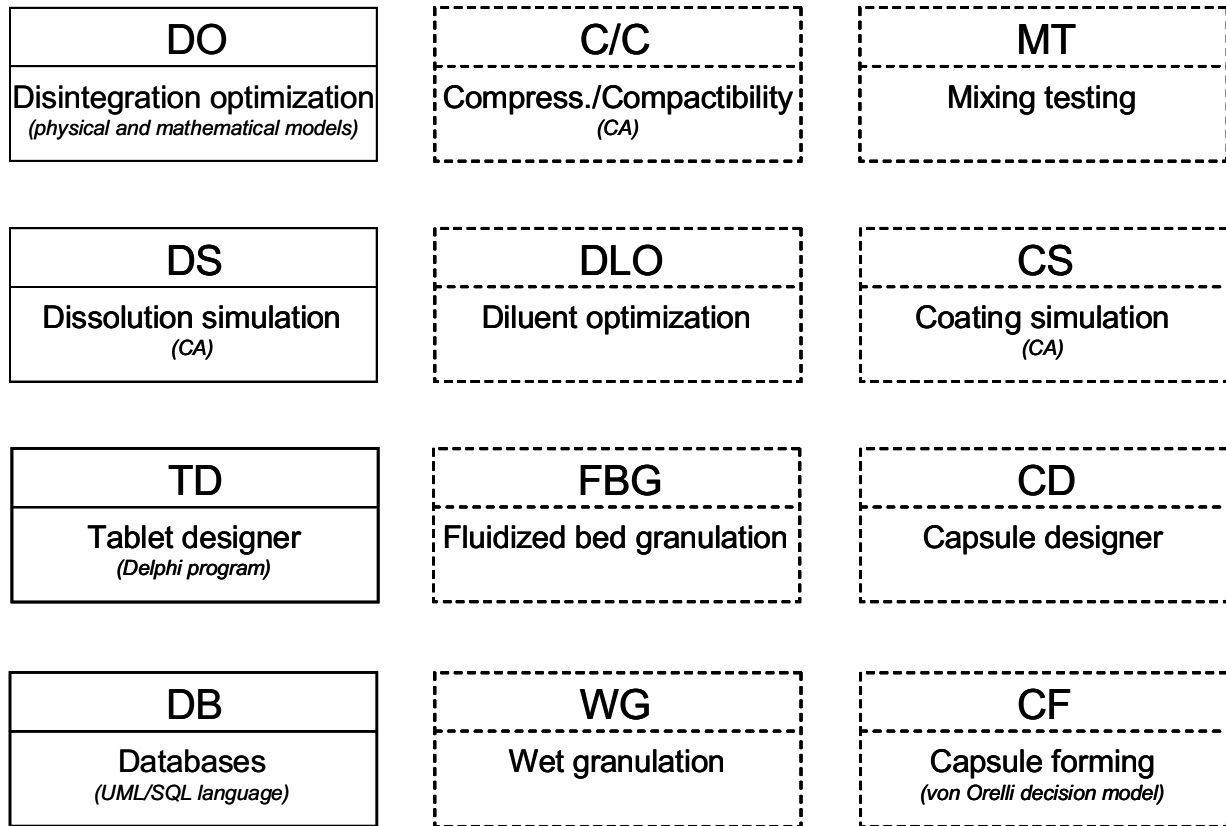


Figure 4.1: Expert system modules: already implemented (continuous lines) and planned for further development (dashed lines).

Each ES module (Figure 4.1) is shortly presented below:

- Disintegration optimisation (DO):

This module calculates the optimum amount of disintegrant to add in a formulation for a shortest disintegration time of a tablet. It uses percolation theory and geometrical and physical models.

- Dissolution simulation (DS):

Provides platform to simulate tablet dissolution using Cellular automata modeling. Tablet components are imported from databases of DB module. Tablet to dissolve *in silico* must be previously designed with TD module.

- Tablet designer (TD):

The name of this module should not be confused with the global tablet formulation design task. This module serves to design tablet pattern and to transform it into a discrete 3D virtual tablet. This tablet model is place in the cubic matrix of DS module for *in silico* dissolution.

- Databases (DB):
This module has a central role in ES. It is composed of databases in which information about substances (API, disintegrant, filler, etc...) are stored. These data will be used by other module of ES to formulate a solid dosage form.
- Compressibility/Compactibility optimisation (C/C):
C/C module will enable to test the compressibility and compactibility of a solid dosage form. The program will use a virtual tablet (like DS module) and will estimate behaviour of the mix under compression according on the base of physical and geometrical properties.
- Diluent optimisation (DLO):
DLO module will enable to choose and to dose diluents in a solid dosage form in order to optimise some of their properties (i.e. compressibility, compactibility, dissolution, etc.).
- Fluidised bed granulation (FBG):
This module will model fluidised bed granulation process.
- Wet granulation (WG):
The same but for wet granulation process.
On the base of the results obtained with FBG and WG it will be possible to advice the best process for granulation.
- Mixing testing (MT):
Should simulate mixing process and detect risks of segregation or over mixing.
- Coating simulation (CS)
CS module will use the same modeling method than DS module but for dissolution simulation of coated tablets.
- Capsule designer (CD):
This module is similar to TD module but for capsule formulation design.
- Capsule forming (CF):
CF module will help to decide whether to formulate a certain mixture with capsules or tablets on the base of von Orelli rules (Van Orelli, 2005).

The list of all modules planned for further development (see Figure 4.1) is not exhaustive. It is possible to add many other modules (e.g. roll compaction modeling, flowability testing) to improve formulation design possibilities and accuracy of ES.

4.1.4. Quality evaluation of the modeling results from ES modules

This section explains how ES should proceed for global formulation design. It describes how the evaluation unit of the system uses data from ES modules to analyse the quality of a formulation at a certain time of the design process.

A schema of the general working of ES is depicted in Figure 4.2. As it is shown on the figure, the quality evaluation unit is a central component of ES. It receives as input the constraints chosen by the user or given by pharmacopoeia (e.g. required dissolution points or minimum hardness). There is possibility for the formulator to turn on/off certain modules and to give a weight to the results from activated modules. Modules weights should be used by the evaluation unit to adjust importance of each property during formulation design.

At this point of development, ingredients to be added to a formulation must be first selected by the user in the DB module (or added if they are not yet available). However, further developments should allow an automatic exchange of data between modules and databases. For example, excipients and their properties should be automatically transferred from databases to ES modules. If the composed mixture does not meet the requirements and the quality standards with one or several modules, other excipients should be selected.

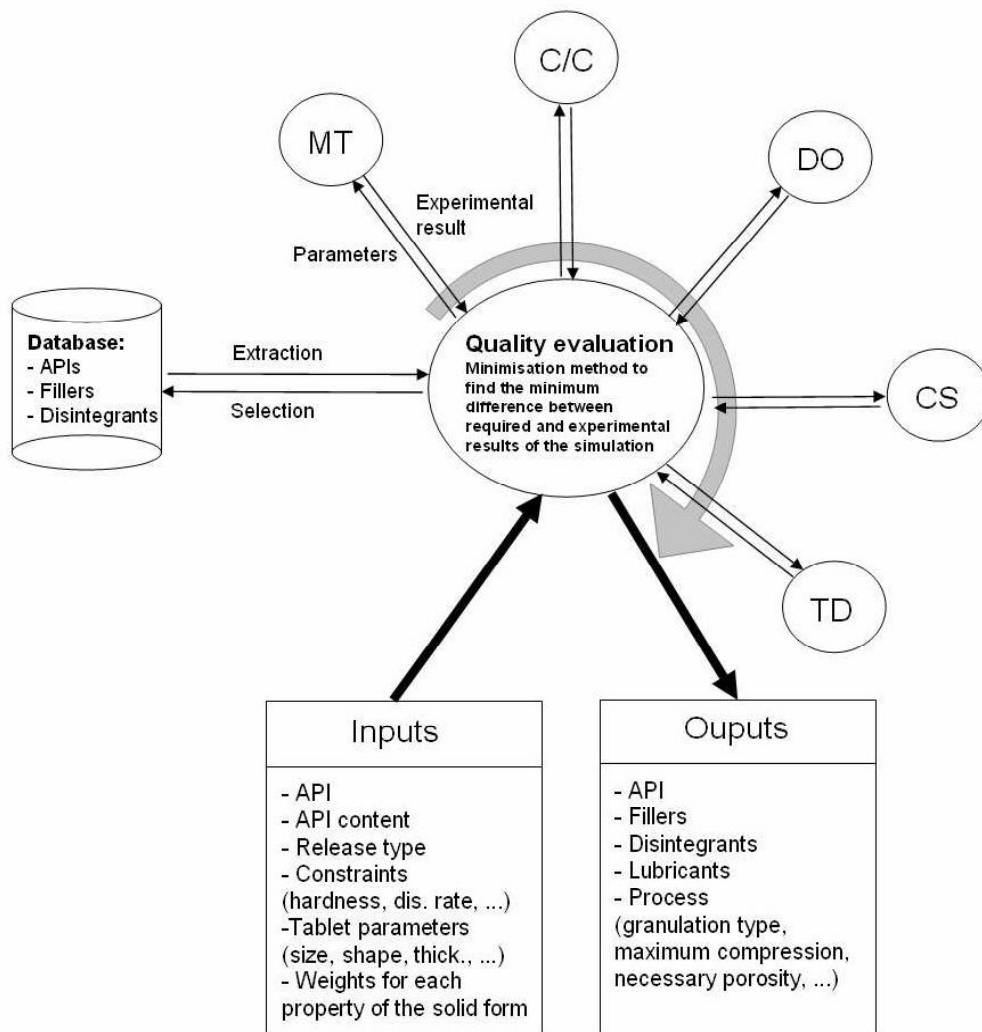


Figure 4.2: Schema of general working of expert system

The result of an *in silico* experience with one of the modules is a function of the factors influencing this result. It can be expressed as follows:

$$R_X^{is} = f(F_1, F_2, \dots, F_n) \quad \text{Equation 59}$$

with R_X^{is} , the *in silico* result from simulation with module X and F_n , a factor n having an influence of the result R_X^{is} .

Let R_X^{req} be the result required by pharmacopoeia or by formulator for a certain formulation property simulated with module X .

To optimise this property, it is necessary to approach R_X^{req} with R_X^{is} :

$$\frac{R_X^{is}}{R_X^{req}} = \alpha \pm \varepsilon \quad \text{Equation 60}$$

with α , the fraction between *in silico* and required results for a given property and ε , the tolerance in precision.

An example of a result R_X^{is} optimisation is shown in Figure 4.3.

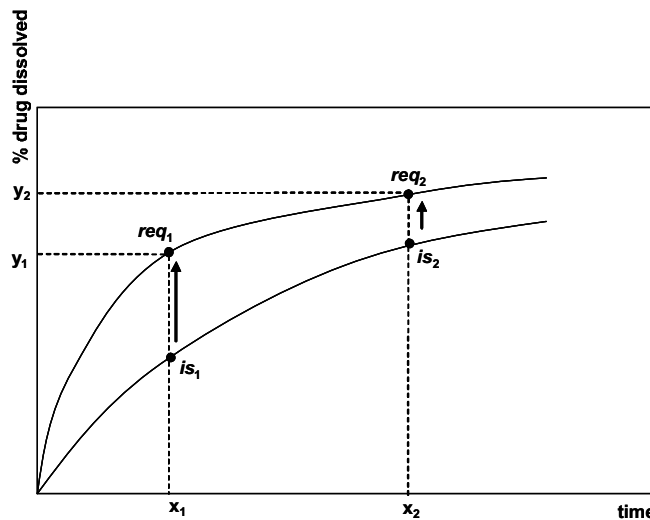


Figure 4.3: Quality evaluation of *in silico* dissolution result. The formulation giving a simulated profile fitting with the curve passing by the required points (req_1 and req_2) will be selected.

This example concerns results obtained with the “Dissolution simulation” (DS) module. Two dissolution points, req_1 and req_2 , are required by pharmacopoeia for time x_1 and x_2 and are given as input of the system by the user. The quality evaluation unit will analyse results R_X^{is} obtained with DS, i.e. *in silico* dissolution profile, until DS find a formulation giving a *in silico* dissolution profile fitting with the profile which passes by req_1 and req_2 points. If is_1 and is_2 are

two *in silico* points at time x_1 and x_2 respectively, dissolution of the designed formulation should give a *in silico* profile with is_1 and is_2 close to req_1 and req_2 .

For a fast approach of R_X^{req} with R_X^{is} , different optimisation algorithms (e.g. Simplex or Nelder-Mead methods) can be used to minimise the difference between required and *in silico* results. Simplex algorithm is a popular algorithm for numerical solution of a linear programming problem. Nelder-Mead method (see example in Figure 4.4) is a numerical method for optimising many-dimensional unconstrained problems by minimising an objective function in a multi-dimensional space.

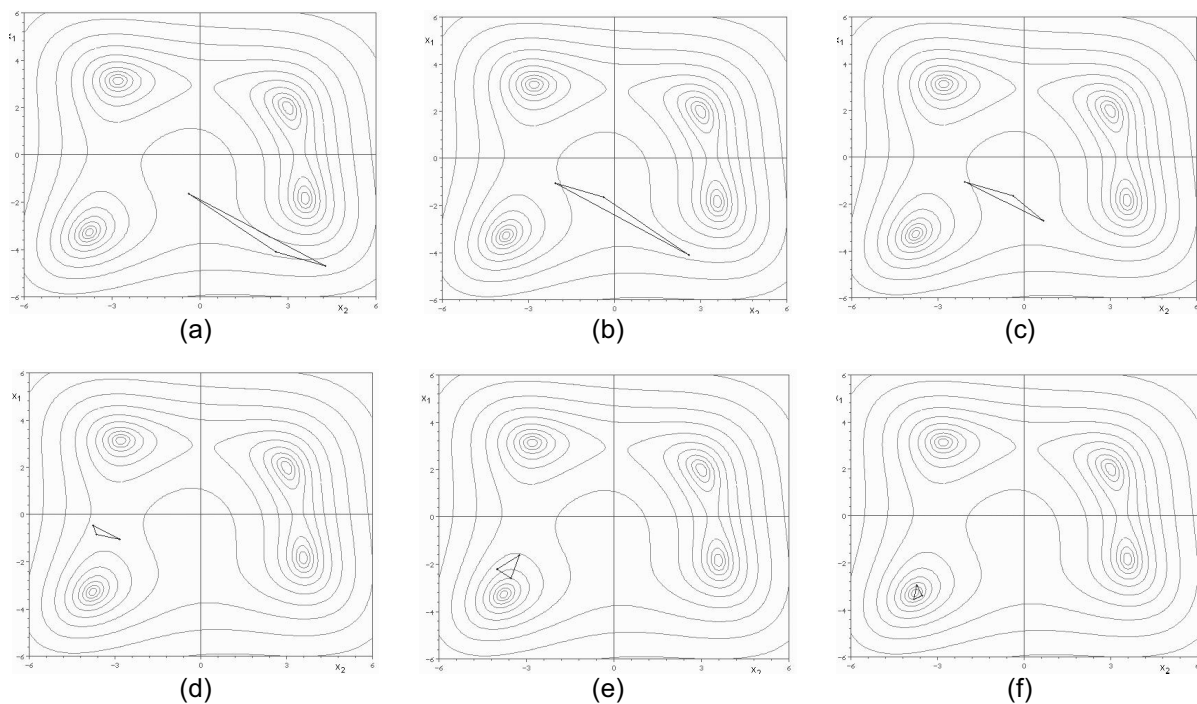


Figure 4.4: Some steps in the research of minimum of a 3D function using “Nelder-mead” method ^[46]

The Nelder-Mead method uses the concept of a simplex, which is a polytope of $N+1$ vertices in N dimensions (e.g. a line segment on a line, a triangle on a plane, a tetrahedron in three-dimensional space). The method approximately finds a locally optimal solution to a problem with N variables when the objective function varies smoothly. In a three-dimensional problem, Nelder-Mead method generates trial designs which are then tested. As each run of the simulation requires high computer capacity, it is important to make good decisions about where to look. Nelder-Mead generates a new test position by extrapolating the behaviour of the objective function measured at each test point arranged as a simplex. The algorithm then chooses to replace one of these test points with the new test point and so the algorithm progresses. The simplest step is to replace the worst point with a point reflected through the

centroid of the remaining N points. If this point is better than the best current point, then the algorithm can try stretching exponentially out along this line. On the other hand, if this new point isn't much better than the previous value then the simulation is stepping across a valley, so it shrinks the simplex towards the best point.

For example, if R_X^{is} function depends on three factors F_1 , F_2 and F_3 , *in silico* experience will be repeated with different factors until $\frac{R_X^{is}}{R_X^{req}} = 1 \pm \varepsilon$.

If several R_X^{is} must be taken into account for an experience with the module X , then the sum of all $\frac{R_X^{is}}{R_X^{req}}$ will be considered:

$$\frac{R_{X_1}^{is}}{R_{X_1}^{req}} + \frac{R_{X_2}^{is}}{R_{X_2}^{req}} + \dots + \frac{R_{X_k}^{is}}{R_{X_k}^{req}} = \alpha_1 + \alpha_2 + \dots + \alpha_k + \varepsilon_{tot} \quad \text{or} \quad \sum_{k=1}^n \frac{R_{X_k}^{is}}{R_{X_k}^{req}} = \sum_{k=1}^n \alpha_k + \varepsilon_{tot} \quad \text{Equation 61}$$

The same evaluation will be done with results from different modules. In this case, each $\frac{R_X^{is}}{R_X^{req}}$ of a module can be multiplied by a weight factor (given by ES user) to adjust importance of certain formulation properties.

4.2. Material and method of implementation

The expert system was implemented on personal computer Dell Optiplex GXC280 with processor Intel Pentium 4, CPU 3.00Ghz, 1.00Gb RAM, equipped with a graphic card Radeon X300 series. The software operating systems Windows XP (SP2) was installed on the computer.

Programs were written in Object Pascal language and Borland Delphi v7.0 (2006) was used as compiler and software development package. Different libraries proposed by Delphi were used for interfaces development (e.g. Visual Component Library). Pascal is an influential imperative programming language. It is a small and efficient language intended to encourage good programming practices using so called structured programming and data structuring. Object Pascal is an object oriented derivative of Pascal language. Object oriented programming is a type of programming in which programmers define not only the data type of a data structure, but also the types of operations (functions) that can be applied to the data structure. In this way, the data structure becomes an "object" that includes both data and functions. In addition, programmers can create relationships between one object and another. For example, objects can inherit characteristics from other objects. One of the main

advantages of object oriented programming techniques compared to procedural programming techniques is that they enable programmers to create modules which do not need to be changed when a new type of object is added. A programmer can simply create a new object that inherits many of its features from existing objects. This makes object-oriented programs easier to modify. Object Pascal is mostly known as the primary programming language of Borland Delphi, which is a software development package supporting Object Pascal. Borland used the name "Object Pascal" for the programming language in the first versions of Delphi, but later renamed it to the "Delphi programming language". As mentioned previously, Borland Delphi is also a compiler, i.e. a computer program (or set of programs) that translates text written in a computer language (the source language, e.g. Object Pascal) into another computer language (the target language). The name "compiler" is primarily used for programs that translate source code from a high-level programming language (directly understandable for the programmer) to a lower level language (e.g., assembly language or machine language) which can be "understood" directly by the computer. Borland Delphi propose different libraries (partially implemented "objects" for programming), e.g. VCL, which is Delphi's object-oriented framework. This library proposes classes (part of source code setting properties and functions of an "object") for Windows objects such as windows, buttons, etc. and you'll also find classes for custom controls such as gauge, timer and multimedia player, along with non-visual objects such as string lists, database tables, and streams.

Databases of DB module were programmed in SQL. SQL, commonly expanded as Structured Query Language, is a computer language designed for the retrieval and management of data in relational database management systems, database schema creation and modification, and database object access control management.

In addition, Mathematica v5.2. software was use for equation simplification and equation solving. Mathematica is a specialised computer program used mainly in scientific and mathematical fields. It provides cross-platform support for tasks such as symbolic or numerical calculations, arbitrary precision arithmetic, data processing and plotting. Mathematica has a programming language which supports functional and procedural programming styles. With Maple and Matlab, it is one of the three main commercial programs of its type. It was originally conceived by Stephen Wolfram, developed by a team of mathematicians and programmers that he assembled and led.

4.3. Developed modules description

4.3.1. Exact prediction of the optimal percentage of disintegrant for a minimal disintegration time of a tablet

The aim of this module is to predict rationally the exact amount of disintegrant to have in a pharmaceutical tablet in order to minimise its disintegration time (DT). This amount, given in % (v/v or w/w) of the powder mix or of the resulting compact, is calculated using percolation theory to model the water diffusion in a tablet. Indeed, shortest DT of a tablet is usually correlated to the fastest diffusion of water within the compact (see sections 3.1.4B and G). The calculation method is given for a compacted binary mixture (drug/disintegrant) model. However, the same method can be applied for a multi components tablet by renormalisation of the system (see section 3.3.1C).

A general solution to the problem is proposed, independent on the chemical properties of the components of the compact. Although the DT value of a tablet, which is not given by the module, strongly depends of the chemical properties of the components, the optimal concentration of these components for the shortest DT can be estimated on the base of geometrical and physical considerations only. For this reason, percolation theory was chosen to model the problem. The calculation method takes into account the porosity of the tablet.

Required information for calculations are:

- Volume of the tablet.
- Mass of the tablet.
- Mean particle sizes of the components.
- True densities of the components.

Two methods of calculation are proposed, depending on the general aspect of the disintegrant particles (non-fibrous or fibrous). Furthermore, the two methods are valid only if all the other components of the tablet (drug, filler, etc.) are non fibrous.

A. Solution for non-fibrous disintegrants

Disintegration Process

In this model it is considered that disintegration of pharmaceutical compact is a subject of the following conditions (see theoretical section):

- A disintegrant with swelling properties is present in the formulation.
- The disintegrant is able to conduct water by diffusion or “wicking”.
- There is porous structure in the tablet which can conduct water by capillary effect to the disintegrant grains.

Particle Size and Shape

Further theoretical postulates are based on the following assumptions:

- Drug and disintegrant particles are assumed to be spherical:

Particles in the system are assumed to be spherical, however a non-fibrous profile is a sufficient condition to apply the model (real powder particles are never perfect spheres).

- Particle size distributions are narrow but can be different for each component:

The model assumes that all particles of a component have the same size but this size can be however different between each component (non isometric system). The mean particle size of a component is considered as the exact and single value for the size of the spheres which model the component. Particle sizes distribution profile of a component must be narrow to ensure a “safe” application of the model.

- There is no significant deformation of drug particles within the compact.

Calculation is base on a geometrical model of non-deformed packed sphere. During compression, the force is distributed to many contact points between particles. Thus, the particles usually do not dramatically deform during compression process. However, some materials may be softer and become flattened during compression. Extreme cases should be considered before application of the model, even if this one tolerates a slight deformation of the particles (if the general packing is not affected). In the same way, it is assumed that brittle particles stay gathered during compression and do not spread within the compact.

Sphere packing in a random close packed sphere system.

A pharmaceutical tablet is a compact of particles arranged in a disordered close packing (particulate disordered media). It was thus assumed that non-fibrous compacted particles can be modelled with a system of spheres randomly close packed, i.e. each sphere of the system is placed at random and is in close contact with its direct neighbours. Such a system is named Random Close Packed (RCP) spheres system (see example in Figure 4.5a).

Observations of different RCP spheres systems revealed that the most stable, probable and smallest local packings of spheres are hexagonal and simple cubic packing (see Figure 4.5b, c).

It has to be pointed out that a RCP system can be composed of spheres of different sizes. Local hexagonal and cubic packing can still be identified inside a heterogeneous system, however only in parts of the system where spheres of similar size are gathered.

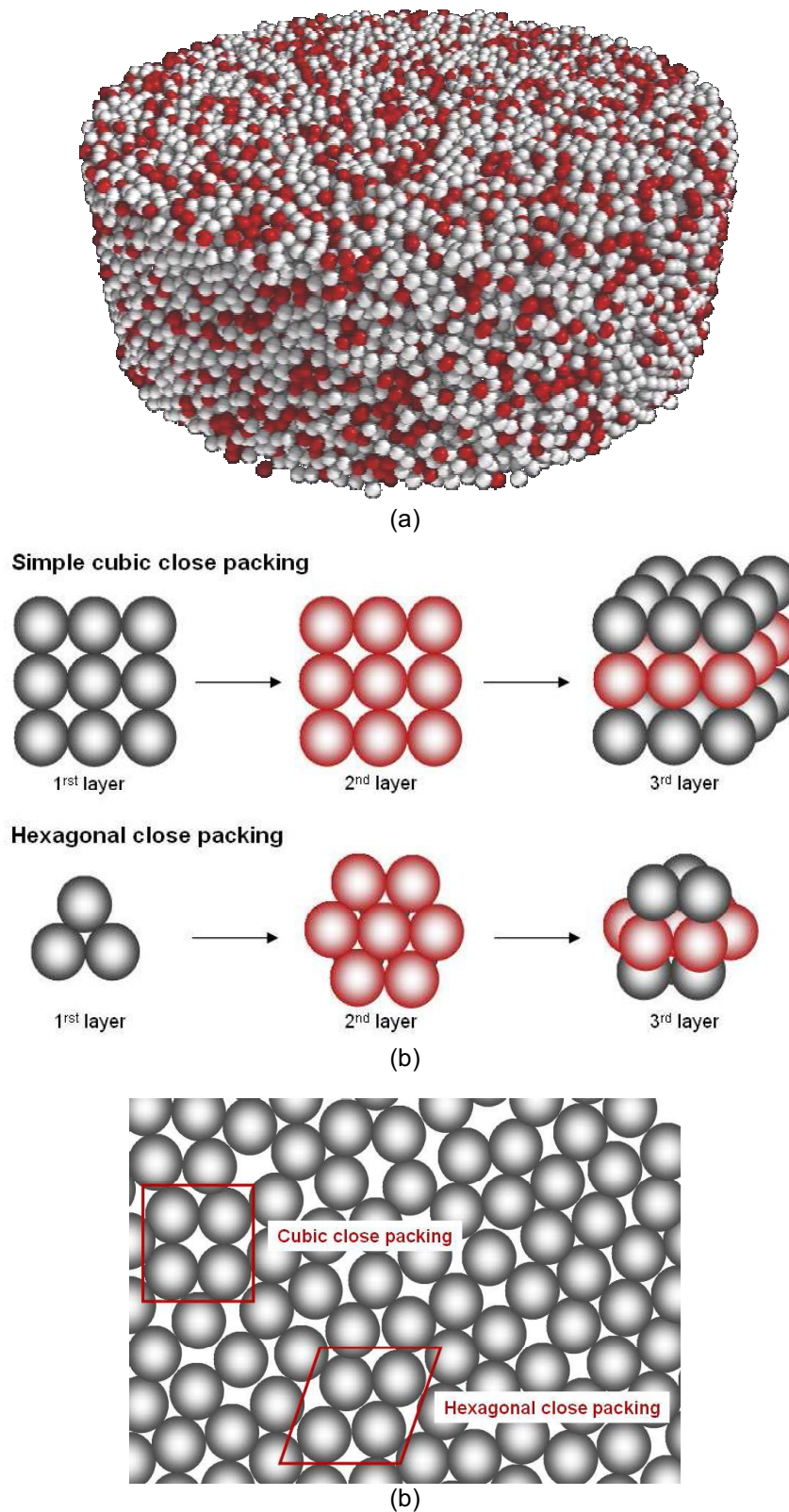


Figure 4.5: Random Close Packed (RCP) spheres system and inner smallest main local packing.
 (a) 3D view of a binary RCP sphere system composed of 120000 mono-disperse spherical beads. ^[45]
 (b) 3D view of hexagonal and simple cubic close packing.
 (c) 2D view of a RCP spheres system with examples (circled in red) of the two smallest and most probable local packing: hexagonal and cubic.

Sphere caging in a binary RCP system.

In binary RCP sphere system composed of small and bigger spheres, small spheres can be caged by bigger spheres if they don't reach a "caging critical size". If the difference of size between the two sphere types is large enough, small spheres can be caged by bigger spheres in a hexagonal close packing (see Figure 4.6).

If a small sphere is too large for being caged in hexagonal packing but is still below the caging critical size, the sphere can be caged in a cubic close packing of bigger spheres (see Figure 4.6). The caged sphere and the caging spheres will form together a Body Centred Cubic (BCC) close packing of spheres. This packing represents the critical packing of the model. Above a critical size of the caged sphere, caging in simple cubic close packing is not possible anymore (Figure 4.6). The caging spheres will be moved apart and the caged sphere will be brought closer to each other (Figure 4.6). For simplification of the model it is considered that if caging spheres of the BCC packing are not in close contact together anymore (close packing), caged spheres can be in contact. In a strict geometrical model, this contact would happen only if the caging spheres are moved apart sufficiently. However, this simplification should be realistic: in a real tablet, slight deformation of the caged particles is sufficient to connect them together with their neighbours, even if their size is just slightly above the caging critical size.

The critical BCC close packing mentioned before represents the limit between two cases. The system is said to be in case I if the smallest spheres can be caged in hexagonal or simple cubic packing. If this is not possible anymore, the system is in case II.

It has to be clearly stated that for case I, it is not mandatory that caged spheres occupy totally the available central space in the hexagonal or simple cubic close packing which are formed by the biggest spheres. For example, it is possible that a sphere is too large to be caged in hexagonal packing but is however smaller than the maximal sphere which can be caged in a simple cubic packing.

Using classical geometry, it is possible to express the radius r of the largest sphere, which can be caged in a simple cubic close packing, in function of the radius R of the spheres forming the packing (a mathematical demonstration is given in Appendix A).

$$r = (\sqrt{3} - 1)R \quad \text{Equation 62}$$

According to Equation 62, a binary system composed of spheres of type A (radius r) and of type B (radius R) will be in case I if r is below or equal to $0.732R$. If r is strictly above $0.732R$ the system will be in case II.

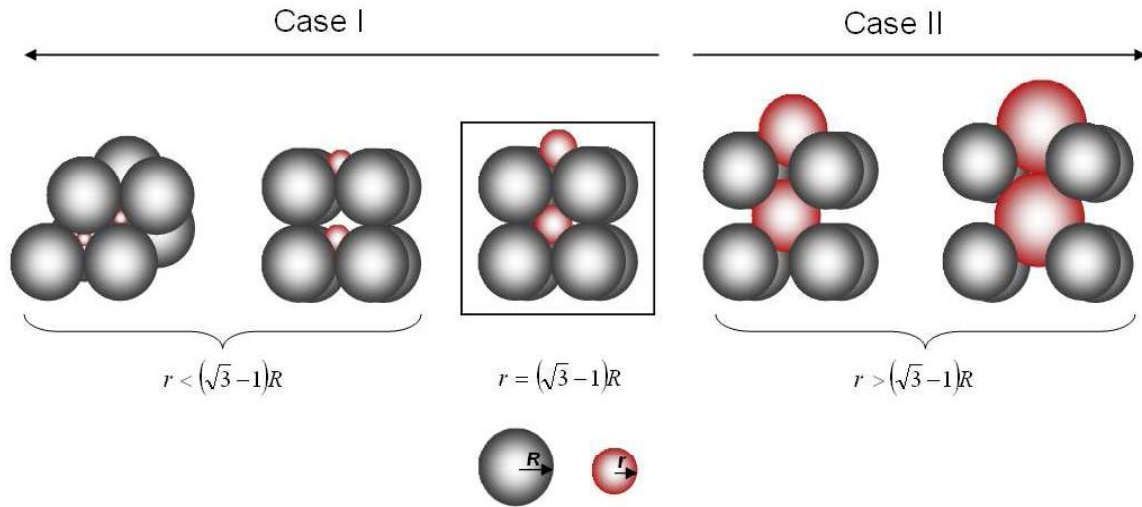


Figure 4.6: Two dimensional view of the evolution of local packing between caged and caging spheres in a RCP system, according to the increase in size of a central sphere. Case I: a disintegrant grain can be caged by drug particles in hexagonal or cubic packing. Case II: disintegrant grain is too large to be caged and can have contacts with other neighbouring disintegrant grains.

Particle caging in a compacted binary mixture of drug/disintegrant particles.

Previous considerations in a RCP spheres system were used to model a compacted binary mixture of spherical disintegrant and drug particles (spherical means here non fibrous). The cases I and II described previously are applied to the caging of disintegrant grains by drug particles. The compacted binary system is in case I if disintegrant particles can be caged by drug particles in a BCC close packing. The compact will be in case II if a disintegrant particle is too large to be caged in a BCC close packing of drug particles. There will then be a possibility for disintegrant particles to have a contact between each other, and if they are numerous enough, to create a continuous cluster through the tablet. If r is the mean particle radius of disintegrant and R the mean particle radius of drug, the case characterising the compacted binary mixture can be calculated as follows:

$$\text{Case I: } r < (\sqrt{3}-1)R \quad \text{Equation 63}$$

$$\text{Case II: } r > (\sqrt{3}-1)R \quad \text{Equation 64}$$

Water diffusion within the compacted binary mixture.

In a compacted binary mixture of disintegrant and drug particles, the water can diffuse between drug particles through capillary system (porous network) and through disintegrant grains (solid network). It is a prerequisite that capillary diffusion is possible only if the porous network is not too hydrophobic. Diffusion through disintegrant particles is possible by default (disintegrant particles are assumed to be hydrophilic and water conductive).

When applying percolation theory to diffusion of water through a compact, it is important to characterise the structures of the water-conducting water networks.

In case I, the network formed by disintegrant grains is included into the porous network, as disintegrant grains are caged into the pores formed by packed drug particles. Porous network and disintegrant grains network exhibit the same structure (see Figure 4.7). It is thus possible to add the porous volume fraction of tablet to disintegrant volume fraction. The sum gives the volume fraction of the tablet in which water can diffuse and represent percolating fraction of the tablet which conduct water. In case I, water is conducted through the porous network by capillary diffusion to disintegrant grains (see Figure 4.8).

For case II, disintegrant particles are not included into the porous network and disintegrant volume fraction cannot be added to pores volume fraction. Indeed, the structures of the two networks are different (Figure 4.7). In case I water is conducted through two separated and “parallel” networks. There is in fact a possible overlapping of the two diffusion networks, but their common volume fraction in the tablet cannot be quantified.

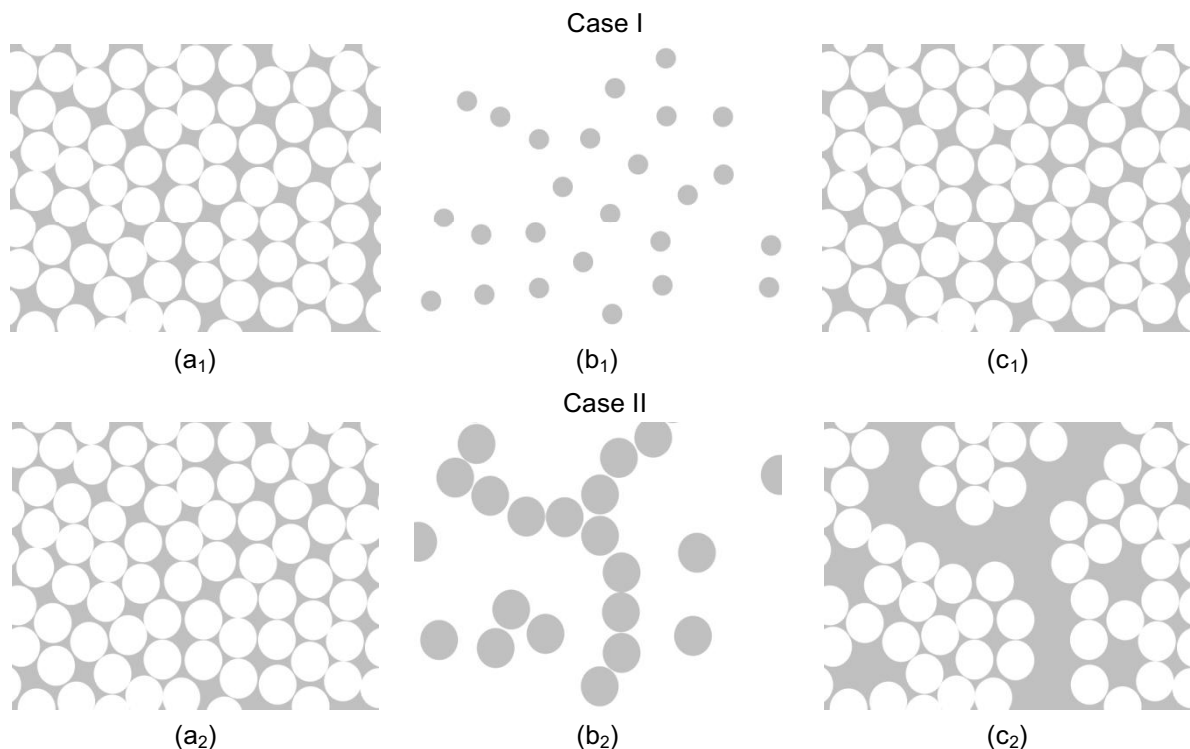


Figure 4.7: Two dimensional view of water-conducting network structures in a compacted binary mixture of drug and disintegrant particles for Case I and II. System fractions in which water can diffuse (pores and disintegrant grains) are colored in grey. White discs represent drug particles.

Case I: When the network between drug particles (a_1) and the network through disintegrant grains (b_1) are added together (c_1), the resulting total network exhibits the same structure than the network between drug particles.

Case II: When the network between drug particles (a_2 , part of the tablet without disintegrant) and the network through disintegrant grains (b_2) are added together (c_2), the resulting total network structure is different from the structure of the network between drug particles.

Furthermore, it has to be remembered that, in case II, disintegrant grains can contact each other if they are direct neighbours in the system. If disintegrant grains are numerous enough in the tablet, they can form a percolating cluster conducting water through the whole compact (see Figure 4.9).

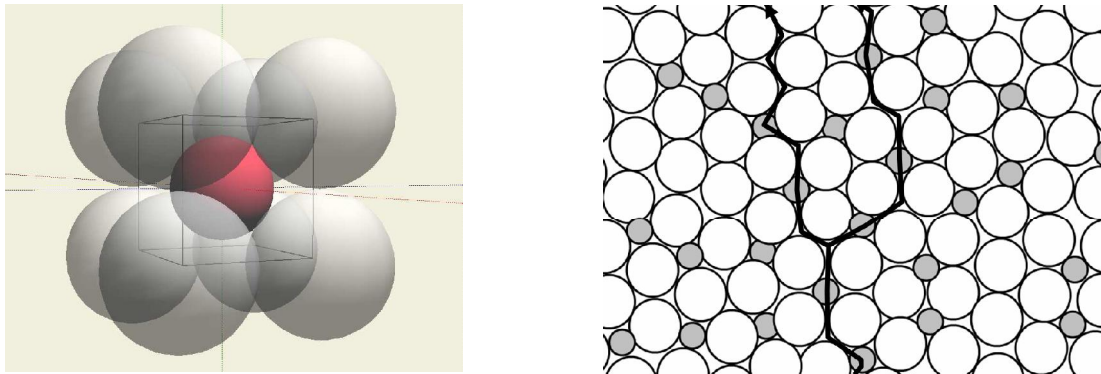


Figure 4.8: Caging of small sphere by bigger ones (left picture) and a matrix of caged spheres modeling a tablet in Case I which is composed of disintegrant particles (grey discs) and drug particles (white discs) (picture at right). Black lines represent the diffusion of water through the combined disintegrant/pores percolation cluster.

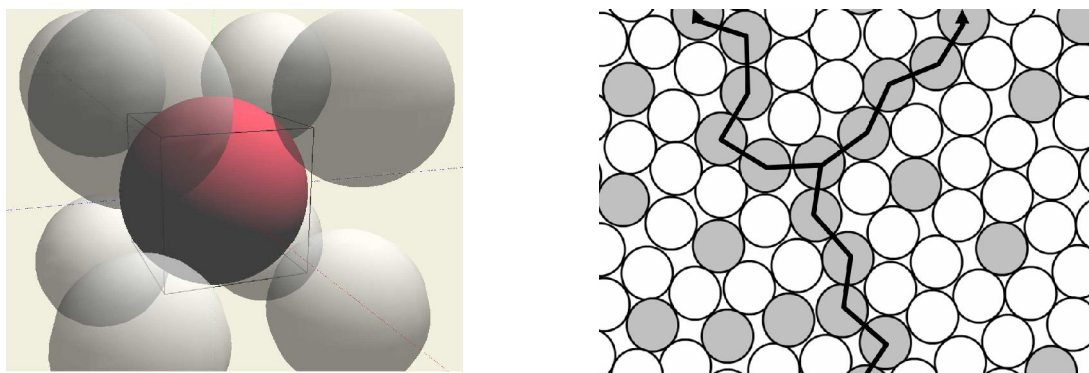


Figure 4.9: Non-caged central sphere in BCC packing (left picture) and a matrix of non-caged spheres modeling a tablet in Case II (grey discs represent disintegrant grains and white discs represent drug particles). Black lines denote water diffusion through a percolating cluster formed by disintegrant grains.

In practical experience it is possible that due to a not absolute perfect mixing, both cases can be present within a tablet (see Figure 4.10). Indeed, an agglomerate resulting of a local accumulation of disintegrant particles can be considered as a disintegrant particle with higher size. If the agglomerate can be caged in a BCC packing, the latter remains in case I. However, if such a caging is not possible, the system switches locally from case I to case II.

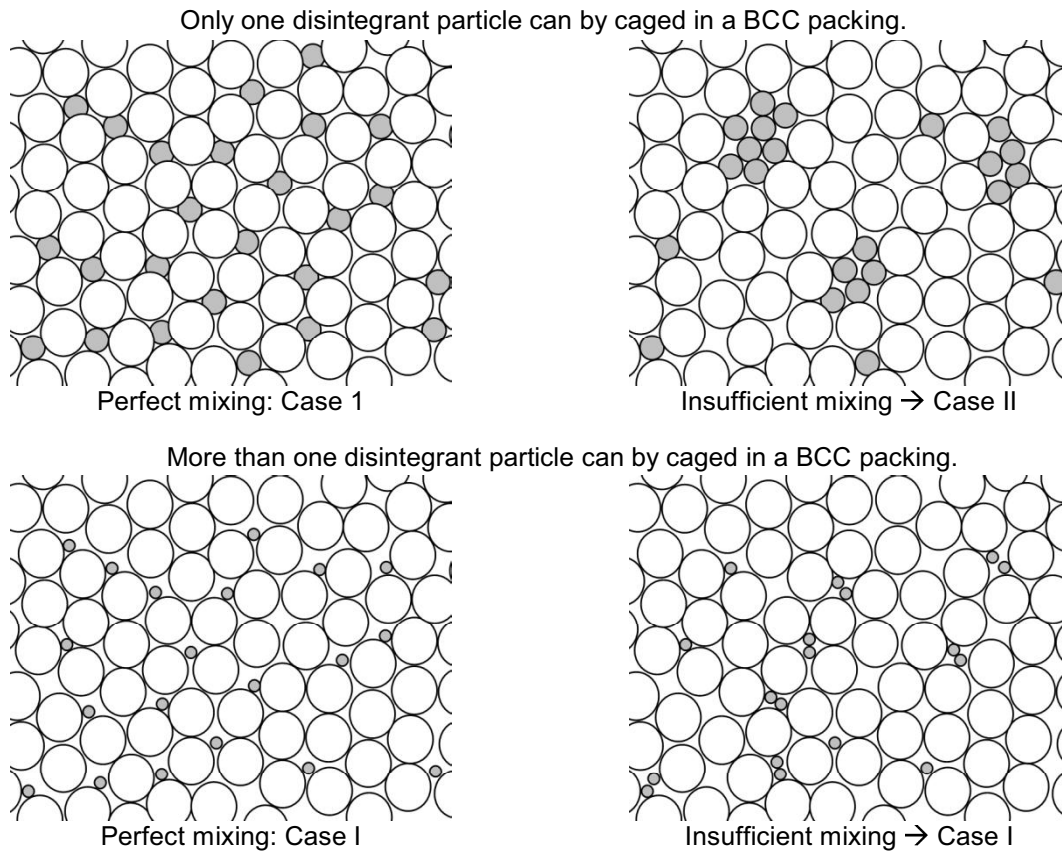


Figure 4.10: Evolution of the case between perfect and insufficient mixing with regard to the disintegrant mean particle size.

Calculation of the optimal disintegrant fraction for the fastest disintegration time of a tablet

As was mentioned previously, the shortest DT of a tablet usually occurs when the diffusion time of water within the compact is minimal. Combination of the presented tablet model with percolation theory enables calculation of the minimum volumetric fraction of a tablet in which water can diffuse. From this fraction, it is possible to deduce the optimum disintegrant fraction. According to percolation theory model, the minimum diffusion time for water is obtained when the water-conducting fraction of the tablet is equal to the percolation threshold of a RCP system.

Below percolation threshold, the water-conducting fraction (pores and disintegrant grains) doesn't form a continuous cluster (see section 3.3.1D) and water cannot diffuse straight through the tablet. In an ideal system, this continuous cluster appears at the exact value of the percolation threshold. Above this critical value, dead end arms start appearing on the main backbone of the continuous cluster. These arms retard water uptake as they absorb part of the liquid during the diffusion process.

The analytical value of site and bond percolation thresholds for RCP systems have been calculated using Monte-Carlo methods and are known with quite high precision (MCLachlan et al., 1990) as reported in Table 4.1. Site percolation threshold was chosen as the most suitable value to be used in modeling and design of robust pharmaceutical formulations.

As it can be seen in the Table 4.1, the threshold values for site and bond percolation (p_{cb} and p_{cs} , respectively) are different for different lattice types. However, the product values of bond thresholds and coordination number (zP_{cb}) are remaining approximately in the same range (average $zP_{cb}=1.5\pm 0.1$). This allows determination of bond percolation threshold in a compact by defining the lattice with a given coordination number. However, the model proposed here is based on site percolation in a multi-particulate system. The product of filling factor v and site percolation threshold, vP_{cs} , is remaining approximately in the same range as well (average $vP_{cs}=0.16\pm 0.02$). In a three dimensional multi-particulate system, the filling factor v represents the solid fraction of the volume. In a system composed of spheres, all randomly packed in close contact (RCP sphere system), v can be expressed through the voids fraction of the volume (porosity ϵ) as $1 - \epsilon$. This shows a key dependency of percolation threshold on porosity.

Table 4.1: Critical parameters for bond and site percolation on a variety of lattices. ^[44]

Lattice*	P_{cb}	P_{cs}	Coordination number, z	Filling factor, v	zP_{cb}	$vP_{cs}=\theta c$
fcc	0.119	0.198	12	0.7405	1.43	0.147
bcc	0.179	0.245	8	0.6802	1.43	0.167
sc	0.247	0.311	6	0.5236	1.48	0.163
Diamond	0.388	0.428	4	0.3401	1.55	0.146
rcp		0.27		0.6		0.162
Average					1.5 ± 0.1	0.16 ± 0.02

*fcc is face-centred cubic, bcc is body-centred cubic, sc is simple cubic, and rcp is random close packed.

As shown in Table 4.1, in case of uncompressed RCP spheres, the solid fraction at what the infinite cluster of disintegrant can be formed is 0.16 ± 0.02 (16%). It is a site percolation threshold for RCP packing. This value can be used for both cases of drug/disintegrant arrangements. Furthermore, it is considered that the porosity is constituted only by the space between drug particles. This space is assumed to be spherical (Figure 4.11). The neglected porosity (outside the model spherical pores) is indeed very small in comparison to the total porosity of a tablet. According to these assumptions, the percolation threshold of the porous fraction (empty spheres in the RCP system) can be considered to be 16 % as well. The critical volumetric ratio of voids to form a water conductive network of hollow interconnected spheres

has to be above 0.16 (v/v). It means that a compact compressed at porosity above 0.16 (v/v) will conduct water through percolating cluster of pores (if hydrophobicity of drug particles is not too high).

In the case I, as it was previously explained, the disintegrant particles volume is included into the porosity one (Figure 4.8) and caged disintegrant particles are assumed to be water conductive. Thus, it can be assumed that the space occupied by voids can be supplemented by the space occupied by the caged disintegrant. When reached by water, disintegrant particles will apply a mechanical force to destroy the compact due to swelling. That leads to the following theoretical assumption: in the case of caging (case I), the cumulative percolating volume is the volume of voids plus the volume of disintegrant.

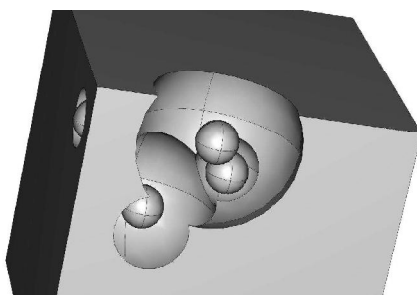


Figure 4.11: 3D representation (idealized model) of pores occupied by disintegrant particles. Four hollow interconnected spheres (pores) entrap small spheres (disintegrant particles).

Porosity of a compact is calculated as a volumetric ratio of pores in the tablet, using the following equation:

$$\varepsilon = 1 - \frac{M_{\text{powder}}}{V_{\text{tab}} \rho_{\text{tab}}} \quad \text{Equation 65}$$

where V_{tab} is the volume of the tablet, M_{powder} is the mass of the tablet and ρ_{tab} the density of the mix. The value ρ_{tab} can be calculated as follows:

$$\rho_{\text{tab}} = v_{\text{drug}} \rho_{\text{drug}} + v_{\text{dis}} \rho_{\text{dis}} = (1 - v_{\text{dis}}) \rho_{\text{drug}} + v_{\text{dis}} \rho_{\text{dis}} \quad \text{Equation 66}$$

where v_{drug} and v_{dis} are the weight fractions of drug and disintegrant respectively, and ρ_{drug} and ρ_{dis} are true densities of drug and disintegrant respectively.

According to above described theoretical assumptions, the following equation can be derived to calculate the location of percolation threshold:

$$X_d = \left(\frac{p_c}{1-\varepsilon} - \varepsilon \right) 100 \quad \text{Equation 67}$$

where X_d is the concentration of disintegrant in a powder mixture (% v/v), p_c is 0.16 ± 0.02 and ε is the porosity of compact. The multiplier $1/(1-\varepsilon)$ is a filling factor. It has to be applied in order to assure that the solid fraction in the final compact will be $1-\varepsilon$, $p_c/(1-\varepsilon)$ is the total percolation ratio. As disintegrant volume is included in porous volume, ε must be subtracted from $p_c/(1-\varepsilon)$ in order to get minimum amount of disintegrant to have a percolating cluster through the tablet. Distinction should be done between the filling factor $p_c/(1-\varepsilon)$ applied to p_c and the pores fraction ε participating to the percolating cluster volume. It has to be noticed that, in case I, if the fraction of disintegrant is too important, there would not be enough voids to cage every disintegrant grain. The grains will remain outside the porous network and, if sufficient amount of disintegrant is present, create an continuous cluster of disintegrant grains, independently of the combined pores/caged disintegrant network. However, it will be shown further that for a disintegrant fraction greater than X_d (Equation 67) the disintegration time will increase again.

In case II, porosity and disintegrant represent two independent networks for the diffusion of water (see previously). Porosity cannot be subtracted from the disintegrant volume. There are two possibilities for water to diffuse through a tablet: through a percolating cluster of pores or through a continuous cluster of disintegrant. As 16 % porosity is often too high for robust tablets, the second solution is preferred, and only the diffusion through disintegrant particles is taken into account. In this respect, Equation 67 is simplified to the following, as ε is not taken into account in the percolating fraction:

$$X_d = \left(\frac{p_c}{1-\varepsilon} \right) 100 \quad \text{Equation 68}$$

Even if porosity does not form alone a percolating cluster, it contributes to the diffusion of water. However, this effect is assumed not to play a significant role due to the swelling of big disintegrant particles, which block the adjacent pores of the percolating cluster of disintegrant.

The resulting equation for both cases can be presented in the form of piecewise function:

$$X_d = \begin{cases} \frac{P_c}{1-\varepsilon} - \varepsilon; & \text{if } \frac{r}{R} \leq \sqrt{3} - 1 \\ \frac{P_c}{1-\varepsilon}; & \text{if } \frac{r}{R} > \sqrt{3} - 1 \end{cases} \quad \text{Equation 69}$$

Equation 69 represents a generalised model to determine the location of percolation thresholds for pharmaceutical compacts, connecting the effect of porosity and the particle size ratio of the components. The value X_d represents the optimum amount of non-fibrous disintegrant for binary fast-disintegrating formulation. If in a binary mixture, the drug particles are highly hydrophobic, capillary diffusion will not be possible. In this case Equation 68 will be used to calculate ratio of disintegrant necessary to get an infinite cluster of disintegrant through the tablet (independently of the value of r/R). Indeed, wicking effect of disintegrant will force the water to cross the system.

Calculation for multi components tablet using renormalisation method.

In case of multi components tablet, the model presented previously can be used by renormalising the system. Basic principle of renormalisation is explained in section 3.3.1C.

Example of application is given with a compacted ternary mixture composed of disintegrant grains, hydrophobic filler particles, and larger dense pellets. The aim is here to design a tablet with a maximum of pellets inside but with a minimum DT, in order to liberate quickly the pellets into the stomach. In this case, it is necessary to design a tablet with a continuous water-conducting network crossing the tablet between pellets. It is then obvious that the fraction situated outside pellets must conduct water. To achieve this, the binary mixture composed of disintegrant/filler must be designed accordingly to the previous model for binary systems. Depending on the difference of size between disintegrant and filler particles, the binary mixture should be designed according to case I or II. When designed, the binary fraction can be considered as one homogeneous water-conducting fraction. Next step is the design of the new binary mixture composed of pellets fraction and disintegrant/filler fraction according to case I (disintegrant/filler fraction can be caged by pellets). This will enable to create a continuous cluster of disintegrant/filler fraction within the tablet. If the compacted ternary mixture is correctly designed, the water will diffuse through disintegrant/filler fraction between pellets and tablet will be fast disintegrated.

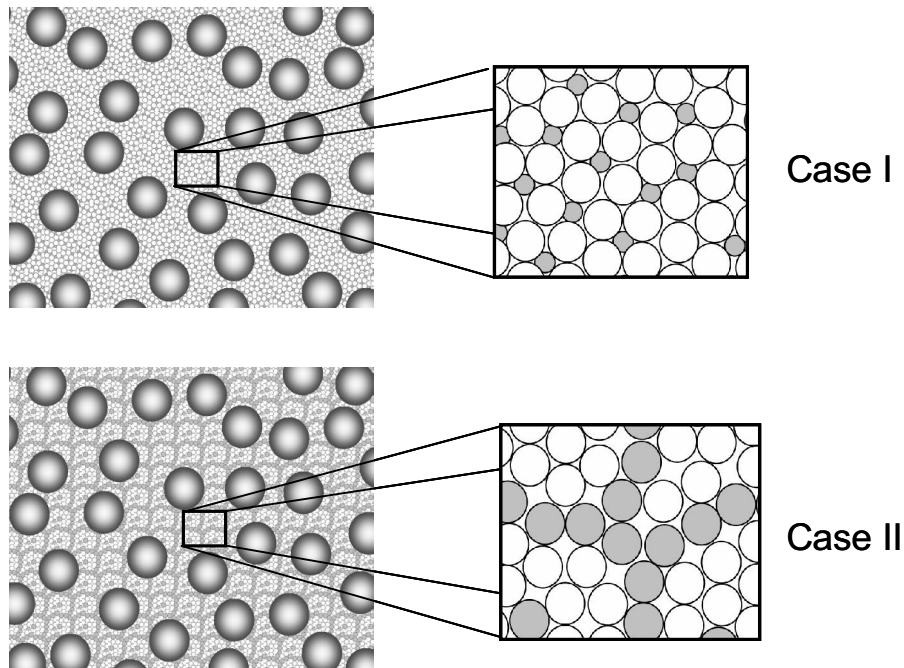


Figure 4.12: Compacted ternary mixture of disintegrant, hydrophobic filler and pellets containing a water-conducting network composed of disintegrant/filler fraction. Two dimensional views of systems with disintegrant/filler fraction in case I and in case II are depicted.

Implemented software for automatic disintegration optimisation

This program is the “Disintegrant Optimisation” (DO) module of the expert system (4.1.3). The module was implemented to enable users of ES to calculate automatically the optimum amount of non-fibrous disintegrant required for the fastest DT of a tablet (an overview of the interface is shown in Figure 4.13). The module can be used separately or in combination with other modules of ES for a complete design process of a tablet.

Software takes in inputs parameters of the tablet itself and parameters of the components of the tablet (see Figure 4.13). Among parameters of the tablet, the diameter and the thickness are required to calculate the volume of the cylindrical tablet as follows:

$$V_{tab} = \pi \left(\frac{d}{2} \right)^2 t \quad \text{Equation 70}$$

where V_{tab} is the cylindrical tablet volume (mm^3), d is the tablet diameter (mm) and t its thickness (mm).

Mean particle diameter of a component is used as a unique particle size value to determine in which case the RCP system is (see Equation 63 and Equation 64). It has to be remembered that mean particle size of a substance can be assume to be the unique value of each of its particles only if the particle size distribution is narrow.

True densities of the components and tablet weight are used to calculate the true density of the mix according to Equation 66. Percolation threshold is given in the form of a range of values (calculation using each extreme value of percolation threshold will be given in output). Percolation threshold of 0.16 (most precisely known value for RCP systems) are registered by default. However, latest published values for RCP thresholds can be given in future.

After decision of the system case (I or II), the program calculates the optimal % (v/v) of disintegrant for the shortest DT using Equation 67 or Equation 68. The optimal % in volume and in mass of the solid fraction (powder mix) is given for each component. Indeed, % in mass of solid fraction are required for preparation of the mix to compress. Tablet volume % of each component and of porosity (see Equation 65) are also given in outputs. The left editing window of the interface resumes parameters in inputs and gives calculated outputs: volume of the tablet, selected system case, volumetric and mass % of drug and excipient (or disintegrant) in solid fraction and volumetric % of drug, excipient and porosity in the tablet.

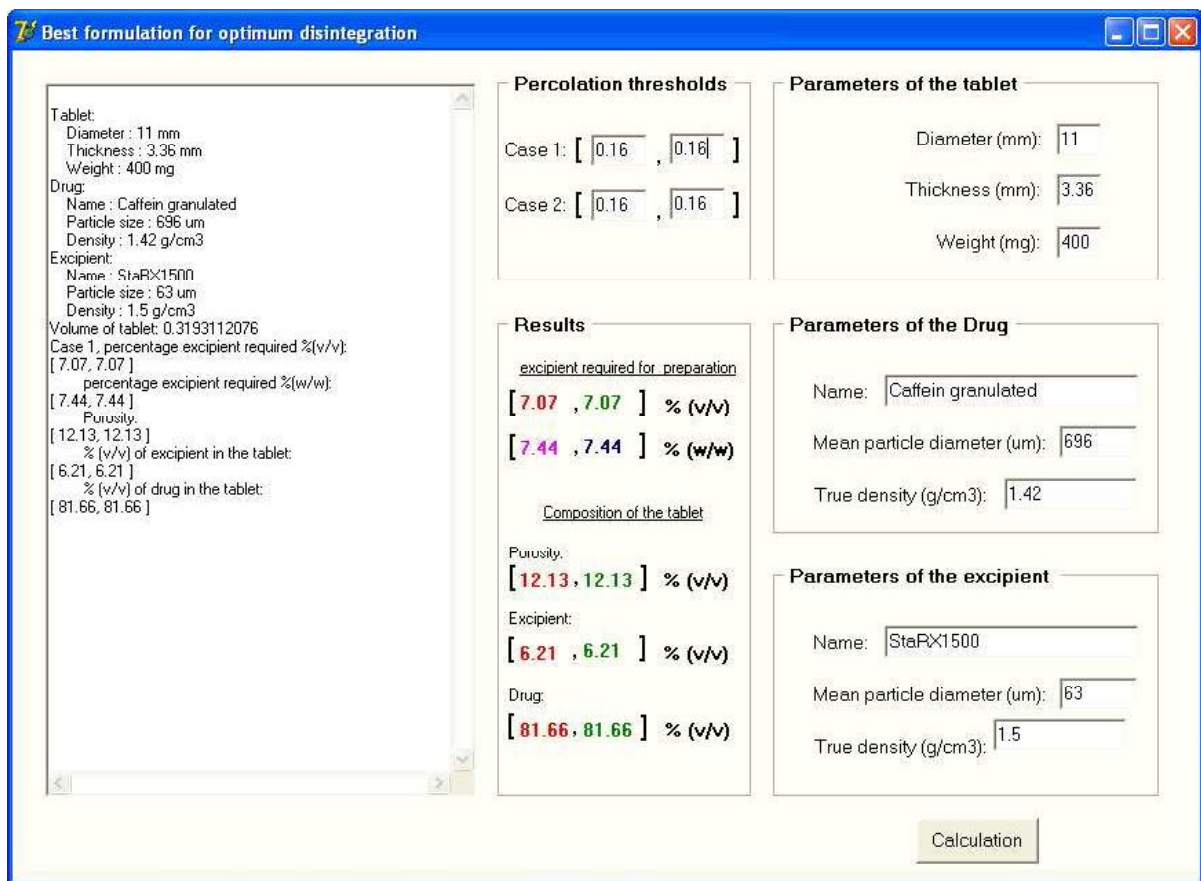


Figure 4.13: View of the interface of DO module of the Expert System after calculation with a binary mixture of Caffeine (drug) and StaRX1500 (disintegrant).

B. Fibrous disintegrants

The model presented previously concerns tablets with non-fibrous disintegrants. For a tablet containing disintegrant exhibiting a fibrous shape (e.g. AcDiSol[®]), another model was developed for calculation of the optimum disintegrant content. This model uses also percolation theory but is with a percolation type.

As said previously, site percolation threshold in a tablet (RCP sphere model) is assumed to be 16 % (v/v) in terms of solid fraction. However, threshold of fibrous material in RCP system should be significantly smaller. Indeed, advised % of AcDiSol[®] is usually from 2 to 4 %. This shift of threshold can be explained with percolation on overlapping spheres.

Overlapping spheres

Overlapping spheres are spheres that have their centres within each other (Figure 4.14). Thus the task is to estimate the amount of spheres N when the percolation takes place. Obviously, the critical value can be expressed as follows:

$$B_c = \frac{4\pi}{3} N_c R^3 \quad \text{Equation 71}$$

where N_c is a critical amount of spheres and R is a sphere radius. Value B_c is a constant of value 2.7 ± 0.1 for spherical particles (MCLachlan et al., 1990)). Thus, an increase in particle radius R will result in decrease in amount N_c of percolating spheres. Important is to note, that value B_c does not depend on the lattice type thus can be applied for RCP systems as pharmaceutical compacts. The physical meaning of the constant B_c is the amount of centres of the spheres (nodes) within one sphere.

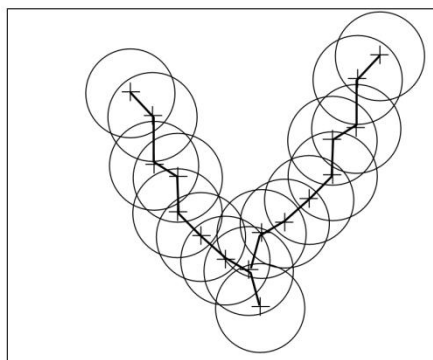


Figure 4.14: Overlapping circles. Bold lines denote percolation path.

Percolation on overlapping ellipsoids of revolution

Fibrous particles like AcDiSol® are approximated as ellipsoids of revolution in this model (see Figure 4.15).

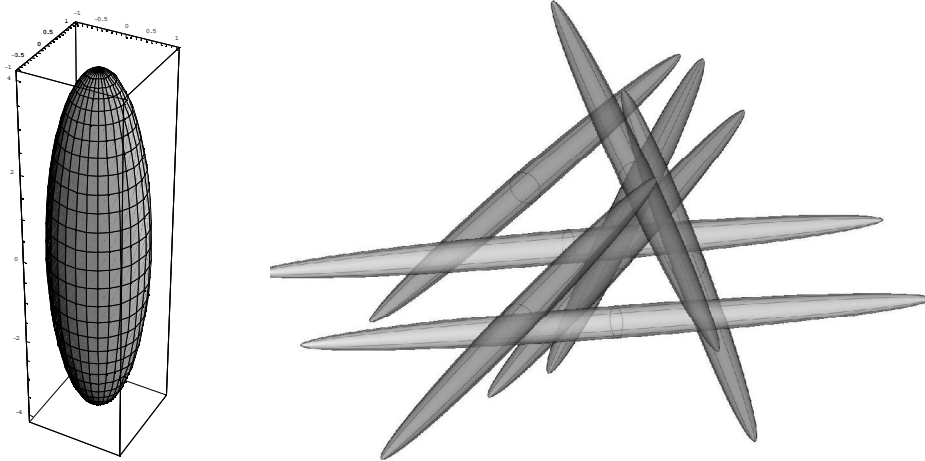


Figure 4.15: Ellipsoid of revolution and packing of fibrous disintegrant particles.

The critical value of B_c is the same as for overlapping spheres. The latter can be proved as follows (Efros, 1982):

Ellipsoid of revolution can be formed from an original sphere (Figure 4.16) by applying the following transformations: $y=y'$, $x'=k_1x$, $z'=k_2z$ (k_1 , k_2 are stretch factors).

If all of the randomly distributed overlapped spheres (and all the points on them) are undergoing the transformation $y=y'$, $x'=k_1x$, $z'=k_2z$, the new values for the coordinates x' and z' are remaining to be randomly distributed as well in the interval from 0 to k_1L (from 0 to k_2L for z), where L is a dimension of the system. The coordinates y remains intact. Thus the concentration N has changed to N' . All of the spheres have been transformed to ellipsoids of revolution with volume:

$$V = k_1 k_2 \frac{4\pi}{3} N' R^3 \quad \text{Equation 72}$$

Thus the new value for constant B has to be introduced $B'=N'V$:

1. $B=B'$. All the nodes (coordinates of the centres of the initial spheres) that were located within certain sphere are now located within an ellipsoid. Indeed if a sphere is deformed, all the outer points remain outside and inner points remain inside. Thus the amount of nodes B' , that are located inside of a deformed sphere is the same as for initial sphere B .

2. If $B > B_c$ then $B > B'_c$ and if $B < B_c$ then $B < B'_c$. Indeed, if prior to the transformation two spheres were overlapping; the ellipsoids will overlap each other as well after transformation (see above). That means that if $B > B_c$ then there is percolation on overlapping spheres and

consequently there is a percolation on overlapping ellipsoids. Converse sentence is true: $B < B_c$ then there is no percolation on overlapping spheres and consequently there is no percolation on overlapping ellipsoids.

3. As the clauses: if $B > B_c$ then $B > B'_c$ and if $B < B_c$ then $B < B'_c$ have to be true for any B , the clause $B_c = B'_c$ is true as well.

Thus we have shown that the critical values B_c for overlapping spheres and ellipsoids of revolution are the same. This has a very important meaning:

- if the spheres (or ellipsoids) are not overlapping, i.e. $B_c < 2.7$ the percolation threshold for such systems is the same as for randomly packed spheres ($p_c = 0.16 \pm 0.02$)
- if $B_c > 2.7$ the critical concentration of ellipsoids necessary to form an infinite percolating cluster is the same as for the overlapping spheres.

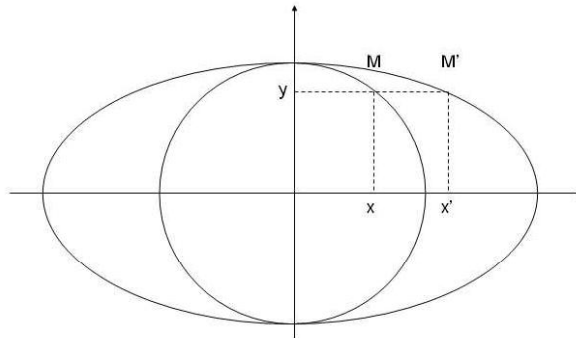


Figure 4.16: Ellipse formed by stretching the original circle.

Calculated values of percolation thresholds for overlapping ellipsoids of revolution

Calculated percolation thresholds on overlapping ellipsoids of revolution of different aspect ratios (major radius divided by minor radius) were published (Garboczi et al., 1995) and are listed in Table 4.2. Furthermore recent numerical findings have revealed a new critical value for overlapping ellipsoids equal to 0.0315 for ellipsoids of aspect ratio 20 (YI et al., 2004).

Table 4.2: Percolation thresholds and geometrical data for randomly oriented overlapping ellipsoids of revolution, placed in a cubic cell of unit edge length.

a/b: aspect ratio

n_c : number of particles at percolation

p_c : volume fraction of particles at percolation (percolation threshold).

Aspect ratio	a	b	n_c	p_c
1/2000	0.000012	0.024	22005	0.0041637
1/1000	0.000024	0.024	22028	0.001275
1/100	0.00024	0.024	21691	0.01248
1/10	0.0025	0.025	17089	0.1058
1/8	0.0030	0.024	18637	0.1262
1/5	0.0044	0.022	21659	0.1757
1/4	0.0055	0.022	20046	0.2003
1/3	0.0070	0.021	20103	0.2289
1/2	0.010	0.020	18209	0.2629
3/4	0.015	0.020	13243	0.2831
1	0.025	0.025	5134	0.2854
3/2	0.030	0.0200	6521	0.2795
2	0.020	0.0100	36235	0.2618
3	0.030	0.0100	20219	0.2244
4	0.040	0.0100	12581	0.1901
5	0.040	0.0080	16557	0.1627
10	0.050	0.0050	17389	0.08703
20	0.060	0.0030	18740	0.04150
30	0.060	0.0020	26679	0.02646
50	0.060	0.0012	41827	0.02646
100	0.060	0.0006	77069	0.006949
200	0.060	0.0003	141458	0.003195
300	0.060	0.0002	204373	0.002052
500	0.060	0.00012	333258	0.001205

Design of a percolating network of fibrous disintegrant particles

Let's consider a compacted mixture of non-fibrous components (drug, filler, etc.) and a fibrous disintegrant. This tablet can be modeled using a RCP spheres system containing ellipsoids of revolution.

According to this model, it is possible to build a hydrophilic continuous cluster of fibrous particles spanning the whole tablet at a critical concentration of disintegrant. In this case, water could diffuse straight through the whole tablet and DT would be minimal.

However, disintegrant particles cannot penetrate inside each other like overlapping spheres. It is then assumed that a simple contact between disintegrant particles corresponds to an overlapping.

In this model, porous volume fraction cannot be added to disintegrant volume fraction as their respective network structures are different (similar demonstration than for non-fibrous disintegrant model in Figure 4.7). It is thus considered that water could diffuse through porous network between drug particles if tablet porosity is at least 16 % (v/v) (porous space formed by fibrous disintegrant particles is neglected) and if pores are not too hydrophobic. As in the previous model, such a porosity value is usually not compatible with robust tablet. It is then considered that, to ensure a direct water uptake by the compact, a continuous network of fibrous disintegrant particles should be installed (see schematic view in Figure 4.17).

To design this network, the mean aspect ratio of fibrous disintegrant particles should be first estimated and compared with aspect ratios in Table 4.2. Percolation threshold on ellipsoids having aspect ratio the closest to the mean aspect ratio of disintegrant fibers should be the most relevant threshold (p_c). $p_c \times 100$ will then give the optimal volumetric % (can be converted in mass % with Equation 66) of disintegrant for the shortest DT of a tablet. Below this value, disintegrant particles will form only isolated clusters, whereas above this %, dead end arms will appear on the backbone of the main percolating cluster and will retard water uptake.

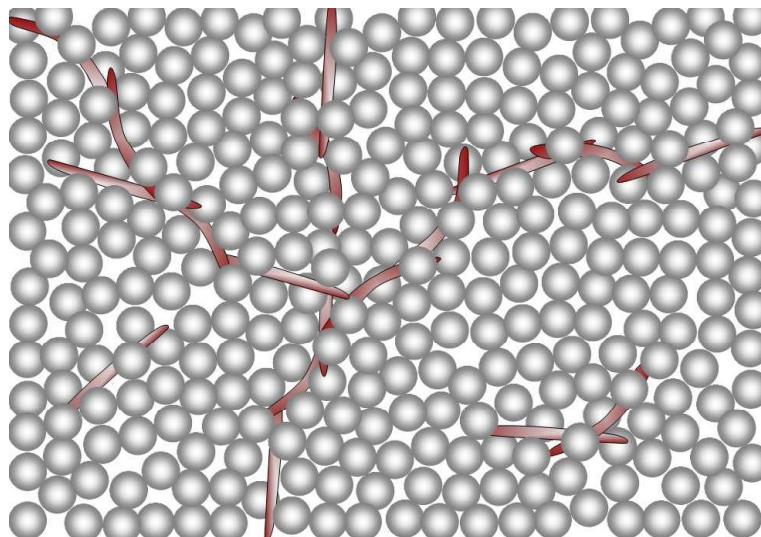


Figure 4.17: Schema of percolating fibrous particle of disintegrant within a compact.

Until now, it was considered in this model that fibrous disintegrant particles stay relatively straight between other components during compression process. However, in case of very

long and thin fibers (high aspect ratio), fibrous particles may get deformed and folded in the final compact. In this case, it is not possible to use directly theoretical values of percolation threshold for straight fibers. However, a folded fiber could be considered as a straight smaller but thicker particle (lower aspect ratio). If only a certain quantity of fibrous particles are totally or partially folded in a tablet, it will change the percolation threshold value for disintegrant. As the percolation threshold value for fibers increases while decreasing their aspect ratio (Berhan et al., 2007a, 2007b), disintegrant percolation threshold of a system containing folded fibers will increase. Unhappily it is not possible to quantify exactly the fraction of folded fibers in a tablet. Furthermore, the curvature and the form of curvature are key parameters for threshold. It is in fact impossible, in such a biased system, to determine exactly the optimum % of disintegrant. In this case, the only possibility to estimate optimum disintegrant content is to choose % disintegrant corresponding to two extreme systems, i.e. a system in which all fibers are straight and a system in which all fibers are folded (see Table 4.2).

Moreover, it may be very difficult to estimate at which aspect ratio fibers of a material would start folding in a compact. Indeed, ability to fold during compression may depend on many factors (e.g. rigidity of the disintegrant material, compression force, etc.).

To formulate of tablet with disintegrant particles of unknown folding capacity, it is advised to use a % disintegrant comprised between threshold for ellipsoids with an aspect ratio close to that of straight disintegrant fiber and threshold for ellipsoid with an aspect ratio close to that of totally folded disintegrant fibers (threshold values could be taken from Table 4.2).

It would be also possible to estimate experimentally the optimum disintegrant % as follows:

- Measure disintegration time of tablets containing a % of disintegrant equal to the percolation threshold of ellipsoids having an aspect ratio close that of a straight disintegrant fiber.
- Same experiment but with a % of disintegrant equal to the percolation threshold of ellipsoids having an aspect ratio close to that of a totally folded disintegrant fiber.
- Comparison of the two measured DT and selection of the best formulation.
- Further approximations can be performed in the same way by ranging at each cycle the previously selected optimum % disintegrant.

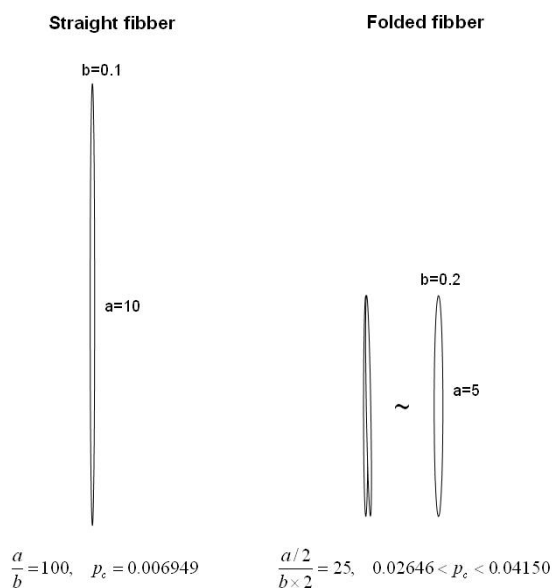


Figure 4.18: Comparison of percolation thresholds for straight fibers (aspect ratio = 100) and for same but totally folded fibers (aspect ratio = 25). Threshold values come from Table 4.2

4.3.2. Dissolution simulation of a pharmaceutical compact using CA modeling

A. General concept and innovative aspect of the simulation

The Dissolution Simulation (DS) module provides a software platform for designing and simulating dissolution of a solid dosage form. Tablet Designer (TD) and Databases (DB) modules will be also presented in this section. They are in fact essential modules to design the virtual tablet and to fill it up with ingredients.

As explained in section 4.1.3, *in silico* tablet pattern is built and discretised with TD module. DB module stores all needed information about active ingredients and excipients. DS module receives in input data discrete tablet model from TD and information on tablet composition from DB. Dissolution simulation algorithm can be executed only after reception of these elements.

Dissolution program uses cellular automata (CA) to imitate natural mechanisms (see section 3.3.2) involved in tablet dissolution process. Indeed, contrary to existing models, the simulation does not use partial differential equations (PDEs) or generalised mathematical descriptions of dissolution profiles. Advantages of this innovative implemented method are the following:

- With CA, a tablet is discretised per units of a cubic matrix. Modeling is thus closer to real dissolution. A tablet is not in fact a homogeneous system but a compacted mixture of particles.

- CA modeling enables an easier control, modification, and design of the system. Rules set, matrix cells states and constants associated to cells can be changed separately and constantly improved.
- Algorithm computation is usually faster for CA simulation than finite or discrete element methods, but slower than PDEs modeling. Computation speed depends however on processor capacity of the computer running the algorithm and on the dissolution system scale (dissolution matrix size).
- It is possible to visualise a virtual tablet during dissolution process. This option depends also on computer capacity and system scale.
- An interesting point with CA modeling is that some non-implemented mechanisms are automatically simulated (water diffusion through fractal porous structure). Indeed, by imitating only simple rules of nature, new complex natural phenomena and structures may appear automatically in the simulation matrix.
- Component particles are discrete models in the system. Furthermore, size, shape and physico-chemical properties of real particles are modeled. It is thus possible to use DS module for designing and developing new excipients by studying the influence of particles shape, swelling force, etc.

B. Tablet pattern design and discretisation using Tablet Designer (TD) module

A virtual tablet can be designed with TD module by setting its shape, dimensions and caps. Tablet pattern will be then exported to the virtual 3D dissolution matrix. This virtual matrix is made up of an ensemble of small cubic cells that represent the discrete units of the CA.

Interface and functionalities of TD module

Interface of the software (see Figure 4.19) is divided into two frames. In the left frame, a tree view list displays various shapes and options to design and assemble different part of a tablet (middle part, bevel edged section and caps). In the right frame, editing windows are displayed to set the tablet parts dimensions (in mm) and the mean particle size (in μm). Two buttons are also provided for visualising the tablet and for creating its discretised model. All components of TD interface are detailed below.

Height different global tablet shapes are proposed in left tree view list: round, oval, diamond, rhombus, pillow, square, oblong and drum. When selecting one shape, a second level appears in the tree list and proposes either to keep a simple flat tablet or to add bevel edged sections. At the same time, editing spaces appear at right to enter horizontal dimensions (e.g. diameter) of the middle part section. If “Central flat part” icon is selected, the right frame displays an editing space to write its height. If the user select “Bevel edged caps”

icon, he must enter horizontal and vertical dimensions of these caps (see example in Figure 4.19). The formulator can then add concave caps either above central flat part or above bevel edged caps. To add concave caps, the user must select “Concave caps” icon and enter their dimensions in editing spaces of the right frame.

It is clear that dimensional information to give in input are adapted to the main shape of the tablet. For example, the design of a round tablet required only diameters and heights of each sections of the tablet. Whereas, in case of diamond or drum shape required information are more complex.

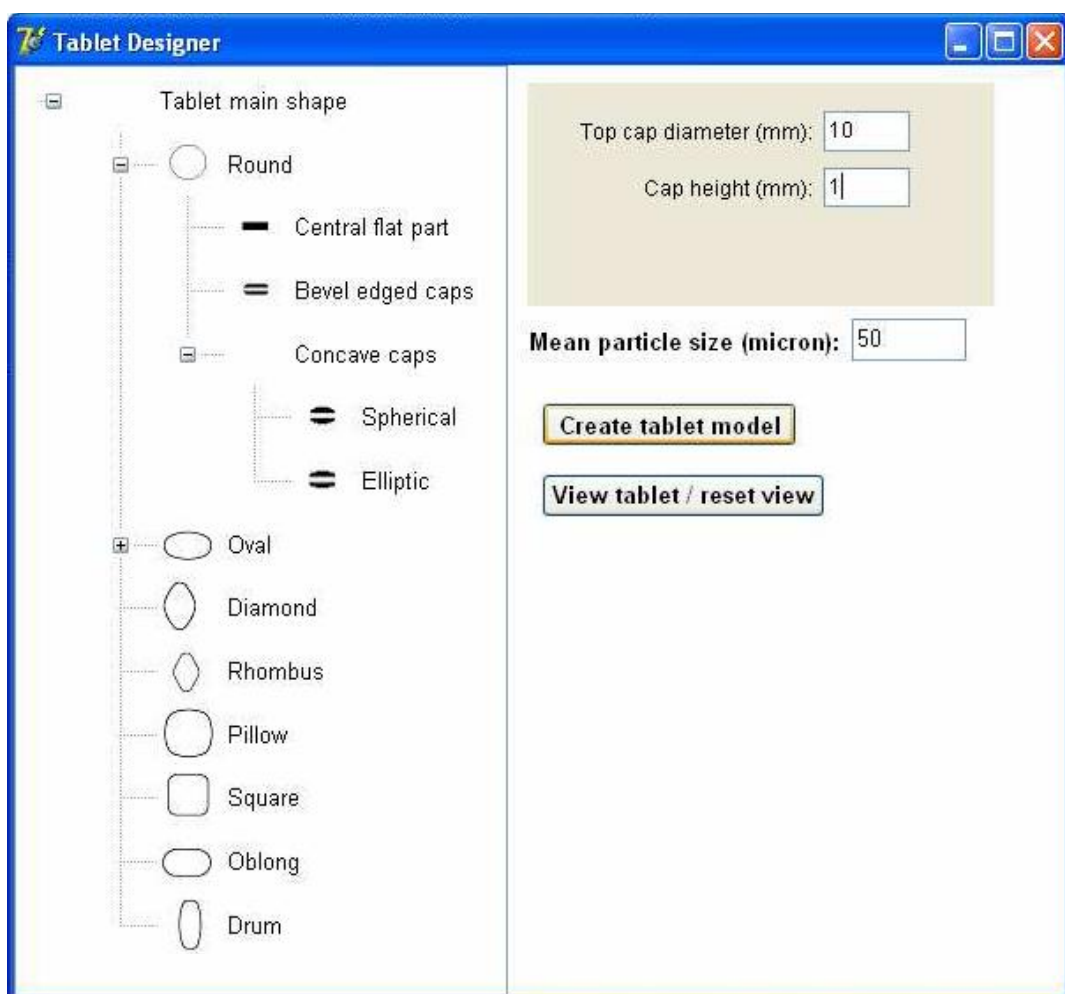


Figure 4.19: Windows interface of “Tablet Designer” module while creation of a spherical tablet.

TD module offers the possibility to visualise at any moment the state of the designed tablet pattern (Figure 4.20). The button “View tablet” displays thus two types of view:

- 3D view of the continuous pattern.
- 2D views of the discretised tablet in the matrix. In this case, each black pixel on the computer screen corresponds to a tablet cell.

“Create tablet model” button enable to run an algorithm that discretised tablet pattern (see next part of this section). This program creates into the dissolution cubic matrix a 3D virtual tablet composed of cells.

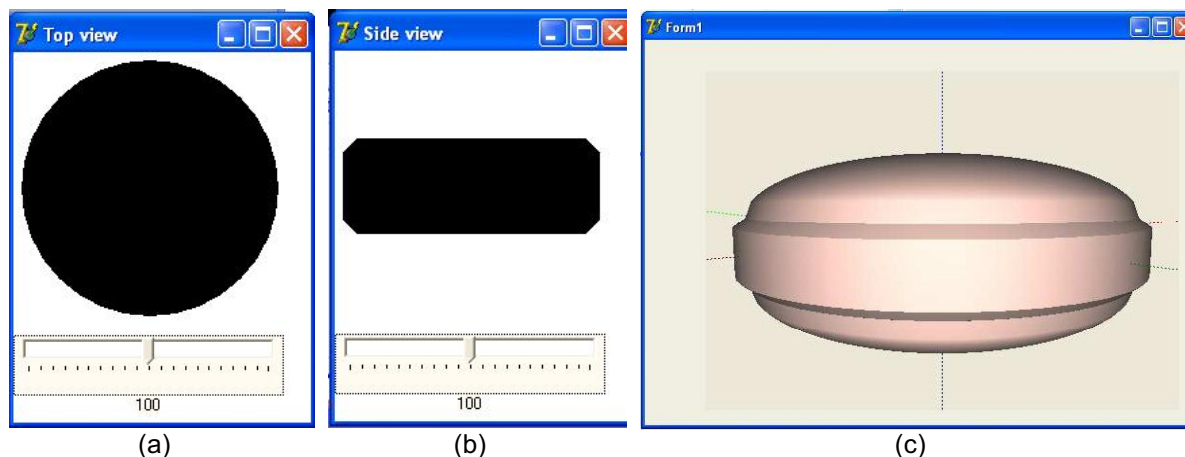


Figure 4.20: Tablet visualisation windows displayed by TD module:

- 2D views of a discretised tablet (round with bevel edged caps): upper view (a) and side view (b). Horizontal trackbars enable to change horizontal (a) and vertical grounds of the views.
- 3D views of the tablet model (round tablet with bevel edged section and spherical concave caps) on top (c). It is possible to rotate the tablet on vertical and horizontal axis with the computer mouse.

The “Mean particle size” editing space enables to set the scale of the dissolution simulation system. Smaller will be this value compared to tablet size smaller and more numerous the virtual particles will be in the tablet model. The difference of size between component particles and the volumetric % of each component in the system is not affected. The scaling option offers the possibility to set priorities in the modeling. A tablet model with more particles per component inside will give a more precise dissolution profile. However, running the algorithm will take more calculation time. Moreover, it is not always possible to simulate the dissolution of a virtual tablet, which contains the same number of particles than a real tablet (it is due to limited computer memory space). If the number of particles in the real tablet to model is too high, a “renormalisation” of the system can be done by the user with the scaling option.

The compromise to find between speed and precision of modeling depends on the memory capacity of the computer and on the calculation power of its processor. The advised operating mode for searching the optimal tablet formulation with respect to dissolution is as follows:

- Large primary formulations screening by running *in silico* dissolution in a small system (reasonable simulation time but imprecise tablet model).
- Fine screening of among the best formulations from primary screening (long simulation time few hours but virtual tablet model very close to real tablet).

Tablet pattern discretisation

After creation with TD module, tablet pattern has to be transformed into discretised model in the dissolution matrix.

Discretisation method is based on Bresenham's algorithms (see examples in Figure 4.21).

Bresenham's line algorithm determines which points in an n-dimensional raster should be plotted in order to form a close approximation to a straight line between two given points (Bresenham, 1965). The algorithm is commonly used to draw lines on a computer screen. Through a minor expansion, the original algorithm for lines can also be used to draw circles. The label "Bresenham" is today often used for a whole family of algorithms, which have actually been developed by successors of Bresenham with a similar basic approach.

Thus, the approach for the *Circle Variant* is also not originally from Bresenham but from Pitteway and van Aken (Pitteway, 1967; Van Aken, 1984).

Bresenham's algorithms are used by TD module to create a discrete tablet in the cubic matrix.

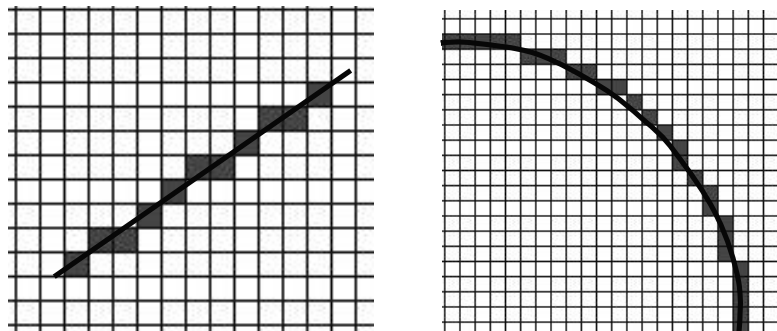


Figure 4.21: Transformation of continuous straight and curved lines into discretised similar lines in a square lattice using Bresenham's algorithms.

Discretisation algorithm is implemented as follows (algorithm schema in Figure 4.22):

- Continuous perimeters of tablet pattern are calculated with dimensions given in input of TD module. These perimeters are then drawn with black line in white Windows frames (the frames are not visible by the user). The algorithms used by the programming language (here Object Pascal) to convert straight and curved lines into pixelised lines are based on Bresenham's family algorithm. The continuous perimeters of the tablet pattern become thus discrete when they are drawn in Windows frames. The number of perimeters required depends of the tablet shape complexity. For example, for a round tablet, only one single perimeter is needed, whereas two different perimeters (along major and minor radii) are required for an oval tablet.

- Each frame used for drawing a perimeter represents a plan of the cubic matrix that crosses the centre of this matrix. Consequently, each pixel of the discrete perimeters has a 3D coordinate in the cubic matrix. Using these coordinates, each black pixel is converted into tablet cell in the matrix.
- The filling of the virtual tablet is performed by piling successively cells layers inside the cage formed by tablet perimeters. Full black slices of the continuous tablet model are first drawn one by one in Windows frames. Black pixels of each slice are then converted into tablet cells in the cubic matrix.

Finally, the cubic dissolution matrix contains a discrete model of the original tablet pattern, which was designed with the TD module. However, at this point, cells of the system (cubic matrix including the virtual tablet) have no “identity”. Next step before performing *in silico* simulation is to attribute to each cell of the tablet an identity corresponding to the substance that the cell is supposed to represent in the system. This task corresponds to the filling of the tablet with ingredients and is the topic of next part of this section.

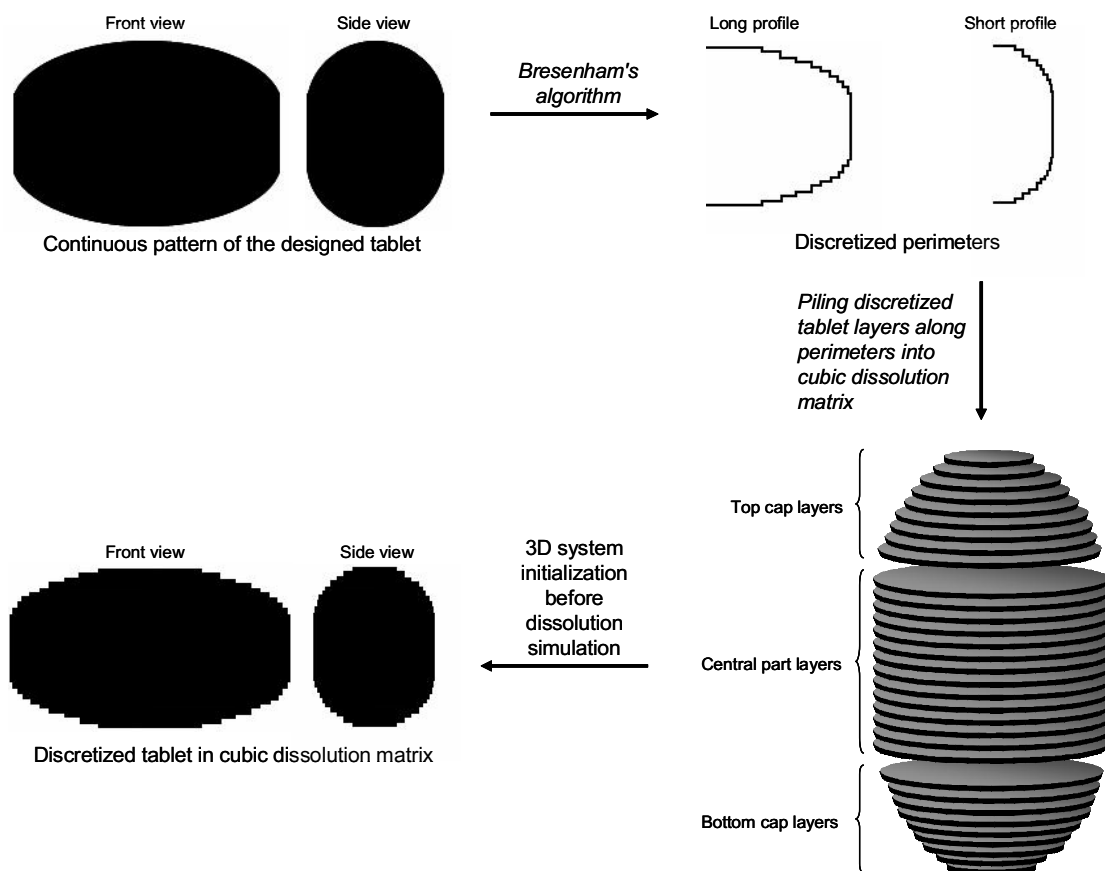


Figure 4.22: Schema of the algorithm used to transform a continuous tablet pattern into a discretised tablet model. The oval tablet in example is small for a visualisation of the discrete aspect of the compact. It is however possible to build bigger tablets (large scale) for which crenellated aspect of the tablet is much smoother (more realistic).

C. Setting up composition of a virtual tablet

This section explains the operating mode and implementation method of setting up *in silico* tablet composition in the dissolution matrix.

Particle-packing algorithm

First step to achieve is to pack randomly ingredients in the virtual tablet (RCP sphere system model, see section 4.3.1B). Ratios between mean particle sizes of the different components are respected. In the dissolution matrix, particles of each component have all the same size. Consequently, volumetric ratios between all ingredients of a formulation are conserved. Particles in the tablet are assumed to be spherical and are modelled with spheres. The spheres are placed at random in the system using a developed packing algorithm (see Figure 4.23).

Packing algorithm proceeds as follows:

- Tablet volume is calculated using tablet dimensions entered in input of TD module.
- Tablet volumetric fraction and mean particle size of each ingredient are given by the user. Volumetric fraction of each ingredient is divided by the volume of a sphere modeling a particle of this ingredient. The rounded result gives the number of particles to pack in the system for each component.
- Before each particle-packing a random number (from 0.0 and 1.0) is generated. The obtained number is compared to tablet volumetric fraction ranges of the components. The ingredient having a volumetric fraction range containing the random number is selected. Thus, probability of selecting a certain ingredient particle is equal to its volumetric ratio in the tablet and the components ratios in the virtual tablet are respected. A virtual particle of the selected ingredient is then placed in a free site of the tablet.

For example: a tablet contains 60 %(v/v) of caffeine (vol. ratio = 0.6), 20 %(v/v) of lactose (vol. ratio = 0.2), 10 %(v/v) of starch (vol. ratio = 0.2) and 10 %(v/v) porosity (vol. ratio = 0.1). The components ranges are for caffeine: [0.0, 0.6[, for lactose: [0.7, 0.8[, for starch: [0.8, 0.9[, and for pores: [0.9, 1[. A random number is generated and has a value = 0.3. Consequently, a virtual Caffeine particle is packed in the system.

This free site to place a new particle is chosen randomly among available sites of the matrix. If a selected site is too small in comparison to the size of a sphere, new random selections are performed until an appropriate site is found.

- After having packed a sphere, the free volume in the system is calculated and the program proceeds to the packing of a new sphere until all spheres of each ingredient are packed in the system.

Packed spheres will be calibrated to be slightly smaller than their true particle size ratio. The reason to this calibration is that particles of the virtual tablet should exhibit a certain deformation similarly to a real compact. This deformation will be obtained by growing particles in the system (see next part of this section).

An example of particle-packing in a virtual tablet volume is shown in Figure 4.23.

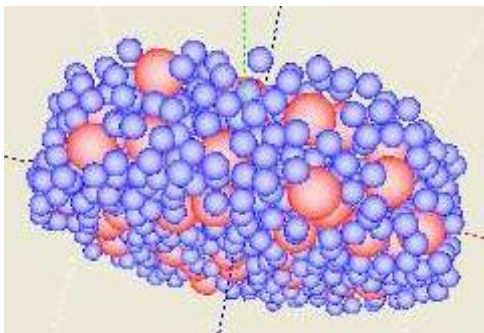


Figure 4.23: Picture of sphere packing in a round flat tablet volume obtained by the placing randomly two different sphere types (different dimensions).

Particle growing

Particle-packing enables allocation of particle spaces in 3D tablet model. Next step is to transform the RCP sphere system into a discrete compacted mixture of ingredients in the dissolution matrix (example in Figure 4.24).

To achieve this task, “seeds” are placed into matrix cells that are positioned at the centre of each particle (see Figure 4.24a₁). A seed is composed of two cells (computational reason) and is randomly oriented. Each particle in the matrix will be created by growing its own seed. Growing process is achieved by transforming each “empty” cell in the Moor neighbourhood of seed cells (see section 3.3.2) into a particle cell. In the same way, each newly created particle cell extends by transforming empty neighbouring cells into particle cells (see Figure 4.24a₁-a₂). A particle does not necessarily only expand in its direct neighbourhood. The expansion radius in Moor neighbourhood at each growing step is proportional to final particle size of an ingredient. This rule enables on one hand to respect particle size ratio between components and on the other hand to ensure their correct volumetric fractions of ingredients in the final tablet.

After a certain number of growing steps, particles will meet each other, i.e. they will share neighbouring cells. In this case, particles will grow round occupied cells, however only until a certain extent. Resulting effect is a deformation aspect of particles, similar to real compacts

(see Figure 4.24a₄). In order to respect the difference of hardness between components, deformation potential of *in silico* particles should be calibrated.

The growing algorithm will stop when the volumetric ratio of each component is obtained and/or when the desired tablet porosity is reached.

The user has the possibility to grow particles separately for each component in order to adjust imprecise volumetric fractions.

The result obtained with the particle growing algorithm is a discrete compacted mixture of ingredients that is ready for *in silico* dissolution in the cubic matrix.

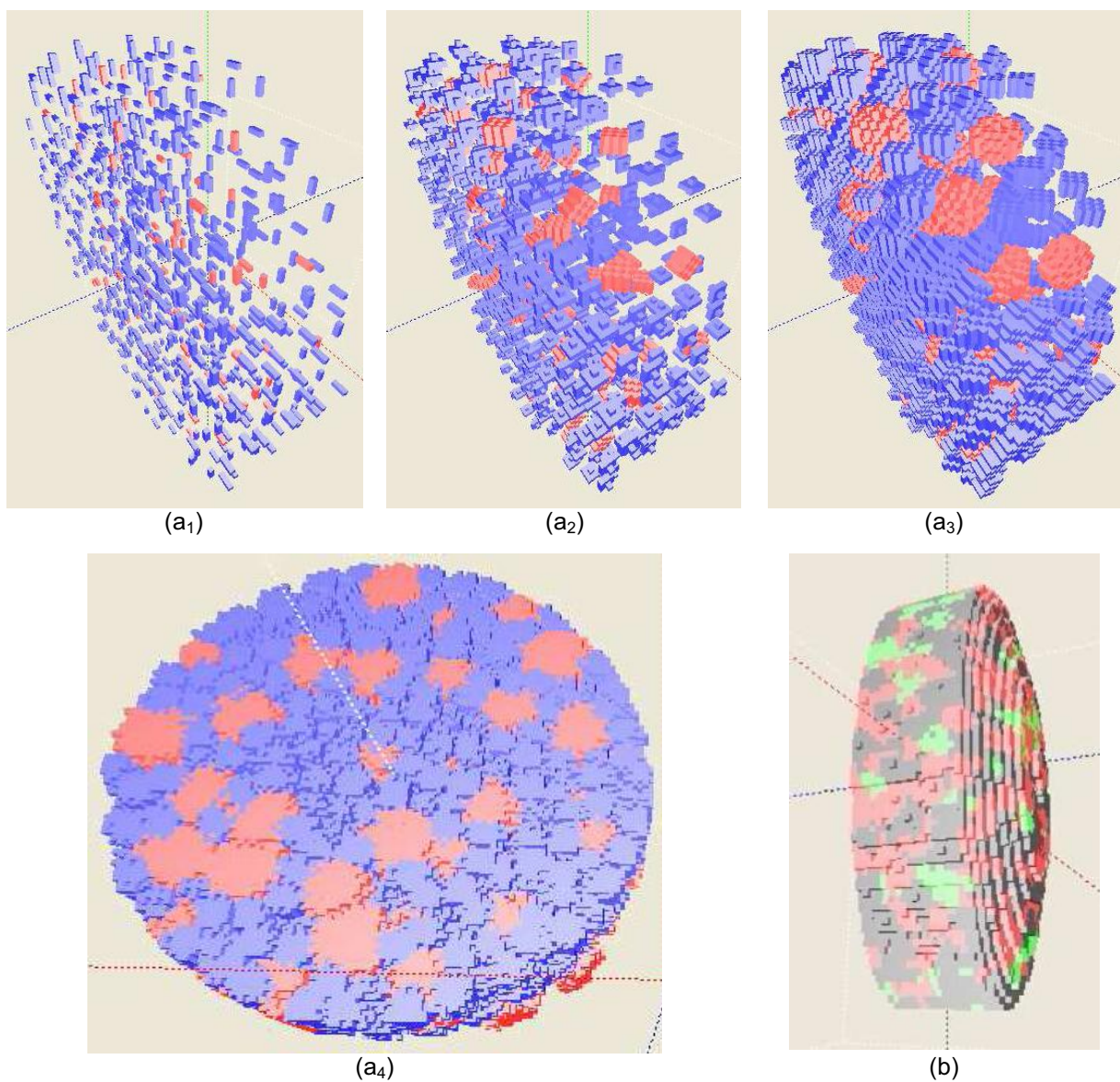


Figure 4.24: Pictures of virtual compacts in the dissolution cubic matrix.

(a₁)-(a₂): Some steps (seeds: a₁, final tablet: a₂) during particle growing process for a round flat tablet.
 (b): Virtual ternary compacted mixture obtained with growing algorithm (oval tablet with concave caps)

Fractal structure within the virtual tablet

Solid and porous clusters in compacted powders mixture usually exhibit fractal structures (see section 3.3.1B). The same characteristics can be observed in large-scale virtual tablets obtained by growing particles. Fractal structures inside *in silico* tablet were not directly programmed. However, they are a direct consequence of the implementation method used to model a compacted and disordered particulate system in a discrete system (matrix). Like in real compacts, this effect will be more apparent if the scale of the tablet is large, i.e. if the number of particles inside the tablet is large. As virtual porous network structure can be fractal, water diffusion within *in silico* tablets during dissolution simulation is expected to be similar to diffusion within real tablets. Overviews of porous structures in a virtual tablet are depicted in Figure 4.25.

It has to be pointed out also that discrete and fractal properties of a randomly filled matrix enable application of Percolation Theory to the model (see section 3.3.1).

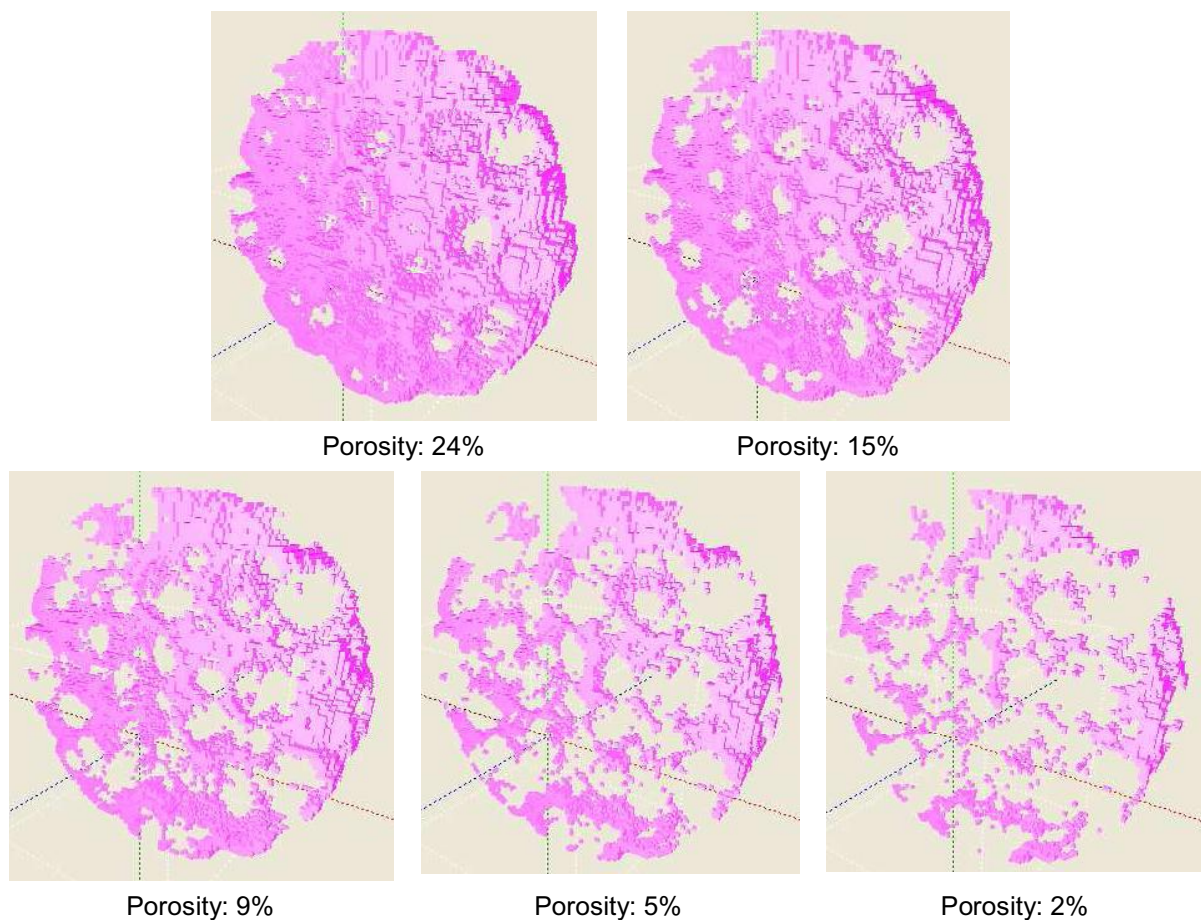


Figure 4.25: Negative views of an *in silico* tablet with various porosity in volumetric %. Only the cell corresponding to pores are colored and visible. Picture shows that pores can take place around and between particles.

Program interface for filling up virtual tablets with ingredients

A user's interface was implemented to provide a tool for filling up the *in silico* tablet with ingredients (see Figure 4.26). Particle-packing algorithm runs automatically, whereas growing algorithm has to be run gradually by pushing successively a button. A visualisation window is displayed in the interface to observe particles growing steps.

Discretised tablet created with TD module is uploaded automatically when filling interface is opened. Mean particle diameters and volumetric ratios of desired components to add in virtual tablet must be given in input by the user (editing spaces at bottom of the interface). Pushing "Distribute centres" button will run particle-packing algorithm. When packing is over, particle seeds are ready for growing into dissolution matrix. Particle growing can be run simultaneously or separately for each component. The user has thus the possibility to finely adjust the volumetric ratio of each ingredient in the tablet. The discrete nature of tablet and particles do not always allow, at this stage of development, to reach volumetric ratios of components exactly equal to target ratios. Some calculation results must in fact be rounded in packing and growing programs for creating a discrete tablet model in a cubic matrix. However precision is enhanced if the system scale is increased (it is equivalent to an enlargement of the number of particles per ingredient). In case of small-scale model, grow constant can be adjusted for each component to reduce imprecision on their respective volumetric concentrations (constant must be entered in editing spaces at bottom of the interface). Grow constants calibrate the expansion radius at each growing step for particles of a component.

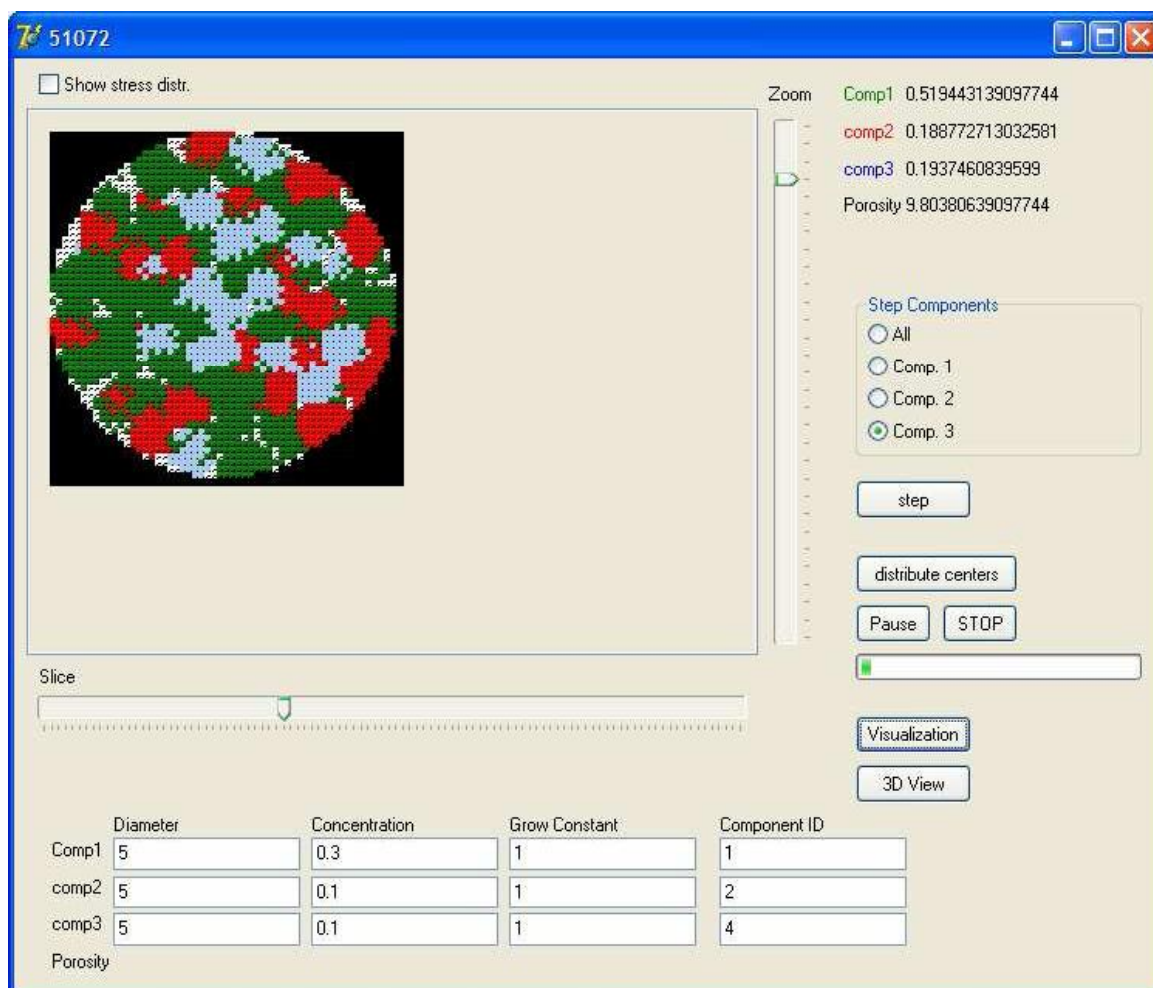


Figure 4.26: Windows interface of virtual tablet filling program.

D. Databases of components, (DB module)

Databases (DB) module has a major importance in the expert system (see section 4.1.3) especially for setting up the virtual tablet composition. DB module is composed of three databases in which are stored information and properties of three different component types: active ingredients, fillers and disintegrants (see overview of the interface in Figure 4.27). New substances can be easily added or removed from the databases. Furthermore, it is possible to add databases of other component types.

For each component type, the database provides an access to descriptive information about substances. Furthermore, it contains solubility constant (SoC) and swelling constant (SwC) of each component and this for different pHs of the dissolution medium. SoC and SwC are specific to the dissolution simulation module. SoC should not be confused with the solubility constant that is commonly determined experimentally (maximum amount of solute dissolved in

a solvent at equilibrium). The functions of SoC and SwC in dissolution simulation are explained in next part of this section.

Before filling up the virtual tablet with substances, the user has to select first in DB module each ingredient he wants to add in the future tablet. After selecting a substance, the “Add to formulation” button must be clicked to transfer substances properties the DS module.

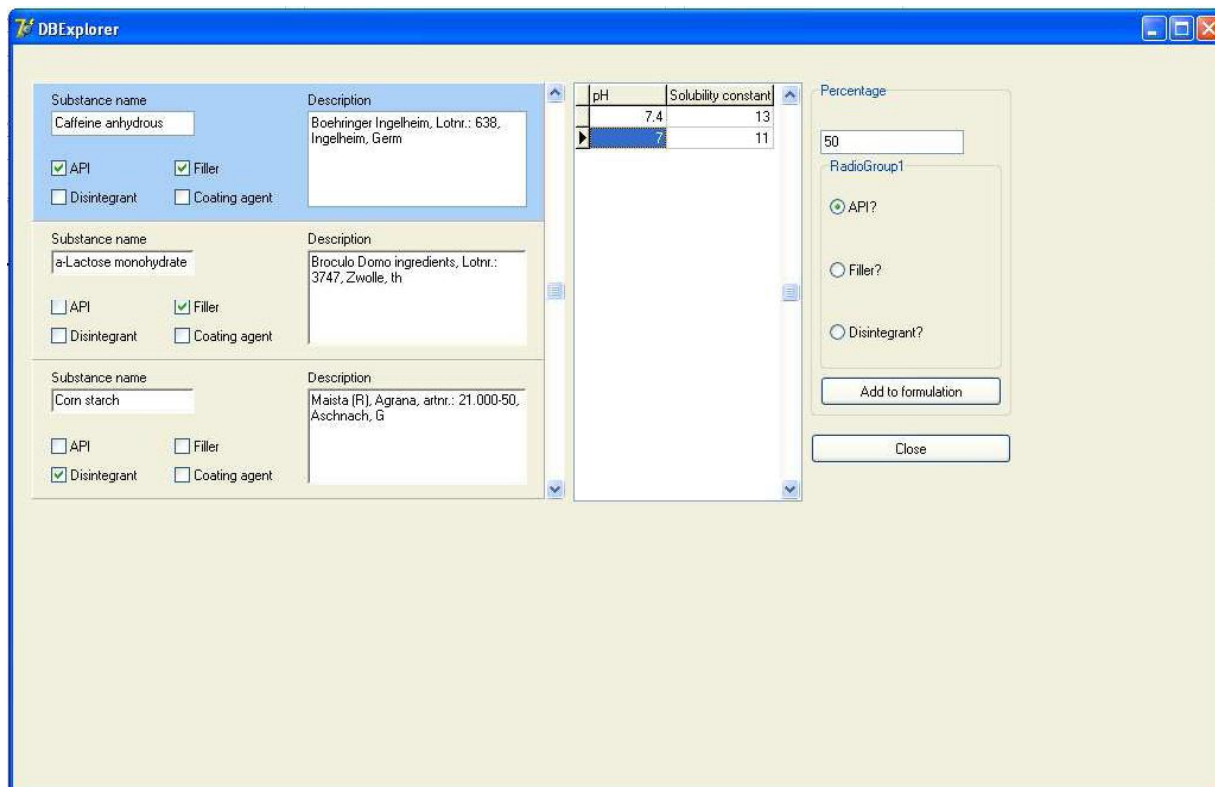


Figure 4.27: DB module interface. Three databases are provided: API, filler and disintegrant databases.

As it was previously pointed out (see section 4.1.3), DB module role is to store data on components and to provide information, not only to DS module, but also to other modules of the expert system. DB module is thus essential for a future automatic scanning of the components to design optimal formulation with all modules of the expert system.

E. Cellular automaton for *in silico* solid dosage form dissolution

General description

This section describes how *in silico* dissolution process is implemented using cellular automata (CA) modeling. Fundamental principles of CA modeling are detailed in section 3.3.2.

The dissolution cellular automaton (DCA) is a three dimensional CA programmed in a virtual cubic matrix. The cubic matrix represents dissolution environment with a tablet at the middle. It is a discrete system composed of cubic units or cells (all of the same volume).

However, matrix cells can have different states among a finite number of possible states. Their state at a certain time depends on the element that they model at this time. States of a cell can be of different types: liquid, gaseous or solid. Cells in “liquid” state model dissolution medium units (usually water). Cells in “gaseous” or “porous” state model empty pores units. Finally, cells in “solid” state model ingredients units.

A solid type cell has always a subtype. The number of possible subtypes is finite: API, filler, disintegrant, etc. Usually a subtype is equal to a state, but some subtypes can have different states: for example, disintegrant subtype can be equal to dry or swollen states.

Time is discrete in CA modeling. A unit of time corresponds to an update of the whole system by the program. The system is considered to be totally updated if the state of all cells has been updated.

To update the state of a cell, the program refers to a rules set. The rules set indicates for each possible state of a cell at time t what will be the state of this cell at time $t+1$. The state of a cell at time $t+1$ always depends on the states of the cells in its 3D Moor neighbourhood at time t (see section 3.3.2). For example, a cell in gaseous state at time t will be in liquid state at time $t+1$ if it has at least one cell in liquid state in its direct Moor neighbour. This rule simulates the entrance of water in a pore (if materials surrounding the pore are not too hydrophobic and pore opening enables capillary diffusion). Thus, after updating the states of all cells in dissolution matrix, the virtual tablet can exhibit a different global state.

The set of rules is not the only element influencing changes of states. Each cell contains in fact two different constants: solubility constant (SoC) and swelling constant SwC. These constants are uploaded from DB module while filling up the matrix with ingredients and play an important role in the dissolution simulation. They are specific to this CA only and give additional indications for updating cells state. Each cell type and subtype has its own constants values.

It has to be remembered to this stage that powder particles in CA are composed of one or more cells. The number of cells necessary to model a particle depends on the size of this particle (see explanations on particle growing algorithm). Furthermore, as said previously, the larger the system will be, the more numerous will be the cells modeling a particle and the more precise the simulation will be.

Updating rules of cells states

As mentioned previously, the state of a cell at next unit of time depends on the states of the neighbouring cells. Additionally, constants of cells influence state updating. SoC is an internal counter of a cell, which gives the number of system update (or time unit) the program has to wait before changing the state of a cell. The lower is the value of SoC for a cell, the less

system updates will be required before changing the state of a cell. SoC enables in fact to calibrate the required time for a solid or gaseous cell to be changed into liquid cell. For API and fillers cells, it is a solubility indication which gives the system the time required for unit of water to solve unit of solid. SwC has a different role in the CA. It does not influence state update with time, but influence states of cells in the neighbourhood of a cell having a SwC. Indeed, Swc calibrates the expansion by swelling of a disintegrant cell. A disintegrant cell will then change porous or liquid cells in its neighbourhood into disintegrant cells with lower SwC. A new disintegrant cell can then also expand but to a lower extent. Lower the SwC value will be the more expansion capacity the disintegrant cell will have. This constant characterises the swelling force of a disintegrant.

- Cells in gaseous state: Porous cells have a very low solubility value. When they have at least one liquid cell in their direct Moor neighbourhood, their state will change into liquid state at next unit time. At this stage of software development, hydrophobicity of a pore and capillary diffusion limitations of water into a pore were not taken into account. However, additional rules for CA cells updating could enable to consider these parameters in the simulation.
- Cells in API state: these cells model active ingredients units. Calibration of their SoC is a very important point to obtain a relevant dissolution profile for a formulated API. A cell that models a unit of soluble drug will have a very low SoC, whereas cell of a poor soluble drug will have a high SoC. At each update of the system, SoC of an API cell will be reduced of a number proportional to the number of liquid (or swollen disintegrant) cells in its direct neighbourhood. An API cell is considered as dissolved and changed into liquid cell when SoC reach a zero value. When an API cell is changed into a liquid cell, the program adds one unit to a "dissolution" counter. This counter calculates the amount of API cells changed into liquid cells. It corresponds to the calculation of the amount of drug dissolved during experimental dissolution test. The cumulative percentage of drug released is then calculated by dividing, at each time unit, the value of the dissolution counter with the number of API cells in the initial virtual tablet. If the modeled drug is very soluble (small SoC value) only few time units will be necessary to dissolve API particles. On the contrary, if the modeled drug is poorly soluble (high SoC value) the complete drug release will be very long, similar to a real case.
- Cells in disintegrant state: these cells have a very high SoC value, as a disintegrant is usually not water-soluble. However, if a formulator wants to simulate another dissolution medium (e.g. ethanol), SoC can be reduced if the modeled disintegrant is soluble in this solvent. Moreover, disintegrant cells have a swelling constant SwC. This constant is

essential for simulating swelling properties of disintegrant. It is assumed in the simulation that disintegrant particles swell inside pores and dissolution medium (porous and liquid cells). In the same way than for a real tablet, an excess of disintegrant can retard drug release by caging API particles caged into a swollen disintegrant mesh. These functionalities enable a first approach to the simulation of retarded or controlled release tablets. Furthermore, API or filler cell consider a swollen disintegrant cell as a liquid cell while applying their updating rules. Water diffusion through disintegrant network is thus simulated.

- Cells in a filler state: They are hybrids between API and disintegrant cells and have a SoC and a SwC. They follow the same dissolution rules than API cells. As filler cells have a swelling constant, it is possible to model filler having a certain swelling capacity.

Figure 4.28 gives an overview of a CA modeling *in silico* dissolution of a tablet

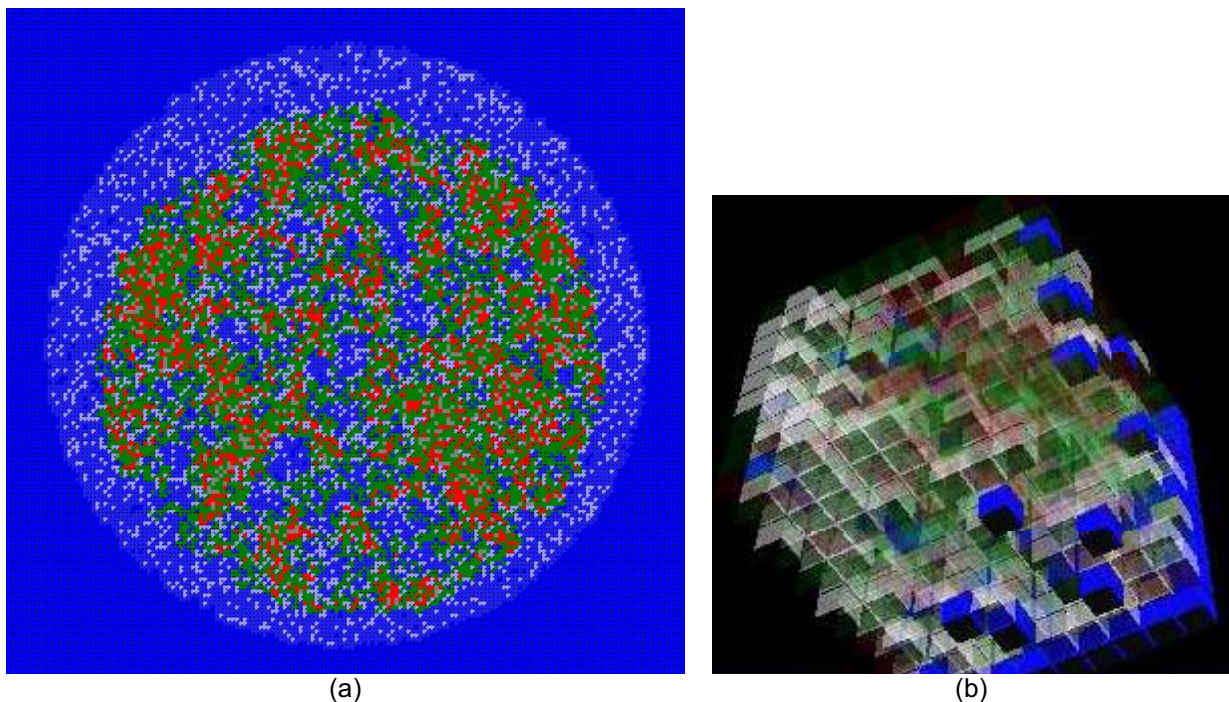


Figure 4.28: Views of virtual tablet under *in silico* dissolution process using CA modeling.

(a): View of a slice in the 3D dissolution matrix showing a partially dissolved tablet composed of: API (green), filler (red), disintegrant (white) and pores (grey). The dissolution medium (blue cells) is visible outside and inside the tablet. Insoluble disintegrant particles (white) remain in the matrix during the whole dissolution process (tablet ghost).

(b): 3D view of part of a virtual tablet while running dissolution algorithm. The small cubes represent cells of the matrix.

Dissolution profiles

The cumulated % of drug released (equal to the cumulated % of API cells changed into liquid cells) at one unit of time (corresponding to a full update of the matrix) is plotted versus unit of times in the main interface of DS module. Dissolution profile is drawn while CA is running.

Time scale can be in seconds or minutes, depending on the SoC value (see further for SoC calibration method). Each new point is linked to the previous one by a line. As the number of system updates (time units) is large, plotted points are numerous and dissolution curve is smooth. However, it has to be remembered that modeling is discrete.

Depending on the virtual tablet composition, *in silico* dissolution curves exhibit different profiles, similarly to experimental dissolution curves (first order, exponential, sigmoid, etc.). An overview of the main interface of DS module, with several drug release profiles drawn inside, is shown in Figure 4.29.

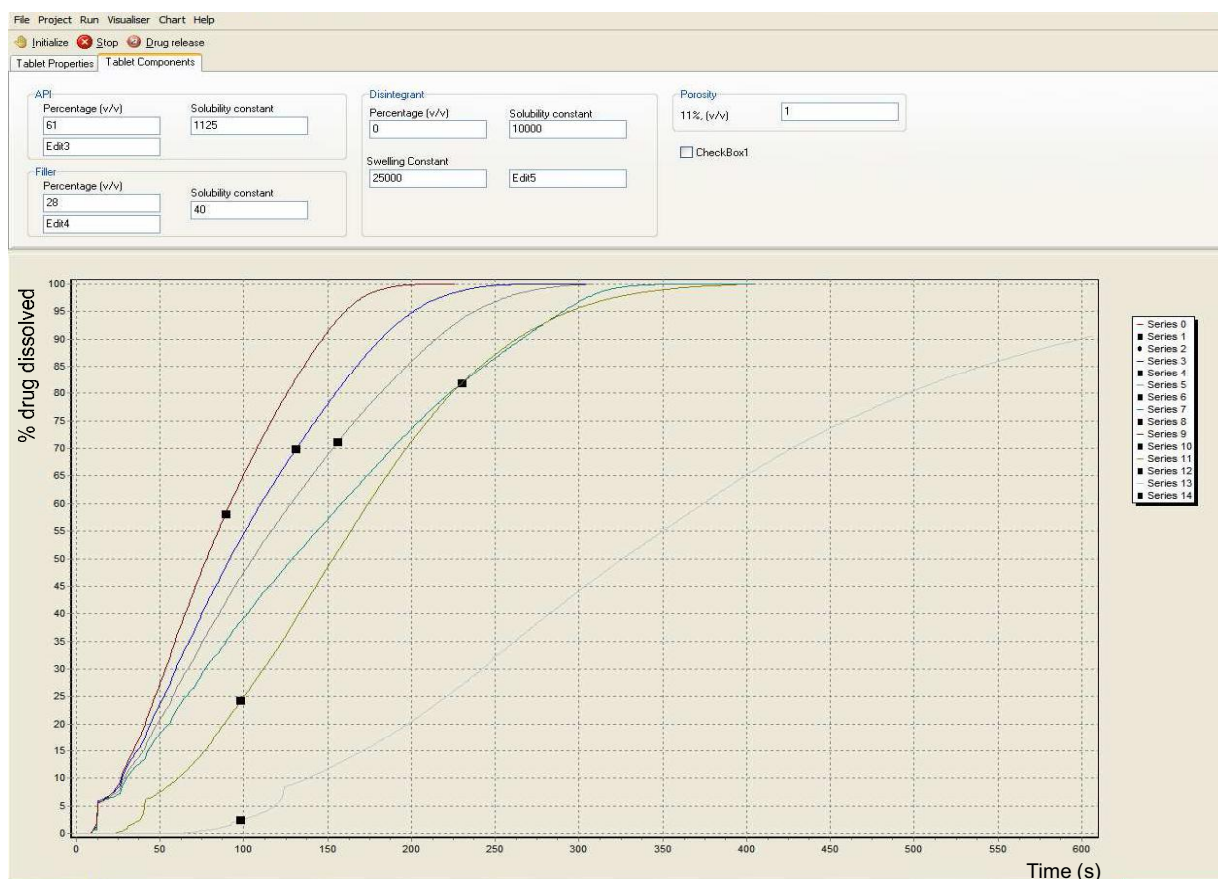


Figure 4.29: Main interface of DS module with some *in silico* dissolution profiles.

A “perturbation” appears on every profile provided by the system and is located at the very beginning of the dissolution curve (see Figure 4.29). A similar break in continuity of the curve

can be observed on profiles obtained with automatic *in situ* dissolution testing machine. With these machines, samples are taken at very short time intervals, which give numerous sampling points and a high precision in the profile. As such a precision is not possible by manual sampling, this perturbation is usually not visible in profiles obtained with classical dissolution testing. This discontinuity in the curve could be explained by faster release of drug particles which are connected to the tablet surface and which are thus in contact with liquid medium at the beginning of the dissolution process.

When a new substance is added into DB module, SoC and/or Swc values must be found. This task is called “calibration”. Once the constant of a substance is calibrated, its value is independent on the composition of a tablet containing this substance. Constants values of a substance will greatly influence *in silico* dissolution profile. The operating mode for calibration of the constants is detailed in the next part of this section. Influence of SoC or SwC on *in silico* dissolution profiles is shown with some examples in Figure 4.30 and Figure 4.31. Figure 4.32 illustrates the influence of disintegrant % on virtual dissolution.

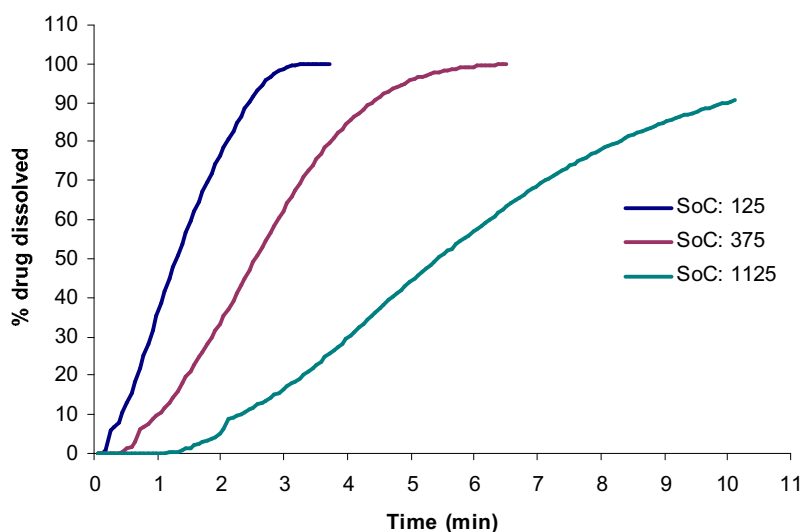


Figure 4.30: *In silico* dissolution profiles of the same tablet with different solubility constants (SoC) values for the API. Virtual tablet composition (in tablet volumetric %): Caffeine (60%), lactose (30%), porosity (10%).

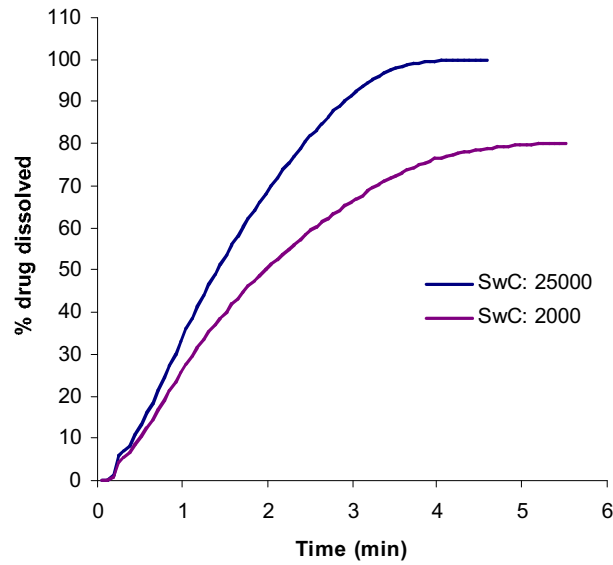


Figure 4.31: *In silico* dissolution profiles of the same tablet with different swelling constants (SwC) values for the disintegrant. Virtual tablet composition (in tablet volumetric %): caffeine (52%), lactose (19%), starch (23%), porosity (6%).

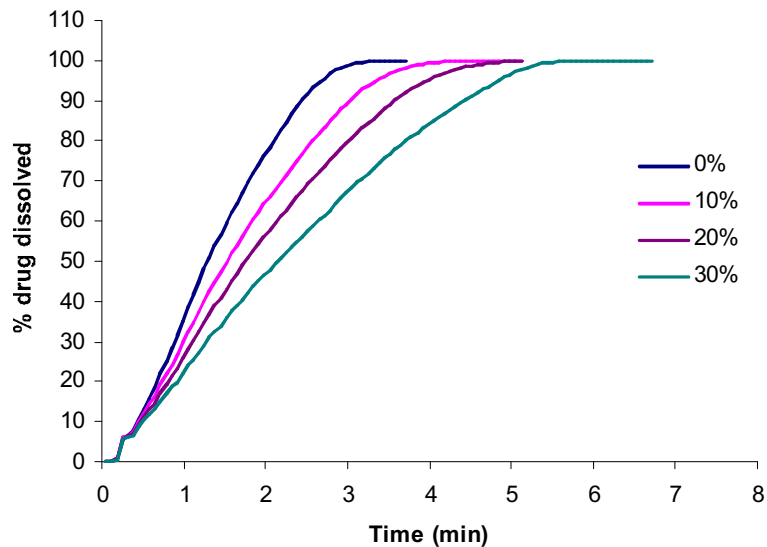


Figure 4.32: *In silico* dissolution profiles of a tablet with different loading amount of starch. Virtual tablet composition (in tablet volumetric %): starch (0-30%), caffeine (60%), lactose (30-0%), porosity (10%).

DS module enables to import experimental dissolution points and to display them in the module interface. This functionality is very important for the calibration of SoC and SwC constants.

F. Operating mode for calibration of solubility and swelling constants of the CA.

If a new ingredient needs to be added in a formulation and is not already in one of the databases, its SoC and/or SwC must be calibrated before running *in silico* dissolution of the virtual tablet.

SoC of substance (e.g. API) can be determined using one single experimental work. Tablet of the pure ingredient must be first compressed. Porosity is estimated, for example with Equation 65. An experimental dissolution test of the resulting compact is then performed with a reasonable number of sampling points (if possible > 10). A virtual tablet of the same dimension and shape should be designed with TD module. The ingredient to calibrate is added into an appropriate database of DB module and an arbitrary SoC is given to the substance. The previously designed tablet has then to be filled up with the ingredient. The same porosity than for the real compact should be installed. Next step is to import experimental dissolution points into DS interface. To achieve SoC calibration of the ingredient, dissolutions simulation of the virtual tablet should be run with different SoC until a virtual profile fits properly with experimental dissolution points. Once calibrated, the SoC will remain the same, independent of the formulation in which it will be added in future. It has however to be pointed out that this SoC is calibrated only for the experimental conditions in which real tablet dissolution was tested (i.e. nature of the dissolution medium, T°, pH, rotation speed of the paddle, etc.).

If SwC of a new substance (e.g. disintegrant) needs to be determined, a similar approach should be carried but with calibration of SwC. Dissolution of a tablet composed of a known ingredient (i.e. already in one database of DB module) and the new substance should be tested. SwC calibration is obtained when *in silico* and experimental dissolution curves are fitting.

In case of a new soluble ingredient exhibiting also swelling properties, SoC and SwC should be changed at the same time while fitting *in silico* and experimental dissolution curves of the pure tableted ingredient. To ensure that calibrations of the two constants are correct, the same operating mode could be repeated with tablets composed of this ingredient and a substance already stored in one of the database.

5. Experimental validation

5.1. Material and methods

5.1.1. Model drugs and excipients

A. Drug substances

Caffeine anhydrous (355 µm mesh)

BASF, Lotnr. 103021AX1D, Ludwigshafen, Germany

(see Figure 5.1)

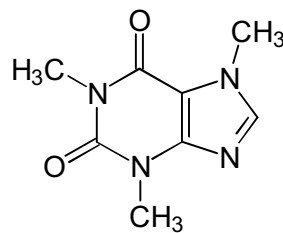


Figure 5.1: Chemical formula of Caffeine

Empirical formula:	C ₈ H ₁₀ N ₄ O ₂
Appearance:	Silky white crystals, usually matted together, or a white crystalline powder, odorless with bitter taste.
Molecular weight:	194.2 g/mol
Melting point:	234 - 239 °C
Solubility (pH 1-10):	Soluble (1 in 60 of water)
Action:	Central nervous stimulant

Paracetamol or Acetaminophen

Rhodia, Lyon, France

RhodapapTM DC90 and DC90Fine (Lotnr. 0014422), two different grades of granulated Paracetamol (90 % w/w) with tableting aids (10 % w/w of a mix of binders, disintegrating agents and lubricant).

(see Figure 5.2)

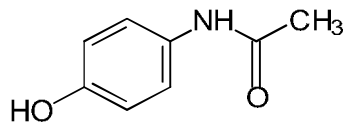


Figure 5.2: Chemical formula of Paracetamol

Empirical formula:	C ₈ H ₉ NO ₂
Appearance:	White crystalline powder, odorless, with a slightly bitter taste.
Molecular weight:	151.2 g/mol
Melting point:	168 – 172 °C
Solubility:	Sparingly soluble in water (1 in 70 of cold water)
Action:	Analgesic, antipyretic.

Aspirin or Acetylsalicylic acid (300 µm mesh)

Sandoz, Lotnr: 82510, Holzkirchen, Germany

(see Figure 5.3)

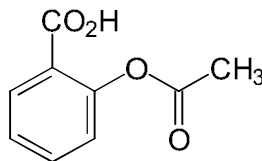


Figure 5.3: Chemical formula of Aspirin

Empirical formula:	C ₉ H ₈ O ₄
Appearance:	White, crystalline powder or colorless crystals
Molecular weight:	180.2 g/mol
Melting point:	136°C (with decomposition)
Solubility:	Slightly soluble in water
Action:	Analgesic, anti-inflammatory, antipyretic.

Indomethacin

Esteve, Lotnr. 98813, Barcelona, Spain

(see Figure 5.4)

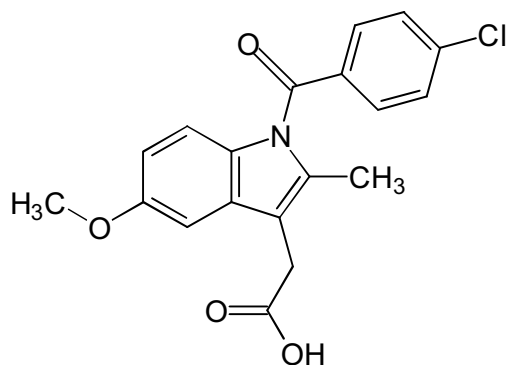


Figure 5.4: Chemical formula of indomethacin

Empirical formula:	C ₁₉ H ₁₆ ClNO ₄
Appearance:	White to brownish-yellow, odorless or almost odorless, crystalline powder.
Molecular weight:	357.8 g/mol
Melting point:	158 - 162
Solubility:	Practically insoluble in water
Action:	Anti-inflammatory, analgesic.

B. Excipients

α -Lactose monohydrate (355 μm mesh)

Broculo Domo ingredients, Lotnr 3747, Zwolle, the Netherlands
(see Figure 5.5)

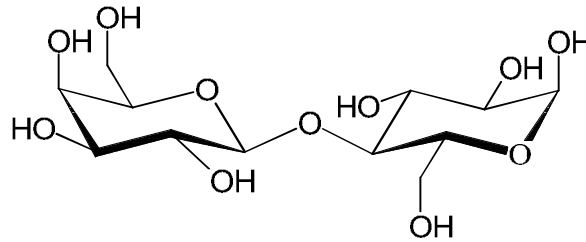


Figure 5.5: Chemical formula of α -Lactose monohydrate

Empirical formula:	$\text{C}_{12}\text{H}_{22}\text{O}_{11}\cdot\text{H}_2\text{O}$
Appearance:	White crystalline or grainy powder, inodorous, with a sweet taste
Molecular weight:	360.3 g/mol
Melting point:	201 - 202 $^{\circ}\text{C}$
Solubility:	very soluble (water)
Technological use:	Lactose is used as filler, binder and adsorbing agent in the tableting and capsule filling processes. For direct tableting, especially spray-dried lactose is suitable.

Partially pregelatinised maize starch (StaRX1500®)

Colorcon, Lotnr. 811024, Dartford Kent, UK

(see Figure 5.6)

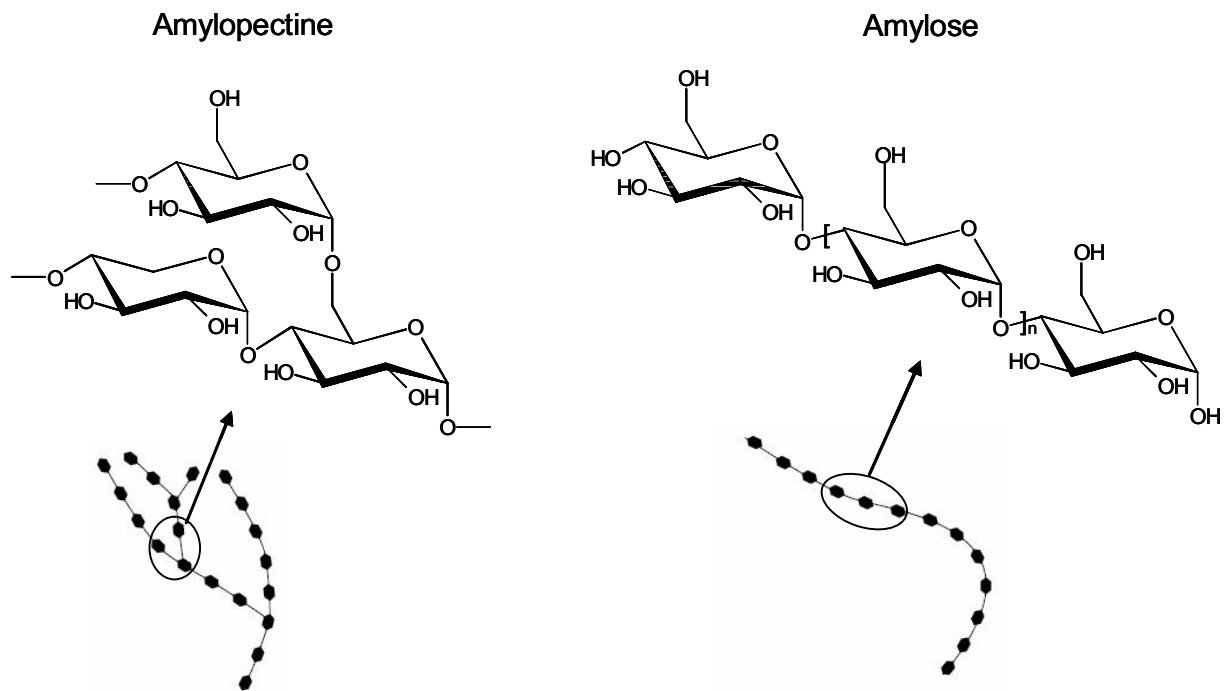


Figure 5.6: Chemical formula of Partially pregelatinised maize starch

Definition:	Maize starch is composed of two polymers: amylose and amylopectine, which are linked within a specific spherical crystalline structure. During partial pregelatinisation, the bond between part of the polymers is broken, giving to StaRX1500® a better flowability and compressibility.
Empirical formula:	$(C_6H_{10}O_5)_n$ with $n = 300-1000$
Appearance:	Odorless, tasteless white powder.
Molecular weight:	Amylose: 50'000-200'000 g/mol Amylopectine: 100'000-1'000'000 g/mol
Solubility:	Insoluble but swells
Technological use:	Performs key functions in direct compression formulations as a binder, disintegrant, flow-aid and self-lubricant.

Croscarmellose (cross-linked carboxymethyl cellulose) (AcDiSol®)

FMC, Lotnr. 14200, Brussels, Belgium

(see Figure 5.7)

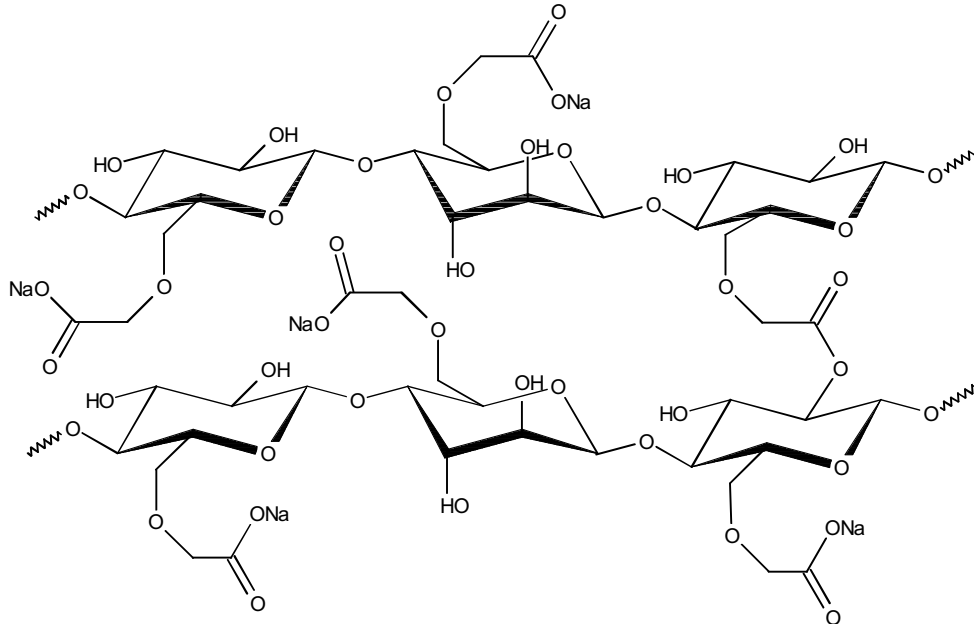


Figure 5.7: Chemical formula of Croscarmellose

Definition	AcDiSol® is an internally cross-linked form of sodium carboxymethylcellulose (NaCMC). It differs from soluble sodium carboxymethylcellulose only in that it has been cross-linked to ensure that the product is essentially water insoluble.
Empirical formula:	$(C_{22}H_{34}O_{15}Na_2)_n$
Appearance:	Odorless, white powder (fibrous particles).
Molecular weight:	584 g/mol
Solubility:	Insoluble but swells.
Technological use:	Aids in the disintegration and dissolution of pharmaceutical tablets (disintegrant). It works by providing a good water uptake, a high capillary action, a rapid swelling and an efficient fluid channeling

Low-Substituted Hydroxypropyl Cellulose (L-HPC)

Shin-Etsu. Lotnr. 5111541, Tokyo, Japan

LH-11 grade

(see Figure 5.8)

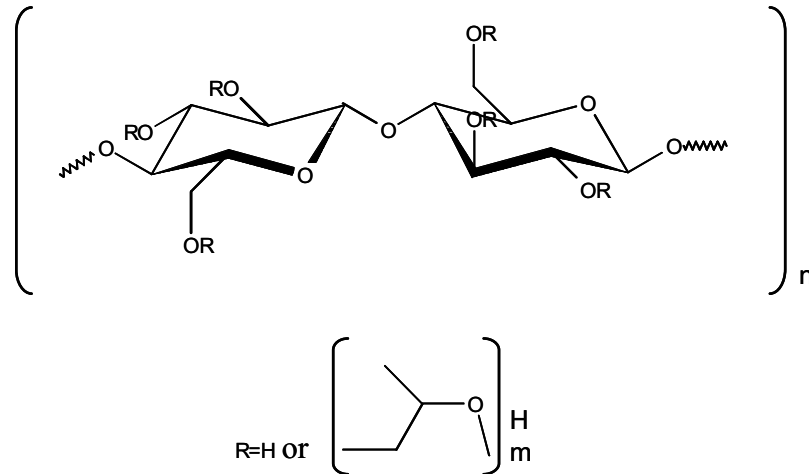


Figure 5.8 : Chemical formula of Low-Substituted Hydroxypropyl Cellulose

Definition:	L-HPC (Low-Substituted Hydroxypropyl Cellulose) is a low-substituted hydroxypropyl ether of cellulose in which quite a small proportion of the three-hydroxyl groups contained in the 1-o-glucopyranosyl ring of the cellulose is etherified with propylene oxide. The different types of L-HPC comprise various combinations of average particle size and hydroxypropoxyl content. Particles of type 11 are highly fibrous (Hydroxypropoxyl Content %:10.0-12.9).
Appearance:	Odorless, white powder (fibrous particles).
Solubility:	Insoluble in water but swells.
Technological use:	L-HPC 11: used as a binder and a disintegrant for solid dosage forms. Applied by direct compression (anti-capping).

5.1.2. Characterisation of the substances

A. Particle size distribution

The average particle size was determined with a Malvern Mastersizer X (Malvern Instruments, Worcestershire, UK). The measurements were carried out at least 3 times for each sample. The average and the median particle size of all granulates was measured using a MS 64-Dry powder feeder (Model MSX 64, Malvern Instruments, Worcestershire, UK).

The following instrument settings have been chosen:

- The air pressure was set between 1-3 bar.
- The number of sweeps was set to 30'000 in a time frame of 60 s.
- The active beam length was set to 10.0 mm with a range lens of 1000 mm.
- A minimum obscuration value between 1-10 % was got in all measurements.

With the software (Malvern) the particle size distribution of the samples including mean and median particle size could be calculated from the raw data. The function "polydispers" was activated. The average particle sizes of all samples mentioned were above or slightly smaller than 50 μm , therefore, the "Fraunhofer" model was chosen (according to the recommendation of Malvern).

B. True density

The true density was measured with a gas displacement pycnometer AccuPycTM 1330 (Micromeritics Instrument Corporation, Nocsoss, USA) with a nominal cell volume of 10 ml. Helium was used as gas. In order to get results with good accuracy, the amount of the sample was chosen so that the measured volume was at least 10 % of the nominal cell volume.

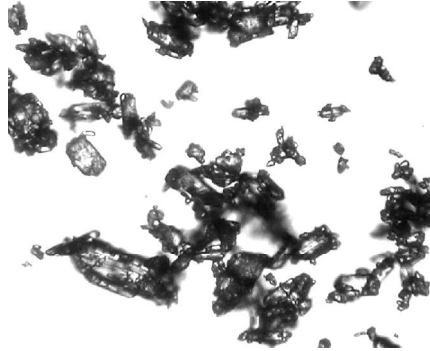
The true density can be expressed as a quotient of mass and volume. The mass was calculated from the difference between the mass of the filled pycnometer and the mass of the empty pycnometer. The volume was determined by purging each sample 20 times with helium. In each run the volume of the sample could be deviated from the difference in volume of the full and the empty pycnometer.

C. Characterisation of the drug substances

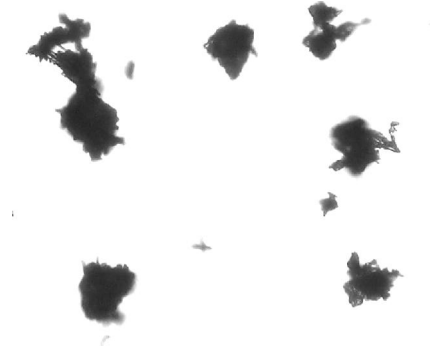
Data for true density (g/cm^3), mean particle size (μm) and general shape of the drug substances used are listed in Table 5.1.

The general shape (fibrous/non fibrous) of the drug and excipients was investigated using scanning electron microscope (XL30 ESEM, Philips, Eindhoven, Netherlands) and an inverted microscope (Hund Wilovert[®], Wetzlar, Germany). The photographs of the drug substances are shown in Figure 5.9.

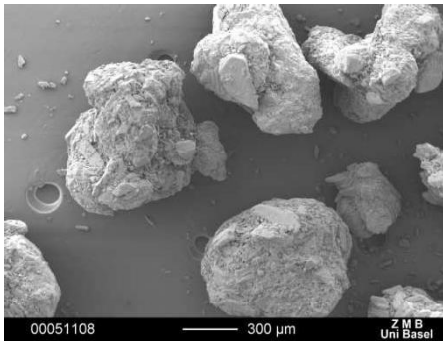
All drug particles exhibit a non-fibrous shape. Even though Caffeine crystals are needle-like they are agglomerated in agglomerates with non-fibrous shape.



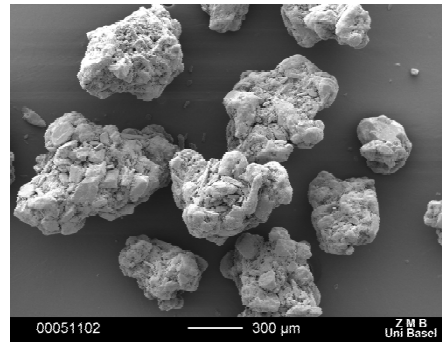
Aspirin (magnification: 25x)



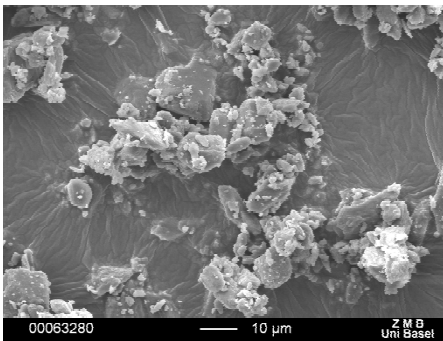
Caffeine (magnification: 25x)



Paracetamol DC90 (magnification: 50x)



Paracetamol DC90Fine (magnification: 50x)



Indomethacin (magnification: 1000x)

Figure 5.9: SEM and microscope photographs of drug substances

Table 5.1: Physical properties of drug substances

Drug Substances	True density (g/cm ³)	Mean particle size (µm)	Shape
Paracetamol			
DC90	1.319	671	non fibrous
DC90Fine	1.290	418	non fibrous
Caffeine			
Powder A	1.460	37.4	non fibrous
Granulated	1.420	727	non fibrous
Powder B	1.440	47	non fibrous
Indomethacin	1.387	9.5	non fibrous
Aspirin	1.376	45	non fibrous

D. Characterisation of the excipients

Data for true density (g/cm³) and mean particle size (µm) of the excipients used are listed in Table 5.2. The general shapes of the excipients were investigated with the same material than drug substances. The photographs of excipients are shown in Figure 5.10. StaRX1500[®] and lactose monohydrate exhibit a non-fibrous shape. L-HPC and AcDiSol[®] are fibrous. L-HPC fibers present a mean aspect ratio higher than AcDiSol[®] fibers; mean length is approximately the same for both material but the width of L-HPC fibers is smaller.

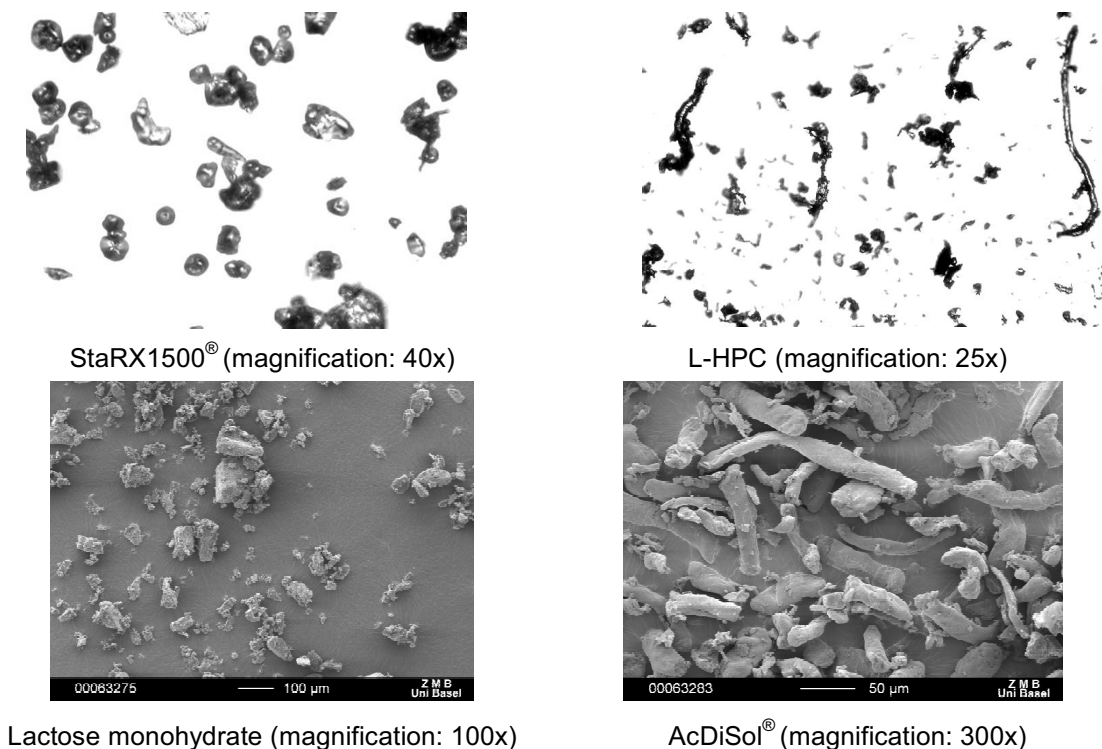


Figure 5.10: SEM and microscope photographs of excipients

Table 5.2: Physical properties of excipients

Drug Substances	True density (g/cm ³)	Mean particle size (µm)	Shape
Partially pregelatinised maize			
StaRX1500 [®] A	1.498	84	non fibrous
StaRX1500 [®] B	1.500	76	non fibrous
Ac-Di-Sol [®]	1.607	45.1	fibrous
L-HPC	1.451	50	fibrous
Lactose monohydrate	1.540	52.2	non fibrous

5.1.3. Tableting

A. Compaction technology

Tablets used for disintegration and dissolution tests were all compressed using the mechanical compaction simulator (Levin et al., 1998) Presster[™] (Metropolitan Computing Corporation, East Hanover, US) with a simulated rotary tablet machine Korsch PH 336 at an output capacity of 10800 tablets per hour, corresponding to a dwell time of 118.3 ms. Description of the simulator and explanations on dwell time are given in section 3.1.2C.

Tablet used for water uptake measurements were compressed using the Zwick[®] 1478 Universal Testing Instrument (Zwick[®] GmbH, Ulm, Germany). The compression and the decompression took place with a speed of 25 mm/min. The ejection speed was 50 mm/min. Before each compression cycle, the punches and the die wall were lubricated with a mixture of magnesium stearate and acetone.

B. Tablet formulations for disintegration testing and water uptake measurement

Two different grades of paracetamol (DC90 and DC90Fine), one grade of indomethacin and three different grades of caffeine (powder (A, B) and granulated) were used as model drugs. Two grades of StaRX1500[®] (A, B) were used as model disintegrants with non-fibrous shape swelling properties. AcDiSol[®] and L-HPC were used as model disintegrants with fibrous shape.

Tablets formulated with non-fibrous disintegrants

Different binary mixtures composed of model drug and non-fibrous disintegrant (see Table 5.3, Table 5.4 and Table 5.5) were chosen as model mixtures to compare calculated and experimental disintegrant thresholds, i.e. the concentration of disintegrant (% v/v of solid fraction) in tablets with the shortest disintegration time.

Experimental data from tablet formulations containing StaRX1500[®] B with caffeine powder B and caffeine granulated (formulations IV and V) are from Luginbuehl's PhD work (Luginbuehl, 1994).

Formulations I-III and VI were prepared with increasing disintegrant percentage. For each formulation drug powder was mixed in a Turbula mixer for 15 min with disintegrant material and stored in a desiccator with silica gel for 12 h (see Table 5.3, Table 5.4 and Table 5.5).

All formulations were compressed targeting certain porosity of compacts. Compressions were performed two times for each Paracetamol formulation (I and II) with different targeted porosities ϵ_t : 10 % and 8 % for formulation I, 10 % and 14 % for formulation II (see Table 5.3). Formulation III with caffeine powder A was compressed with $\epsilon_t=14$ % (Table 5.4). Tablet containing caffeine granulated (formulation IV) and caffeine powder B (formulation V) were both compressed $\epsilon_t=12$ % (Luginbuehl, 1994) (Table 5.4). Targeted porosity for formulation VI (indomethacin) was $\epsilon_t=10$ % (Table 5.5).

Round, flat, 10 mm diameter tablets were prepared for formulations I-III and VI using the compaction simulator Presster[™]. A rotary tablet machine Korsch PH 336 was simulated at an output capacity of 10800 tablets per hour corresponding to a dwell time of 118.3 ms. Targeted weight of the tablets was 380 mg. Minimum distance between punches at dwell time were adjusted on Presster[™] for each different drug/disintegrant ratios of the formulations to respect targeted porosities ϵ_t of the tablets.

For formulations IV and V, round flat, 11 mm diameter tablets were compressed with a weight of 400 ± 2 mg, a height of 3.19 ± 0.02 mm and a porosity of 12 ± 0.2 % (v/v) with a compression force of 10 kN (Luginbuehl, 1994).

Table 5.3: Formulations with Paracetamol as model drug and starch as model disintegrant. Each Paracetamol grade (DC90 and DC90Fine) was compressed with starch at two different targeted porosities (ϵ_t).

Formulation I Paracetamol DC90 / StaRX1500 [®] A				Formulation II Paracetamol DC90Fine / StaRX1500 [®] A			
$\epsilon_t = 10\%$		$\epsilon_t = 8\%$		$\epsilon_t = 10\%$		$\epsilon_t = 14\%$	
StaRX1500 [®] (in solid fraction)		StaRX1500 [®] (in solid fraction)		StaRX1500 [®] (in solid fraction)		StaRX1500 [®] (in solid fraction)	
%(v/v)	%(w/w)	%(v/v)	%(w/w)	%(v/v)	%(w/w)	%(v/v)	%(w/w)
0.00	0.00	0.00	0.00	0.00	0.00	0.00	0.00
5.00	5.65	5.00	5.64	1.00	1.16	2.00	2.32
7.00	7.88	7.00	7.88	2.00	2.32	3.00	3.47
8.00	9.00	8.00	8.99	3.00	3.47	4.00	4.62
9.00	10.11	9.00	10.10	4.00	4.62	5.00	5.76
10.00	11.22	10.00	11.21	5.00	5.77	6.00	6.90
15.00	16.71	11.00	12.31	6.00	6.91	8.00	9.17
20.00	22.14	15.00	16.70	7.00	8.05	15.00	17.01
40.00	43.12	20.00	22.11	8.00	9.18	20.00	22.50
50.00	53.21			9.00	10.31		
				10.00	11.44		
				15.00	17.03		
				20.00	22.52		
				30.00	33.26		
				40.00	43.67		
				50.00	53.76		

Table 5.4: Formulations with Caffeine as model drug and starch as model disintegrant. Experimental results with formulation IV and V are from (Luginbuehl, 1994).

Formulation III Caffeine powder A / StaRX1500 [®] A		Formulation IV Caffeine granulated / StaRX1500 [®] B		Formulation V Caffeine powder B/ StaRX1500 [®] B	
$\epsilon_t = 14\%$		$\epsilon_t = 12\%$		$\epsilon_t = 12\%$	
StaRX1500 [®] (in solid fraction)		StaRX1500 [®] (in solid fraction)		StaRX1500 [®] (in solid fraction)	
%(v/v)	%(w/w)	%(v/v)	%(w/w)	%(v/v)	%(w/w)
0.00	100.00	0.00	0.00	0.00	0.00
5.81	94.19	2.37	2.50	9.66	10.00
11.63	88.37	4.75	5.00	14.51	15.00
19.77	80.23	7.13	7.50	19.39	20.00
20.93	79.07	9.51	10.00	24.28	25.00
22.09	77.91	11.92	12.50	29.19	30.00
23.26	76.74	14.32	15.00	39.07	40.00
24.42	75.58	19.12	20.00	49.03	50.00
29.07	70.93	28.85	30.00	59.07	60.00
34.88	65.12	38.67	40.00	69.18	70.00
		48.61	50.00	79.37	80.00
		58.66	60.00	89.65	90.00
		68.82	70.00		
		79.10	80.00		
		89.49	90.00		

Table 5.5: Formulation with indomethacin as model drug and starch as model disintegrant.

Formulation VI	
Indomethacin/ StaRX1500 [®] A	
$\varepsilon_t = 10\%$	
StaRX1500 [®] (in solid fraction)	
%(v/v)	%(w/w)
0.00	0.00
5.56	6.01
11.11	11.96
18.89	20.20
20.00	21.37
21.11	22.53
22.22	23.70
27.78	29.48
33.33	35.21
44.44	46.51

Tablets formulated with fibrous disintegrants

Different binary model mixtures (drug/fibrous disintegrant, see Table 5.6) were used to compare experimental and calculated disintegrant thresholds with regard to the shortest DT or the highest water uptake constant of tablets.

Tablets with formulation VII, VIII (caffeine) and IX (indomethacin) were prepared with the same methods than with formulations I-III and VI. All tablets were compressed at targeted porosity $\varepsilon_t = 10\%$. For formulations VII and VIII, round flat, 10mm diameter tablets with a targeted weight of 380 mg were prepared using the compaction simulator Presster[™].

For formulation IX, round, flat, 11 mm diameters tablets were compressed using Zwick[®] 1478 Universal Testing Instrument at a targeted weight of 300 mg. However, the low compactibility of indomethacin/AcDiSol[®] mixtures did not allow to reach targeted porosity of $\varepsilon_t = 10\%$ for formulation IX. Average porosity of the resulting tablets was $12.97 \pm 0.40\%$ (Table 5.6).

Table 5.6: Formulations composed of caffeine and indomethacin as model drugs, and AcDiSol[®] and L-HPC as model disintegrants (fibrous).

Formulation VII Caffeine powder A / AcDiSol [®]		Formulation VIII Caffeine powder A / L-HPC		Formulation IX Indomethacin / AcDiSol [®]	
$\varepsilon_t = 10\%$		$\varepsilon_t = 10\%$		$\varepsilon_t = 10\%$	
StaRX1500 [®] (in solid fraction)		StaRX1500 [®] (in solid fraction)		StaRX1500 [®] (in solid fraction)	
%(v/v)	%(w/w)	%(v/v)	%(w/w)	%(v/v)	%(w/w)
0.00	0.00	0.00	0.00	0.00	0.00
0.56	0.62	0.56	0.54	1.00	1.16
1.11	1.23	1.11	1.08	1.50	1.73
2.22	2.46	2.22	2.15	2.00	2.31
3.33	3.68	3.33	3.23	2.70	3.11
4.44	4.90	4.44	4.31	3.00	3.46
5.56	6.12	5.56	5.38	5.00	5.74
6.67	7.33	8.89	8.62	10.00	11.40
7.78	8.55	11.11	10.79		
8.89	9.75				
10.00	10.96				
11.11	12.16				

C. Preparation of the tablet formulations for dissolution testing

Caffeine (powder A) and Aspirin were used as model drugs, StaRX1500[®] as model swelling disintegrant and α -lactose monohydrate as model filler. Round, flat, 10 mm diameter tablets with a targeted weight of 380 mg were compressed with PressterTM for all formulations.

Pure caffeine, Aspirin and lactose tablets were first compressed to calibrate their respective solubility constants (SoC) in CA. The SoC of a substance cell in the CA determines the number of update necessary to dissolve virtually this substance, i.e. to change the solid state of corresponding cell into a liquid state (see sections 4.3.2E, F). Another mandatory condition for such a change of state is that the substance cell should have at least one liquid cell as direct neighbour in the matrix. Targeted porosity $\varepsilon_t=30\%$ for the three ingredients tablets. This porosity was chosen to facilitate the dissolution of the tablets, especially for poor soluble substances like Aspirin. An important point is that SoC is theoretically independent of the porosity chosen for calibration only if the virtual tablet is designed with the same porosity than the real tablet.

Different formulations (X-XIII) composed of a drug, a filler and possibly a disintegrant were then chosen as model mixtures and compressed similarly with a targeted porosity $\varepsilon_t=9\%$. Substances percentage (v/v tablet) for the different tableted formulations are listed in Table 5.7).

Table 5.7: Targeted composition (% v/v of the tablet) for experimental and *in silico* dissolution of tablets formulations X-XIII tablets.

Pure caffeine tablets			
Caffeine powder A		Porosity	
70		30	
Pure Aspirin tablets			
Aspirin		Porosity	
70		30	
Formulation X tablets			
Caffeine powder A	StaRX1500 [®]	α lactose monohydrate	Porosity
51.70	20.68	18.61	9.00
Formulation XI tablets			
Caffeine powder A	StaRX1500 [®]	α lactose monohydrate	Porosity
65.32	20.68	5.00	9.00
Formulation XII tablets			
Caffeine powder A	StaRX1500 [®]	α lactose monohydrate	Porosity
65.32	10.00	15.68	9.00
Formulation XIII tablets			
Caffeine powder A	StaRX1500 [®]	α lactose monohydrate	Porosity
50	20	18	12
Formulation XIV tablets			
Aspirin	StaRX1500 [®]	α lactose monohydrate	Porosity
60.00	0.00	26.00	14.00

5.1.4. Characterisation of the tablets

A. Porosity calculation

Tablets were weighted using Mettler Toledo AX204 DeltaRange[®] balance. Tablets diameters and thicknesses were measured using a micrometer digital caliper. Porosity was calculated for each tablet with equations Equation 65, Equation 66 and Equation 70 (see section 4.3.1).

B. Characteristics of the tablets used for disintegration and water uptake testing

Tablets formulated with non-fibrous disintegrants

Characteristics of formulations I-VI tablets are resumed in Table 5.8.

Table 5.8: Characteristics of formulations I-VI tablets.

Formulations	Tablets parameters			
	Weight (mg)	Thickness (mm)	Diameter (mm)	Porosity (% v/v)
Formulation I				
Paracetamol DC90 / StaRX1500 [®] A				
Targeted porosity=10 %	378.8 ± 0.6	3.95 ± 0.06	10	9.7 ± 1.5
Targeted porosity=8 %	380.1 ± 0.5	3.95 ± 0.02	10	8.4 ± 0.4
Formulation II				
Paracetamol DC90Fine / StaRX1500 [®] A				
Targeted porosity=10 %	375.6 ± 3.5	4.31 ± 0.18	10	10.0 ± 0.0
Targeted porosity=14 %	381.0 ± 1.1	4.33 ± 0.06	10	15.1 ± 0.8
Formulation III				
Caffeine powder A / StaRX1500 [®] A				
Targeted porosity=14 %	380.9 ± 0.6	3.76 ± 0.01	10.03 ± 0.00	14.4 ± 0.2
Formulation IV				
Caffeine granulated / StaRX1500 [®] B				
Targeted porosity=12 %	400.0 ± 2.0	-	11	12.0 ± 0.2
Formulation V				
Caffeine powder B/ StaRX1500 [®] B				
Targeted porosity=12 %	400.0 ± 2.0	-	11	12.0 ± 0.2
Formulation VI				
Indomethacin/ StaRX1500 [®] A				
Targeted porosity=10 %	381.6 ± 2.3	3.82 ± 0.03	10.01 ± 0.01	10.4 ± 0.3

Targeted weights were respected with a maximum difference of 1.6 mg for formulation I ($\epsilon_t=8\%$), formulation II ($\epsilon_t=14\%$), formulation III, IV, V and VI. For formulation I ($\epsilon_t=10\%$) and formulation II ($\epsilon_t=10\%$), tablets exhibited a difference in weight of 7.9 mg maximum with the targeted value of 380mg. However, deviations in weights were compensated with reductions in thickness and all formulations had calculated porosities close to their respective targeted porosities values: maximum difference of 1.8 % for formulation I ($\epsilon_t=10\%$) and of 1.9 % for formulation II ($\epsilon_t=14\%$).

Tablets formulated with fibrous disintegrants

Characteristics of formulations I-VI tablets are resumed in Table 5.9.

Table 5.9: Characteristics of formulations I-VI tablets.

Formulations	Tablets parameters			
	Weight (mg)	Thickness (mm)	Diameter (mm)	Porosity (% v/v)
Formulation VII Caffeine powder A / AcDiSoL [®] Targeted porosity=10%	380.9±1.3	3.70±0.02	10	10.12±0.26
Formulation VIII Caffeine powder A / L-HPC Targeted porosity=10%	380.5±1.0	3.72±0.02	10.03±0.01	12.97±0.40
Formulation IX Indomethacin/ AcDiSoL [®] Targeted porosity=10%	301.3±0.8	2.56±0.04	11	11.34±1.25

Targeted weights were respected (maximum difference of 2.1 mg for Formulation IX). For formulation VII, measured porosity of the tablets was close to $\epsilon_t=10\%$. However, a mean deviation of 2.97 % for formulation VIII and of 1.34 % for formulation IX was calculated ($\epsilon_t=10\%$).

C. Characterisation of the tablets for dissolution testing

Dimensional characteristics and calculated porosities of tablets are listed in Table 5.10. Targeted weights were respected with a maximum mean deviation of 1.4 mg (pure lactose tablets). Measured porosities of tablets were close to targeted values with a maximum difference of 1.86 % for pure caffeine compacts, except for formulation XIII, whose tablets exhibited a mean porosity higher of 4.44 % to targeted value (see Table 5.10).

Table 5.10: Characteristics of tablets for dissolution testing

Formulations	Tablets parameters			
	Weight (mg)	Thickness (mm)	Diameter (mm)	Porosity (% v/v)
Pure caffeine (Targeted porosity=30 %)	379.4±0.7	4.62±0.02	10.02±0.01	28.14±0.40
Pure lactose (Targeted porosity=30 %)	381.4±1.8	4.43±0.01	10.03±0.00	29.27±0.23
Pure Aspirin (Targeted porosity=30 %)	381.4±1.4	5.03±0.02	10.02±0.00	30.12±0.47
Formulation X Caffeine powder A / StaRX1500 [®] / Lactose (Targeted porosity=9 %)	380.7±1.3	3.52±0.01	10.04±0.01	9.30±0.14
Formulation XI Caffeine powder A / StaRX1500 [®] / Lactose (Targeted porosity=9 %)	380.8±1.0	3.54±0.01	10.04±0.01	9.56±0.40
Formulation XII Caffeine powder A / StaRX1500 [®] / Lactose (Targeted porosity=9 %)	380.4±1.0	3.56±0.02	10.03±0.01	10.21±0.32
Formulation XIII Caffeine powder A / StaRX1500 [®] / Lactose (Targeted porosity=12 %)	380.7±1.25	3.65±0.01	10.02±0.01	12.36±0.28
Formulation XIV Aspirin / Lactose (Targeted porosity=14 %)	380.8±1.5	3.96±0.01	10.02±0.00	14.44±0.19

5.1.5. Tablet testing methods

A. Disintegration testing

Disintegration time of the different tablet formulations was determined with an apparatus according to the specifications of Ph. Eur. 2002 (Disintegration apparatus: Sotax DT 3, Allschwil/Basel, Switzerland) (see schema in section 3.1.4). The distilled water at 37±0.1 °C was used as disintegration media. A total of six tablets were disintegrated for each measurement (two times three tablets). DT of each tablet was checked separately by visual inspection.

B. Water sorption measurement

The sorption ability of formulation IX was determined with a Krüss Processor Tensiometer K100 Mk2 (©Krüss GmbH, Hamburg, Germany) and the software LabDesk™ K100 Version 3.0, Artnr.: SW32 (©Krüss GmbH, Hamburg, Germany). Three tablets were tested separately.

All samples were put into a glass tube with a porous glass base and placed in contact with the test liquid, which was distilled water.

The increase of square mass of the samples were monitored and plotted against time (g^2/min , see Figure 5.11) in order to get the slope K according to the modified Washburn equation (Luginbuehl et al., 1994):

$$M^2(t) = K.t \quad \text{Equation 73}$$

M is the absorbed mass of water at a certain time t . K stands for a velocity constant of the water uptake.

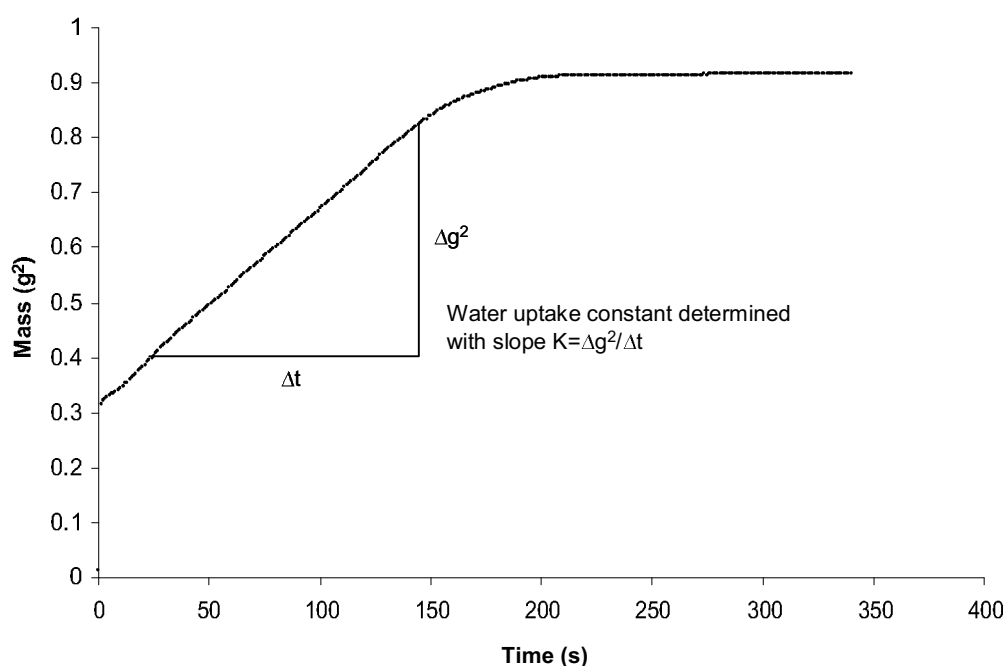


Figure 5.11: The water sorption constant K can be determined by plotting the increase of square mass against time. The water uptake curve in the figure was measured for indomethacin tablets with a 1 % (v/v solid fraction) AcDiSol[®].

C. Dissolution testing

The dissolution testing was performed using an apparatus of type II according to USP (Sotax AT7, Sotax AG, Basel, Switzerland) equipped with paddles. The speed of paddles was set to a constant speed of 50 rpm. The vessels were containing 500 ml dissolution medium for all experiments and a temperature of 37.2 ± 0.1 °C. The dissolution medium was distilled water at pH=6.8 for caffeine tablets and distilled water buffered at pH=6.8 with potassium phosphate, monobasic and NaOH for Aspirin tablets. Sink conditions were respected for each dissolution test. Samples (2 ml) of dissolution medium were removed at regular time intervals. An equal

volume of dissolution medium at 37.2 ± 0.1 °C was added to maintain a constant volume. These exchanges of volume were taken into account in percentage drug release calculations.

5.2. Results and discussion

5.2.1. Validation of Disintegration Optimisation module

A. Non-fibrous disintegrants

Experimental disintegrant thresholds

DT of compacted binary mixtures Paracetamol/StaRX1500[®] (Table 5.3), Caffeine/StaRX1500[®] (Table 5.4) and Indomethacin/StaRX1500[®] (Table 5.5) with increasing loading amount of StaRX1500[®] were measured. Disintegration results are shown below.

Disintegrant percentage of the tablets with having a minimum disintegration time was determined for each formulation (written in bold in DT values tables). Even though Equation 69 gives disintegrant percentage (v/v) of solid fraction, corresponding disintegrant percentage of total tablet are added in DT tables. Concentrations of disintegrant in total compact volume may be useful to study the state of the whole system when disintegrant grains percolate. However, in further discussions, percentage means volumetric percentage of the solid fraction of a tablet.

It has to be remembered that disintegration curve of a binary compacted mixture drug/swelling disintegrant usually exhibits a V-shape profile and can be described using percolation theory. The lowest point of the curve should correspond to the optimal disintegrant percentage with regard to the lowest disintegration time of the tablet (see 3.3.1D).

As it can be seen in Figure 5.12, DT of formulation I tablets ($\epsilon_t = 10$ %) is increasing with increasing disintegrant percentage until a concentration of disintegrant of 7 % disintegrant (DT = 158 ± 12.26 s. At 8 % disintegrant, DT decreases (148.17 ± 20.70 sec), but increases again for higher StaRX1500[®] % until a DT of 300.17 ± 25.39 s for 40 % disintegrant. A localized V-shape profile in the disintegration curve can thus be identified for 8 % disintegrant. Paracetamol DC90 and DC90Fine grades are in fact preparations for direct compression. Their small granules contain already 1-2 % disintegrant (exact value was not communicated) which leads to the following hypothesis: by swelling, added StaRX1500[®] first reduces the efficiency of the internal disintegrant of DC90 particles and DT of formulation I tablets thus increases until 7 % StaRX1500[®] in tablets. However, at 8 %, a water-conducting network of StaRX1500[®] grains and pores may appear as system is in case I (see Table 5.19). With higher StaRX1500[®] %, excess of swollen disintegrant and dead-end arms on the percolating network backbone may explain the longer DT after 8 % (see section 3.3.1D). Consequently, the experimental

disintegrant threshold for formulation I tablets with $\varepsilon_t = 10\%$ is assumed to be 8% (see Table 5.11).

Formulation I was also compressed with $\varepsilon_t = 8\%$ of the tablets. A similar disintegration curve is observed (see Figure 5.13), with a local V-shape profile having its lower point at 10% StaRX1500[®] for a DT=159.67±9.16s (Table 5.12). The increase of DT before this threshold is however less important than for formulation I with $\varepsilon_t = 10\%$ and tablet with 0% disintegrant have the lower DT. One reason which may explain this difference with formulation I at $\varepsilon_t = 10\%$ is the lower porosity of the tablets (8.4±0.4%). Indeed, it is possible that internal disintegrant of DC90 granules is not sufficient for conducting water directly within the whole tablet. After 10% disintegrant, DT increases again and reaches a maximum of 336.33±30.79 s for a concentration of 15% StaRX1500[®]. The experimental disintegrant threshold for formulation I tablets with $\varepsilon_t = 8\%$ is assumed thus assumed to be 10%(v/v) of solid fraction.

However, it was noticed that for formulation I, DT profiles show a lower point at the end of the curve. Corresponding disintegrant percentage could present a second threshold appearing when too many starch particles are present in the system. In this case, caging of all disintegrant grains by drug particles is not possible and a continuous cluster formed of disintegrant grains may appear at high disintegrant percentage. However, corresponding DT is longer than the one at selected disintegrant thresholds (10%).

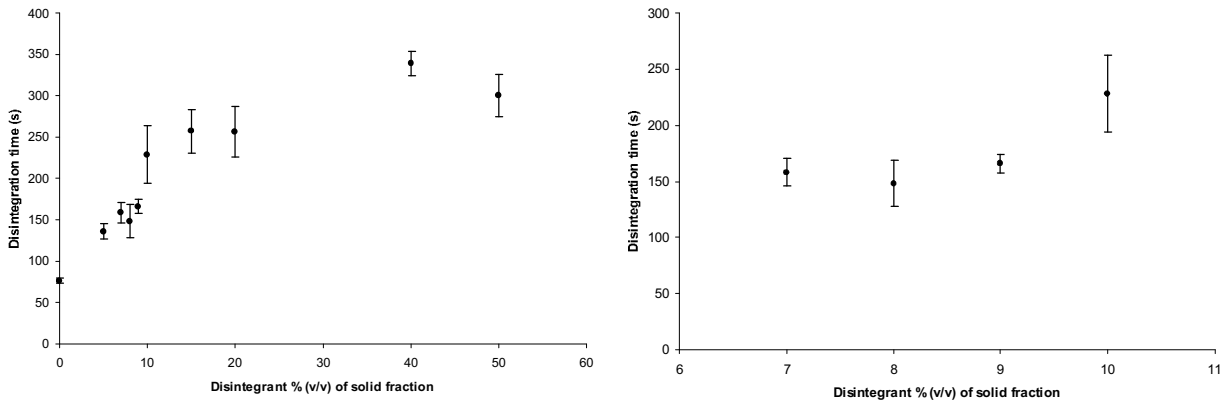


Figure 5.12: Disintegration time of tablets composed of Paracetamol DC90 and StaRX1500® A (Formulation I: $\epsilon_t = 10\%$) with increasing StaRX1500® % (v/v, solid fraction) from 0% to 50% and from 7% to 10%.

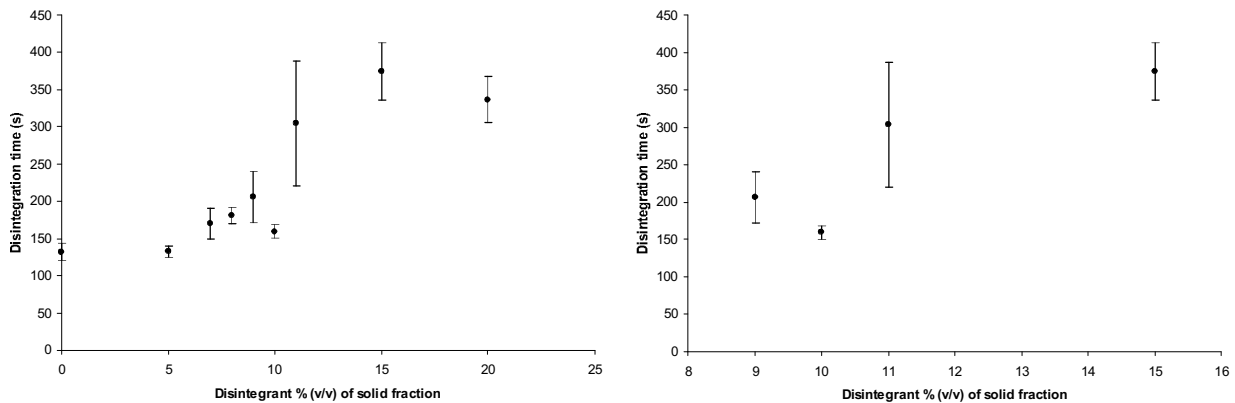


Figure 5.13: Disintegration time of tablets composed of Paracetamol DC90 and StaRX1500® A (Formulation I: $\epsilon_t = 8\%$) with increasing StaRX1500® volumetric ratio (of solid fraction) from 0% to 20% and from 9% to 15%.

Table 5.11: DT of formulation I tablets: Paracetamol DC90/StaRX1500® A ($\epsilon_t=10\%$):

StaRX1500® %(v/v)		Av. DT (sec.)	Stdev. DT
Solid fraction	Tablet		
0	0.0	76.17	3.06
5	4.5	135.67	9.07
7	6.4	158.00	12.26
8	7.3	148.17	20.70
9	8.2	166.00	8.29
10	9.2	228.33	34.49
15	13.6	256.83	25.93
20	18.2	256.17	30.42
40	35.4	339.17	14.72
50	43.6	300.17	25.39

Table 5.12: DT results of formulation I tablets: Paracetamol DC90/StaRX1500® A ($\epsilon_t=8\%$):

StaRX1500® %(v/v)		Av. DT (sec.)	Stdev. DT
Solid fraction	Tablet		
0	0.0	132.1	11.36
5	4.6	132.6	7.94
7	6.4	169.6	20.37
8	7.3	180.6	10.86
9	8.2	206.1	34.23
10	9.2	159.6	9.16
11	10.	304.1	83.51
15	13.	374.6	38.81
20	18.	336.3	30.79

Disintegration profile of Paracetamol DC90Fine tablets (formulation II) with $\epsilon_t = 10\%$ is shown in Figure 5.14 and corresponding values are listed in Table 5.13. An increase in DT is observed between 0% and 1% StaRX1500[®] (+2.83 s). As DC90Fine granules also contain 1-2% disintegrant internally, this small increase could be explained by the reduction of internal disintegrant efficiency when a small amount of StaRX1500[®] is added into tablets. However, when StaRX1500[®] percentage increases more, DT of tablets decreases until the lowest value of the curve (23.83 ± 0.98 s) corresponding to tablet with 5% disintegrant. From 5% to 15%, DT increases again slightly until 33.33 ± 1.51 s. From 15% to 50% disintegrant, DT increases then dramatically until a maximum of 192.33 ± 7.20 s. The global disintegration curve shows a non symmetric V-shape profile with less abrupt left arm. Experimental disintegrant threshold for formulation II tablets at $\epsilon_t = 10\%$ corresponds to lowest point of the curve, i.e. tablet with 5%(v/v) StaRX1500[®].

For tablets with formulation I and compressed at $\epsilon_t = 14\%$, DT slightly decreases first and increases in two steps when concentration of disintegrant increases (see Figure 5.15 and Table 5.14). However, the maximum difference of DT is 1s between 0% and 5% and is probably due to imprecision in DT testing, imperfect mixing or differences in tablet dimensions and weights. This part of the curve is thus assumed to be linear. When StaRX1500[®] % increases over 5%, DT increases significantly from 26.17 ± 1.47 s to 42.67 ± 2.07 s. Experimental disintegrant threshold is thus assumed to be 5%.

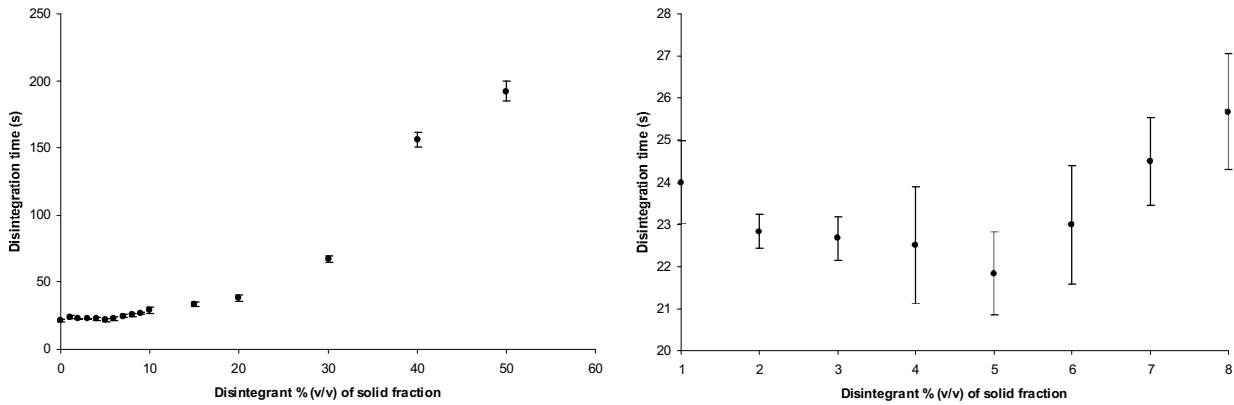


Figure 5.14: Disintegration time of tablets composed of Paracetamol DC90Fine and StaRX1500[®] A (Formulation II: $\epsilon_t = 10\%$) with increasing StaRX1500[®] percentage (v/v, solid fraction) from 0 % to 50 % and from 1 % to 8 %.

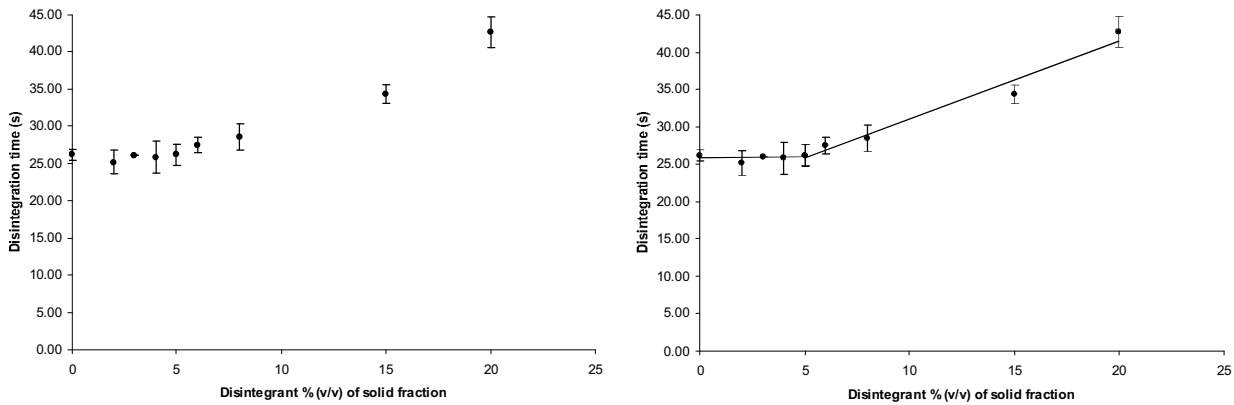


Figure 5.15: Disintegration time of tablets composed of Paracetamol DC90Fine and StaRX1500[®] A (Formulation II: $\epsilon_t = 14\%$) with increasing StaRX1500[®] % (v/v, solid fraction) from 0 % to 20 % (trend lines of the two identified parts of the curves are depicted in left picture)

Table 5.13: DT of formulation II tablets: Paracetamol DC90Fine/StaRX1500[®] A ($\epsilon_t=10\%$)

StaRX1500 [®] %(v/v)		Av. DT [s]	Stdev. DT
Solid fraction	Tablet		
0	0.0	21.17	0.75
1	0.9	24.00	0.98
2	1.8	22.83	0.41
3	2.7	22.67	0.52
4	3.6	22.50	1.38
5	4.5	21.83	0.98
6	5.4	23.00	1.41
7	6.3	24.50	1.05
8	7.2	25.67	1.37
9	8.1	26.67	1.03
10	9.0	29.00	2.00
15	13.5	33.33	1.51
20	18.0	38.33	2.42
30	27.0	67.00	2.28
40	36.0	156.33	5.54
50	45.0	192.33	7.20

Table 5.14: DT results of formulation II tablets: Paracetamol DC90Fine/StaRX1500[®] A ($\epsilon_t=14\%$)

StaRX1500 [®] %(v/v)		Av. DT [s]	Stdev. DT
Solid fraction	Tablet		
0	0.0	26.17	0.75
2	1.7	25.17	1.60
3	2.6	26.00	0.00
4	3.4	25.83	2.14
5	4.3	26.17	1.47
6	5.1	27.50	1.05
8	6.8	28.50	1.76
15	12.6	34.33	1.21
20	16.7	42.67	2.07

For formulation III tablets with $\varepsilon_t = 14\%$ and containing caffeine grade A, DT decreases dramatically when disintegrant percentage (v/v) increase from 0% to 5.81% (see Figure 5.16 and Table 5.15). The steepness of the curve becomes less abrupt from 5.81% and reaches a minimum for 19.77% disintegrant (24.50 ± 0.55 s). While concentration of StaRX1500[®] increases from 20.93% to 23.26% the DT of tablets decreases of 1.5 s only. Over 23.26%, only a small increase of DT is observed (11.5 s). The part of the curve between 19.77% and 34.88% disintegrant is almost linear, thus selected experimental disintegrant threshold is 19.77%.

The behaviour of DT describes an asymmetric “V”-shaped profile for formulation IV tablets, in particular between 0% and 19.12% disintegrant (see Figure 5.17 and Table 5.16). DT of the tablets continues to increase over 19.12% and reach a maximum of 3692 ± 220 s for 79.10% disintegrant. The minimum DT of 112 ± 14 s for 7.13% disintegrant represents the experimental disintegrant threshold for this formulation.

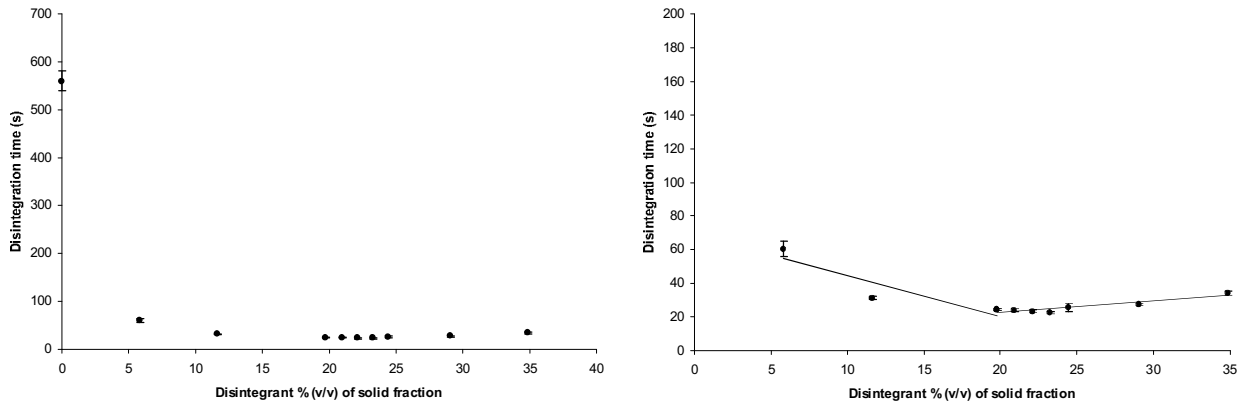


Figure 5.16: Disintegration time of tablets composed of Caffeine powder A and StaRX1500® A (Formulation III: $\epsilon_t = 14\%$) with increasing StaRX1500® percentage (v/v, solid fraction) from 0% to 38.88% and from 5.81% to 34.88%. Trend lines of the two identified parts of the curve are depicted in left picture

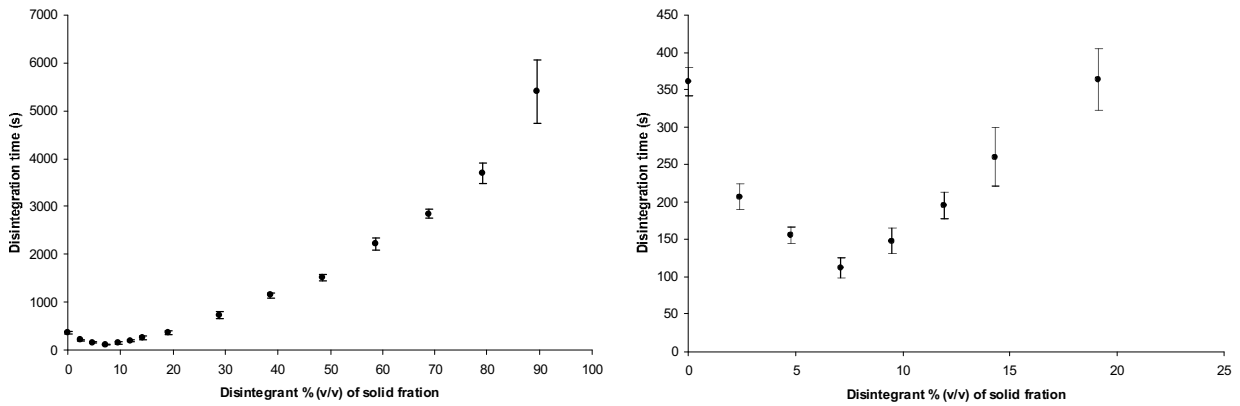


Figure 5.17: Disintegration time of tablets composed of Caffeine granulated and StaRX1500® B (Formulation IV: $\epsilon_t = 12\%$) with increasing StaRX1500® volumetric ratio (of solid fraction) from 0% to 89.49% and from 0% to 19.12%.

Table 5.15: DT of formulation III tablets: Caffeine powder A/StaRX1500® A ($\epsilon_t=14\%$)

StaRX1500® %(v/v)		Av. DT [s]	Stdev. DT
Solid fraction	Tablet		
0.00	0.00	560.17	19.91
5.81	4.95	60.33	4.63
11.63	9.94	31.17	0.98
19.77	16.95	24.50	0.55
20.93	17.96	24.00	1.10
22.09	18.90	23.33	1.03
23.26	19.89	22.50	0.55
24.42	20.88	25.50	2.19
29.07	24.93	27.17	0.55
34.88	29.82	34.00	1.33

Table 5.16: DT of formulation IV tablets: Caffeine granulated/StaRX1500® B ($\epsilon_t=12\%$)

StaRX1500® %(v/v)		Av. DT [s]	Stdev. DT
Solid fraction	Tablet		
0.00	0.00	361	19
2.37	2.09	207	17
4.75	4.18	156	11
7.13	6.27	112	14
9.51	8.37	148	17
11.92	10.49	196	18
14.32	12.60	260	39
19.12	16.83	364	41
28.85	25.39	734	67
38.67	34.03	1144	61
48.61	42.78	1514	61
58.66	51.62	2220	135
68.82	60.56	2844	99
79.10	69.61	3692	220
89.49	78.75	5400	659

DT curve for formulation V tablets exhibits an asymmetric V-shape profile with a minimum DT of 28 ± 1 s for tablets containing 19.39 % disintegrant (see Figure 5.18). The left arm of the curve goes from 317 ± 10 s (0 % dis.) to this minimum (Table 5.17). DT is increasing dramatically when percentage StaRX1500[®] B is over 59.07 %. A maximum of 4672 ± 502 s is reached for a disintegrant concentration of 89.65 %. Left arm of the curve is less steep than right arm; however the difference of DT between 0 % and 28 % is 289 s. Thus this part of the curve is not assumed to be a linear segment of the profile. Experimental disintegrant threshold is thus 19.39 % disintegrant.

The DT curve for formulation VI tablets decreases dramatically of more than 1123 s between 0 % and 5.56 % disintegrant in tablets. This high steepness at this part of the profile is probably due to the low porosity ($\epsilon_t = 10$ %) of the tablets and to the high hydrophobicity of indomethacin. Indeed, pure indomethacin tablets were not disintegrated after 22 min (see Figure 5.19 and Table 5.18). DT continues decreasing but with lighter steepness between 5.56 % (DT= 196.33 ± 37.48 s) and 20 % (DT= 63.33 ± 4.76 s) points. Between 21.11 % and 55.56 % the curve decreases and increases again but DT variations are very low maximum (22.53 s) in comparison to the whole profile. Thus, this part of the curve can be assumed to be linear. The experimental disintegrant threshold for formulation VI was chosen at 20 %.

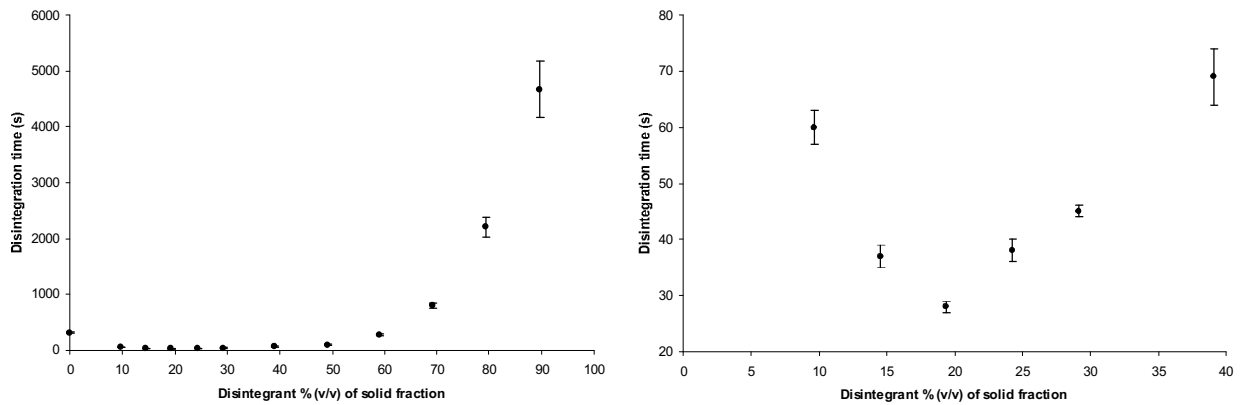


Figure 5.18: Disintegration time of tablets composed of Caffeine powder B and StaRX1500[®] B (Formulation V: $\epsilon_t = 12\%$) with increasing StaRX1500[®] volumetric ratio (of solid fraction) from 0 % to 89.65 % and from 9.66 % to 39.07 %.

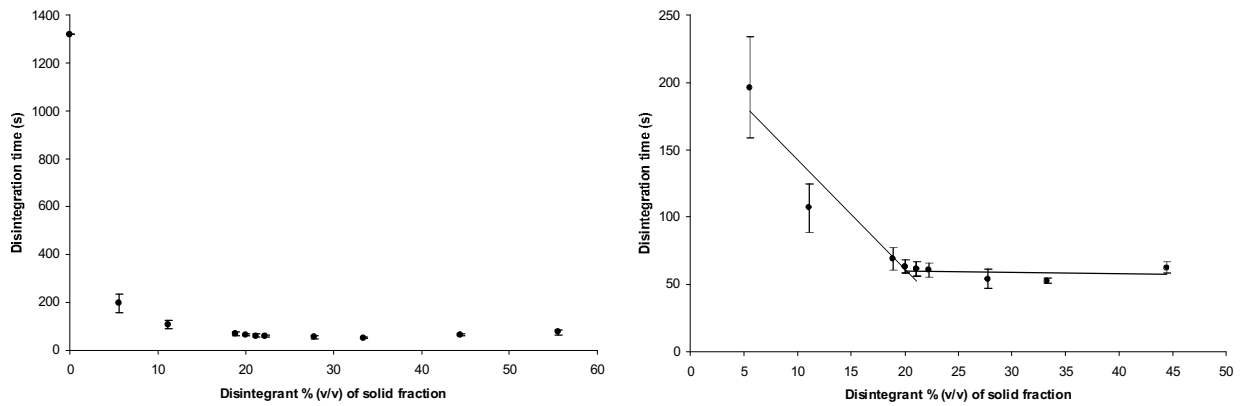


Figure 5.19: Disintegration time of tablets composed of indomethacin and StaRX1500[®] A (Formulation VI: $\epsilon_t = 10\%$) with increasing StaRX1500[®] volumetric ratio (of solid fraction) from 0 % to 55.56 % and from 5.56 % to 44.44 %.

Table 5.17: DT of formulation V: Caffeine powder B/StaRX1500[®] B ($\epsilon_t=12\%$)

StaRX1500 [®] %(v/v)		Av. DT [s]	Stdev. DT
Solid fraction	Tablet		
0.00	0.00	317	10
9.66	8.50	60	3
14.51	12.77	37	2
19.39	17.06	28	1
24.28	21.37	38	2
29.19	25.69	45	1
39.07	34.38	69	5
49.03	43.15	100	7
59.07	51.98	268	17
69.18	60.88	798	41
79.37	69.85	2209	173
89.65	78.89	4672	502

Table 5.18: DT of formulation VI: Indomethacin/StaRX1500[®] A ($\epsilon_t=10\%$)

StaRX1500 [®] %(v/v)		Av. DT [s]	Stdev. DT
Solid fraction	Tablet		
0.00	0.0	>	0.00
5.56	5.0	196.33	37.48
11.11	10.0	106.83	18.15
18.89	16.9	69.17	8.70
20.00	18.0	63.33	4.76
21.11	18.9	61.67	5.54
22.22	19.9	60.83	5.12
27.78	24.8	54.33	6.98
33.33	29.6	52.80	2.17
44.44	40.1	62.67	4.32
55.56	49.7	75.33	9.58

Comparison of experimental and calculated threshold

Theoretical disintegrant thresholds (i.e. optimum disintegrant concentration for a shortest disintegration time of drug/disintegrant tablets) were calculated with Equation 69 after determination of the system case with Equation 62. Calculated values of r/R , corresponding cases, and calculated and experimental thresholds are reported in table Table 5.19 for each formulation.

Table 5.19: Calculated and experimental values of disintegrant thresholds for formulation I-VI tablets. Ratios r/R and corresponding system cases are indicated. R and r represent the mean radius of a drug particle and disintegrant grain respectively.

Formulations	r/R	Case	Disintegrant thresholds	
			Calculated	Experimental
Formulation I Paracetamol DC90 / StaRX1500 [®] A				
Targeted porosity=10 %	0.125	I	8.02	8
Targeted porosity=8 %	0.125	I	9.07	10
Formulation II Paracetamol DC90Fine / StaRX1500 [®] A				
Targeted porosity=10 %	0.201	I	7.78	5
Targeted porosity=14 %	0.201	I	3.75	5
Formulation III Caffeine powder A / StaRX1500 [®] A				
Targeted porosity=14 %	2.246	II	18.69	19.77
Formulation IV Caffeine granulated / StaRX1500 [®] B				
Targeted porosity=12 %	0.105	I	6.18	7.13
Formulation V Caffeine powder B/ StaRX1500 [®] B				
Targeted porosity=12 %	1.617	II	18.18	19.39
Formulation VI Indomethacin/ StaRX1500 [®] A				
Targeted porosity=10 %	8.842	II	17.86	20

Theoretical disintegrant thresholds are plotted versus experimental thresholds in Figure 5.8. It can be seen that the points on this chart are split into two clusters: a left bottom cluster corresponding to case 1 systems and an upper left cluster corresponding to case 2 systems. The region between the two clusters corresponds to pharmaceutical compacts having very low porosity (0-4 %, see Equation 69). As it is very hard to achieve such a low porosity practically, there are no data points shown for disintegrant percentage in that range.

The points have a regression coefficient of adjusted $R^2 = 0.959$. It can be deduced that there is a good linear correlation between experimental and calculated thresholds. The trend line has however a small deviation from $y=x$ line. The theoretical assumptions of the model for non-fibrous disintegrant (section 4.3.1A) assume a certain deviation of the predicted thresholds. This deviation takes into account the fact that the threshold for the spherical systems may vary from system to system with respect of the system size (number of particles in a compact). As the pharmaceutical compact is not an infinite system, the deviation may become higher with significant decrease of the particle number. Any percolating system at the vicinity of the percolation threshold is tending to expose a very stochastic behaviour, which is amplified with decrease of the particles number.

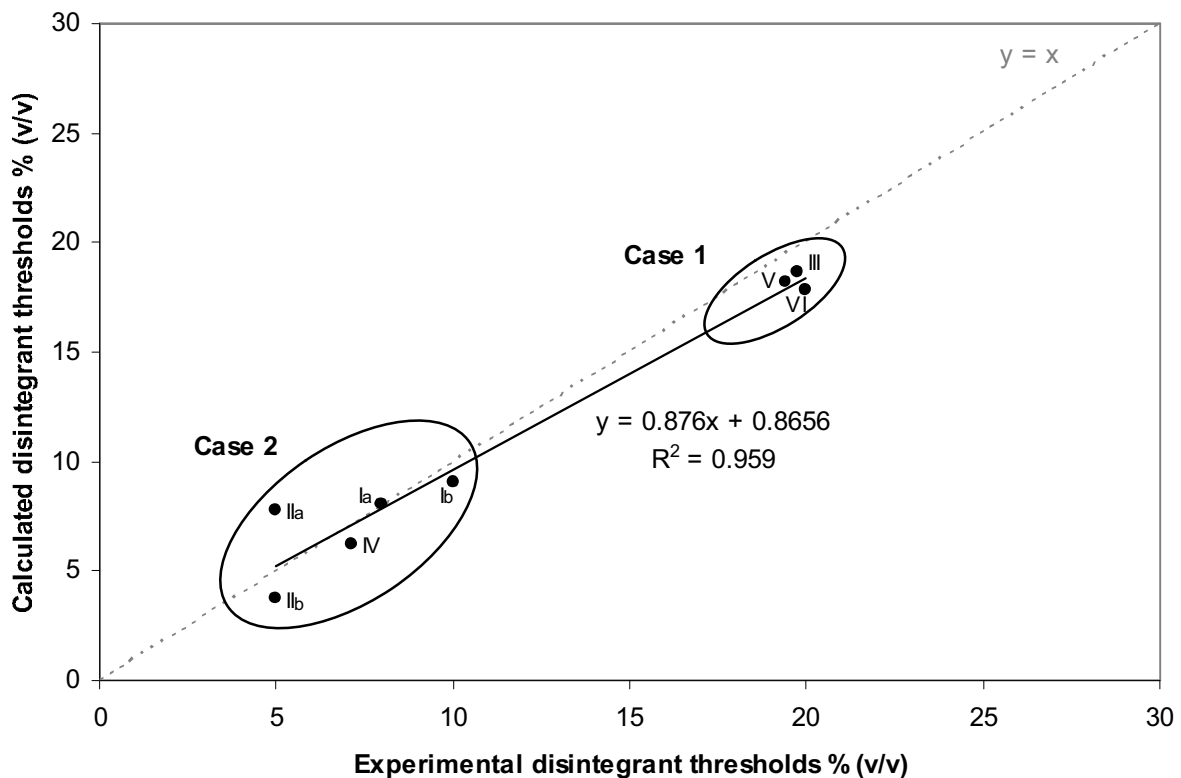


Figure 5.20: Estimated vs. experimental percentage (v/v) of disintegrant (disintegrant thresholds) at minimum disintegration time of formulations I-VI tablets.

Ia: formulation I with $\epsilon_t = 10\%$, Ib: formulation I with $\epsilon_t = 8\%$, IIa: formulation II with $\epsilon_t = 10\%$, IIb: formulation II $\epsilon_t = 14\%$

The non-fibrous model of “Disintegration Optimisation” module leads to possible optimisation of a formulation by just increasing or decreasing the porosity of a compact to shift the effective percolation threshold to the most optimal region. Furthermore, these findings explain the tablet formulations, where the disintegration time is sensitive to the tableting force.

It shows the importance to keep the thickness and the mass of a tablet constant during the compaction process.

In this study, it became evident that the percolation threshold of the disintegrant or the combination of the disintegrant with a hydrophilic porous network, which forms an infinite cluster, plays an outstanding role in the disintegration process of a tablet. In addition, it was possible to predict with a high precision this percolation threshold for tablet formulations consisting of binary mixtures. In this context, it is important to take into account the particle size ratio of the components and effects of porosity. It could be shown that the range of concentrations where the percolation effect occurs is very narrow. Thus, it can be easily overlooked if the experimental design is performed without a previous estimation of the location of the percolation threshold. On the other hand it has to be kept in mind that the determination of the percolation threshold leads to the formulation with the optimal disintegration time, but it does not give an answer about the absolute value of the disintegration time. This time depends on the formulation, that is, on its hydrophobicity and on the disintegrant involved. It has to be taken into account that the proposed method and formulation strategy is not limited to binary compositions only, but can be used with ternary mixtures by applying the renormalisation technique (Kimura et al., 2007). The important points are to know which formulation will show the minimum of the disintegration time, that is, to determine the percolation threshold and the behaviour of the disintegration time in the vicinity of the threshold and the sensitivity to the compaction pressure to obtain if the expected disintegration time is reached for a robust formulation.

B. Fibrous disintegrants

The disintegration times of formulation VII (caffeine/AcDiSol[®]) and formulation VIII (caffeine/L-HPC) tablets with increasing loading amount of fibrous disintegrant were measured. Experimental disintegrant thresholds of formulations were determined from DT profiles. It is assumed here that thresholds correspond to the disintegrant percentage in tablets having the shortest disintegration time, i.e. tablets with a percolating cluster of disintegrant fibers conducting water.

During disintegration tests with formulation IX tablets (indomethacin/ AcDiSol[®]), compacted fragments of pure indomethacin remained intact on the mesh of the disintegration apparatus during more than 60 min. It was thus difficult to determine experimentally the disintegrant threshold using disintegration testing. Consequently, the threshold of formulation IX tablets was determined measuring water sorption of tablets with loading amount of disintegrant (see table Table 5.6).

Figure 5.21 shows the DT profile of formulation VII tablets with increasing fibrous disintegrant percentage. DT values for each percentage AcDiSol[®] in tablets are listed in table Table 5.20. A minimum of disintegration time (15.33 ± 0.52 s) has been reached at 2.22 % of disintegrant. The decrease of DT is very abrupt between 0 % and 0.56 % disintegrant (mean difference $DT > 913$ s). The steepness of the curve is reduced between 0.56 % and 2.22 % (16.67 s difference). After a critical value at 2.22 % disintegrant, DT increases moderately and reaches a maximum of 91.50 ± 3.08 s for a concentration of 11.11 %. The very asymmetric V-shape profile of DT curve (very low right arm) is due to the low swelling rate of AcDiSol[®] fibers. After threshold, the dead ends do appear on main percolating backbone formed by disintegrant fibers. However, unlike formulations with StaRX1500[®], wetted AcDiSol[®] does not block the pores by intensive swelling. According to previous observations, disintegrant threshold is 2.22 % for formulation VII.

The disintegration profile of tablets composed of caffeine and L-HPC (formulation VIII, Figure 5.22) shows a rapid decrease of DT between 0 % and 1.11 % (from 612.17 ± 130.24 s to 88.83 ± 14.99 s, see Table 5.21). Next points of the curve show a slower decrease until 5.56 % (until 16.00 ± 2.10 s) and a small increase after this disintegrant percentage (6 s). However, between 3.33 % and 11.11 %, the variation is very small in comparison with the whole DT profile. These variations are not being significant and may be due to variations during mixing process between the tablets or imprecision of DT measurements. Consequently, it is assumed that the part of the curve between 3.33 % and 11.11 % is almost flat. The inflexion point at 3.33 % is thus the experimental disintegrant threshold.

As L-HPC fibers have a higher aspect ratio than AcDiSol[®] fibers (see section 5.1.2D), L-HPC threshold should be lower than AcDiSol[®] threshold (see section 4.3.1B). Moreover, calculated porosity of tablets with L-HPC is 2 % higher than tablets with AcDiSol[®]. According to these observations, the following hypothesis was done: because of their high aspect ratio L-HPC fibers are probably folding between drug particles during compression of the tablet. As it was explained in section 4.3.1B of this thesis, fibers have a percolation threshold that is higher if they are folded than if they keep a straight position.

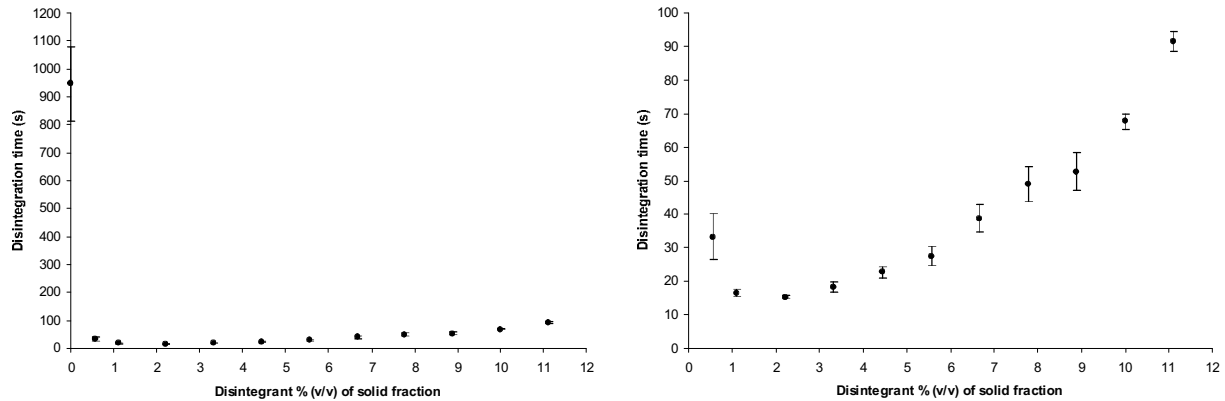


Figure 5.21: Disintegration time of tablets composed of Caffeine powder A and AcDiSol® (Formulation VII: $\epsilon_t = 10\%$) with increasing AcDiSol® volumetric ratio (of solid fraction) from 0.00 % to 11.11 % and from 0.56 % to 11.11 %.

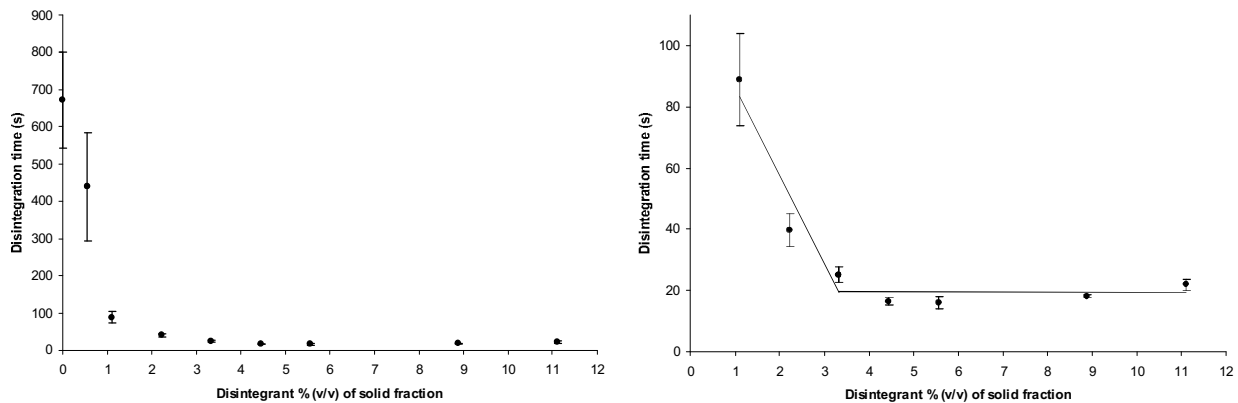


Figure 5.22: Disintegration time of tablets composed of Caffeine powder A and L-HPC (Formulation VIII: $\epsilon_t = 10\%$) with increasing L-HPC volumetric ratio (of solid fraction) from 0.00 % to 11.11 % and from 1.11 % to 11.11 %.

Table 5.20: DT of formulation VII tablets: Caffeine powder A/StarX1500® A ($\epsilon_t=10\%$)

AcDiSol® %(v/v)		Av. DT [s]	Stdev. DT
Solid fraction	Tablet		
0.00	0.00	946.83	133.04
0.56	0.50	33.17	6.82
1.11	1.00	16.50	1.05
2.22	1.99	15.33	0.52
3.33	3.01	18.33	1.51
4.44	3.99	22.67	1.63
5.56	5.00	27.50	2.81
6.67	5.99	38.67	4.08
7.78	6.98	48.83	5.15
8.89	7.97	52.67	5.57
10.00	8.99	67.67	2.25
11.11	9.97	91.50	3.08

Table 5.21: DT of formulation VIII tablets: Caffeine powder A/L-HPC ($\epsilon_t=10\%$)

L-HPC %(v/v)		Av. DT [s]	Stdev. DT
Solid fraction	Tablet		
0.00	0.00	672.17	130.24
0.56	0.49	439.25	144.72
1.11	0.96	88.83	14.99
2.22	1.93	39.83	5.27
3.33	2.90	25.17	2.48
4.44	3.87	16.50	1.22
5.56	4.85	16.00	2.10
8.89	7.76	18.20	0.45
11.11	9.70	22.00	1.79

Experimental disintegrant threshold for formulation IX was determined by measuring water sorption of the tablets with increasing loading amount of disintegrant. Water uptake constants K were calculated according to the method presented in section 5.1.5B. Water uptake graph is shown in Figure 5.23 and values of constants K are listed in Table 5.22.

Experimental data have shown the leveling off of the water uptake constant at the values above 3 % v/v of AcDiSol[®]. The small decrease of K at 5 % disintegrant is probably due to variation during mixing between tablets (high standard deviation) or imprecision in measurements. As K increases only slightly at 10 % in comparison to its value at 3 %, this part of the graph is assumed as almost horizontal. Thus, the disintegrant concentration of 3 % is experimental disintegrant threshold for formulation IX.

Additionally, K values were normalised by inversion and different fittings of general equation of percolation theory (see Equation 46) using a threshold value $p_c=0.0315$ into experimental points were tested. The theoretical threshold value was calculated value for ellipsoid of revolution of aspect ratio 20 (4.3.1B) and mean aspect ratio of AcDiSol[®] fibers was situated in the range 15-20 using SEM photographs 5.1.2D. The best fitting of the equation of percolation theory into the experimental data in the vicinity of this threshold had yielded a value for critical exponent β (strength of the infinite cluster) equal to 0.39. The quality of fit had yielded $R^2=0.998$. This value used for β is in a good agreement with known value of β for 3-dimensional systems (0.41) (YI et al., 2004).

It is possible to conclude that the behaviour of AcDiSol[®] particles was well approximated by percolation of overlapping ellipsoids of revolution (see section 4.3.1B). The minimal volumetric concentration of AcDiSol[®] that assures inclusion of all disintegrant particles into infinite cluster was found at 3 % (v/v). This value represents the minimum amount for a shortest disintegration time of tablet containing AcDiSol[®]. Thus, according to the previous theoretical considerations and percolation on overlapping ellipsoids, the critical value of fibrous disintegrant particles does not depend on particle length only but on the aspect ratio.

However, DT profile of formulation VII has shown an AcDiSol[®] threshold slightly smaller (2.22 %) than formulation VIII. The reason to this could be the difference of methods used for threshold determination (disintegration and water sorption). Furthermore, as tablets are not ideal infinite system, percolation threshold values may show small variations (see section 3.3.1).

In addition, experimental L-HPC threshold for formulation VIII was approximately the same than AcDiSol[®] threshold for formulation IX. These two values should be different according to the different aspect ratios between fibers of the two excipients. It is supposed that L-HPC fibers are folding in a compact because of the large aspect ratio.

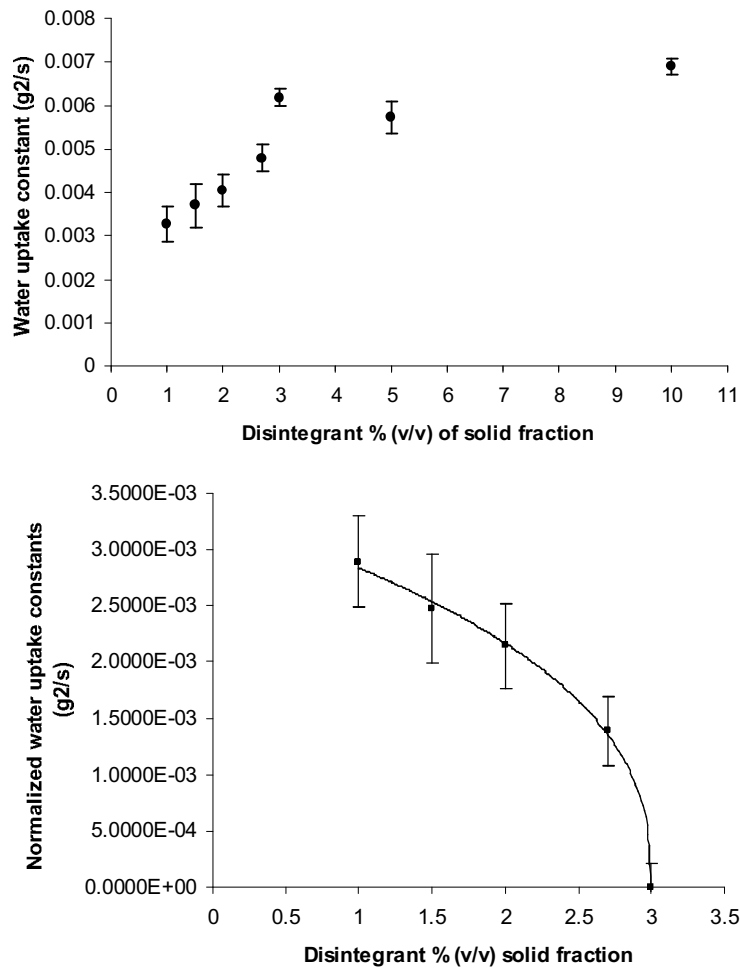


Figure 5.23: Water uptake measurement of formulation IX

Table 5.22: Water uptake of formulation IX:
Indomethacin/AcDiSol[®] ($\epsilon_t=10\%$)

L-HPC%(v/v)		WU const. [g2/s]	Stdev. WU
Solid fraction	Tablet		
1.00	0.90	0.003279	0.000405
1.50	1.33	0.003698	0.000490
2.00	1.78	0.004029	0.000374
2.70	2.39	0.004785	0.000301
3.00	2.64	0.006173	0.000208
5.00	4.41	0.005718	0.000359
10.00	8.78	0.006895	0.000176

5.2.2. Validation of the dissolution simulation module

All dissolution simulations shown below were performed using DS module of the expert system. Virtual tablet patterns were designed using TD program by respecting shapes and dimensions of the tablets to model. Tablet compositions were set up according to real tablet formulations and porosities using packing program. The aspect ratios between mean particle sizes of the different ingredients were conserved. Little differences however appeared between *in silico* and experimental tablet compositions. These small variations in percentages are due to rounded values of ingredients percentage during discretisation process of tablets. The differences are however reduced when increasing the scale of the system (increase of the numbers of CA cells per ingredient particles).

A. Determination of CA solubility constants of the drugs

Drug release of pure caffeine and Aspirin tablets were measured experimentally (see Figure 5.24 and Figure 5.25). *In silico* dissolution profiles of corresponding virtual tablets were fitted with experimental dissolution points by changing solubility constants (SoC) values of the drugs. The SoC leading to the best fittings for each API were selected and entered in input of drug database (DB module). These SoC were used for further dissolution simulations of compacted formulations containing corresponding drugs.

Pure caffeine and Aspirin tablets showed first order release profiles. A percentage of 90 % of caffeine were dissolved after 7.30 min (see Table 5.23). For Aspirin, 90 % release occurred at 300 min (see Table 5.23). Maximum percentage release measured experimentally for pure Aspirin tablets were only 95.57 ± 0.65 % (450 min). A partial degradation of Aspirin during dissolution process could explain this incomplete release.

The best fitting of virtual dissolution profile with experimental release points of pure caffeine tablets is shown in Figure 5.24. Differences in release time between the two curves is 0.35 min at 50 % and 2.8 min at 90 % (see Table 5.23). This deviation at 90 % could not be reduced more. According to the high standard deviations of experimental points before 90 %, this fitting is satisfying enough and corresponding caffeine SoC was conserved for further simulations.

For pure Aspirin tablets, the difference between experimental and *in silico* release values is 6min at 50 % and 50 min at 90 % release (see Table 5.23). This fitting was however the best possible for pure Aspirin tablets and the obtained Aspirin SoC value was kept.

The calibration of α -lactose monohydrate SoC was not possible following the same method than for caffeine and Aspirin, as this filler does not absorb UV. Consequently, it was not possible to measure lactose concentrations of dissolution samples for plotting a dissolution curve. The time for 100 % release of pure lactose tablets were thus estimated visually.

According to visual inspections, mean value for 100 % release 34.06 ± 3.59 min (see Table 5.23). The calibration of SoC for lactose was performed by generating *in silico* dissolution profiles of virtual lactose tablets with different SoC values until the simulated profile reach 100 % dissolution at 34 min. The corresponding SoC value was entered for lactose in drug database of DB module.

Table 5.23: Experimental and virtual tablets compositions and dissolution times of pure drug tablets.

Pure caffeine tablets		
Components	Tablet composition (%v/v)	
	Experimental	in silico
Caffeine	71.86	70.62
Porosity	28.14	29.38
% drug released	Dissolution times (min)	
	Experimental	in silico
50	1.75	2.1
90	7.30	4.5

Pure Aspirin tablets		
Components	Tablet composition (%v/v)	
	Experimental	in silico
Aspirin	69.88	-
Porosity	30.12	-
% drug released	Dissolution times (min)	
	Experimental	in silico
50	118.00	124.00
90	300.00	250.00

Pure lactose tablets		
Components	Tablet composition (%v/v)	
	Experimental	in silico
Lactose	70.73	-
Porosity	29.27	-
% drug released	Dissolution times (min)	
	Experimental	In silico
100	34.06	-

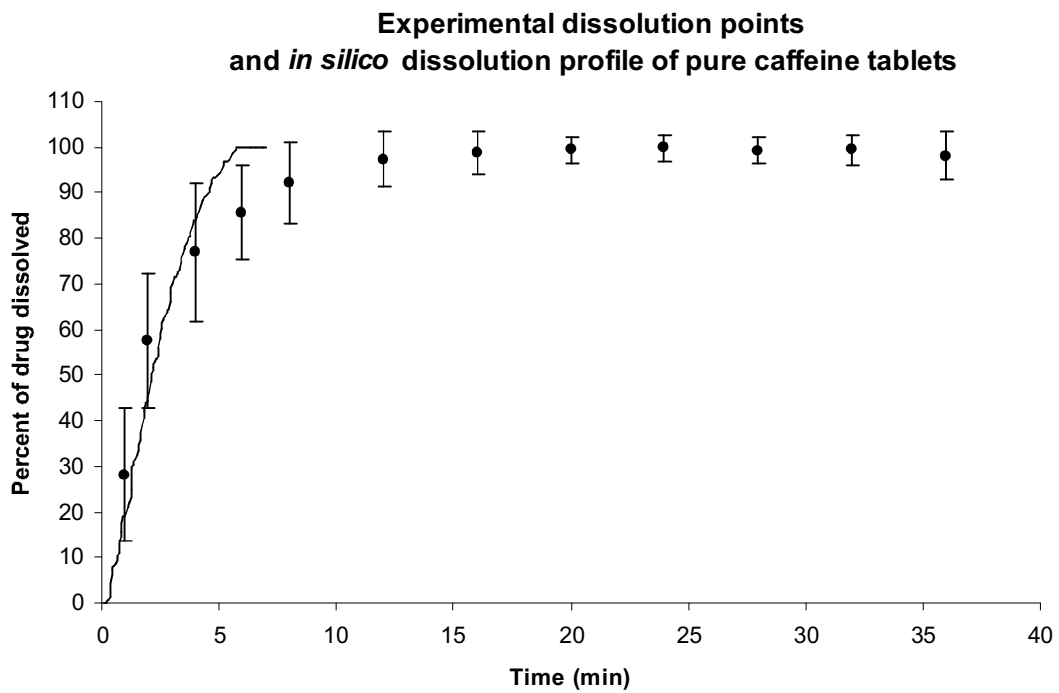
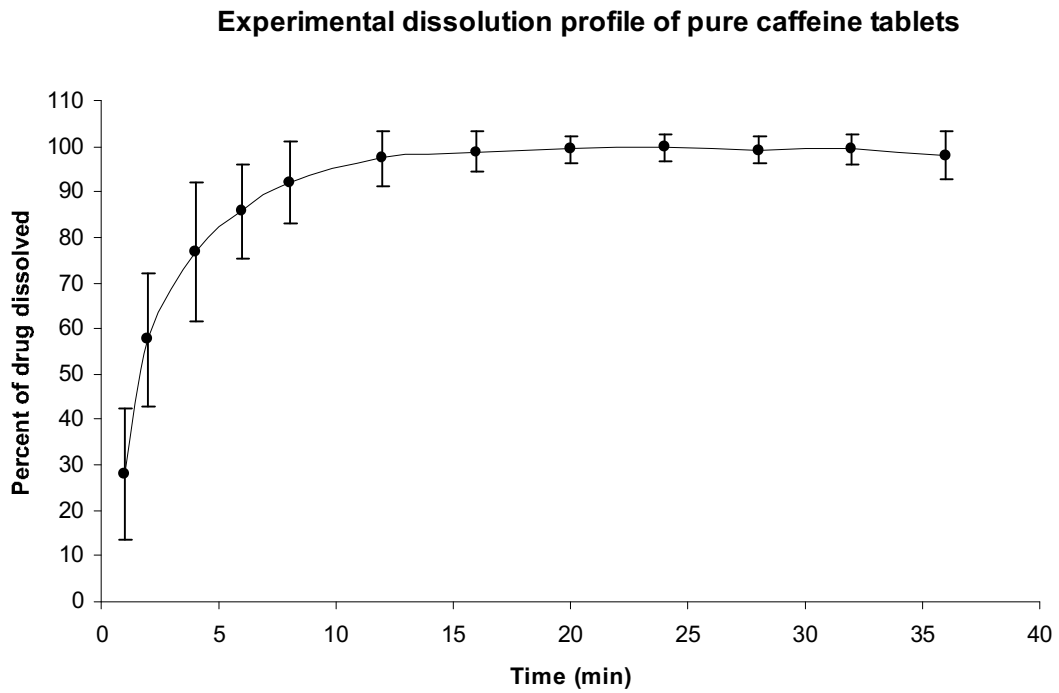
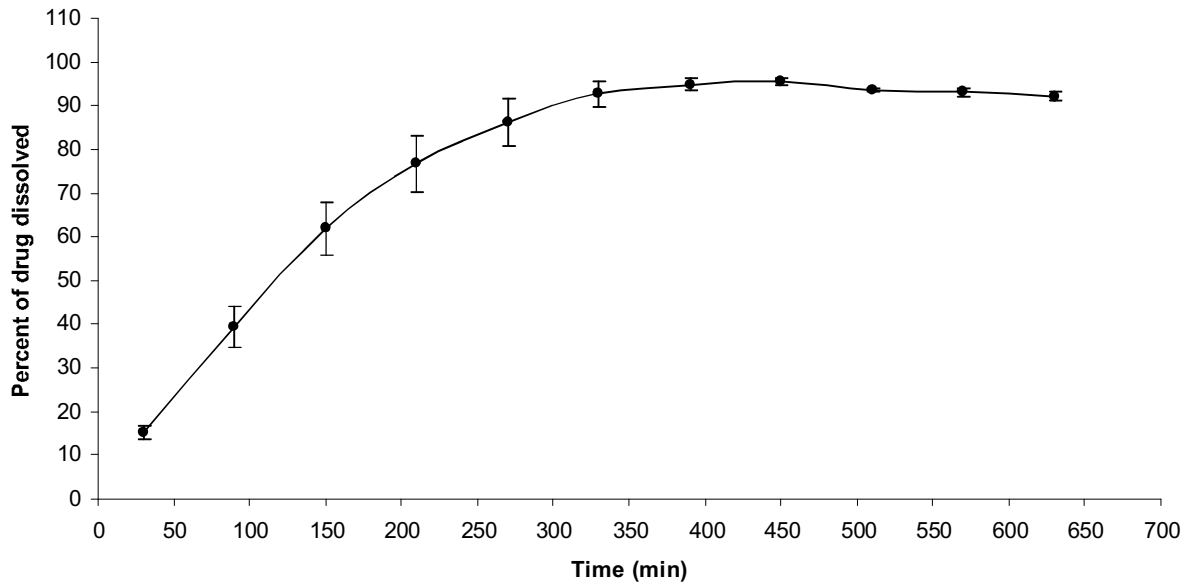


Figure 5.24: Experimental dissolution profile (top) and *in silico* dissolution profile fitted with experimental points (bottom): pure caffeine tablets.

Experimental dissolution profile of pure aspirin tablets



Experimental dissolution points and *in silico* dissolution profile of pure aspirin tablets

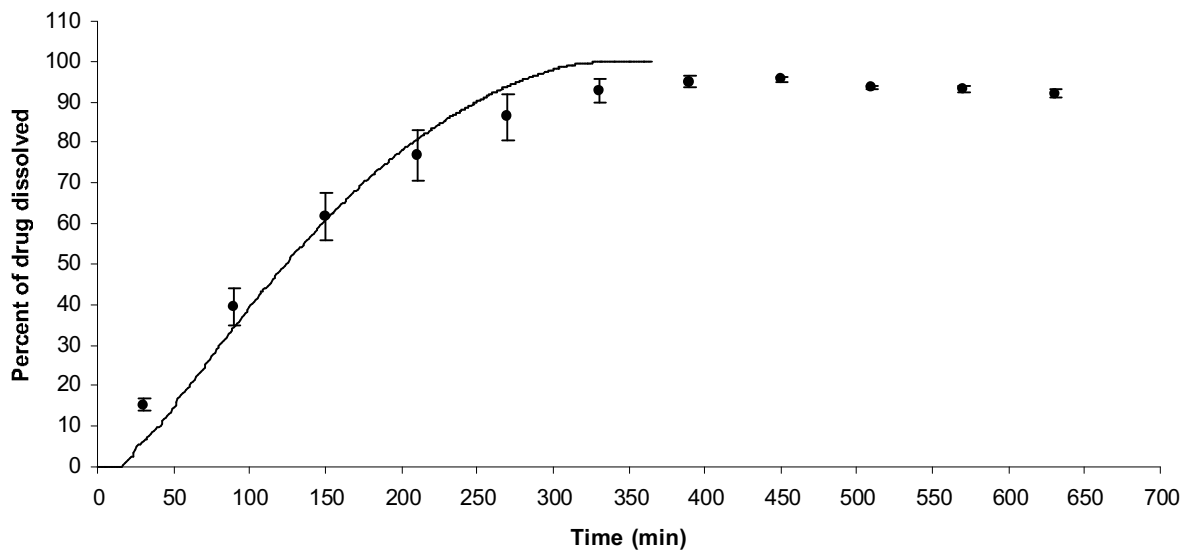


Figure 5.25: Experimental dissolution profile (top) and *in silico* dissolution profile fitted with experimental points (bottom): pure Aspirin tablets.

B. Comparison of *in silico* and experimental dissolution profiles

Experimental and *in silico* dissolution profiles of different compacted mixtures with caffeine as model drug, lactose as model filler and StaRX1500[®] as model disintegrant are shown below (see Figure 5.26-Figure 5.29). Tablets compositions (volumetric %) of the corresponding formulations (X-XIII) are listed in Table 5.24 and compared with virtual tablets compositions used for dissolution simulation. For both experimental and virtual dissolution profiles, Table 5.24 gives dissolution times at 50 % and at 90 % release. Porosity was targeted at 9 % for formulations X-XII tablets and at 12 % for formulation XIII. The SwC of StaRX1500[®] was calibrated by adjusting *in silico* profile of formulation X with corresponding experimental dissolution points. All dissolution profiles were of first order.

For formulation X, virtual and experimental dissolution profiles showed differences of only 0.20 min at 50 % release and 0.58 min at 90 %. The fitting is thus satisfying for this formulation. It has to be however remembered that *in silico* curve was adjusted to experimental points for calibration of the SwC of StaRX1500[®].

For formulation XI, dissolution profile of virtual tablet showed a good fitting with experimental points; differences in release time were only 0.07 min at 50 % release and 0.05 min at 90 %. It was thus assumed that SoC and SwC were properly calibrated as the simulation detected the changes in lactose and caffeine concentration in this formulation in comparison to formulation X (see Table 5.24). Consequently, the same SoC value for caffeine and lactose and the same SwC value for StaRX1500[®] were kept for further simulations.

Fitting of *in silico* curve with experimental dissolution points showed only a small deviation of release times for formulation XII tablets; 0.38 min at 50 % and 0.73 min at 90 % release. However, these differences are more significant in comparison with the small dissolution time of formulation XII tablet (1.49 min at 90 % release). Influence of imprecision in virtual tablet composition (see Table 5.24) is in fact less negligible for very fast release tablets than for slow release tablets. However, an increase in scale of the dissolution system should give more precise composition and consequently reduce differences in release times between *in silico* and experimental profiles. Furthermore, as percentage of StaRX1500[®] is lower in formulation XII than in formulation XI, it could be supposed that the rule for swelling disintegrant in the CA should be improved.

For formulation XIII, differences of 0.5 min and 0.97 at 50 % and 90 % release can be observed. Tablets are dissolved almost as fast as formulation XII tablets. The percentage of StaRX1500[®] is close to the one of formulation X and XI who exhibited a good fitting between *in silico* and experimental dissolution profiles. Consequently, it seems that the rule for updating

swelling disintegrant cells in the CA is not the reason for differences in release time. More probably imprecision in composition could explain these variations.

Table 5.24: Experimental and virtual tablets compositions and dissolution times of formulations X-XIII tablets.

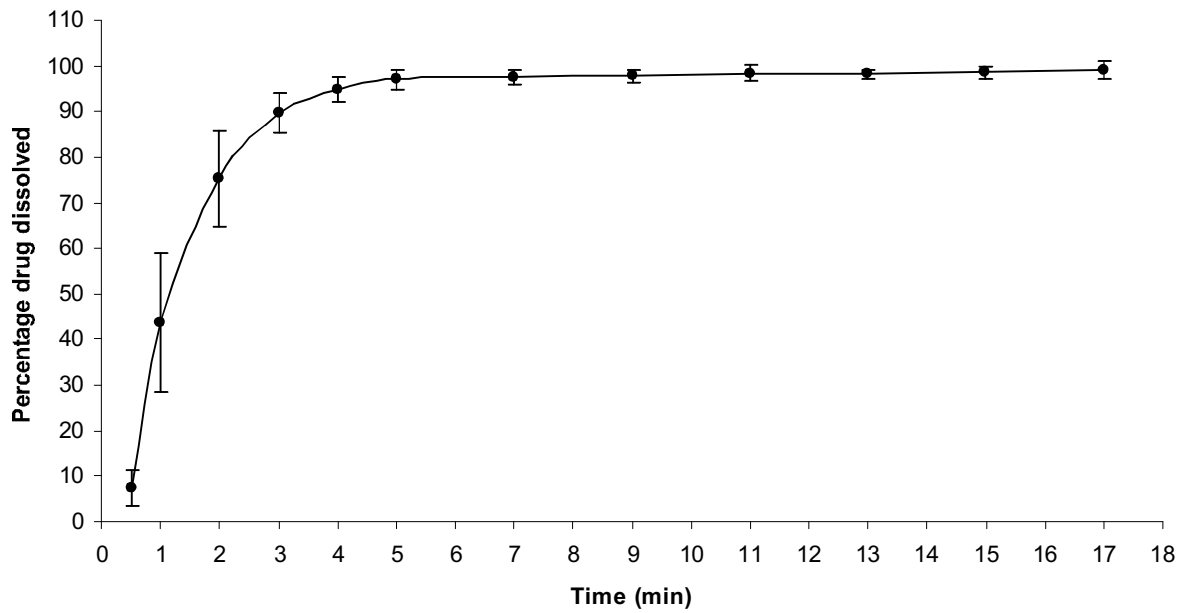
Formulation X tablets		
Components	Tablet composition (%v/v)	
	Experimental	<i>in silico</i>
Caffeine	51.53	51.94
Lactose	20.61	18.88
StaRX1500®	18.55	19.37
Porosity	9.30	9.80
% drug released	Dissolution times (min)	
	Experimental	<i>in silico</i>
50	1.20	1.40
90	3.00	3.58

Formulation XI tablets		
Components	Tablet composition (%v/v)	
	Experimental	<i>in silico</i>
Caffeine	64.92	65.83
Lactose	4.97	5.63
StaRX1500®	20.55	17.02
Porosity	9.56	11.52
% drug released	Dissolution times (min)	
	Experimental	<i>in silico</i>
50	1.55	1.62
90	4.00	3.95

Formulation XII tablets		
Components	Tablet composition (%v/v)	
	Experimental	<i>in silico</i>
Caffeine	64.45	63.33
Lactose	15.47	15.39
StaRX1500®	9.87	10.41
Porosity	10.21	10.88
% drug released	Dissolution times (min)	
	Experimental	<i>in silico</i>
50	0.84	1.22
90	1.49	2.22

Formulation XIII tablets		
Components	Tablet composition (%v/v)	
	Experimental	<i>in silico</i>
Caffeine	49.80	52.46
Lactose	17.93	13.52
StaRX1500®	19.92	21.59
Porosity	12.36	12.42
% drug released	Dissolution times (min)	
	Experimental	<i>in silico</i>
50	0.68	1.18
90	1.64	2.61

Experimental dissolution profile of formulation X tablets



Experimental dissolution points and *in silico* dissolution profile of formulation X tablets

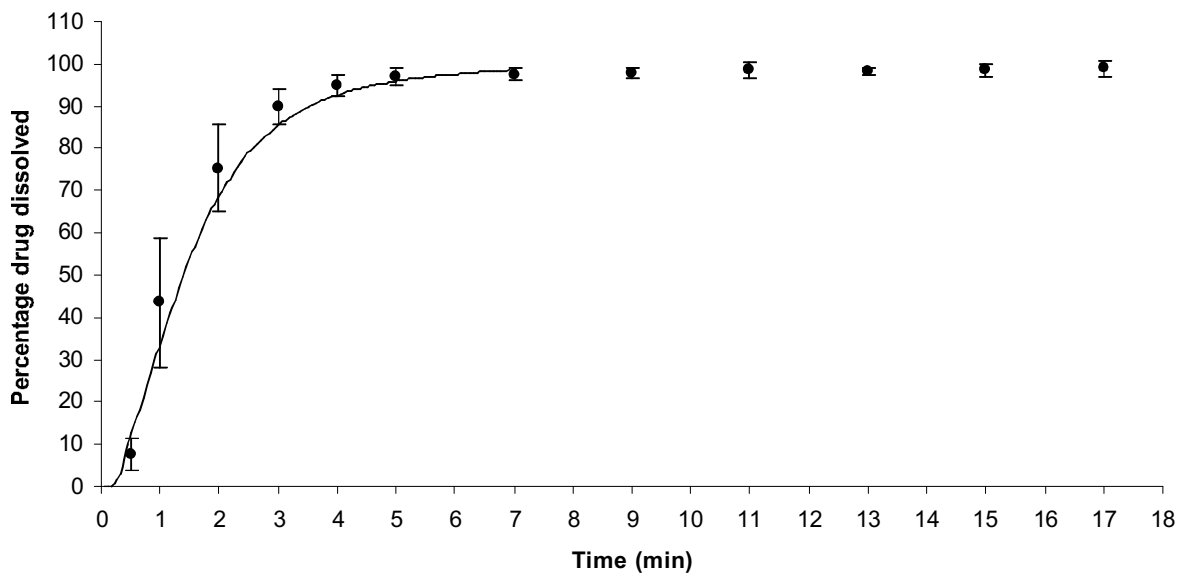
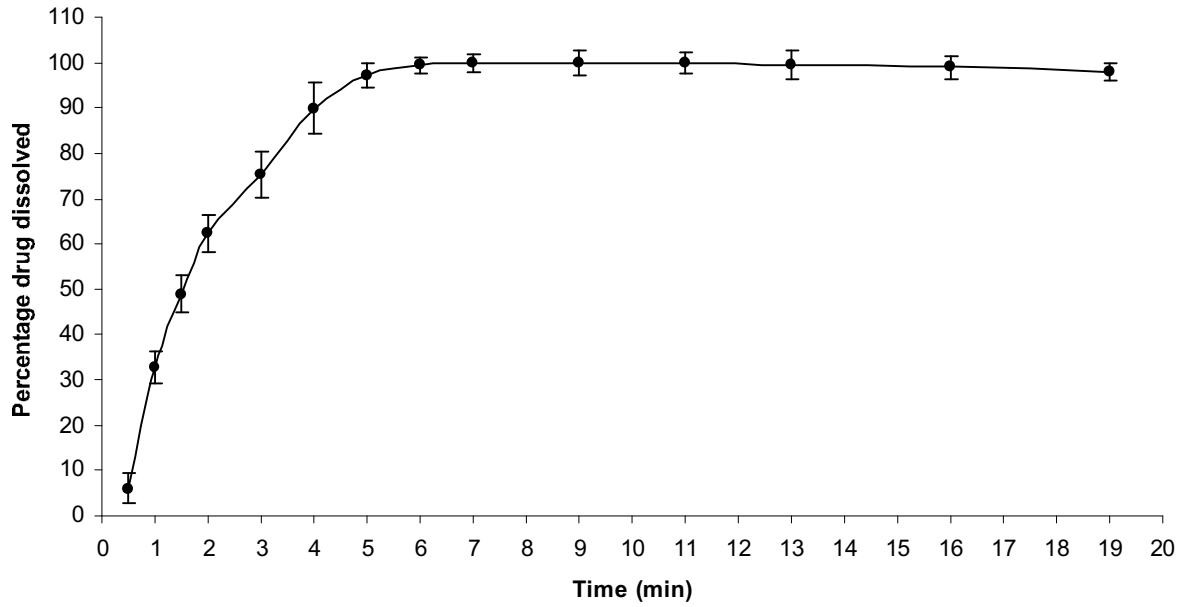


Figure 5.26: Experimental dissolution profile (top) and *in silico* dissolution profile fitted with experimental points (bottom): formulation X tablets.

Experimental dissolution profile of formulation XI tablets



Experimental dissolution points and *in silico* dissolution profile of formulation XI tablets

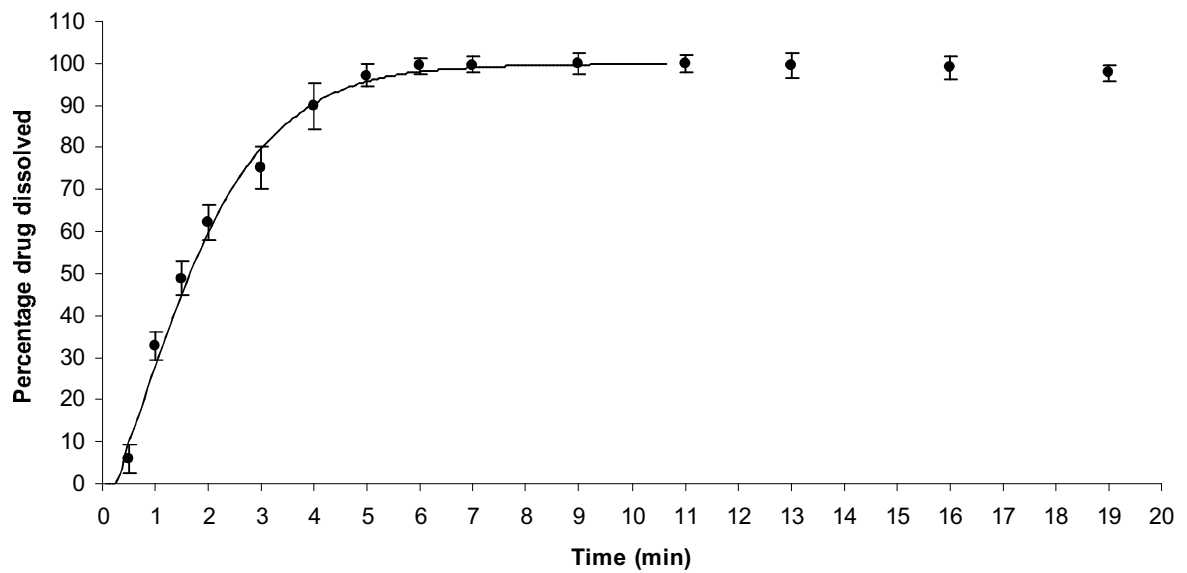


Figure 5.27: Experimental dissolution profile (top) and *in silico* dissolution profile fitted with experimental points (bottom): formulation XI tablets.

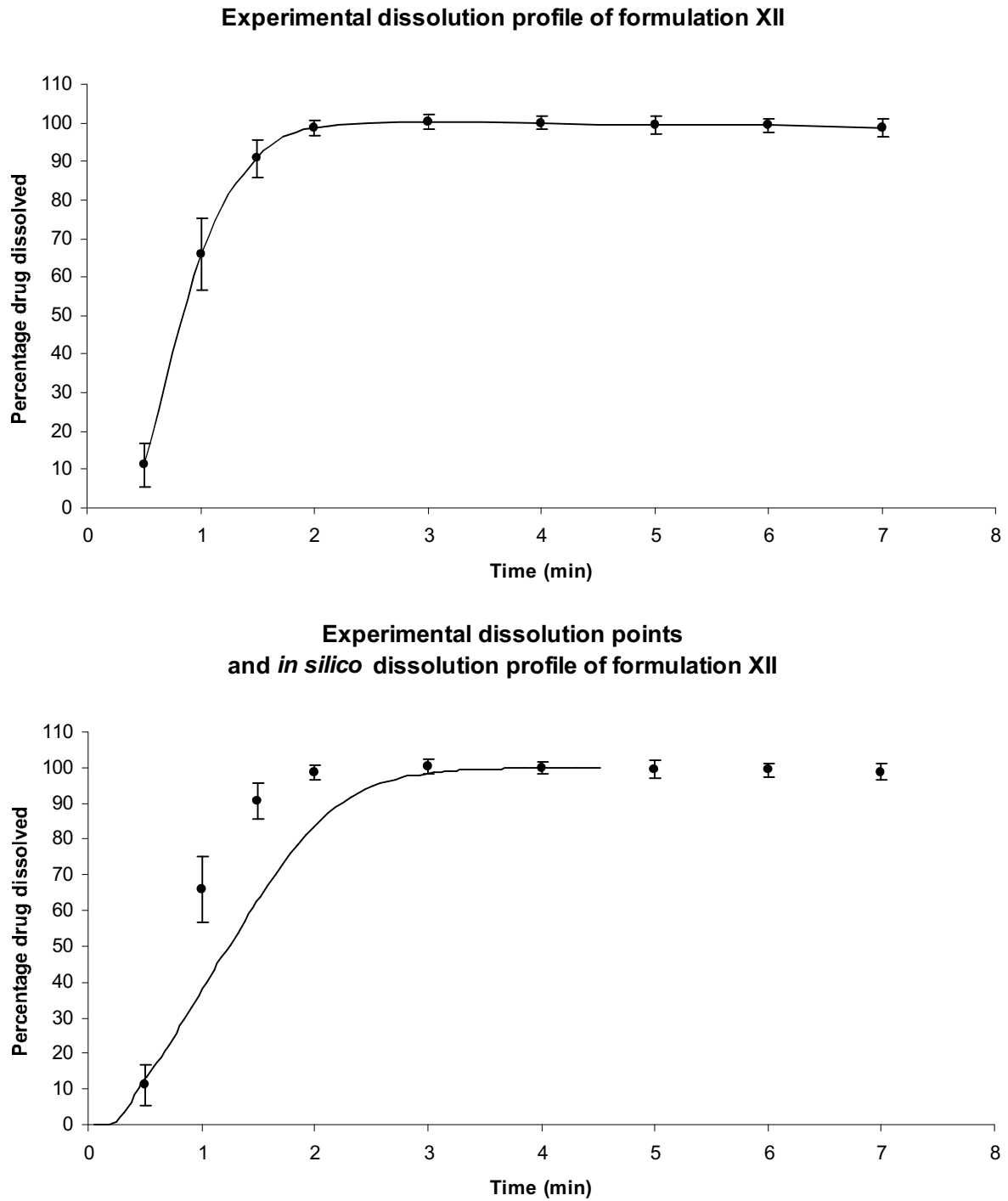
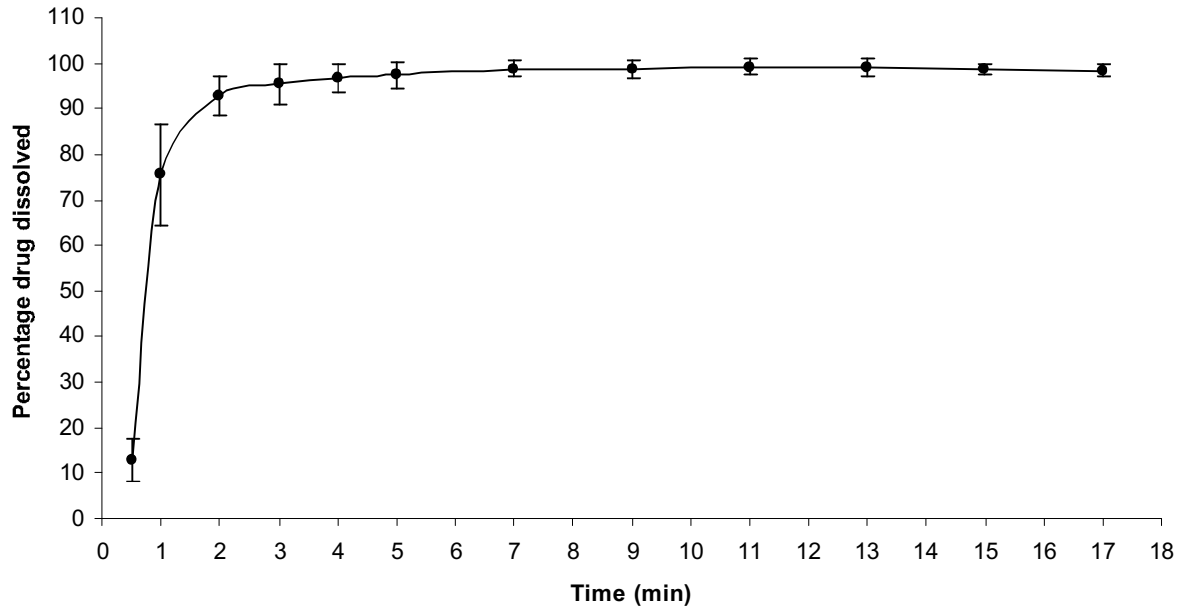


Figure 5.28: Experimental dissolution profile (top) and *in silico* dissolution profile fitted with experimental points (bottom): formulation XII tablets.

Experimental dissolution profile of formulation XIII tablets



Experimental dissolution points and *in silico* dissolution profile of formulation XIII tablets

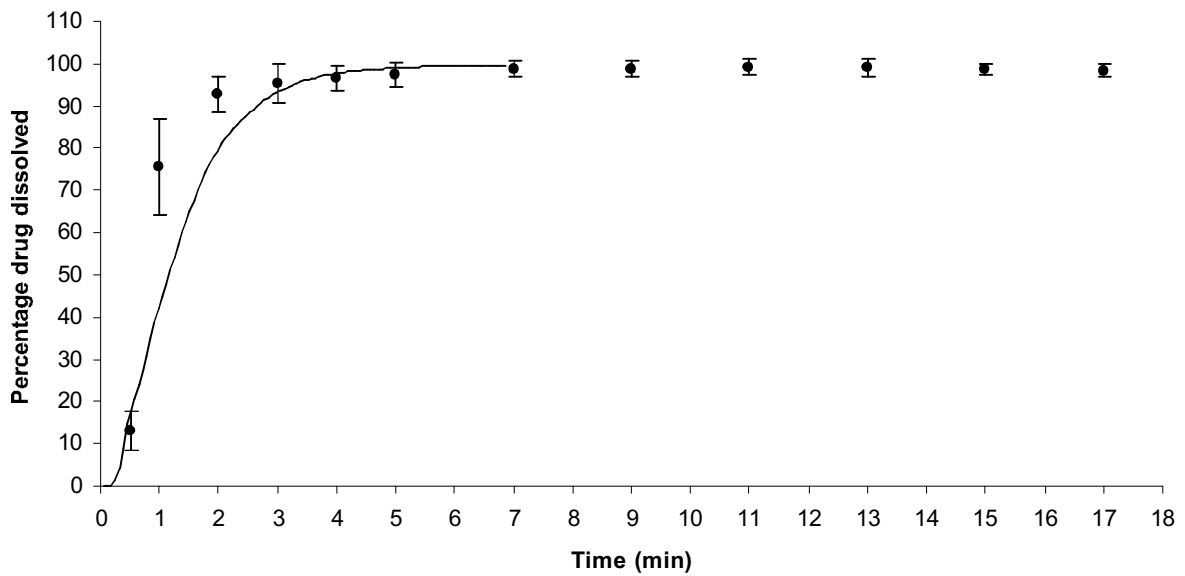


Figure 5.29: Experimental dissolution profile (top) and *in silico* dissolution profile fitted with experimental points (bottom): formulation XIII tablets.

The experimental and *in silico* release of formulation XIV tablets with Aspirin as model drug and lactose as model filler are shown below in Figure 5.30. The curves exhibit a first order profile. Targeted porosity of real and virtual tablets was 14 %.

The experimental release of formulation XIV tablets didn't reach 90 %. This incomplete release could be attributed to partial degradation of Aspirin during the dissolution process.

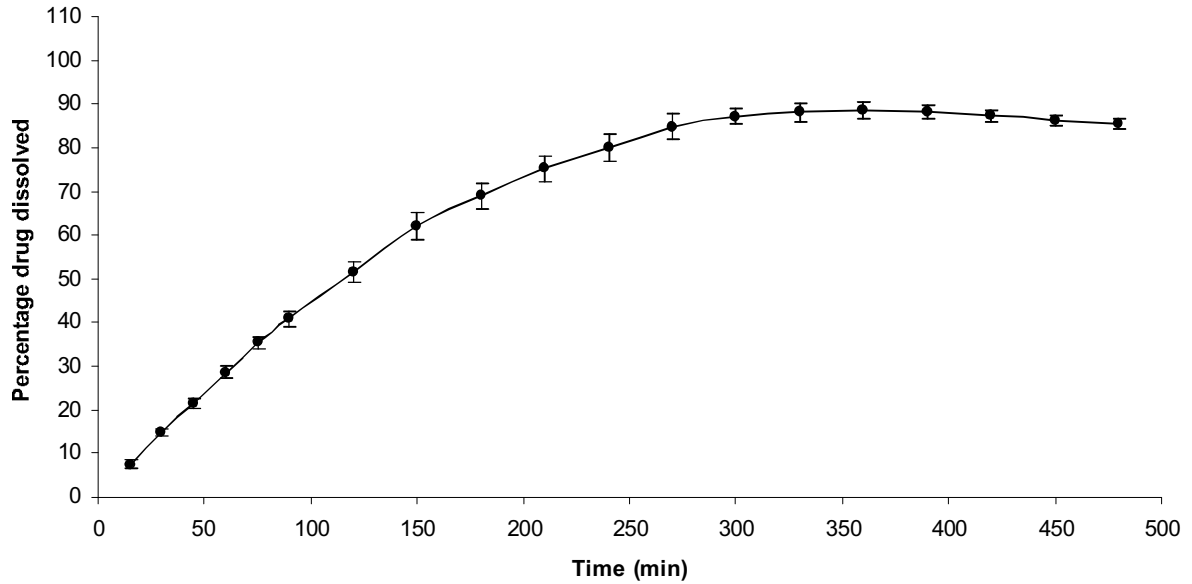
The *in silico* dissolution was however executed until 100 % release as this degradation effect is not simulated.

The drug release difference between *in silico* and experimental profiles 8 min at 50 % and 75 min at 88 %. The difference at 50 % is rather small in comparison to the total release time of the formulation XIV tablets. However, as possible degradation of Aspirin occurred during dissolution, differences in release times increase between virtual and real tablets for higher dissolution percentages.

Table 5.25: Experimental and virtual tablets compositions and dissolution times of formulation XIV tablets.

Formulation XIV tablets		
Components	Tablet composition (%v/v)	
	Experimental	<i>in silico</i>
Aspirin	59.69	62.60
Lactose	25.87	23.51
Porosity	14.44	13.89
% drug released	Dissolution times (min)	
	Experimental	<i>in silico</i>
50	115	123
88	320	245

Experimental dissolution profile of formulation XIV tablets



**Experimental dissolution points
and *in silico* dissolution profile of formulation XIV tablets**

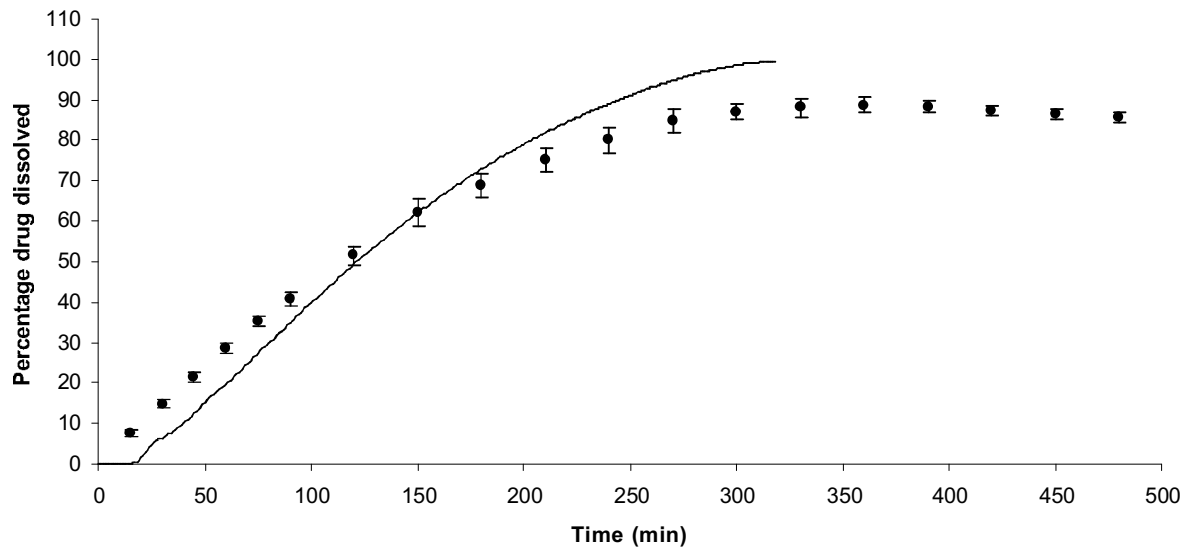


Figure 5.30: Experimental dissolution profile (top) and *in silico* dissolution profile fitted with experimental points (bottom): formulation XIV tablets.

The DS module has shown of good relevancy for simulating composition of a tablet. The desired percentage of ingredients and the random packing of particles in virtual compact were satisfying even though some imprecisions exist between real and *in silico* tablet composition (discretisation effect). A sufficient scale for the tablet in dissolution matrix should however limit these variations. Moreover, it has to be pointed out that composition of the real tablet is likely not perfectly precise. The targeted percentages of the different ingredients were in fact set up with targeted tablet porosity, but the values shown in Table 5.24 and Table 5.25 are values of percentage ingredients corrected calculated tablets porosity (calculated themselves with dimensions and weights measured with real tablets). Thus, the difference between this composition and the virtual one should be negligible, except maybe for very fast release tablets.

The dissolution profiles obtained with CA simulation showed a rather good fitting with experimental points, despite a less satisfying relevancy of the profiles for of very fast release tablets. The implemented software for dissolution simulation represents however an innovative approach for dissolution simulation of solid dosage forms. It could become a useful tool for formulators for screening many different formulations before experimental dissolution testing. Reduction of the time for formulation task is not the only advantage of this approach. As it uses CA modeling, it is possible to add easily new rules for system cells updates according to the latest findings in dissolution mechanisms and thus to improve the relevancy of the tool.

The speed of simulation on a standard personal computer is rather high (around 10 min for caffeine tablets and around 30 min for Aspirin tablets at system scale factor 180) for small system scale but can be much longer if the system scale is close to the one of a real compacted mixture. The constant increase of computer processors and memory capacities should reduce constantly in future the time for dissolution simulation using CA.

6. Conclusions and outlook

The presented work was a contribution to set up the scientific backbone and to develop some modules of an innovative expert system (ES) for solid dosage formulation design.

The backbone of the ES is based on mathematical and physical models only and was built on a modular architecture. Each module of the system models or simulates a certain property of solid dosage form. It is possible to either use ES modules separately or to perform a full formulation design taking into account, at the same time, *in silico* results from all modules. In the latter case, a central calculation unit is in charge of the evaluation of the obtained results with each module. The corresponding algorithm receives as input different constraints on dosage form properties, which are chosen by the user or given by pharmacopoeia. In addition, a weight should be associated with each module to adjust its influence on evaluation process and to propose the best compromise for the final formulation. At this stage of development, the global formulation process with all modules together is not fully automatic. However, scientific and practical bases to achieve this task were set up. The implemented modules of the ES are currently: “Disintegration Optimisation” (DO) module, “Dissolution Simulation” (DS) module and “Databases” (DB) module.

DO module enables to calculate the optimum amount of disintegrant to minimise the disintegration time of a tablet. The calculation is based on simple geometrical and physical considerations and uses percolation theory in Random Close Packed (RCP) sphere systems as a model. It is assumed that minimum disintegration time occurs when a continuous cluster conducting water starts percolating the whole tablet. This cluster is formed of disintegrant particles and/or tablet pores. Solutions proposed by the model depend on the general aspect of the disintegrant particles (non-fibrous or fibrous) used in the formulation. In case of compacted binary mixture of drug/non-fibrous disintegrant, the following piecewise function was found:

$$X_d = \begin{cases} \frac{p_c}{1-\varepsilon} - \varepsilon; & \text{if } \frac{r}{R} \leq \sqrt{3} - 1 \\ \frac{p_c}{1-\varepsilon}; & \text{if } \frac{r}{R} > \sqrt{3} - 1 \end{cases}$$

where X_d is the volumetric percentage of disintegrant in the tablet (solid fraction), ε is the tablet porosity, r is the mean radius of disintegrant grains, R is the mean radius of drug particles and p_c is the used percolation threshold value for RCP spheres systems (0.16).

In case of fibrous disintegrant, fibers were approximated with ellipsoids of revolution. In this case, the optimal disintegrant concentration (% v/v solid fraction) is assumed to be equal to the calculated percolation threshold value on overlapping ellipsoids having an aspect ratio (major radius/minor radius of ellipse) close to the one of a disintegrant fiber.

Different compacted binary mixtures (drug/disintegrant) with increasing loading amount of disintegrant were disintegrated. The experimental disintegrant thresholds have shown a good correlation with calculated disintegrant thresholds. The models proposed were validated with compacted binary mixtures but they can be applied to tablets with more ingredients using renormalisation.

The DS module is a software platform for the simulation of tablet dissolution. It uses Cellular Automata (CA) modeling for mimicking natural mechanisms involved in real dissolution process. A discrete virtual tablet pattern must be first designed with the "Tablet Designer" program. This pattern is then discretised into a virtual tablet model, which is placed in a cubic matrix. The different ingredients of the formulation are selected from DB module. This module contains databases of components (drug, excipients and fillers databases) where information about substances are stored. The selected composition is then set up into the virtual tablet using a packing and particle-growing algorithm. The particles in the resulting tablet are randomly disposed and exhibit deformed shape after execution of the algorithm. The virtual tablet is an ensemble of different matrix cells, which can be of different types. Cells of the tablet are in fact units of the dissolution system (unit of ingredients, pores or dissolution medium). The state of each cell of the system is changed at each unit of time. A unit of time corresponds to an update of the whole system (all cells of the matrix). The change in state of a cell depends on the one hand on the states of neighbouring cells, and on the other hand on its solubility constant (SoC) and/or swelling constant (SwC). SoC and Swc are constants, which are specific to the CA and were preliminary calibrated by fitting *in silico* dissolution curves of pure compacted drug tablets with experimental dissolution points of corresponding tablets.

Experimental dissolution profiles of different compacted mixtures composed of a drug, a filler and a disintegrant were compared with *in silico* dissolution profiles of similar virtual tablets. Simulated profiles fitted rather well the experimental dissolution points of tested compacted mixtures.

The possible applications of this tool are various: computer-aided formulation design (CAfD), research activities to reveal the influence of different parameters, design and development of new excipients and education purposes (companies, universities). This DS module represents also an ultimate tool to keep and use the gained expert knowledge and experience of formulators.

Only several modules of the ES were implemented during this PhD work. To achieve a complete formulation design toolbox, i.e. taking into account all properties and parameters influencing solid dosage form quality, further development is required. The DS module uses tablet model with deformed particles similarly to real compacts. The compressibility and compactibility of substances were not taken into account at this stage of development. Furthermore, the DS module does not model the density distribution of the material inside the tablet. It would be thus interesting to consider particle deformation and stress distribution with respect to the physical properties for each component. Moreover, tablet coating was not programmed but this option can be added to CA by using layers of cells with coating agent characteristics. Finally, the loading-up of the system's database with more API and excipients properties should be continued.

7. References

Ahlnock C, Alderborn G: Moisture adsorption and tableting. II. The effect on tensile strength and air permeability of the relative humidity during storage of tablets of 3 crystalline materials. *International Journal of Pharmaceutics* 1989;56(2):143-150.

Alderborn G, Nystroem C: Intermolecular bonding forces, in Alderborn G, Nystroem C (eds): *Pharmaceutical powder compaction technology*. New York, Marcel Dekker, 1996a, pp 20-23.

Alderborn G, Nystroem C: Nomenclature, in Alderborn G, Nystroem C (eds): *Pharmaceutical powder compaction technology*. New York, Marcel Dekker, 1996b.

Atkins PW, De Paula J: *Atkins' Physical Chemistry*, Oxford University Press, 2002.

Augsburger LL: *Disintegrants: Lecture: Tablets and Capsules: Design and Formulation, PHAR 535: Pharmaceutics*, 2007, vol 2007.

Baker RW, Lonsdale HS: Controlled release: mechanism and rates, in Taquary AC, Lacey RE (eds): *Controlled release of biologically active agents*. New York, Plenum Press, 1974, pp 15-71.

Banker GS, Anderson NR: Tablets, in Lachman L, Lieberman HA, Kanig JL (eds): *The theory and practice of industrial pharmacy*. Philadelphia, Lea & Febiger, 1986, pp 293-345.

Barat A, Ruskin HJ, Crane M: Probabilistic models for drug dissolution. Part 1. Review of Monte Carlo and stochastic cellular automata approaches. *Simulation Modeling Practice and Theory* 2006;14(7):843-856.

Barton A: *Handbook of solubility parameters and other cohesion parameters*, CRC press Inc., 2000, vol 177-185.

Bateman SD: 1996;20(3):174-184.

Ben Aim R, Le Goff P: La coordination des empilements désordonnés de sphères. Application aux mélanges binaires de sphères. *Powder Technol.* 1968-1969;2:1-12.

Bergler S: *Introduction to Expert Systems*, 2007.

Berhan L, Sastry AM: Modeling percolation in high-aspect-ratio fiber systems. I. Soft-core versus hard-core models. *Phys. Rev. E* 2007a;75(041120):1-8.

Berhan L, Sastry AM: Modeling percolation in high-aspect-ratio fiber systems. II. The effect of waviness on the percolation onset. *Phys. Rev. E* 2007b;75(041121):1-7.

Berry H, Ridout CW: *J. Pharm. Pharmacol.* 1950;2:619-629.

Bolhuis G, Smallenbroek A, Lerk C: Interaction of tablet disintegrants and magnesium stearate during mixing, I: Effect on tablet disintegration. *Pharm. Sci.* 1981;70:1328-1336.

Bolhuis GK, Van Kamp HV, Lerk CF, Sessink GM: On the mechanism of action of modern disintegrants. *Acta Pharm. Techn.* 1982;28:111-114.

- Bollaert C, Guyot-Herman AM: Etude des propriétés d'agents de désagrégation dérivés de l'amidon de maïs: les Esma Farin. Labo Pharma Probl. Tech. 1984;32:682-689.
- Bolzolakis J, Augsburger L: Role of disintegrants in hard gelatin capsules. J Pharm. Pharmacol. 1984;36:77-84.
- Bolzolakis J, Small L, Augsburger L: Effect of disintegrants on drug dissolution from capsules filled on a dosator-type automatic capsule-filling machine. Int. J. Pharm. 1982;12:341-349.
- Bonny JD: Wirkstoffreisetzung aus Matrix-Retardformen: Die Bedeutung der fraktalen Geometrie und der Perkolationstheorie.; PhD Thesis, University of Basel, 1992.
- Bonny JD, Leuenberger H: Determination of fractal dimensions of matrix-type solid dosage forms and their relation with drug dissolution kinetics. Eur. J. Pharm. Biopharm. 1993a;39:31-37.
- Bonny JD, Leuenberger H: Matrix type controlled release systems II. Percolation effects in non-swellable matrices. Pharm. Acta Helv. 1993b;68:25-33.
- Bonny JD, Leuenberger H: Matrix type controlled release systems. I. Effect of percolation on drug dissolution kinetics. Acta Helv. 1993c;66:160-164.
- Boon J-P: Advanced Research Workshop on Lattice Gas Automata Theory, Implementation, and Simulation. J. Stat. Phys. 1992;68(3/4).
- Borst I, Ugwu S, Beckett AH: New and extended applications for USP drug release apparatus 3. Dissolution Technologies 1997;4(1):11-15.
- Bradshaw D: Financial Times 1989.
- Bresenham JE: Algorithm for Computer Control of a Digital Plotter. IBM Systems Journal 1965;4(1):25-30.
- Broadbent SR, Hammersley JM: Percolation processes. I. Crystals and mazes. Proceedings of the Cambridge Philosophical Society, Mathematical and physical science 1957;53:629-641.
- Brunner L: Reaktionsgeschwindigkeit in heterogenen Systemen. Z. Phys. Chem. 1904;43:56-102.
- Brunner L, Tolloczko S: Über die Auflösungs-geschwindigkeit Fester Körper. Z. Phys. Chem. 1900;35:283-290.
- Bunde A, Kantelhardt W: Diffusion and conduction in percolation systems: theory and applications, in Heitjans P, Kärger J (eds): Diffusion in Condensed Matter. Berlin, Springer, 2005, pp 895-914.
- Burks AW: Von Neumann's self-reproducing automata, in burks AW (ed): Essays on Cellular Automata, University of Illinois Press, 1970, pp 3-64.
- Byl J: Self-reproduction in small cellular automata. Physica D 1989;34:259-299.
- Callahan P: What is the Game of Life?, Math.com, 2007.
- Caraballo I, Fernandez-Arevalo M, Holgado MA, Rabasco AM: Percolation theory: application to the study of the release behaviour from inert matrix systems. Int. J. Pharm. 1993;96:175-181.
- Caraballo I, Melgoza LM, Alvarez-Fuentes J, Soriano MC, Rabasco AM: Design of controlled release inert matrices of naltrexone hydrochloride based on percolation concepts. Int. J. Pharm. 1999;181:23-30.

- Caraballo I, Millan M, Rabasco AM: Relationship between drug percolation threshold and particle size in matrix tablets. *Pharm. Res.* 1996;13(3):387-390.
- Caramella C, Colombo P, Conte U, Ferrari F, Gazzaniga A, La Manna A, Peppas NA: The mechanisms of disintegration of compressed particulate systems. *Polymer Bull* 1987a;18:541-544.
- Caramella C, Colombo P, Conte U, Ferrari F, Gazzaniga A, LaManna A, Peppas NA: A physical analysis of the phenomenon of tablet disintegration. *International Journal of Pharmaceutics* 1988;44(1-3):177-186.
- Caramella C, Colombo P, Conte U, Ferrari F, La Manna A, Van Kamp HV, Bolhuis GK: Water uptake and disintegrating force measurements: towards a general understanding of disintegration mechanisms. *Drug Dec. Ind. Pharm.* 1986;12(1986a):1749-1766.
- Caramella C, Colombo P, Conte U, Gazzaniga A, La Manna A: The role of swelling in the disintegration process. *Int. J. Pharm. Techn. Prod. Manuf.* 1984;5(1984):1-5.
- Caramella C, Colombo P, Conte U, La Manna A: Tablet disintegration uptake: the dynamic approach. *Drug Dev. Ind. Pharm.* 1987b;13:2111-2145.
- Caramella C, Ferrari F, Bonferoni MC, Ronchi M: Disintegrants in solid dosage forms. *Drug Dev. Ind. Pharm.* 1990;2561-2577.
- Carr RL: Evaluating flow properties of solids. *Chem. Eng.* 1965;18:163-168.
- Carstensen JT: *Pharmaceutical systems. Solid dosage forms.* New York and London, Academic Press, 1973, vol I, pp 205.
- Carstensen JT: *Drug stability - Principles and Practices.* New York, Marcel Dekker, 1995, pp 25.
- Carstensen JT, Kothari R, Prasad VK, Sheridan J: Time and temperature dependence of disintegration and correlation between dissolution and disintegration rate constants. *J Pharm Sci* 1980a;69(3):290-4.
- Carstensen JT, Lai T-F, Prasad VK: USP dissolution IV: Comparison of methods. *J. Pharm. Sci.* 1978;67(9):1303-1307.
- Carstensen JT, Lai TY-F, Toure P, Sheridan J: Repose angles as a function of the supporting surface. *International Journal of Pharmaceutics* 1980b;5(2):157-160.
- Carter JC: *The role of disintegrants in solid oral dosage manufacturing, 2007, vol 2007.*
- Celik M: Overview of compaction data analysis techniques. *Drug Development and Industrial Pharmacy* 1992;18(6-7):767-780.
- Chopard B, Droz M: *Cellular Automata Modeling of Physical Systems,* Cambridge University Press, 1998.
- Chopard B, Droz M, Kolb M: Cellular automata approach to non-equilibrium diffusion and gradient percolation. *J. Phys. A.* 1989;22:1609-1619.
- Chow S, Ki F: Statistical comparison between dissolution profiles of drug products. *Journal of Biopharmaceutical Statistics* 1997;7(2):241-258.
- Christensen FN, Hansen FY, Bechgaard H: Physical interpretation of parameters in the Rosin-Rammler-Sperling-Weibull distribution for drug release from controlled release dosage forms. *J. Pharm. Pharmacol.* 1980;32:580-582.
- Codd EF: *Cellular Automata,* Academic Press, 1968.

Colombo P, Caramella C, Conte U, La Manna A, Guyot-Herman AM, Ringard J: Disintegration force and tablet properties. *Drug Dev. Ind. Pharm.* 1981;7:135-153.

Colombo P, Conte U, Caramella C, Geddo M, La Manna A: Disintegrating force as a new formulation parameter. *J. Pharm. Sci.* 1984;73(1984):701-705.

Colombo P, Conte U, Caramella C, La Manna A, Guyot-Herman AM, Ringard J: Force de delitement des comprimés, II. *Farm. Ed. Prat.* 1980;35(1980):391-402.

Commons RC, Bergen A, Walker GC: Influence of starch concentration on the disintegration time of tolbutamide tablets. *J. Pharm. Sci.* 1968;57:1253-1254.

Cook MK: *Drug. Cosm. Ind. Sept.* 1975.

Cooper AR, Eaton LE: Compaction behaviour of several ceramic powders. *Journal of the American Ceramic Society* 1962;45(3):97-101.

Costa P, Sousa Lobo JM: Modeling and comparison of dissolution profiles. *European Journal of Pharmaceutical Sciences* 2001;13(2):123-133.

Couvreur P: Les mécanismes de désintégration de comprimés à base d'agents amylacés Université Catholique de Louvain, 1975.

Couvreur P, Gillard J, Roland M: Incidence des cinétiques d'absorption d'eau sur le délitement des comprimés pharmaceutiques à base d'agents amylacés. *Ann. Pharm. Fr.* 1976;34(3-4):123-132.

Couvreur P, Gillard J, Van den Schrieck HG, Roland M: Mécanisme de désintégration des comprimés à base d'amidon. *J. Pharm. Belg.* 1974;29:399-414.

Deleuil M: Approche du comportement des poudres. *STP Pharma* 1987;8:668-675.

Derjaguin BV: The force between molecules. *Sci. Am.* 1960;203(1):47-53.

Derjaguin BV, Abrikosova II, Lifshitz EM: Direct measurement of molecular attraction between solids separated by a narrow gap. *Quart. Rev. Chem. Soc.* 1956;10:195-329.

Desai SJ, Singh P, Simonelli AP, Higuchi WI: Investigation of factors influencing release of solid drug dispersed in inert matrices. IV. Some studies involving the polyvinyl chloride matrix. *J. Pharm. Sci.* 1966a;55:1235-1239.

Desai SJ, Singh P, Simonelli AP, Higuchi WI: Investigation of factors influencing release of solid drug dispersed in inert matrices. III. Quantitative studies involving the polyethylene plastic matrix. *J. Pharm. Sci.* 1966b;55:1230-1234.

Deware J: *Systems International* 1989;7(7):12-17.

Dokoumetzidis A, Macheras P: A century of dissolution research: From Noyes and Whitney to the Biopharmaceutics Classification System. *International Journal of Pharmaceutics* 2006;321:1-11.

Doolen G: Lattice Gas Method for Partial Differential Equations, in Doolen G (ed), Addison-Wesley, 1990.

Down GRB, McMullen JN: The effect of interparticulate friction and moisture on the crushing strength of sodium chloride compacts. *Powder Technology* 1985;42(2):169-174.

Duberg M, Nystroem C: *Int. J. Pharm. Technol. Prod. Manuf.* 1985;6:17.

- Dupuis A, Chopard B: An object oriented approach to lattice gas modeling. *Future generation computer systems* 2000;16:523-532.
- Efros AL: *Physics and Geometry of Disorder. Percolation theory*, in Russian, Nauka, Moscow, 1982.
- Ehrburger F, Misono S, Lahaye J: Conducteurs granulaires, théories, caractéristique et perspectives.: *Journée des études de la Société des Electriciens et des Electroniciens*. Paris, 1990, pp 197-204.
- Ellis SR, Wright JL: Modeling of aqueous transport in rigid porous matrices near the percolation threshold. *Pharmaceutical Research* 2006;23(10).
- Essam JW: *Percolation theory. Reports on Progress in Physics* 1980;43.
- Fassihi A: Mechanisms of disintegration and compactability of disintegrants in a direct compression system. *Int. J. Pharm.* 1986;32(93-96).
- FDA: *Guidance for industry. Waiver of in vivo bioavailability and bioequivalence studies for immediate-release solid oral dosage forms based on a biopharmaceutics classification system*. 2000.
- Flory PJ: Molecular size distribution in three dimensional gelation I-III. *Journal of the American Chemical Society* 1941;63(11):3083-3090, 3091-3096, 3096-3100.
- Frisch U, Hasslacher B, Pomeau Y: Lattice gas automata for the Navier-Stokes equation. *Phys. Rev. Lett.* 1986;56(14):1505-1508.
- Fuertes I, Miranda A, Millan M, Caraballo I: Estimation of the percolation thresholds in acyclovir hydrophilic matrix tablets. *Eur. J. Pharm. Biopharm.* 2006;64(3):336-342.
- Fukuzawa H, Nakai Y: 87th annual meeting of the pharmaceutical soc. of japan. Kyoto, 1967.
- Fürher C: Substance behaviour in direct compression. *Lab. Pharma. Probl. Technol.* 1977;269:759-762.
- Ganguly N, Sikdar BK, Deutsch A, Canright G, Chaudhuri PP: A Survey on Cellular Automata. in press:1-30.
- Garboczi EJ, Snyder KA, Douglas JF: Geometrical percolation threshold of overlapping ellipsoids. *Physical Review* 1995;21(1):819-828.
- Gardner M: The fantastic combinations of John Conway's new solitaire game life. *Scientific American* 1970;220(4):120.
- Gibaldi M, Feldman S: Establishment of sink conditions in dissolution rate determinations - theoretical considerations and application to nondisintegrating dosage forms. *J. Pharm. Sci.* 1967;56(1238-1242).
- Goldsmith JA, Randall N, Ross SD: On methods of expressing dissolution rate data. *J. Pharm. Pharmacol.* 1978;30:347-349.
- Gonsalves R.J. *UoBNY: Java Applet: Percolation*, vol 2007.
- Gould H, Tobochnik J, Christian W: *Percolation*, in J. B (ed): *An Introduction to Computer Simulation Methods: Applications to Physical Systems*. Boston, Addison Wesley 3rd edition, 2006, pp 443-470.
- Gould P, Tan S: The effect of recompression on the dissolution of wet massed tablets containing superdisintegrants. *Drug Dev Ind Pharm.* 1986;12:1929-1945.
- Gray WA: *The packing of solid particles*. London, Chapman and Hall, 1968, pp 100-102.
- Gregg SJ, Sing KSW: *Adsorption, Surface Area, and Porosity*. New York, Academic Press, 1967.

- Guyot-Herman AM, Ringard J: Disintegration mechanisms of tablets containing starches. Hypothesis about the particle/particle repulsive force. *Drug Dev. Ind. Pharm.* 1981;7:155-177.
- Guyot-Hermann AM: Tablet disintegration and disintegrating agents. *S.T.P. Pharma Sci.* 1992;2(6):445-462.
- Guyot-Hermann AM, Ringard J: Hypothesis about the particle-particle repulsive forces. *Drug Dev. Ind. Pharm.* 1981;7:155-177.
- Hancock BC, York P, Rowe RC: The use of solubility parameters in pharmaceutical dosage form design. *International Journal of Pharmaceutics* 1997;148(14):1-21.
- Hansen CM: The three dimensional solubility parameter-key to paint component affinities, 1: solvents, plasticisers, polymers and resins. *J. Paint. Technol.* 1967a;39:104-117.
- Hansen CM: The three dimensional solubility parameter-key to paint component affinities, 2. Dyes, emulsifiers, mutual solubility and compatibility, and pigments. *J. Paint. Technol.* 1967b;39:505-510.
- Hanson R, Gray V: *Handbook of Dissolution Testing*. Hockessin, Dissolution Technologies Inc., 2004.
- Hastedt JE, Wright JL: Diffusion in porous materials above the percolation threshold. *Pharm. Res.* 1990;7(9):893-901.
- Hausner HH: Friction conditions in a mass of metal powder. *Int. J. Powder Metall.* 1967;3:7-13.
- Heckel RW: An analysis of powder compaction phenomena. *Transactions of the Metallurgical Society of AIME* 1961a;221:1001-1008.
- Heckel RW: Density pressure relationships in powder compaction. *Transactions of the Metallurgical Society of AIME* 1961b;221:671-675.
- Hellman NN, Boesch TF, Melvin EH: Starch Granule Swelling in Water Vapor Sorption. *J. Am. Chem. Soc.* 1952;74(2):348-350.
- Hess H: Tablets under microscope. *Pharm. Technol.* 1978;2:38-57.
- Higuchi WI, Hiestand EN: Dissolution rates of finely divided drug powders. I. Effect of a distribution of particle sizes in a diffusion-controlled process. *J. Pharm. Sci.* 1963a;52:67-71.
- Higuchi WI, Rowe EL, Hiestand EN: Dissolution rates of finely divided drug powders. II. Micronized methylprednisolone. *J. Pharm. Sci.* 1963b;52:162-164.
- Higushi T, R. N, Busse L, Swintosky J: The physics of tablets compression, II. The influence of degree of compression on properties of tablets. *J. Am. Pharm. Assoc. Sci. Ed.* 1953;42(4):194-197.
- Hildebrand JH, Scott RL: *The solubility of nonelectrolytes*. New York, Reinhold, 1950.
- Hill JW, Petrucci RH: *General Chemistry*, Prentice Hall, 1999.
- Hixson AW, Crowell JH: Dependence of reaction velocity upon surface and agitation. *Ind. Eng. Chem.* 1931;23:923-931.
- Hopfenberg HB: Controlled release polymeric formulations, in Paul DR, Harris FW (eds): *ACS Symposium Series 33*. Washington DC, American Chemical Society, 1976, pp 26-31.
- Huettenrauch R, Keiner I: Neues hochwirksames sprengmittel fur komprimierte. *Pharmazie* 1973;28(H2):137.

- Hussain AS, Lesko LJ, Lo KY, Shah VP, Volpe D, Williams RL: The Biopharmaceutics Classification System: Highlights of the FDA's Draft Guidance. Dissolution Technologies 1999.
- I.S.I: Lattice Gas Dynamics and Foundations of Hydrodynamics, in Monaco R (ed), World Scientific, 1989.
- Ingram J, Lowenthal W: Mechanisms of action of starch as a disintegrant. J. Pharm. Sci. 1966;55:614-617.
- Israelachvili JN: Intermolecular and Surface Forces. London, Academic Press, 1985.
- Israelachvili JN, Tabor D: Prog. Surf. Membr. Sci. 1973;7.(1).
- Jetzer W, Leuenberger H, Sucker H: The compressibility and compatibility of pharmaceutical powders. Pharmaceutical Technology 1983;7(4):33-39.
- Jorgensen WL, Duffy EM: Prediction of drug solubility from structure. Advanced Drug Delivery Reviews 2002;54(3):355-366.
- Kanig JL, Rudnic EM: The mechanisms of disintegration action. Pharm. Technol. 1984;4:50-63.
- Katsura N, Mitsuoka T, Shimosaka A, Shirakawa Y, Hidaka J: Development of new simulation method for flow behaviour of granular materials in a blast furnace using cellular automaton. ISIJ International 2005;45(10):1396-1405.
- Kawakita K, Lüdde K-H: Some considerations on powder compression equations. Powder Technology 1970/71;4:61-68.
- Kimura G, Puchkov M, Betz G, Leuenberger H: Percolation Theory and the Role of Maize Starch as a Disintegrant for a Low Water-Soluble Drug. Pharmaceutical Development and Technology 2007;12(1):11 - 19.
- King PR, Buldyrev SV, Dokholyan NV, Havlin S, Lopez E, Paul G, Stanley HE: Percolation theory. DIALOG [London Petrophysical Society Newsletter] 2002;10/3.
- Kitazawa S, Johno I, Ito Y, Teramura S, Okada J: Effects of hardness on the disintegration time and the dissolution rate of uncoated caffeine tablets. J. Pharm. Pharmacol. 1975;27:765-770.
- Kitazawa S, Johno I, Ito Y, Tokuzo M, Okada J: Interpretation of dissolution rate data from in vivo testing of compressed tablets. J. Pharm. Pharmacol. 1977;29:453-459.
- Koch HP: The rotating flask method. Choice of an alternative methodology in dissolution testing. Pharm. Ind. 1982;44(8):838-842.
- Koch HP: Die Technik der Dissolutionsbestimmung (Teil 2). Pharm. Acta Helv. 1984;59(4):130-139.
- Korschmeyer RW, Gurny R, Doelker EM, Buri P, Peppas NA: Mechanism of solute release from porous hydrophilic polymers. Int. J. Pharm. 1983;15:25-35.
- Krausbauer E, Puchkov M: Expert system software for solid dosage formulation design: Pharmaceutical Sciences World Congress. Amsterdam, Netherlands, 2007.
- Kuentz M, Leuenberger H: Pressure susceptibility of polymer tablets as a critical property: a modified Heckel equation. Journal of Pharmaceutical Sciences 1999a;88(2):174-179.

- Kuentz M, Leuenberger H: A new approach to tablet strength of a binary mixture consisting of a well and a poorly compactable substance. *European Journal of Pharmaceutics and Biopharmaceutics* 2000;49(2):151-152.
- Kuentz M, Leuenberger H, Kolb M: Fracture in disordered media and tensile strength of microcrystalline cellulose tablets at low relative densities. *International Journal of Pharmaceutics* 1999b;182(2):243-255.
- Lai S: *Pharm. Technol. Eur.* 1996;8(9):60-68.
- Langenbucher F: In vitro assesment of dissolution kinetics: description and evaluation of a column-type method. *Journal of Pharmaceutical Sciences* 1969;58:1265-1272.
- Langenbucher F: Linearization of dissolution rate curves by the Weibull distribution. *J. Pharm. Pharmacol.* 1972;24:979-981.
- Langton CG: Self-reproducing in cellular automata. *Physica D* 1984;10:135-144.
- Langton CG: Editor's Introduction. *Artificial Life* 1994;1(v-viii).
- Langton CG, Taylor C, Farmer JD: *Artificial Life II*, Addison-Wesley, 1992.
- Lanz M: *Pharmaceutical powder technology: towards a science based understanding of the behaviour of powder systems* Universität Basel, 2006.
- Leuenberger H: The application of percolation theory in powder technology. *Adv. Powder Technol.* 1999;10(4):323-353.
- Leuenberger H: Solubilization systems: The impact of percolation theory and fractal geometry, in L. R (ed): *Water insoluble drug formulation*, CRC, 2000, pp 569-590.
- Leuenberger H, Lanz M: Powder - the fourth state of aggregation? *Pharm. Tech. Japan* 2002;18(7):995-1001.
- Leuenberger H, Lanz M: *Pharmaceutical Powder Technology-from Art to Science: the challenge of FDA's PAT initiative*. *Advanced Powder Technology* 2005;16(1-36).
- Leuenberger H, Rohera BD: Fundamentals of powder compression. I. The compactibility and compressibility of pharmaceutical powders. *Pharm. Res.* 1986;3(1):12-22.
- Leuenberger H, Rohera BD, Haas C: Percolation theory - a novel approach to solid dosage form design. *Int. J. Pharm.* 1987a;38:109-115.
- Leuenberger H, Rohera BD, Hass C: Percolation theory-a novel approach to solid dosage form design. *Int. J. Pharm.* 1987b;38:109-115.
- Levich V: *Physicochemical Hydrodynamics*. New Jersey, Prentice Hall, 1962.
- Levin M, Tsygan L, Duckler S: *Press simulation apparatus and methods*. US, 1998.
- Levy G: Effect of certain tablet formulation factors on dissolution rate of the active ingredient. I. Importance of using appropriate agitation intensities for in vitro dissolution rate measurements to reflect in vivo conditions. *J. Pharm. Sci.* 1963;52(11):1039-1146.
- List PH, Muazzam UA: Swelling: the force that disintegrates. *Drugs made in Germany* 1979;22:161-170.
- Livi R, Ruffo S, Ciliberto S: *Chaos and Complexity*, in Buiatti M (ed), World Scientific, 1988, pp 450.

- Löbenberg R, Amidon GL: Modern bioavailability, bioequivalence and biopharmaceutics classification system. New scientific approaches to international regulatory standards. *European Journal of Pharmaceutics and Biopharmaceutics* 2000;50:3-12.
- Louie AS, Brown MS, Kim A: Measuring the Return on Modeling and Simulation Tools in Pharmaceutical Development. *Health Industry Insights* 2007(January):1-23.
- Lowenthal W: Disintegration of tablets. *J. Pharm. Sci.* 1972a;61(11):1695-1711.
- Lowenthal W: Mechanism of action of starch as a tablet disintegrant. V. Effect of starch grain deformation. *J. Pharm. Sci.* 1972b;61:455-459.
- Lowenthal W: Mechanism of action of tablet disintegrants. *Pharm. Acta Helv.* 1973;48:589-609.
- Lowenthal W, Burruss R: Mechanism of starch as a tablet disintegrant, IV. Effect of medicaments and disintegrants on mean pore diameter and porosity. *J. Pharm. Sci.* 1971;60:1325-1332.
- Luginbuehl R: Anwendung der Perkolationstheorie zur Untersuchung des Zerfallsprozesses, der Wasseraufnahme und der Wirkstofffreisetzung von binaeren Tablettensystemen. PhD Thesis; University of Basel: Basel 1994.
- Luginbuehl R, Leuenberger H: Use of percolation theory to interpret water uptake, disintegration time and intrinsic dissolution rate of tablets consisting of binary mixtures. *Pharm. Acta Helv.* 1994;69(3):127-134.
- Macheras P, Athanassios I: *Modeling in Biopharmaceutics, Pharmacokinetics, and Pharmacodynamics.* New York, Springer, 2006.
- Macheras P, Iliadis A: *The Geometry of Nature: Modeling in Biopharmaceutics, Pharmacokinetics and Pharmacodynamics,* Springer; 1 edition, 2005, pp 442.
- Madore BF, Freedman WL: Computer simulation of the Belousov-Zhabotinsky reaction. *Science* 1983;222:615-616.
- Mandelbrot BB: *Fractals: Form, Chance, and Dimensions.* San Francisco, W. H. Freeman, 1977.
- Mandelbrot BB: *The Fractal Geometry of Nature,* W. H. Freeman and Company, 1982.
- Manneville P, Boccara N, Vichniac GY: Cellular Automata and Modeling of Complex Physical Systems, in Bideau R (ed), *Springer Proceeding in Physics* 46, 1989.
- Marsac J, Shamblin L, Taylor S: Theoretical and Practical Approaches for Prediction of Drug-Polymer Miscibility and Solubility. *Pharmaceutical Research* 2006;23(10):2417-2426.
- Marshall K: Monitoring punch forces and punch movements as an aid to developing robust tablet formulations. *Drug. Dev. Ind. Pharm.* 1989;15:2153-2176.
- Martin AN, Bustamante P, Chun AHC: *Physical Pharmacy: Physical Chemical Principles in the Pharmaceutical Sciences,* Lippincott Williams & Wilkins, 1993.
- Masteau JC, Thomas C, Chulia D: Influence of the isobaric contact time on different tablet properties: 2nd World Meeting, *Pharm. Biopharm. Pharmaceutical Technol.* Paris, 1998, pp 149-150.
- MCLachlan DS, Blaszkiewicz M, al. e: Electrical resistivity of composites. *J. Am. Ceram. Soc.* 1990;73(8):2187-2203.
- Melia CD, Davis SS: Mechanisms of drug release from tablets and capsules. I: Disintegration. *Aliment. Pharmacol. Therap.* 1989;3:223-232.

- Meyer MC, Straughn AB, Mhatre RM, Shah VP, Williams RL, Lesko LJ: Lack of in-vitro / in-vivo correlation of 50 mg and 250 mg primidote tablets. *Pharm. Res.* 1998;15:1085-1089.
- Millan M, Caraballo I, Rabasco AM: The role of the drug/excipient particle size ratio in the percolation model for tablets. *Aaps pharmaceutica* 1998;15(2):216-220.
- Miranda A, Millan M, Caraballo I: Estimation of the percolation thresholds in acyclovir hydrophilic matrix tablets. *Eur. J. Pharm. Biopharm.* 2006a;64(3):336-342.
- Miranda A, Millan M, Caraballo I: Study of the critical points of HPMC hydrophilic matrices for controlled drug delivery. *International Journal of Pharmaceutics* 2006b;311(1-2):75-81.
- Miranda A, Millan M, Caraballo I: Investigation of the influence of particle size on the excipient percolation thresholds of HPMC hydrophilic matrix tablets. *Journal of Pharmaceutical Sciences* 2007;96(10):2746-2756.
- Mitchell AG, Down GRB: Recrystallisation after powder compaction. *International Journal of Pharmaceutics* 1984;22(2-3):337-344.
- Modrzejewski F, Wochna L: Study of the swelling power of tablet disintegrants. *Acta Pol. Pharm.* 1965;22(4):305-310.
- Muazzam UA: Untersuchungen zum Mechanismus des Tablettenerfalls, 1979.
- Muller FX, Augsburger LL: The role of the displacement-time waveform in the determination of Heckel behaviour under dynamic conditions in a compaction simulator and a fully-instrumented rotary tablet machine. *J. Pharm. Pharmacol.* 1994;46(6):468-475.
- Mulye NV, Turco SJ: A simple model based on first order kinetics to explain release of highly water soluble drugs from porous dicalcium phosphate dihydrate matrices. *Drug Dev. Ind. Pharm.* 1995;21:943-953.
- Munday DL, Fassihi AR: In-vitro / in-vivo correlation studies on a novel controlled release theophylline delivery system and on Theo-Dur tablets. *Int. J. Pharm.* 1995;118:251-255.
- Nakai Y, Nakajuna S: Relationship between configuration of starch grains in tablet and tablet disintegration. *Yakugaku Zasshi* 1977;97:1168-1173.
- Nernst W: Theorie der Reaktionsgeschwindigkeit in heterogenen Systemen. *Z. Phys. Chem.* 1904;47:52-55.
- Niebergall PJ, Goyan JE: Dissolution rate studies. I. Continuous recording technique for following rapid reaction in solution. *J. Pharm. Sci.* 1963;52:29-33.
- Nogami H, Nagai T, Fukuska E, Sonobe T: Disintegration of Aspirin tablets containing potato starch and microcrystalline cellulose in various concentrations. *Chem. Pharm. Bull* 1969;17:1450-1455.
- Nogami H, Nagai T, Uchida H: Studies on powdered preparation. XIV. Wetting of powder bed and disintegration time of tablet. *Chem. Pharm. Bull* 1966;14:152-158.
- Nokhodchi A, Ford JL, Rowe PH, Rubinstein MH: The effects of compression rate and force on the compaction properties of different viscosity grades of hydroxypropylmethylcellulose. *Int. J. Pharm.* 1996;129(1-2):21-31.
- Nyström C, Alderborn G, Duberg M, Karehill P-G: Bonding surface area and bonding mechanism - Two important factors for the understanding of powder compactability. *Drug. Dev. Ind. Pharm.* 1993;19(17-18):2143-2196.

- Omohundro S: Modeling cellular automata with partial differential equations. *Physica D* 1984;10:128-134.
- Oono Y, Kohmoto M: A discrete model for chemical turbulence. *Phys. Rev. Lett.* 1985;55:2927-2931.
- Parrot EL: *Pharmaceutical dosage forms: Tablets*. New York, Marcel Decker Inc., 1981a, vol 2, pp 178.
- Parrot EL: Compression, in Lieberman HA, Lachman L, Schwartz BJ (eds): *Pharmaceutical dosage forms: Tablets*. New York, Marcel Decker Inc., 1981b, vol 2, pp 201-243.
- Parrot EL: Compression, in Lieberman HA, Lachman L (eds): *Pharmaceutical Dosage Forms: Tablets*. New York, Marcel Decker, 1981c.
- Partridge D, Hussain KM: *Knowledge-Based Information Systems*, McGraw Hill, 1994.
- Patel N, Hopponen R: Mechanism of action of starch as a disintegrating agent in Aspirin tablets. *J. Pharm. Sci.* 1966;55(10):1065-1068.
- Peck GE, Baley GJ, McCurdy VE, Banker GS: Tablet Formulation Design, in Lieberman HA, Lachman L, Schwartz BJ (eds): *Pharmaceutical Dosage Forms: Tablets*. New York, Marcel Decker, 1989, vol 1, pp 75-130.
- Pedersen PV, Myrick JW: Versatile kinetic approach to analysis of dissolution data. *J. Pharm. Sci.* 1978;67:1450-1455.
- Perdang JM: *Cellular Automata: Prospect in Astrophysical Applications*, in Lejeune A (ed), World Scientific, 1993.
- Pernarowski M, Woo W, Searl R: Continuous flow apparatus for the determination of dissolution characteristics of tablets and capsules. *Journal of Pharmaceutical Sciences* 1968;57:1419-1421.
- Pesavento U: An implementation of von Neumann's self-reproducing machine. *Artificial Life* 1995;2:337-354.
- Picker KM: The 3-D model: comparison of parameters obtained from and by simulating different tableting machines. *AAPS PharmSciTech* 2003;4(3):35.
- Pires A, Landau DP: *Computational Physics and Cellular Automata*, in Herrmann H (ed), World Scientific, 1990.
- Pitteway MLV: Algorithm for Drawing Ellipses or Hyperbolae with a Digital Plotter. *Computer J.* 1967;10(3):282-289.
- Ponchel G, Duchene D: Evaluation of formalincaseine as a tablet disintegrant. *Drug Dev. Ind. Pharm.* 1990;16:613-628.
- Poole J: Some experiences in the evaluation of formulation variables in drug availability. *Drug Information Bulletin* 1969;3:8-16.
- Preston K, Duff M: *Modern Cellular Automata: Theory and Applications*, Plenum press, 1984.
- Prista LN, Alves AC, Morgado RM: *Técnica Farmacêutica e Farmácia Galênica*. Lisboa, Fundação Calouste Gulbenkian, 1995, vol I, pp 453-454.
- Ragnarsson G: Force-displacement and network measurements, in Alderborn G, Nystroem C (eds): *Pharmaceutical powder compaction technology - Drugs and the pharmaceutical sciences*. New York, Decker, 1996.

- Ramani KV, Patel MR, Patel SK: An expert system for drug preformulation in a pharmaceutical company. *Interfaces, Journal of INFORMS* 1992;22(2):101-108.
- Reggia A, Armentrout SL, Chou H-H, Peng Y: Simple systems that exhibit self-directed replication. *Science* 1993;259:1282.
- Ringard J, Guyot-Herman AM: Influence de l'établissement d'un réseau hydrophile et continue d'amidon sur les propriétés des comprimés. *J. Pharm. Belg.* 1978;33:99-110.
- Ringard J, Guyot-Herman AM: Mechanism de la désagrégation. Répercussions pratiques sur la formulation des comprimés. *Labo Pharma Probl. Tech.* 1982;30:7-18.
- Ringard J, Guyot-Herman AM, Robert H: Détermination de l'absorption d'eau et du mouillage en surface des comprimés dans le cadre d'une étude sur le délitement. *Labo Pharma Probl. Tech.* 1977;25:409-415.
- Ringard J, Guyot-Hermann AM: Calculation of disintegrant critical concentration in order to optimise tablets disintegration. *Drug Dev Ind Pharm.* 1988;14(15-17):2321-2339.
- Romero P, Costa JB, Castel-Maroteaux X, Chulia D: Statistical optimisation of a controlled release formulation obtained by a double compression process: application of a hadamard matrix and a factorial design, in Wells JI, Rubinstein MH (eds): *Pharmaceutical Technology, Controlled Drug Release*. New York, Ellis HArwood, 1991, vol 2, pp 44-58.
- Rowe RC: Adhesion of film coatings to tablet surfaces - a theoretical approach based on solubility parameters. *Int. J. Pharm.* 1988;41:219-222.
- Rowe RC: *Manufacturing Intelligence*. 1993(14):13-15.
- Rowe RC: *PDA J. Pharm. Sci. Technology* 1995;49:257-261.
- Rowe RC, Hall J, Roberts RJ: *R.J. Pharm. Technol. Eur.* (in press).
- Rowe RC, Roberts RJ: Artificial intelligence in pharmaceutical product formulation: knowledge-based and expert systems. *Research Focus* 1998;1(4):153-159.
- Rubio GI: *An. Fac. Quim. Farm. Chile.* 1957;9:249.
- Rumpf H: *Agglomeration*. New York, Interscience Publishers, 1962a.
- Rumpf H: The strength of granules and agglomerates, in Knepper WA (ed): *Agglomeration*. New York, Interscience Publishers, 1962b.
- Ryshkewitch E: Compression strength of porous sintered alumina and zirconia. *Journal of the American Ceramic Society* 1953;36(2):65-68.
- Schmidt PC, Vogel PJ: Force-time curves of a modern rotary tablet machine I. Evaluation techniques and characterisation of deformation behaviour of pharmaceutical substances. *Drug. Dev. Ind. Pharm.* 1994;20(921-934).
- Schwartz BJ, Simonelli AP, Higuchi WI: Drug release from wax matrice. II. Application of a mixture theory to the sulfanilamide-wax system. *J. Pharm. Sci.* 1968a;57:278-282.
- Schwartz BJ, Simonelli AP, Higuchi WI: Drug release from wax matrices. I. Analysis of data with first-order kinetics and with the diffusion-controlled model. *J. Pharm. Sci.* 1968b;57:274-277.
- Seager H, Burt I, Ryder J, Rue P, Murray S: *Int. J. Pharm. Technol. Prod. Manuf.* 1979;1(36).

- Sell PS: Expert systems—a practical introduction, Camelot Press, 1985.
- Shangraw R, Mitrevej A, Shah M: A new era of tablet disintegrants. *Pharm. Techn.* 1980;4:49-57.
- Shotton E, Hersey JA, Wray PE: Compaction and compression, in Lachmann L, Liebermann HA, Kanig JL (eds): *Theory and practice of industrial pharmacy*. Philadelphia, Lea and Febiger, 1976a, pp 303-306.
- Shotton E, Leonard GS: Effect of intragranular and extragranular disintegrating agents on particle size of disintegrated tablets. *J. Pharm. Sci.* 1976b;65:1170-1174.
- Stamm A, Gissinger D, Boymond C: Quantitative evaluation of the wettability of powders. *Drug Dev. Ind. Pharm.* 1984;10:381-408.
- Stauffer D, Aharony A: *Introduction to percolation theory, Second Edition*. CRC Press: Florida 33431, USA, 1994:181 pp.
- Stockmayer WH: Theory of molecular size distribution and gel formation in branched-chain polymers. *Journal of Chemical Physics* 1943;11(2):45-55.
- Stricker H: *Pharm. Ind.* 1991;53:571-578.
- Stricker H: *Pharm. Ind.* 1994;56:641-647.
- Surleve A: *Etude de quelques agents de désagrégation modernes. Optimisation de la formulation biopharmaceutique des comprimés*, 1981.
- Thomas M: *Manufacturin Intelligence* 1991(7):6-8.
- Toffoli T: Cellular automata as an alternative to (rather than an approximation of) differential equations in modeling physics. *Physica D* 1984;10:117-127.
- Toffoli T, Farmer D: *Cellular Automata Proceedings of an Interdisciplinary Workshop*. North-Holland, Physica D, 1984, vol 10.
- Train D: An investigation into the compaction of powders. *J. Pharm. Pharmac.* 1956;8:745-760.
- Tson Y, Hammerstrom T, Sathe P, Shah V: Statistical assessment of mean difference between two dissolution data sets. *Drug. Information Journal* 1996;30:1105-1112.
- Ulam S: Random processes and transformations: *Proc. Int. Congr. Math.*, 1952, vol 2, pp 264-275.
- Valvani SC, Yalkowsky SH: Solubility and partitioning in drug design, in Yalkowsky SH, Sinkula AA, Valvani SC (eds): *Physical chemical properties of drugs*. New York, Marcel Dekker, 1980.
- Van Aken JR: An Efficient Ellipse Drawing Algorithm. *CG&A* 1984;4(9):24-35.
- Van Kamp H, Bolhuis G, de Boer A, Lerk C, Lie-A-Huen L: The role of water uptake of tablet disintegration. *Pharm. Acta Helv.* 1986;61:22-29.
- Van Krevelen DW, Hoftyzer PJ: *Properties of polymers: their estimation and correlation with chemical structur*. Elsevier, Amsterdam 1976.
- Van Orelli J: *Search for Technological Reasons to develop a Capsule or a Tablet Formulation* University of Basel, 2005.

- Varelas CG, Dixon DG, Steiner C: Zero-order release from biphasic polymer hydrogels. *J. Control. Release* 1995;34:185-192.
- Velasco MV, Munoz-Ruiz A, Monedero MC, Munoz NM, Jimenez-Castellanos MR: Study of post-compressional parameters in the friction properties of maltodextrins. *Int. J. Pharm.* 1997;155:35-43.
- Vichniac GY: Simulating physics with cellular automata. *Physica D* 1984:96-116.
- Von Orelli J: Search for Technological Reasons to develop a Capsule or a Tablet Formulation University of Basel, 2005.
- Vudathala GK, Rogers JA: Dissolution of fludrocortisone form phospholipid coprecipitates. *J. Pharm. Sci.* 1992;82:282-286.
- Wadke DA, Serajuddin ATM, Jacobson H: Preformulation testing, in Lieberman HA, Lachman L, Schwartz BJ (eds): *Pharmaceutical dosage forms: Tablets*. New York, Marcel Dekker, 1989, vol 1, pp 1-73.
- Wagner JG: Interpretation of percent dissolved-time plots derived from In vitro testing of conventional tablets and capsules. *J. Pharm. Sci.* 1969;58:1253-1257.
- Walko JZ: *Innovation* 1989;24(28).
- Washburn EW: The dynamics of capillary flow. *The physical review* 1921;17:273-283.
- Weibull W: A statistical distribution function of wide applicability. *Journal of Applied Mechanics* 1951;18:293-297.
- Wells J: Pharmaceutical preformulation: physicochemical properties of drug substances, in Aulton ME (ed): *Pharmaceutics: The Science of Dosage Form Design*. Amsterdam, Churchill Livingstone, 2001, vol 1, pp 113-138.
- Wikipedia: Expert System, 2007.
- Winfree A, Winfree E, Seifert H: Organizing centers in a cellular excitable medium. *Physica D* 1985;17:109-115.
- Wolfram S: *Theory and Application of Cellular Automata*. World Scientific 1986.
- Wolfram S: *Cellular Automata and Complexity*, Reading MA, 1994.
- Wolfram S: *A New Kind of Science*, Wolfram Media, Inc., 2002.
- Wood M: *Lab. Equipment Digest* 1991(December):17-19.
- Woodhead PJ, Newton JM: The influence of deposition method on the packing uniformity of powder beds. *J. Pharm. Pharmac.* 1983;35:133-137.
- Yang L, Venkatesh G, Fassihi R: Characterisation of compressibility and compactibility of poly(ethylene oxide) polymers for modified release application by compaction simulator. *J. Pharm. Sci.* 1996;85(10):1085-1090.
- YI YB, Sastry AM: Analytical approximation of the percolation threshold for overlapping ellipsoids of revolution. *Proc. R. Soc. Lond.* 2004;460:2353-2380.
- Yuasa H, Kanya Y: Studies on internal structure of tablet. II. Effect of the critical disintegrator amount on the internal structure of tablets. *Chem. Pharm. Bull* 1986;34:5133-5139.

Zou RP, Yu AB: Evaluation of the packing characteristics of mono-spherical particles. *Powder Technol.* 1996;88:71-79.

Zygourakis K, Markenscoff PA: Computer-aided design of bioerodible devices with optimal release characteristics: a cellular automata approach. *Biomaterials* 1996;17:125-135.

8. Image credits

1 G.K. Raju, Purdue University, Indianapolis, USA

2 Joshi V: Excipient Choice in Solid Dosage Forms, 2007.

3 modified from Gabaude C: De la poudre au comprimé: une stratégie de caractérisation pour un développement rationnel Université de Limoges, 1999.

4 modified from Alderborn G, Nystroem C: Intermolecular bonding forces, in Alderborn G, Nystroem C (eds): Pharmaceutical powder compaction technology. New York, Marcel Dekker, 1996, p21.

5 Leuenberger H: Feste Arzneiformen: Universität Basel lecture manuscripts. Basel, 2004.

6 Guntermann A: Evaluation of Presster™ Compaction Simulator. Freiburg, Germany, 2004.

7 Davis, Raymond E., H. Clark Metcalfe, John E. Williams, and Joseph F. Castka. Modern Chemistry: Annotated Teacher's Edition. Austin: Holt, Reinhart and Winston, 2002.

http://www.nisd.net/secww/science/science-taks/Solubility%20Factors_files/frame.htm#slide0001.htm

8 Department of Chemistry, University of Illinois at Chicago, 2007.

http://www.chem.uic.edu/marek/apintropage/ap_notes/chapter11/chapter11.htm

9 modified from Guyot-Hermann AM: Tablet disintegration and disintegrating agents. S.T.P. Pharma Sci. 1992;2(6):445-462.

10 modified from Kanig JL, Rudnic EM: The mechanisms of disintegration action. Pharm. Technol. 1984;4:50-63

11 screenshots from video

Zhao N, Augsburg L: Functionality Comparison of 3 Classes of Superdisintegrants in Promotin Aspirin Tablet Disintegration and Dissolution. AAPS PharmSciTech 2005;6(4):634-640.

<http://www.aapspharmscitech.org/view.asp?art=pt060479>

12 modified Melia CD, Davis SS: Mechanisms of drug release from tablets and capsules. I: Disintegration. Aliment. Pharmacol. Therap. 1989;3:223-232.

13 modified from Guyot-Hermann AM: Tablet disintegration and disintegrating agents. S.T.P. Pharma Sci. 1992;2(6):445-462

14 Hanson R, Gray V: Handbook of Dissolution Testing. Hockessin, Dissolution Technologies Inc., 2004, pp 21-22.

15 modified from: Macheras P, Athanassios I: Modeling in Biopharmaceutics, Pharmacokinetics, and Pharmacodynamics. New York, Springer, 2006, pp 90-95

16 modified from Martin AN, Bustamante P, Chun AHC: Physical Pharmacy: Physical Chemical Principles in the Pharmaceutical Sciences, Lippincott Williams & Wilkins, 1993.

17 Hanson R, Gray V: Handbook of Dissolution Testing. Hockessin, Dissolution Technologies Inc., 2004, p36-37.

-
- 18 Bergler S: Introduction to Expert Systems, 2007.
- 19 Rowe RC, Roberts RJ: Artificial intelligence in pharmaceutical product formulation: knowledge-based and expert systems. *Research Focus* 1998;1(4):153-159.
- 20 screenshots from: Java Applet runs: Gonsalves R.J., 2007.
http://www.physics.buffalo.edu/gonsalves/ComPhys_1998/Java/Percolation.html
- 21 Stauffer D, Aharony A: Introduction to percolation theory, Second Edition. CRC Press: Florida 33431, USA, 1994, p72
- 22 Edkins J, 2007.
<http://gwydir.demon.co.uk/jo/tess/index.htm>
- 23 Wikipedia, 2007
http://en.wikipedia.org/wiki/Bethe_lattice
- 24 Graphics Application Lab., 2007
<http://jade.cs.pusan.ac.kr/~pgkim/images/voronoi.jpg>
- 25 University of Massachusetts, Lowell R. , 2007.
<http://ulcar.uml.edu/RPI/BinBrowser/Cube.gif>
- 26 Southern Methodist University, Department of Mathematics, 2007.
<http://www.smu.edu/math/research/foam.jpg>
- 27 modified from Essam JW: Percolation theory. *Reports on Progress in Physics* 1980; 43, p843
- 28 Gould H, Tobochnik J, Christian W: Percolation, in J. B (ed): *An Introduction to Computer Simulation Methods: Applications to Physical Systems*. Boston, Addison Wesley 3rd edition, 2006, p456.
- 29 How Long Is the Coast of Britain? Statistical Self-Similarity and Fractional Dimension
<http://www.answers.com/topic/how-long-is-the-coast-of-britain-statistical-self-similarity-and-fractional-dimension>
- 30 modified form efg's Web Sites, Koch curve, 2007
<http://www.efg2.com/Lab/FractalsAndChaos/vonKochCurve.htm>
- 31 modified from Wikipedia: Sierpinski triangle, 2007.
http://en.wikipedia.org/wiki/Sierpinski_triangle
- 32 modified from HYPO: serveur WEB de l'enseignement secondaire postobligatoire, Menger sponge, 2007
<http://hypo.ge-dip.etat-ge.ch/www/math/html/root.html>
- 33 Vassallo C: Indentation angle and fractal dimension, 2007
<http://perso.orange.fr/charles.vassallo/fr/art/dimension.html>
- 34 Bunde A, Kantelhardt W: Diffusion and conduction in percolation systems: theory and applications, in Heitjans P, Kärger J (eds): *Diffusion in Condensed Matter*. Berlin, Springer, 2005
<http://www.uni-giessen.de/physik/theorie/theorie3/publications/JWK-Springer1.pdf>
- 35 Gould H, Tobochnik J, Christian W: Percolation, in J. B (ed): *An Introduction to Computer Simulation Methods: Applications to Physical Systems*. Boston, Addison Wesley 3rd edition, 2006, p461-463
- 36 modified from Mathworld W: Von Neumann neighbourhood, 2007.
- 37 modified form Mathworld W: Moore Neighbourhood, 2007.

38 modified from Wikipedia: Cellular automata, 2007.

39 Callahan P: What is the Game of Life?, Math.com, 2007.

40 modified from Wikipedia: Conway's Game of Life. 2007.

41 produced with the Applet: Hensel A: Game of Life, Math.com, 2007.

42 from Katsura N, Mitsuoka T, Shimosaka A, Shirakawa Y, Hidaka J: Development of new simulation method for flow behaviour of granular materials in a blast furnace using cellular automaton. ISIJ International 2005;45(10):1396-1405.

43 Screenshots from Zygourakis K: Cellular Automaton for Surface Erosion, 2007

44 modified MCLachlan DS, Blaszkiewicz M, al. e: Electrical resistivity of composites. J. Am. Ceram. Soc. 1990;73(8):2187-2203.

45 Department of Applied Mathematics ANU: Packing of 120,000 mono-disperse spherical beads, 2007.

46 Wikipedia: Nelder-Mead method, 2007.

9. Appendix

List of abbreviations:

Av.	average
Calc. ρ	calculated density of the mixture
CF	compression force
pCF	pre-compression force
D	diameter of the tablet
Dis.	disintegrant
DT	disintegration time
H	thickness, height of the tablet
MDBP	minimum distance between upper and lower punches during compression with Presster™ simulator
pMDBP	minimum distance between upper and lower punch during pre-compression with Presster™ simulator
Sol. frac.	solid fraction of the tablets
Stdev	standard deviation
T	temperature of disintegration or dissolution medium
Tab.	tablet
Targ. thick.	targeted thickness of the tablet during compression
W	weight of the tablet
%(v/v)	volumetric percentage
%(w/w)	mass percentage
ε_t	targeted porosity of the tablets during compression

Appendix A: Calculation of the radius of the largest sphere being caged by four bigger spheres in a BCC close packing.

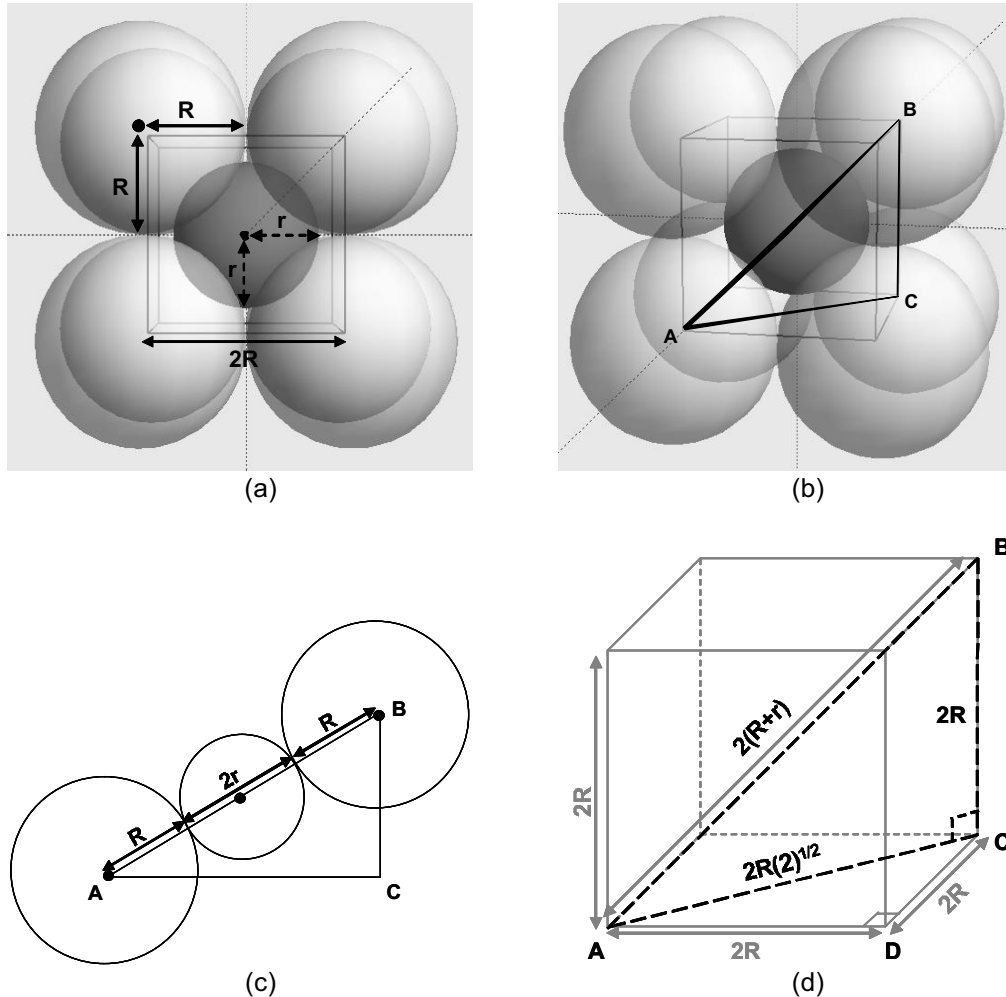


Figure: 9.1 Spheres in a BCC close packing and corresponding schemas for calculation of the radius of the largest caged sphere.

(a) Top view of a five spheres in a BCC close packing.

(b) Perspective view of five spheres in a BCC close packing with a right triangle ABC inside.

(c) Alignment of the centres of three spheres on the diagonal (AB) of the ABC right triangle.

(d) Schema of the BCC lattice cube. The hypotenuse (AB) of the right triangle (dashed lines) is the diagonal of the cube. The second longer side (AC) of the triangle is the diagonal of the bottom face of the cube. The third side (BC) of the triangle is an edge of the cube.

In a Body Centred Cubic (BCC) close packing of spheres, the radius r of the largest central sphere which can be caged by four other spheres of radii R was determined using Euclidian geometry as follows:

- In a BCC close packing, all spheres are in contact with their respective direct neighbours (Figure: 9.1a, b).
- A BCC lattice contains a cube having its corners corresponding to centres of the four external spheres of the packing (see Figure: 9.1a, b, d).
- The BCC lattice cube contains a right triangle ABC with an hypotenuse (AB) equal to a diagonal of the cube, a side (AC) equal to the diagonal of the bottom face of the cube and a side (BC) equal to an edge of the cube (see Figure: 9.1b, d).
- The centre of the inner sphere and the centres of two external spheres of the BCC close packing are aligned on the hypotenuse (AB) of the ABC triangle.
- The diagonal length of the cube of the BCC lattice is then equal to the sum of the diameter of the central sphere and the radii of the two neighbouring external spheres (Figure: 9.1c, d):

$$AB = R + 2r + R = 2(R + r)$$

- The length of the smallest side (BC) of the triangle ABC is equal to two radii of the external spheres of the BCC close packing (Figure: 9.1d):

$$BC = 2R$$

- AC is the diagonal of the bottom face of the BCC lattice cube (Figure: 9.1d) and the length of AC can be determined using Pythagorean Theorem in the triangle ACD:

$$(AC)^2 = (CD)^2 + (AD)^2 = 2(2R)^2$$

$$\text{which gives } AC = 2R\sqrt{2}$$

Pythagorean Theorem in the right triangle ABC is as follows:

$$(AB)^2 = (BC)^2 + (AC)^2$$

By replacing AC, BC and AC by their previously determined values, it gives:

$$(2(R + r))^2 = (2R)^2 + (2R\sqrt{2})^2 = 12R^2$$

$$\Leftrightarrow 2(R + r) = \sqrt{12R^2} = 2R\sqrt{3}$$

$$\Leftrightarrow r = \frac{2R\sqrt{3} - 2R}{2}$$

$$\Leftrightarrow r = R(\sqrt{3} - 1)$$

In a BCC close packing of spheres, the radius of the largest sphere which can be caged by four spheres of radii R is $r = R(\sqrt{3} - 1)$.

Appendix B Composition of the formulations

Formulation I ($\epsilon_t = 10\%$) Paracetamol DC90 (drug) / StaRX1500 [®] A (dis.)				Formulation I ($\epsilon_t = 8\%$) Paracetamol DC90 (drug) / StaRX1500 [®] A (dis.)			
% Dis. (v/v sol. frac.)	% Dis. (w/w)	Calc. ρ (g/cm ³)	Targ. thick. (mm)	% Dis. (v/v sol. frac.)	% Dis. (w/w)	Calc. ρ (g/cm ³)	Targ. thick. (mm)
0	0.00	1.319	3.67	0	0.00	1.319	3.99
5	5.65	1.329	3.64	5	5.64	1.329	3.96
7	7.88	1.333	3.63	7	7.88	1.333	3.94
8	9.00	1.335	3.62	8	8.99	1.335	3.94
9	10.11	1.337	3.62	9	10.10	1.337	3.93
10	11.22	1.339	3.61	10	11.21	1.339	3.93
15	16.71	1.349	3.59	11	12.31	1.341	3.92
20	22.14	1.359	3.56	15	16.70	1.349	3.90
40	43.12	1.396	3.47	20	22.11	1.359	3.87
50	53.21	1.414	3.42				

Formulation II ($\epsilon_t = 10\%$) Paracetamol DC90Fine (drug) / StaRX1500 [®] A (dis.)				Formulation II ($\epsilon_t = 14\%$) Paracetamol DC90Fine (drug) / StaRX1500 [®] A (dis.)			
% Dis. (v/v sol. frac.)	% Dis. (w/w)	Calc. ρ (g/cm ³)	Targ. thick. (mm)	% Dis. (v/v sol. frac.)	% Dis. (w/w)	Calc. ρ (g/cm ³)	Targ. thick. (mm)
0	0.00	1.290	3.75	0	0.00	1.290	4.36
1	1.16	1.292	3.74	2	2.32	1.299	4.33
2	2.32	1.295	3.74	3	3.47	1.303	4.32
3	3.47	1.297	3.73	4	4.62	1.308	4.30
4	4.62	1.300	3.72	5	5.76	1.312	4.29
5	5.77	1.302	3.72	6	6.90	1.316	4.28
6	6.91	1.305	3.71	8	9.17	1.324	4.25
7	8.05	1.307	3.70	15	17.01	1.351	4.16
8	9.18	1.309	3.70	20	22.50	1.369	4.11
9	10.31	1.312	3.69				
10	11.44	1.314	3.68				
15	17.03	1.326	3.65				
20	22.52	1.337	3.62				
30	33.26	1.360	3.56				
40	43.67	1.382	3.50				
50	53.76	1.403	3.45				

Formulation III ($\epsilon_t=14\%$) Caffeine powder A (drug) / StaRX1500 [®] A (dis.)				Formulation VI ($\epsilon_t=10\%$) Indomethacin (drug) / StaRX1500 [®] A (dis.)			
% Dis. (v/v sol. frac.)	% Dis. (w/w)	Calc. ρ (g/cm ³)	Targ. thick. (mm)	% Dis. (v/v sol. frac.)	% Dis. (w/w)	Calc. ρ (g/cm ³)	Targ. thick. (mm)
0.00	100.00	1.500	3.8	0.00	0.00	1.387	3.88
5.81	94.19	1.500	3.8	5.56	6.01	1.394	3.86
11.63	88.37	1.500	3.8	11.11	11.96	1.401	3.84
19.77	80.23	1.500	3.8	18.89	20.20	1.410	3.81
20.93	79.07	1.500	3.8	20.00	21.37	1.411	3.81
22.09	77.91	1.500	3.8	21.11	22.53	1.413	3.81
23.26	76.74	1.500	3.8	22.22	23.70	1.414	3.80
24.42	75.58	1.500	3.8	27.78	29.48	1.421	3.78
29.07	70.93	1.500	3.8	33.33	35.21	1.427	3.77
34.88	65.12	1.500	3.8	44.44	46.51	1.440	3.73
				55.56	57.60	1.452	3.70

Formulation VII ($\epsilon_t=10\%$) Caffeine powder A (drug) / AcDiSol [®] (dis.)				Formulation VIII ($\epsilon_t=10\%$) Caffeine powder A (drug) / L-HPC (dis.)			
% Dis. (v/v sol. frac.)	% Dis. (w/w)	Calc. ρ (g/cm ³)	Targ. thick. (mm)	% Dis. (v/v sol. frac.)	% Dis. (w/w)	Calc. ρ (g/cm ³)	Targ. thick. (mm)
0.00	0.00	1.450	3.58	0.00	0.00	1.500	3.58
0.56	0.62	1.451	3.58	0.56	0.54	1.500	3.58
1.11	1.23	1.452	3.58	1.11	1.08	1.499	3.59
2.22	2.46	1.454	3.58	2.22	2.15	1.499	3.59
3.33	3.68	1.456	3.57	3.33	3.23	1.498	3.59
4.44	4.90	1.458	3.57	4.44	4.31	1.498	3.59
5.56	6.12	1.460	3.57	5.56	5.38	1.497	3.59
6.67	7.33	1.461	3.57	8.89	8.62	1.496	3.59
7.78	8.55	1.463	3.56	11.11	10.79	1.495	3.60
8.89	9.75	1.465	3.56				
10.00	10.96	1.467	3.56				
11.11	12.16	1.469	3.55				

Formulation IX ($\epsilon_t=10\%$) Indomethacin (drug) / AcDiSol [®] (dis.)			
% Dis. (v/v sol. frac.)	% Dis. (w/w)	Calc. ρ (g/cm ³)	Targ. thick. (mm)
0.00	0.00	1.387	2.28
1.00	1.16	1.390	2.27
1.50	1.73	1.391	2.27
2.00	2.31	1.392	2.27
2.70	3.11	1.394	2.26
3.00	3.46	1.395	2.26
5.00	5.74	1.400	2.25
10.00	11.40	1.412	2.24

Formulation X ($\epsilon_t=9\%$)			
Caffeine (drug) / StaRX1500 [®] (dis.) / α lactose monohydrate (filler)			
	Caffeine powder A	StaRX1500 [®]	α lactose monohydrate
% (v/v) tablet:	51.70	20.68	18.61
% (v/v) sol. frac.:	56.82	22.73	20.45
% (w/w):	56.51	22.60	20.89
Calc. ρ (g/cm ³):	1.508		

Formulation XI ($\epsilon_t=9\%$)			
Caffeine (drug) / StaRX1500 [®] (dis.) / α lactose monohydrate (filler)			
	Caffeine powder A	StaRX1500 [®]	α lactose monohydrate
% (v/v) tablet:	65.32	20.68	5.00
% (v/v) sol. frac.:	71.78	22.73	5.49
% (w/w):	71.67	22.69	5.63
Calc. ρ (g/cm ³):	1.502		

Formulation XII ($\epsilon_t=9\%$)			
Caffeine (drug) / StaRX1500 [®] (dis.) / α lactose monohydrate (filler)			
	Caffeine powder A	StaRX1500 [®]	α lactose monohydrate
% (v/v) tablet:	65.32	10.00	15.68
% (v/v) sol. frac.:	71.78	10.99	17.23
% (w/w):	71.45	10.94	17.61
Calc. ρ (g/cm ³):	1.507		

Formulation XIII ($\epsilon_t=12\%$)			
Caffeine (drug) / α lactose monohydrate (filler)			
	Caffeine powder A	StaRX1500 [®]	α lactose monohydrate
% (v/v) tablet:	49.80	19.92	17.93
% (v/v) sol. frac.:	56.82	22.73	20.45
% (w/w):	56.51	22.60	20.89
Calc. ρ (g/cm ³):	1.508		

Formulation XIV ($\epsilon_t=14\%$)		
Aspirin (drug) / α lactose monohydrate (filler)		
	Aspirin	α lactose monohydrate
% (v/v) tablet:	60.00	26
% (v/v) sol. frac.:	69.77	30.23
% (w/w):	67.45	32.55
Calc. ρ (g/cm ³):	1.426	

Appendix C Tableting

Formulation I ($\epsilon_t = 10\%$): Paracetamol DC90 (drug) / StaRX1500 [®] A (dis.)											
Compression parameters and tablet properties											
% dis. (v/v sol. frac.)	Tab.	W (mg)	H (mm)	CF (kN)	MDBP (mm)	% dis. (v/v sol. frac.)	Tab.	W (mg)	H (mm)	CF (kN)	MDBP (mm)
0	1	381.1	4.09	15.5	2.60	10	1	380.2	3.90	35.0	1.28
	2	378.8	4.10	14.7	2.60		2	379.1	3.92	35.8	1.28
	3	380.7	4.12	15.0	2.60		3	377.3	3.93	36.0	1.28
5	1	381.2	4.03	22.4	2.15	15	1	378.8	3.94	38.5	1.05
	2	377.2	3.96	21.8	2.15		2	378.9	3.92	39.0	1.05
	3	377.5	4.01	22.2	2.15		3	379.3	3.95	38.8	1.05
7	1	378.5	3.99	25.3	1.92	20	1	378.8	3.90	44.0	0.78
	2	378.3	3.97	26.2	1.92		2	379.5	3.91	42.9	0.78
	3	378.5	3.96	25.9	1.92		3	378.8	3.92	42.6	0.78
8	1	378.8	3.97	27.9	1.78	40	1	378.8	3.90	39.2	0.75
	2	379.0	3.94	28.4	1.78		2	378.4	3.90	40.2	0.75
	3	378.7	3.96	28.4	1.78		3	376.3	3.89	39.6	0.75
9	1	378.1	3.93	34.8	1.45	50	1	377.9	3.89	38.6	0.70
	2	378.4	3.95	34.7	1.45		2	377.8	3.90	40.3	0.70
	3	379.1	3.92	34.1	1.45		3	379.1	3.92	39.3	0.70

Formulation I ($\epsilon_t = 10\%$): Paracetamol DC90 (drug) / StaRX1500[®] A (dis.)
 Averages values: compression parameters, tablet properties, calculated mixture density, porosity and volumetric % of disintegrant in total tablet.

% dis. (v/v sol. frac.)	W (mg)	H (mm)	CF (kN)	MDBP (mm)	Calc. ρ (g/cm ³)	Porosity (% vol. tab.)	% dis. (v/v tab.)
0	380.2	4.10	15.1	2.60	1.32	10.6	0.0
5	378.6	4.00	22.1	2.15	1.33	9.3	4.5
7	378.4	3.97	25.8	1.92	1.33	9.0	6.4
8	378.8	3.96	28.2	1.78	1.34	8.7	7.3
9	378.5	3.93	34.5	1.45	1.34	8.4	8.2
10	378.9	3.92	35.6	1.28	1.34	8.0	9.2
15	379.0	3.94	38.8	1.05	1.35	9.1	13.6
20	379.0	3.91	43.2	0.78	1.36	9.2	18.2
40	377.8	3.90	39.7	0.75	1.40	11.6	35.4
50	378.3	3.90	39.4	0.70	1.42	12.8	43.6

Formulation I ($\epsilon_t = 8\%$): Paracetamol DC90 (drug) / StaRX1500[®] A (dis.)											
Compression parameters and tablet properties											
% dis. (v/v sol. frac.)	Tab.	W (mg)	H (mm)	CF (kN)	MDBP (mm)	% dis. (v/v sol. frac.)	Tab.	W (mg)	H (mm)	CF (kN)	MDBP (mm)
0	1	379.2	3.98	20.0	2.80	10	1	381.5	3.93	32.7	2.30
	2	380.6	3.99	19.8	2.80		2	380.0	3.94	32.4	2.30
	3	382.1	4.00	20.5	2.80		3	377.9	3.91	31.6	2.30
	4	380.5	4.00	19.8	2.80		4	380.5	3.95	32.4	2.30
	5	379.1	3.98	19.8	2.80		5	381.2	3.95	31.9	2.30
	6	379.5	3.99	20.0	2.80		6	381.3	3.95	32.4	2.30
5	1	379.1	3.96	24.1	2.60	11	1	379.6	3.93	33.6	2.30
	2	378.8	3.96	23.4	2.60		2	379.4	3.94	31.2	2.30
	3	379.0	3.96	24.3	2.60		3	382.1	3.96	33.2	2.30
	4	381.3	3.98	24.5	2.60		4	381.7	3.95	32.8	2.30
	5	380.1	3.98	23.5	2.60		5	378.9	3.93	31.7	2.30
	6	379.9	3.97	24.1	2.60		6	380.9	3.95	32.4	2.30
7	1	380.6	3.95	26.8	2.50	15	1	381.0	3.95	38.7	2.10
	2	379.8	3.96	26.6	2.50		2	379.7	3.92	39.0	2.10
	3	380.6	3.96	26.1	2.50		3	379.6	3.92	39.1	2.10
	4	381.1	3.96	26.6	2.50		4	380.2	3.95	38.7	2.10
	5	380.2	3.95	26.1	2.50		5	383.2	3.98	39.4	2.10
	6	381.3	3.97	27.0	2.50		6	380.4	3.95	38.3	2.10
8	1	379.6	3.94	29.2	2.40	20	1	379.2	3.91	45.4	1.90
	2	379.1	3.94	28.8	2.40		2	379.9	3.90	43.5	1.90
	3	381.5	3.96	29.2	2.40		3	380.1	3.96	44.8	1.90
	4	380.6	3.96	29.4	2.40		4	380.6	3.93	44.0	1.90
	5	379.7	3.94	28.9	2.40		5	380.0	3.93	44.1	1.90
	6	377.7	3.94	28.4	2.40		6	380.5	3.92	44.4	1.90
9	1	377.9	3.93	28.5	2.40						
	2	378.6	3.95	29.5	2.40						
	3	380.0	3.93	29.3	2.40						
	4	382.3	3.98	30.1	2.40						
	5	377.3	3.93	28.2	2.40						
	6	378.4	3.93	28.7	2.40						

Formulation I ($\epsilon_t = 8\%$): Paracetamol DC90 (drug) / StaRX1500[®] A (dis.)
Averages values: compression parameters, tablet properties, calculated mixture density, porosity and volumetric % of disintegrant in total tablet.

% dis. (v/v sol. frac.)	W (mg)	H (mm)	CF (kN)	MDBP (mm)	Calc. ρ (g/cm ³)	Porosity (% vol. tab.)	% dis. (v/v tab.)
0	380.2	3.99	20.0	2.80	1.319	8.03	0.0
5	379.7	3.97	24.0	2.60	1.329	8.33	4.6
7	380.6	3.96	26.5	2.50	1.333	8.16	6.4
8	379.7	3.95	29.0	2.40	1.335	8.24	7.3
9	379.1	3.94	29.1	2.40	1.337	8.41	8.2
10	380.4	3.94	32.2	2.30	1.339	8.15	9.2
11	380.4	3.94	32.5	2.30	1.341	8.40	10.1
15	380.7	3.95	38.9	2.10	1.349	8.92	13.7
20	380.1	3.93	44.4	1.90	1.359	9.28	18.1

Formulation II ($\epsilon_t = 10\%$): Paracetamol DC90Fine (drug) / StaRX1500 [®] A (dis.)									
Compression parameters and tablet properties									
% dis. (v/v sol. frac.)	Tab.	W (mg)	H (mm)	MDBP (mm)	% dis. (v/v sol. frac.)	Tab.	W (mg)	H (mm)	MDBP (mm)
0	1	377.4	4.49	2.65	8	1	377.2	4.33	2.37
	2	378.0	4.50	2.65		2	376.8	4.36	2.37
	3	379.0	4.50	2.65		3	377.9	4.33	2.37
1	1	377.5	4.47	2.59	9	1	377.2	4.31	2.30
	2	378.5	4.47	2.59		2	377.8	4.29	2.30
	3	377.4	4.47	2.59		3	377.8	4.34	2.30
2	1	377.4	4.45	2.55	10	1	376.5	4.29	2.25
	2	376.1	4.43	2.55		2	375.0	4.28	2.25
	3	378.0	4.43	2.55		3	377.4	4.27	2.25
3	1	377.8	4.43	2.54	15	1	377.0	4.27	2.20
	2	378.1	4.42	2.54		2	376.8	4.28	2.20
	3	378.0	4.42	2.54		3	376.7	4.27	2.20
4	1	376.5	4.43	2.53	20	1	376.0	4.23	2.10
	2	377.1	4.42	2.53		2	375.5	4.24	2.10
	3	377.3	4.42	2.53		3	375.1	4.25	2.10
5	1	377.4	4.43	2.52	30	1	369.1	4.11	1.80
	2	376.8	4.43	2.52		2	371.4	4.09	1.80
	3	377.3	4.42	2.52		3	371.8	4.10	1.80
6	1	377.4	4.43	2.51	40	1	366.2	3.91	1.30
	2	375.6	4.44	2.51		2	369.3	3.94	1.30
	3	377.4	4.43	2.51		3	370.0	3.95	1.30
7	1	377.1	4.40	2.44	50	1	368.4	3.91	1.00
	2	377.3	4.37	2.44		2	367.2	3.93	1.00
	3	377.9	4.40	2.44		3	366.4	3.92	1.00

Formulation II ($\epsilon_t = 10\%$): Paracetamol DC90Fine (drug) / StaRX1500[®] A (dis.)
Averages values: compression parameters, tablet properties, calculated mixture density, porosity and volumetric % of disintegrant in total tablet.

% dis. (v/v sol. frac.)	W (mg)	H (mm)	MDBP (mm)	Calc. ρ (g/cm ³)	Porosity (% vol. tab.)	% dis. (v/v tab.)
0	378.1	4.50	2.65	1.290	10.0	0.0
1	377.8	4.47	2.59	1.292	10.0	0.9
2	377.2	4.44	2.55	1.295	10.0	1.8
3	378.0	4.42	2.54	1.297	10.0	2.7
4	377.0	4.42	2.53	1.300	10.0	3.6
5	377.2	4.43	2.52	1.302	10.0	4.5
6	376.8	4.43	2.51	1.305	10.0	5.4
7	377.4	4.39	2.44	1.307	10.0	6.3
8	377.3	4.34	2.37	1.309	10.0	7.2
9	377.6	4.31	2.30	1.312	10.0	8.1
10	376.3	4.28	2.25	1.314	10.0	9.0
15	376.8	4.27	2.20	1.326	10.0	13.5
20	375.5	4.24	2.10	1.337	10.0	18.0
30	370.8	4.10	1.80	1.360	10.0	27.0
40	368.5	3.93	1.30	1.382	10.0	36.0
50	367.3	3.92	1.00	1.403	10.0	45.0

Formulation II ($\epsilon_t = 14\%$): Paracetamol DC90Fine (drug) / StaRX1500[®] A (dis.)
Compression parameters and tablet properties.

% dis. (v/v sol. frac.)	Tab.	W (mg)	H (mm)	CF (kN)	MDBP (mm)	% dis. (v/v sol. frac.)	Tab.	W (mg)	H (mm)	CF (kN)	MDBP (mm)
0	1	380.1	4.38	7.1	3.67	6	1	380.7	4.33	8.0	3.55
	2	381.6	4.38	7.0	3.67		2	380.9	4.33	7.9	3.55
	3	383.4	4.39	7.3	3.67		3	380.0	4.34	8.1	3.55
	4	382.8	4.38	7.1	3.67		4	382.2	4.37	8.0	3.55
	5	382.5	4.38	7.2	3.67		5	380.6	4.34	8.0	3.55
	6	383.2	4.38	7.1	3.67		6	381.7	4.36	8.2	3.55
2	1	382.0	4.38	7.4	3.65	8	1	380.3	4.31	8.1	3.53
	2	381.4	4.39	6.9	3.65		2	381.2	4.33	8.2	3.53
	3	378.1	4.35	6.9	3.65		3	380.4	4.32	8.1	3.53
	4	384.2	4.38	7.6	3.65		4	379.7	4.31	8.0	3.53
	5	383.3	4.39	7.3	3.65		5	381.5	4.32	8.1	3.53
	6	383.2	4.39	7.5	3.65		6	382.2	4.32	8.2	3.53
3	1	381.8	4.35	7.4	3.64	15	1	379.2	4.25	8.7	3.40
	2	382.1	4.37	7.3	3.64		2	377.8	4.25	9.2	3.40
	3	381.1	4.36	7.6	3.64		3	379.4	4.27	8.7	3.40
	4	381.9	4.38	7.6	3.64		4	380.4	4.26	9.0	3.40
	5	381.5	4.35	7.4	3.64		5	379.7	4.26	9.1	3.40
	6	381.1	4.36	7.7	3.64		6	381.0	4.29	8.8	3.40
4	1	381.1	4.37	7.4	3.63	20	1	378.8	4.22	9.8	3.30
	2	381.5	4.37	7.3	3.63		2	378.3	4.19	9.7	3.30
	3	383.6	4.38	7.7	3.63		3	378.3	4.22	9.3	3.30
	4	381.3	4.38	7.2	3.63		4	379.7	4.20	10.2	3.30
	5	382.0	4.37	7.4	3.63		5	380.2	4.22	10.4	3.30
	6	379.9	4.36	7.2	3.63		6	379.4	4.23	9.4	3.30
5	1	382.9	4.35	8.1	3.57						
	2	382.0	4.35	7.9	3.57						
	3	379.5	4.33	7.6	3.57						
	4	381.8	4.34	8.3	3.57						
	5	379.6	4.35	7.5	3.57						
	6	379.9	4.35	7.4	3.57						

Formulation II ($\epsilon_t = 14\%$): Paracetamol DC90Fine (drug) / StaRX1500[®] A (dis.)
Averages values: compression parameters, tablet properties, calculated mixture density,
porosity and volumetric % of disintegrant in total tablet.

% dis. (v/v sol. frac.)	W (mg)	H (mm)	CF (kN)	MDBP (mm)	Calc. ρ (g/cm ³)	Porosity (% vol. tab.)	% dis. (v/v tab.)
0	382.3	4.38	7.1	3.67	1.290	13.9	0.0
2	382.0	4.38	7.3	3.65	1.299	14.5	1.7
3	381.6	4.36	7.5	3.64	1.303	14.5	2.6
4	381.6	4.37	7.4	3.63	1.308	15.0	3.4
5	381.0	4.35	7.8	3.57	1.312	14.9	4.3
6	381.0	4.35	8.0	3.55	1.316	15.2	5.1
8	380.9	4.32	8.1	3.53	1.324	15.2	6.8
15	379.6	4.26	8.9	3.40	1.351	16.1	12.6
20	379.1	4.21	9.8	3.30	1.369	16.3	16.7

Formulation III ($\varepsilon_t = 14\%$) Caffeine powder A (drug) / StaRX1500[®] A (dis.)
 Compression parameters and tablet properties.

% dis. (v/v sol. frac.)	Tab.	W (mg)	H (mm)	D (mm)	CF (kN)	MDBP (mm)
0.00	1	380.0	3.76	10.03	13.7	2.90
	2	380.5	3.75	10.03	13.4	2.90
	3	381.0	3.76	10.03	13.2	2.90
	4	381.1	3.75	10.03	13.5	2.90
	5	381.1	3.75	10.02	13.2	2.90
	6	381.5	3.75	10.02	13.9	2.90
5.81	1	379.2	3.75	10.02	13.1	2.90
	2	381.3	3.77	10.04	12.7	2.90
	3	379.9	3.77	10.03	12.6	2.90
	4	380.1	3.76	10.03	13.2	2.90
	5	381.6	3.78	10.04	13.2	2.90
	6	381.1	3.77	10.04	12.8	2.90
11.63	1	382.3	3.77	10.03	13.9	2.85
	2	383.3	3.76	10.02	14.0	2.85
	3	381.1	3.76	10.03	13.4	2.85
	4	380.9	3.77	10.04	13.8	2.85
	5	380.5	3.76	10.04	13.4	2.85
	6	380.4	3.76	10.04	13.7	2.85
19.77	1	380.2	3.75	10.03	15.1	2.75
	2	380.1	3.75	10.03	14.2	2.75
	3	381.1	3.75	10.02	15.2	2.75
	4	381.1	3.75	10.03	14.9	2.75
	5	381.8	3.75	10.03	14.8	2.75
	6	381.8	3.76	10.03	14.7	2.75
20.93	1	380.6	3.75	10.03	14.7	2.75
	2	380.9	3.77	10.03	14.5	2.75
	3	381.3	3.75	10.02	14.7	2.75
	4	380.4	3.75	10.02	14.5	2.75
	5	382.6	3.75	10.02	15.1	2.75
	6	383.7	3.77	10.02	14.8	2.75
22.09	1	381.3	3.75	10.03	15.0	2.75
	2	378.9	3.76	10.03	14.6	2.75
	3	381.7	3.76	10.03	14.9	2.74
	4	380.0	3.75	10.03	14.8	2.74
	5	381.1	3.75	10.03	15.0	2.74
	6	381.4	3.76	10.03	14.6	2.74
23.26	1	378.9	3.74	10.03	14.9	2.72
	2	378.3	3.73	10.03	14.5	2.72
	3	378.9	3.75	10.03	14.8	2.72
	4	381.5	3.76	10.03	14.9	2.72
	5	378.5	3.75	10.03	14.9	2.72
	6	381.2	3.75	10.02	15.2	2.72

Formulation III (continued) ($\epsilon_t = 14\%$) Caffeine powder A (drug) / StaRX1500[®] A (dis.)
Compression parameters and tablet properties.

% dis. (v/v sol. frac.)	Tab.	W (mg)	H (mm)	D (mm)	CF (kN)	MDBP (mm)
24.42	1	379.4	3.74	10.03	15.3	2.71
	2	379.3	3.75	10.03	15.1	2.71
	3	381.0	3.74	10.03	15.4	2.71
	4	383.2	3.77	10.02	15.4	2.71
	5	381.4	3.75	10.02	15.3	2.71
	6	381.2	3.75	10.03	15.8	2.71
29.07	1	382.9	3.77	10.03	15.5	2.71
	2	379.7	3.76	10.03	14.4	2.71
	3	381.8	3.76	10.02	15.3	2.71
	4	379.7	3.76	10.03	14.9	2.71
	5	380.3	3.76	10.03	15.0	2.71
	6	380.8	3.76	10.02	14.9	2.71
34.88	1	380.8	3.76	10.02	15.5	2.70
	2	380.6	3.76	10.02	15.5	2.70
	3	381.1	3.77	10.02	15.6	2.70
	4	382.3	3.77	10.02	16.0	2.70
	5	382.9	3.78	10.04	15.6	2.70
	6	380.8	3.77	10.03	15.8	2.70

Formulation III ($\epsilon_t = 14\%$) Caffeine powder A (drug) / StaRX1500[®] A (dis.) ($\epsilon_t = 14\%$):
Averages values: compression parameters, tablet properties, calculated mixture density,
porosity and volumetric % of disintegrant in total tablet.

% dis. (v/v sol. frac.)	W (mg)	H (mm)	D (mm)	CF (kN)	MDBP (mm)	Calc. ρ (g/cm ³)	Porosity (% vol. tab.t)	% dis. (v/v tab.)
0.00	380.9	3.75	10.03	13.5	2.90	1.500	14.3	0.00
5.81	380.5	3.77	10.03	12.9	2.90	1.500	14.8	4.95
11.63	381.4	3.76	10.03	13.7	2.85	1.500	14.5	9.94
19.77	381.0	3.75	10.03	14.8	2.75	1.500	14.3	16.95
20.93	381.6	3.76	10.02	14.7	2.75	1.500	14.2	17.96
22.09	380.7	3.76	10.03	14.8	2.74	1.500	14.4	18.90
23.26	379.6	3.75	10.03	14.9	2.72	1.500	14.5	19.89
24.42	380.9	3.75	10.03	15.4	2.71	1.500	14.2	20.88
29.07	380.9	3.76	10.03	15.0	2.71	1.500	14.5	24.93
34.88	381.4	3.77	10.03	15.7	2.70	1.500	14.5	29.82

Formulation VI ($\epsilon_t = 10\%$) Indomethacin (drug) / StaRX1500 [®] A (dis.)								
Compression parameters and tablet properties								
% dis. (v/v sol. frac.)	Tab.	W (mg)	H (mm)	D (mm)	pCF (kN)	pMDBP (mm)	CF (kN)	MDBP (mm)
0.00	1	381.40	3.88	10.00	1.80	4.00	10.50	3.20
	2	377.30	3.85	10.00	2.20	3.80	10.30	3.20
	3	379.50	3.85	10.00	2.40	3.80	11.10	3.20
	4	376.60	3.86	10.02	1.60	4.00	9.90	3.20
	5	377.70	3.86	10.00	1.60	4.00	10.30	3.20
	6	377.70	3.86	10.02	1.50	4.00	10.00	3.20
5.56	1	376.70	3.84	10.01	1.70	4.00	10.50	3.15
	2	381.80	3.87	10.02	1.80	4.00	10.30	3.15
	3	377.30	3.83	10.03	1.60	4.00	10.40	3.15
	4	379.30	3.85	10.00	1.60	4.00	10.50	3.15
	5	379.80	3.85	10.00	1.50	4.00	11.00	3.15
	6	377.40	3.85	10.00	1.60	4.00	10.60	3.15
11.11	1	377.30	3.81	10.01	1.50	4.00	11.70	3.05
	2	379.10	3.82	10.02	1.70	4.00	11.90	3.05
	3	380.50	3.85	10.03	1.50	4.00	12.40	3.05
	4	379.90	3.84	10.02	1.50	4.00	11.50	3.05
	5	379.10	3.82	10.01	1.60	4.00	12.10	3.05
	6	376.70	3.82	10.01	1.50	4.00	11.20	3.05
18.89	1	381.10	3.82	10.01	1.80	3.90	13.50	2.95
	2	382.20	3.83	10.02	1.80	3.90	13.60	2.95
	3	382.60	3.83	10.02	1.70	3.90	13.50	2.95
	4	380.70	3.82	10.01	1.70	3.90	13.20	2.95
	5	378.90	3.83	10.01	1.60	3.90	12.80	2.95
	6	383.40	3.85	10.02	1.70	3.90	13.50	2.95
20.00	1	383.10	3.84	10.01	1.80	3.90	13.50	2.95
	2	381.90	3.84	10.02	1.80	3.90	13.00	2.95
	3	381.10	3.82	10.01	1.70	3.90	13.40	2.95
	4	381.60	3.82	10.00	1.80	3.90	13.00	2.95
	5	380.70	3.82	10.01	1.70	3.90	13.10	2.95
	6	381.70	3.82	10.01	1.80	3.90	13.30	2.95
21.11	1	383.00	3.84	10.02	1.70	3.90	13.20	2.95
	2	381.40	3.84	10.00	1.60	3.90	12.70	2.95
	3	382.10	3.83	10.01	1.70	3.90	13.30	2.95
	4	381.40	3.83	10.02	1.80	3.90	13.10	2.95
	5	380.80	3.84	10.06	1.80	3.90	13.00	2.95
	6	382.00	3.84	10.02	1.80	3.90	12.90	2.95

Formulation VI (continued) ($\epsilon_t = 10\%$) Indomethacin (drug) / StaRX1500[®] A (dis.)
Compression parameters and tablet properties

% dis. (v/v sol. frac.)	Tab.	W (mg)	H (mm)	D (mm)	pCF (kN)	pMDBP (mm)	CF (kN)	MDBP (mm)
22.22	1	381.40	3.82	10.02	1.60	3.90	13.50	2.94
	2	379.30	3.80	10.01	1.70	3.90	13.60	2.94
	3	382.90	3.82	10.02	1.80	3.90	13.70	2.94
	4	381.20	3.82	10.02	1.70	3.90	13.50	2.94
	5	380.90	3.83	10.02	1.70	3.90	13.30	2.94
	6	381.20	3.83	10.04	1.60	3.90	13.20	2.94
27.78	1	381.70	3.82	10.03	1.60	3.90	14.30	2.92
	2	382.80	3.82	10.02	1.60	3.90	14.50	2.90
	3	381.60	3.81	10.02	1.60	3.90	14.30	2.90
	4	381.40	3.82	10.02	1.60	3.90	15.10	2.88
	5	382.50	3.84	10.02	1.60	3.90	14.50	2.88
	6	383.60	3.83	10.01	1.80	3.90	14.40	2.88
33.33	1	385.10	3.84	10.02	1.70	3.90	15.80	2.85
	2	384.70	3.85	10.00	1.40	3.90	15.00	2.85
	3	383.80	3.83	10.02	1.60	3.90	15.20	2.85
	4	382.40	3.83	10.02	1.60	3.90	15.30	2.85
	5	383.20	3.83	10.02	1.60	3.90	14.80	2.85
	6	383.50	3.84	10.02	1.70	3.90	14.90	2.85
44.44	1	383.00	3.77	10.01	1.50	3.90	22.00	2.45
	2	384.70	3.77	10.01	1.60	3.90	23.30	2.45
	3	385.20	3.77	10.00	1.50	3.90	23.10	2.45
	4	384.40	3.76	10.00	1.60	3.90	22.80	2.45
	5	384.40	3.76	10.00	1.50	3.90	22.70	2.45
	6	386.00	3.78	10.00	1.60	3.90	23.00	2.45
55.56	1	383.60	3.76	10.02	1.40	3.90	27.50	2.25
	2	384.40	3.78	10.02	1.40	3.90	27.30	2.25
	3	384.60	3.75	10.01	1.40	3.90	29.20	2.25
	4	386.30	3.77	10.00	1.50	3.90	29.10	2.20
	5	385.50	3.75	10.01	1.50	3.90	29.90	2.20
	6	-	-	-	-	-	-	-

Formulation VI (continued) ($\epsilon_t = 10\%$) Indomethacin (drug) / StaRX1500[®] A (dis.)
Averages values: compression parameters, tablet properties, calculated mixture density,
porosity and volumetric % of disintegrant in total tablet.

% dis. (v/v sol. frac.)	W (mg)	H (mm)	D (mm)	pCF (kN)	pMDBP (mm)	CF (kN)	MDBP (mm)	Calc. ρ (g/cm ³)	Porosity (% vol. tab.t)	% dis. (v/v tab.)
0.00	378.37	3.86	10.01	1.85	3.93	10.35	3.20	1.387	10.16	0.0
5.56	378.72	3.85	10.01	1.63	4.00	10.55	3.15	1.394	10.30	5.0
11.11	378.77	3.83	10.02	1.55	4.00	11.80	3.05	1.401	10.33	10.0
18.89	381.48	3.83	10.02	1.72	3.90	13.35	2.95	1.410	10.33	16.9
20.00	381.68	3.83	10.01	1.77	3.90	13.22	2.95	1.411	10.20	18.0
21.11	381.78	3.84	10.02	1.73	3.90	13.03	2.95	1.413	10.70	18.9
22.22	381.15	3.82	10.02	1.68	3.90	13.47	2.94	1.414	10.54	19.9
27.78	382.27	3.82	10.02	1.63	3.90	14.52	2.89	1.421	10.74	24.8
33.33	383.78	3.84	10.02	1.60	3.90	15.17	2.85	1.427	11.04	29.6
44.44	384.62	3.77	10.00	1.55	3.90	22.82	2.45	1.440	9.80	40.1
55.56	384.68	3.76	10.01	1.44	3.90	28.60	2.23	1.452	10.59	49.7

Formulation VII ($\epsilon_t = 10\%$) Caffeine powder A (drug) / AcDiSol® (dis.)											
Compression parameters and tablet properties.											
% dis. (v/v sol. frac.)	W (mg)	H (mm)	D (mm)	CF (kN)	MDBP (mm)	% dis. (v/v sol. frac.)	W (mg)	H (mm)	D (mm)	CF (kN)	MDBP (mm)
0.00	1	378.7	3.70	15.1	2.95	5.56	1	378.0	3.67	15.5	2.87
	2	381.4	3.71	15.6	2.95		2	381.4	3.69	15.5	2.87
	3	381.9	3.73	14.8	2.95		3	380.7	3.69	15.4	2.87
	4	383.1	3.73	15.5	2.95		4	378.6	3.69	14.5	2.87
	5	379.7	3.71	14.4	2.95		5	380.5	3.70	15.4	2.87
	6	383.4	3.76	15.5	2.95		6	377.6	3.68	14.6	2.87
	7	383.6	3.73	15.4	2.95		7	381.1	3.69	15.6	2.87
	8	382.7	3.72	15.2	2.95		8	380.3	3.68	15.1	2.87
	9	379.9	3.72	13.9	2.95		9	380.2	3.67	15.1	2.87
0.56	1	379.9	3.72	14.1	2.95	6.67	1	379.9	3.69	15.2	2.90
	2	382.2	3.73	14.4	2.95		2	381.6	3.71	14.2	2.90
	3	380.4	3.72	14.2	2.95		3	382.1	3.70	15.1	2.90
	4	379.0	3.71	13.8	2.95		4	381.2	3.71	15.0	2.90
	5	381.3	3.72	14.3	2.95		5	379.9	3.68	14.6	2.90
	6	378.8	3.71	14.2	2.95		6	381.1	3.68	14.3	2.90
	7	378.7	3.71	13.8	2.95		7	379.9	3.69	14.6	2.90
	8	380.2	3.71	14.3	2.95		8	380.8	3.69	14.8	2.90
	9	379.6	3.71	13.8	2.95		9	380.4	3.70	14.7	2.90
1.11	1	380.3	3.71	14.6	2.95	7.78	1	379.9	3.68	15.3	2.87
	2	383.5	3.74	14.7	2.95		2	379.9	3.69	14.4	2.87
	3	380.0	3.71	14.7	2.95		3	380.3	3.66	14.9	2.87
	4	379.8	3.71	14.6	2.95		4	378.9	3.68	14.4	2.87
	5	381.5	3.72	14.4	2.95		5	380.4	3.69	14.8	2.87
	6	382.3	3.72	15.0	2.95		6	380.0	3.69	14.6	2.87
	7	379.1	3.71	13.9	2.95		7	382.5	3.71	15.4	2.87
	8	380.0	3.71	14.7	2.95		8	381.0	3.69	14.8	2.87
	9	381.6	3.71	14.6	2.95		9	380.5	3.69	15.1	2.87
2.22	1	381.2	3.72	14.6	2.95	8.89	1	379.8	3.68	15.3	2.85
	2	380.3	3.71	14.1	2.95		2	379.9	3.67	15.1	2.85
	3	380.9	3.71	14.6	2.95		3	381.8	3.68	15.5	2.85
	4	381.5	3.71	14.4	2.95		4	381.9	3.69	15.7	2.85
	5	379.6	3.71	14.2	2.95		5	379.3	3.69	15.0	2.85
	6	382.3	3.71	14.6	2.95		6	378.7	3.68	14.8	2.85
	7	379.9	3.71	14.2	2.95		7	-	-	-	2.85
	8	379.2	3.71	14.1	2.95		8	379.2	3.68	14.9	2.85
	9	380.8	3.71	13.9	2.95		9	380.3	3.69	15.1	2.85
3.33	1	380.6	3.69	15.2	2.90	10.00	1	380.8	3.68	15.1	2.85
	2	382.2	3.70	15.2	2.90		2	382.6	3.69	15.5	2.85
	3	382.9	3.71	15.6	2.90		3	382.5	3.68	15.2	2.85
	4	382.2	3.70	15.2	2.90		4	384.3	3.70	15.5	2.85
	5	383.4	3.71	15.7	2.90		5	381.1	3.69	14.7	2.85
	6	381.5	3.69	14.9	2.90		6	381.1	3.68	15.4	2.85
	7	381.6	3.71	15.5	2.90		7	379.7	3.66	15.0	2.85
	8	380.6	3.69	15.0	2.90		8	381.1	3.68	14.8	2.85
	9	382.1	3.70	15.3	2.90		9	379.9	3.68	14.9	2.85
4.44	1	381.1	3.70	14.8	2.90	11.11	1	380.3	3.67	14.8	2.85
	2	382.7	3.71	14.9	2.90		2	382.0	3.70	14.7	2.85
	3	382.1	3.70	15.2	2.90		3	381.8	3.68	15.2	2.85
	4	382.2	3.72	14.5	2.90		4	381.5	3.70	15.0	2.85
	5	382.2	3.71	15.3	2.90		5	381.3	3.68	15.5	2.85
	6	380.2	3.69	14.6	2.90		6	382.3	3.70	15.0	2.85
	7	381.0	3.70	14.7	2.90		7	382.5	3.68	15.4	2.85
	8	382.3	3.71	14.9	2.90		8	381.2	3.68	14.9	2.85
	9	381.0	3.71	14.7	2.90		9	381.7	3.68	14.7	2.85

Formulation VII ($\epsilon_t = 10\%$) Caffeine powder A (drug) / AcDiSol® (dis.)
 Averages values: compression parameters, tablet properties, calculated mixture density, porosity and volumetric % of disintegrant in total tablet.

% dis. (v/v sol. frac.)	W (mg)	H (mm)	CF (kN)	MDBP (mm)	Calc. ρ (g/cm ³)	Porosity (% vol. tab.t)	% dis. (v/v tab.)
0.00	381.6	3.72	15.0	3.0	1.450	10.00	0.00
0.56	380.0	3.72	14.1	3.0	1.451	10.25	0.50
1.11	380.9	3.72	14.6	3.0	1.452	10.10	1.00
2.22	380.6	3.71	14.3	3.0	1.454	10.18	1.99
3.33	381.9	3.70	15.3	2.9	1.456	9.72	3.01
4.44	381.6	3.71	14.8	2.9	1.458	10.04	3.99
5.56	379.8	3.68	15.2	2.9	1.460	10.07	5.00
6.67	380.8	3.69	14.7	2.9	1.461	10.21	5.99
7.78	380.4	3.69	14.9	2.9	1.463	10.23	6.98
8.89	380.1	3.68	15.2	2.9	1.465	10.31	7.97
10.00	381.5	3.68	15.1	2.9	1.467	10.10	8.99
11.11	381.6	3.69	15.0	2.9	1.469	10.26	9.97

Formulation VIII ($\epsilon_t = 10\%$) Caffeine powder A (drug) / L-HPC (dis.)											
Compression parameters and tablet properties.											
% dis. (v/v sol. frac.)	Tab.	W (mg)	H (mm)	CF (kN)	MDBP (mm)	% dis. (v/v sol. frac.)	Tab.	W (mg)	H (mm)	CF (kN)	MDBP (mm)
0.00	1	382.5	3.73	13.9	2.95	4.44	1	381.6	3.72	15.5	2.80
	2	382.2	3.75	14.1	2.95		2	381.3	3.72	-	2.80
	3	381.1	3.73	15.3	2.90		3	382.4	3.72	15.8	2.80
	4	381.1	3.73	14.7	2.90		4	381.7	3.73	15.4	2.80
	5	381.3	3.73	14.8	2.90		5	382.0	3.73	16.0	2.80
	6	381.2	3.73	14.9	2.90		6	380.8	3.71	15.9	2.80
	7	383.4	3.75	15.2	2.90		7	381.7	3.71	15.7	2.80
	8	382.1	3.73	15.4	2.90		8	381.8	3.72	15.7	2.80
	9	383.3	3.74	15.2	2.90		9	380.2	3.72	15.4	2.80
0.56	1	382.1	3.75	15.1	2.88	5.56	1	380.0	3.71	15.6	2.80
	2	382.4	3.75	15.6	2.88		2	381.6	3.71	15.5	2.80
	3	384.1	3.75	15.5	2.88		3	381.2	3.72	16.0	2.80
	4	382.3	3.73	15.6	2.88		4	382.0	3.73	16.0	2.80
	5	381.6	3.74	15.0	2.88		5	381.8	3.72	15.8	2.80
	6	380.4	3.73	15.3	2.88		6	381.8	3.72	15.8	2.80
	7	382.6	3.74	15.3	2.88		7	381.1	3.71	15.5	2.80
	8	378.9	3.70	14.8	2.88		8	380.5	3.71	15.5	2.80
	9	383.0	3.74	15.5	2.88		9	381.5	3.72	15.9	2.80
1.11	1	381.8	3.74	16.4	2.80	8.89	1	381.3	3.72	15.3	2.80
	2	381.9	3.75	17.0	2.80		2	380.8	3.72	14.8	2.80
	3	381.2	3.73	16.4	2.80		3	380.5	3.71	15.5	2.80
	4	381.2	3.71	16.6	2.80		4	379.2	3.69	15.2	2.80
	5	380.3	3.72	16.4	2.80		5	382.0	3.71	15.4	2.80
	6	382.4	3.75	16.8	2.80		6	379.0	3.69	15.3	2.80
	7	376.5	3.7	16.1	2.80		7	382.6	3.73	15.7	2.80
	8	381.0	3.73	16.8	2.80		8	380.5	3.72	15.0	2.80
	9	381.1	3.71	16.3	2.80		9	379.0	3.69	14.9	2.80
2.22	1	380.4	3.74	16.4	2.80	11.11	1	380.5	3.73	15.2	2.80
	2	381.1	3.74	15.8	2.80		2	381.3	3.71	15.0	2.90
	3	382.0	3.72	17.0	2.78		3	381.7	3.72	15.0	2.90
	4	383.2	3.72	17.2	2.78		4	380.3	3.72	15.3	2.90
	5	381.6	3.72	16.9	2.78		5	379.7	3.72	14.9	2.90
	6	380.1	3.73	16.2	2.78		6	380.3	3.71	15.2	2.90
	7	381.6	3.71	16.7	2.78		7	384.0	3.73	15.1	2.90
	8	382.0	3.72	16.9	2.78		8	383.0	3.74	15.3	2.90
	9	382.4	3.73	16.7	2.78		9	381.1	3.71	15.2	2.90
3.33	1	379.6	3.70	16.5	2.78		1	380.5	3.73	15.2	2.80
	2	380.4	3.71	16.1	2.78		2	381.3	3.71	15.0	2.90
	3	381.3	3.72	16.3	2.78		3	381.7	3.72	15.0	2.90
	4	380.5	3.72	15.6	2.80		4	380.3	3.72	15.3	2.90
	5	381.4	3.72	15.8	2.80		5	379.7	3.72	14.9	2.90
	6	380.3	3.72	15.3	2.80		6	380.3	3.71	15.2	2.90
	7	379.9	3.69	15.5	2.80		7	384.0	3.73	15.1	2.90
	8	381.8	3.71	15.4	2.80		8	383.0	3.74	15.3	2.90
	9	380.1	3.71	15.3	2.80		9	381.1	3.71	15.2	2.90

Formulation VIII ($\epsilon_t = 14\%$) Caffeine powder A (drug) / L-HPC (dis.)
 Averages values: compression parameters, tablet properties, calculated mixture density,
 porosity and volumetric % of disintegrant in total tablet.

% dis. (v/v sol. frac.)	W (mg)	H (mm)	CF (kN)	MDBP (mm)	Calc. ρ (g/cm ³)	Porosity (% vol. tab.t)	% dis. (v/v tab.)
0.00	382.0	3.74	14.8	2.91	1.500	13.19	0.00
0.56	381.9	3.74	15.3	2.88	1.500	13.24	0.49
1.11	380.8	3.73	16.5	2.80	1.499	13.20	0.96
2.22	381.6	3.73	16.6	2.78	1.499	13.00	1.93
3.33	380.6	3.71	15.8	2.79	1.498	12.83	2.90
4.44	381.5	3.72	15.7	2.80	1.498	12.83	3.87
5.56	381.3	3.72	15.7	2.80	1.497	12.75	4.85
8.89	380.5	3.71	15.2	2.80	1.496	12.67	7.76
11.11	381.3	3.72	15.1	2.89	1.495	12.73	9.70

Formulation IX ($\epsilon_t = 10\%$) Indomethacin (drug) / AcDiSol[®] (dis.)
Tablet properties.

% dis. (v/v sol. frac.)	Tab.	W (mg)	H (mm)	% dis. (v/v sol. frac.)	Tab.	W (mg)	H (mm)
0.00	Not compactible at the desired porosity (laminating tablets)			2.70	1	2.53	301.6
					2	2.59	302.0
					3	2.59	301.5
1.00	1	2.43	300.0	3.00	1	2.59	301.9
	2	2.57	302.0		2	2.58	300.8
	3	2.59	300.0		3	2.59	302.5
1.50	1	2.57	301.0	5.00	1	2.57	301.0
	2	2.57	301.0		2	2.57	301.7
	3	2.59	301.0		3	2.57	301.2
2.00	1	2.55	299.7	10.00	1	2.59	301.9
	2	2.57	301.6		2	2.57	302.5
	3	2.56	301.4		3	2.54	302.3

Formulation IX ($\epsilon_t = 10\%$) Indomethacin (drug) / AcDiSol[®] (dis.)

Averages values: tablet properties, calculated mixture density, porosity and volumetric % of disintegrant in total tablet. (Round flat of diameter is 11mm)

% dis. (v/v sol. frac.)	W (mg)	H (mm)	Calc. ρ (g/cm ³)	Porosity (% vol. tab.t)	% dis. (v/v tab.)
0.00			pure indo. tablets not compactible		
1.00	2.53	300.7	1.390	10.03	0.90
1.50	2.58	301.0	1.391	11.63	1.33
2.00	2.56	300.9	1.392	11.15	1.78
2.70	2.57	301.7	1.394	11.39	2.39
3.00	2.59	301.7	1.395	12.01	2.64
5.00	2.57	301.3	1.400	11.88	4.41
10.00	2.57	302.2	1.412	12.25	8.78

Caffeine powder A pure ($\epsilon_t=30\%$) (tablets for CA solubility constant calibration)
Average values of tablet properties and porosity.

Comp. parameters	Tablet 1	Tablet 2	Tablet 3	Tablet 4	Tablet 5	Tablet 6	Average	Stdev
Thickness (mm)	4.60	4.58	4.63	4.63	4.62	4.64	4.62	0.02
Diameter (mm)	10.03	10.02	10.01	10.01	10.03	10.03	10.02	0.01
Weight (mg)	379.6	379.4	379.3	380.6	378.3	379.4	379.4	0.7
Up. Punch pos.	4.20	4.21	4.22	4.22	4.22	4.22	4.22	0.01
Comp. Force (kN)	2.1	2.4	2.0	2.1	2.1	2.1	2.1	0.1
Density (g/cm ³)					1.450			
Porosity	27.97	27.55	28.21	27.96	28.53	28.63	28.14	0.40

Aspirin pure ($\epsilon_t=30\%$) (tablets for CA solubility constant calibration)
Average values of tablet properties and porosity.

Comp. parameters	Tablet 1	Tablet 2	Tablet 3	Tablet 4	Tablet 5	Tablet 6	Average	Stdev
Thickness (mm)	5.06	5.04	5.03	5.02	5.04	5.00	5.03	0.02
Diameter (mm)	10.02	10.02	10.02	10.02	10.02	10.02	10.02	0.00
Weight (mg)	379.7	379.8	381.5	383.0	382.7	381.6	381.4	1.4
Up. Punch pos.	4.6	4.6	4.6	4.6	4.6	4.6	4.6	0.0
Comp. Force (kN)	0.5	0.6	0.7	0.5	0.7	0.6	0.6	0.1
Density (g/cm ³)					1.376			
Porosity	30.82	30.53	30.08	29.66	30.00	29.64	30.12	0.47

A lactose monohydrate pure ($\epsilon_t=30\%$) (tablets for CA solubility constant calibration)
Average values of tablet properties and porosity.

Comp. parameters	Tablet 1	Tablet 2	Tablet 3	Tablet 4	Average	Stdev
Thickness (mm)	4.42	4.43	4.43	4.45	4.43	0.01
Diameter (mm)	10.03	10.03	10.03	10.03	10.03	0.00
Weight (mg)	381.5	380.1	380.2	383.9	381.4	1.8
Up. Punch pos.	4.0	4.0	4.0	4.0	4.00	0.00
Comp. Force (kN)	1.5	1.6	1.6	1.6	1.6	0.1
Density (g/cm ³)					1.540	
Porosity	29.05	29.47	29.45	29.09	29.27	0.23

Formulation X ($\epsilon_t=9\%$) Caffeine powder A (drug) / StaRX1500[®] (dis.) / Lactose monohydrate (filler)
Average values of tablet properties, calculated density of the mixture and porosity.

Comp. parameters	Tablet 1	Tablet 2	Tablet 3	Tablet 4	Tablet 5	Tablet 6	Average	Stdev
Thickness (mm)	3.52	3.51	3.52	3.52	3.53	3.51	3.52	0.01
Diameter (mm)	10.04	10.03	10.03	10.03	10.04	10.04	10.04	0.01
Weight (mg)	382.2	378.9	381.0	380.3	382	379.7	380.7	1.3
Up. Punch pos.	1.8	1.8	1.8	1.8	1.8	1.8	1.8	0.0
Comp. Force (kN)	37.5	36.2	37.3	36.5	37.2	37.1	37.0	0.5
Density (g/cm ³)					1.508			
Porosity	9.07	9.42	9.18	9.35	9.38	9.41	9.30	0.14

Formulation XI ($\epsilon_t=9\%$) Caffeine powder A (drug) / StaRX1500[®] (dis.) / Lactose monohydrate (filler)
Average values of tablet properties, calculated density of the mixture and porosity.

Comp. parameters	Tablet 1	Tablet 2	Tablet 3	Tablet 4	Tablet 5	Tablet 6	Average	Stdev
Thickness (mm)	3.54	3.54	3.55	3.55	3.54	3.54	3.54	0.01
Diameter (mm)	10.03	10.02	10.04	10.04	10.04	10.04	10.04	0.01
Weight (mg)	381.4	381.7	381.7	379.7	380.6	379.5	380.8	1.0
Up. Punch pos.	1.8	1.8	1.8	1.8	1.8	1.8	1.8	0.0
Comp. Force (kN)	37.8	36.9	37.3	36.8	36.1	36.3	36.9	0.6
Density (g/cm ³)					1.502			
Porosity	9.23	8.98	9.59	10.07	9.60	9.86	9.56	0.40

Formulation XII ($\epsilon_t=9\%$) Caffeine powder A (drug) / StaRX1500[®] (dis.) / Lactose monohydrate (filler)
Average values of tablet properties, calculated density of the mixture and porosity.

Comp. parameters	Tablet 1	Tablet 2	Tablet 3	Tablet 4	Tablet 5	Tablet 6	Average	Stdev
Thickness (mm)	3.55	3.57	3.56	3.57	3.53	3.56	3.56	0.02
Diameter (mm)	10.04	10.03	10.04	10.03	10.01	10.04	10.03	0.01
Weight (mg)	380.0	380.8	380.7	381.3	378.6	380.9	380.4	1.0
Up. Punch pos.	1.8	1.8	1.8	1.8	1.78	1.78	1.79	0.01
Comp. Force (kN)	35.9	37.6	36.6	37.1	37.5	37.7	37.1	0.7
Density (g/cm ³)					1.507			
Porosity	10.28	10.42	10.37	10.30	9.57	10.32	10.21	0.32

Formulation XIII ($\epsilon_t=14\%$) Aspirin (drug) / Lactose monohydrate (filler)
Average values of tablet properties, calculated density of the mixture and porosity.

Comp. parameters	Tablet 1	Tablet 2	Tablet 3	Tablet 4	Tablet 5	Tablet 6	Average	Stdev
Thickness (mm)	3.95	3.95	3.97	3.96	3.96	3.95	3.96	0.01
Diameter (mm)	10.02	10.02	10.02	10.02	10.02	10.02	10.02	0.00
Weight (mg)	379.0	379.2	382.8	381.1	381.6	380.9	380.8	1.5
Up. Punch pos.	3.48	3.48	3.48	3.48	3.48	3.48	3.48	0.00
Comp. Force (kN)	3.2	3.2	3.5	3.2	3.3	3.4	3.3	0.1
Density (g/cm ³)					1.426			
Porosity	14.69	14.65	14.27	14.44	14.32	14.27	14.44	0.19

Appendix D Disintegration tests and water uptake measurement of tablets

Formulation I ($\epsilon_t = 10\%$) Paracetamol DC90 (drug) / StaRX1500[®] A (dis.)
Disintegration time of the tablets

% dis. (v/v, sol. frac.)	DT (sec.)						Av. DT (sec.)	Stdev. DT	Av. T (°C)
	Tab. 1	Tab. 2	Tab. 3	Tab. 4	Tab. 5	Tab. 6			
0	77	78	80	72	73	77	76.17	3.06	36.9
5	127	130	147	126	141	143	135.67	9.07	36.9
7	148	156	164	140	170	170	158.00	12.26	36.9
8	154	159	180	124	129	143	148.17	20.70	36.9
9	162	171	171	152	165	175	166.00	8.29	36.9
10	196	250	256	174	244	250	228.33	34.49	36.9
15	226	246	279	230	278	282	256.83	25.93	36.9
20	230	232	253	241	271	310	256.17	30.42	37.1
40	333	336	369	331	332	334	339.17	14.72	37.0
50	282	282	315	273	310	339	300.17	25.39	36.9

Formulation I ($\epsilon_t = 8\%$) Paracetamol DC90 (drug) / StaRX1500[®] A (dis.)
Disintegration time of the tablets

% dis. (v/v, sol. frac.)	DT (sec.)						Av. DT (sec.)	Stdev. DT	Av. T (°C)
	Tab. 1	Tab. 2	Tab. 3	Tab. 4	Tab. 5	Tab. 6			
0	122	123	148	124	132	144	132.17	11.36	37.0
5	138	139	140	120	127	132	132.67	7.94	37.0
7	154	160	174	154	168	208	169.67	20.37	37.0
8	174	190	198	170	176	176	180.67	10.86	37.0
9	176	206	258	163	208	226	206.17	34.23	37.0
10	164	164	166	146	154	164	159.67	9.16	37.0
11	248	375	437	225	255	285	304.17	83.51	37.0
15	339	407	433	337	355	377	374.67	38.81	37.0
20	314	316	322	326	345	395	336.33	30.79	37.0

Formulation II ($\epsilon_t = 10\%$) Paracetamol DC90Fine (drug) / StaRX1500[®] A (dis.)
Disintegration time of the tablets

% dis. (v/v, sol. frac.)	DT (sec.)						Av. DT (sec.)	Stdev. DT	Av. T (°C)
	Tab. 1	Tab. 2	Tab. 3	Tab. 4	Tab. 5	Tab. 6			
0	21	21	22	20	21	22	21.17	0.75	37
1	22	22	24	22	23	24	24.00	0.98	37
2	23	23	23	22	23	23	22.83	0.41	37
3	22	23	23	22	23	23	22.67	0.52	37
4	20	22	23	23	23	24	22.50	1.38	37
5	22	22	22	20	22	23	21.83	0.98	37
6	21	22	24	23	23	25	23.00	1.41	37
7	23	25	26	24	24	25	24.50	1.05	37
8	24	25	28	25	26	26	25.67	1.37	37
9	25	27	27	26	27	28	26.67	1.03	37
10	27	29	31	-	-	-	29.00	2.00	37
15	32	33	36	32	33	34	33.33	1.51	37
20	34	38	39	38	40	41	38.33	2.42	37
30	65	65	71	66	67	68	67.00	2.28	37
40	148	154	158	156	157	165	156.33	5.54	37
50	194	196	200	180	188	196	192.33	7.20	37

Formulation II ($\epsilon_t = 14\%$) Paracetamol DC90Fine (drug) / StaRX1500[®] A (dis.)
Disintegration time of the tablets

% dis. (v/v, sol. frac.)	DT (sec.)						Av. DT (sec.)	Stdev. DT	Av. T (°C)
	Tab. 1	Tab. 2	Tab. 3	Tab. 4	Tab. 5	Tab. 6			
0	26	25	27	26	26	27	26.17	0.75	37
2	24	24	24	25	26	28	25.17	1.60	37
3	26	26	26	26	26	26	26.00	0.00	37
4	24	25	26	25	25	30	25.83	2.14	37
5	26	27	27	24	25	28	26.17	1.47	37
6	26	27	28	27	28	29	27.50	1.05	37
8	30	30	30	27	28	26	28.50	1.76	37
15	33	33	35	34	35	36	34.33	1.21	37
20	40	42	42	42	44	46	42.67	2.07	37

Formulation III ($\epsilon_t = 14\%$) Caffeine powder A (drug) / StaRX1500[®] A (dis.)
Disintegration time of the tablets

% dis. (v/v, sol. frac.)	DT (sec.)						Av. DT (sec.)	Stdev. DT	Av. T (°C)
	Tab. 1	Tab. 2	Tab. 3	Tab. 4	Tab. 5	Tab. 6			
0.00	588	537	541	574	568	553	560.17	19.91	37
5.81	60	62	64	54	56	66	60.33	4.63	37
11.63	30	31	32	30	32	32	31.17	0.98	37
19.77	24	24	25	24	25	25	24.50	0.55	37
20.93	24	24	26	23	23	24	24.00	1.10	37
22.09	24	24	24	22	22	24	23.33	1.03	37
23.26	22	22	23	22	23	23	22.50	0.55	37
24.42	25	25	25	26	26	26	25.50	2.19	37
29.07	26	26	26	28	28	29	27.17	0.55	37
34.88	36	36	36	32	32	32	34.00	1.33	37

Formulation VI ($\epsilon_t = 10\%$) Indomethacin DC90Fine (drug) / StaRX1500® A (dis.)
Disintegration time of the tablets

% dis. (v/v, sol. frac.)	DT (sec.)						Av. DT (sec.)	Stdev. DT	Av. T (°C)
	Tab. 1	Tab. 2	Tab. 3	Tab. 4	Tab. 5	Tab. 6			
0.00	>1320	>1320	>1320	>1320	>1320	>1320	>1320.00	0.00	37
5.56	188	237	238	142	172	201	196.33	37.48	37
11.11	73	107	123	106	110	122	106.83	18.15	37
18.89	65	74	77	54	69	76	69.17	8.70	37
20.00	64	65	68	55	61	67	63.33	4.76	37
21.11	52	59	67	62	64	66	61.67	5.54	37
22.22	63	65	66	54	55	62	60.83	5.12	37
27.78	46	49	51	57	58	65	54.33	6.98	37
33.33	50	51	54	-	54	55	52.80	2.17	37
44.44	62	68	68	58	60	60	62.67	4.32	37
55.56	61	71	75	73	87	85	75.33	9.58	37

Formulation VII ($\epsilon_t = 10\%$) Caffeine powder A (drug) / AcDiSol® A (dis.)
Disintegration time of the tablets

% dis. (v/v, sol. frac.)	DT (sec.)						Av. DT (sec.)	Stdev. DT	Av. T (°C)
	Tab. 1	Tab. 2	Tab. 3	Tab. 4	Tab. 5	Tab. 6			
0.00	857	1062	1112	785	851	1014	946.83	133.04	37
0.56	22	34	28	38	38	39	33.17	6.82	37
1.11	16	17	18	15	16	17	16.50	1.05	37
2.22	15	15	16	15	15	16	15.33	0.52	37
3.33	18	18	20	16	18	20	18.33	1.51	37
4.44	20	22	22	24	24	24	22.67	1.63	37
5.56	28	28	29	22	28	30	27.50	2.81	37
6.67	36	40	44	33	37	42	38.67	4.08	37
7.78	44	44	48	49	50	58	48.83	5.15	37
8.89	44	51	54	50	58	59	52.67	5.57	37
10.00	67	70	70	64	67	68	67.67	2.25	37
11.11	92	93	94	86	90	94	91.50	3.08	37

Formulation VIII ($\epsilon_t = 10\%$) Caffeine powder A (drug) / L-HPC (dis.)
Disintegration time of the tablets

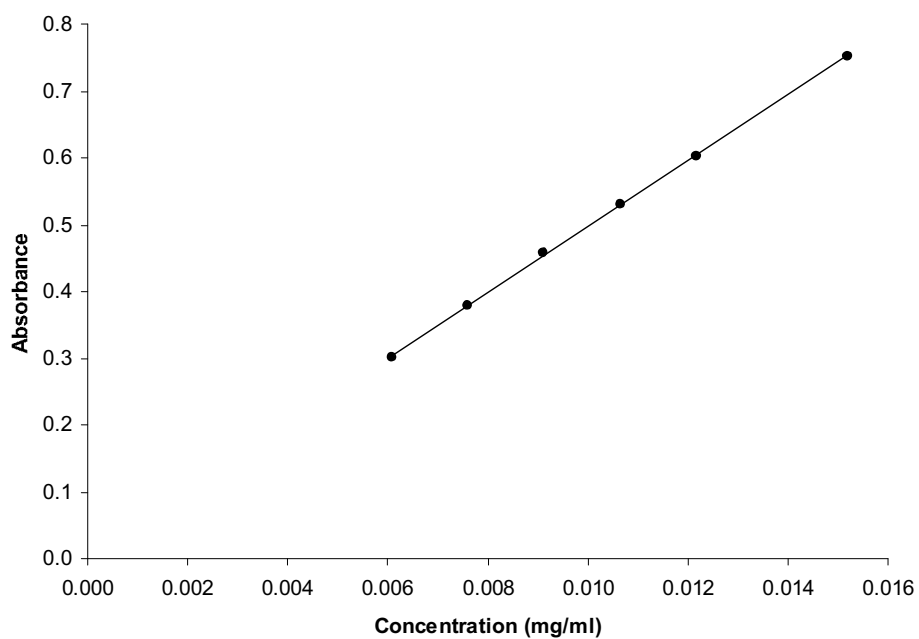
% dis. (v/v, sol. frac.)	DT (sec.)						Av. DT (sec.)	Stdev. DT	Av. T (°C)
	Tab. 1	Tab. 2	Tab. 3	Tab. 4	Tab. 5	Tab. 6			
0.00	516	573	624	687	760	873	672.17	130.24	37
0.56	252	419	489	597	-	-	439.25	144.72	37
1.11	79	100	110	73	76	95	88.83	14.99	37
2.22	34	36	42	39	39	49	39.83	5.27	37
3.33	22	22	26	27	27	27	25.17	2.48	37
4.44	15	16	16	18	18	16	16.50	1.22	37
5.56	14	15	19	14	16	18	16.00	2.10	37
8.89	18	18	19	18	18	-	18.20	0.45	37
11.11	20	21	21	22	23	25	22.00	1.79	37

Formulation IX ($\epsilon_t = 10\%$) Indomethacin (drug) / AcDiSol[®] (dis.)
Water uptake (WU) constants

% dis. (v/v, sol. frac.)	WU (g ² /sec)			Av. WU (sec.)	Stdev.WU
	Tab. 1	Tab. 2	Tab. 3		
0.00	-	-	-	-	-
1.00	0.002814	0.003558	0.003464	0.003279	0.000405
1.50	0.004159	0.003184	0.003751	0.003698	0.000490
2.00	0.004460	0.003832	0.003794	0.004029	0.000374
2.70	0.004970	0.004947	0.004438	0.004785	0.000301
3.00	0.006359	0.005949	0.006211	0.006173	0.000208
5.00	0.005973	0.005874	0.005308	0.005718	0.000359
10.00	0.006767	0.006821	0.007096	0.006895	0.000176

Appendix E Calibration curves

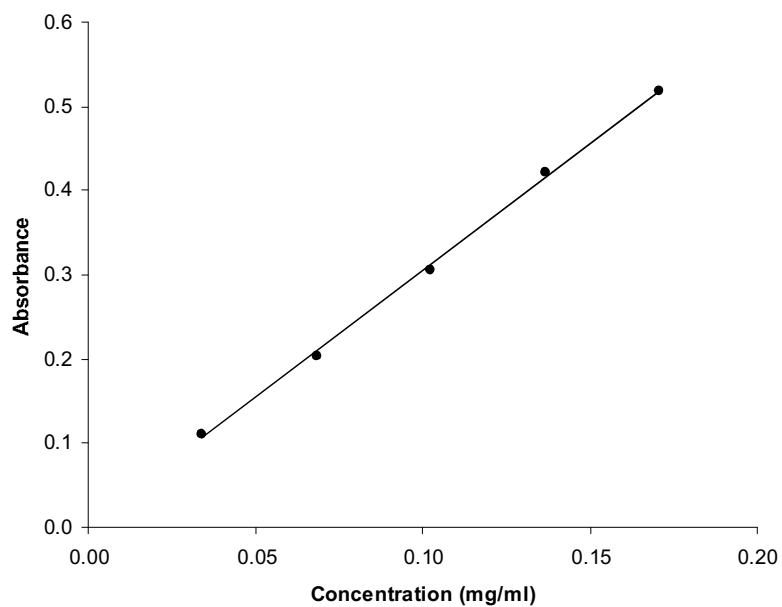
UV absorbance data of caffeine powder A in pH 6.8 water 272 nm					
Solution	Solution 1 %(v/v).	Dilution		Concentration (mg/ml)	Absorbance
		Solution 1 (ml)	Distilled water (ml)		
1	100	-	-	0.0152	0.751
2	80	40	50	0.01216	0.603
3	70	35	50	0.01064	0.531
4	60	30	50	0.00912	0.457
5	50	25	50	0.0076	0.378
6	40	20	50	0.00608	0.301



Calibration curve of caffeine powder A in pH 6.8 water at 272 nm
($y = 49.258x + 0.0044$, $R^2 = 0.9998$)

UV absorbance data of Aspirin in pH 6.8 phosphate buffer at 265 nm

Solution	solution 1 %(v/v)	Dilution		Concentration (mg/ml)	Absorbance
		Solution 1	Distilled water		
1	100	0	10	0.171	0.518
2	80	8	10	0.137	0.421
3	60	6	10	0.103	0.306
4	40	4	10	0.068	0.204
5	20	2	10	0.034	0.111



Calibration curve of Aspirin powder A in pH 6.8 phosphate buffer at 265 nm
($y = 3.0166x + 0.0027$, $R^2 = 0.9989$)

Appendix F Experimental drug release data

Drug release data of pure caffeine tablets ($\epsilon_t=30\%$)								
Time (min)	% drug release						Average values	Stdev
	Tab. 1	Tab. 2	Tab. 3	Tab. 4	Tab. 5	Tab. 6		
0	0.00	0.00	0.00	0.00	0.00	0.00	0.00	0.00
1	28.02	16.94	21.36	56.35	26.91	19.34	28.15	14.47
2	57.42	63.02	39.91	64.18	78.67	42.16	57.56	14.62
4	66.09	88.89	53.90	72.61	92.83	86.67	76.83	15.21
6	71.07	93.01	79.24	79.85	95.97	94.74	85.65	10.30
8	78.04	94.89	97.41	84.01	100.82	97.71	92.15	9.02
12	87.72	97.58	103.63	92.96	102.71	99.46	97.34	6.08
16	91.49	96.79	104.19	97.40	102.72	100.40	98.83	4.62
20	95.38	96.25	102.59	100.48	101.92	99.47	99.35	2.96
24	97.00	95.17	101.51	102.23	101.64	100.81	99.73	2.91
28	97.14	94.64	102.31	101.43	100.97	99.07	99.26	2.93
32	96.19	94.63	102.32	102.50	100.84	99.47	99.32	3.26
36	94.19	89.28	102.05	101.57	101.10	100.27	98.08	5.18
T (C°)	37.0	37.2	37.0	37.3	37.0	37.1	37.1	0.13

Drug release data of pure Aspirin tablets ($\epsilon_t=30\%$)								
Time (min)	% drug release						Average values	Stdev
	Tab. 1	Tab. 2	Tab. 3	Tab. 4	Tab. 5	Tab. 6		
30	14.73	15.62	17.34	14.86	12.83	15.93	15.22	1.50
90	40.80	40.79	39.74	46.30	32.18	36.52	39.39	4.73
150	62.48	65.67	63.33	68.62	51.47	59.45	61.84	5.94
210	77.97	82.21	79.91	80.92	65.16	73.98	76.69	6.34
270	88.38	90.84	86.97	90.45	75.98	85.10	86.29	5.49
330	94.39	94.39	92.78	95.13	87.04	92.87	92.77	2.95
390	95.22	96.09	94.63	96.45	92.37	95.11	94.98	1.44
450	95.74	95.46	94.90	95.95	94.84	96.54	95.57	0.65
510	93.56	93.02	92.99	94.16	94.10	94.00	93.64	0.54
570	93.03	92.74	92.33	92.87	92.69	94.87	93.09	0.90
630	91.99	91.33	91.30	92.73	91.66	93.73	92.12	0.95
T (C°)	37.2	37.2	37.2	37.2	37.2	37.2	37.2	0.0

Visual estimation of the time for 100 % release of pure lactose monohydrate tablets ($\epsilon_t=30\%$)

	% drug release				Average values	Stdev
	Tab. 1	Tab. 2	Tab. 3	Tab. 4		
Time(min) for 100 % release	39.45	32.28	32.25	32.26	34.06	3.59
T (C°)	37.2	37.2	37.2	37.2	37.2	0.0

Drug release data of **formulation X** tablets ($\xi_i=9\%$)
Caffeine powder A (drug) / StaRX1500[®] (dis.) / Lactose monohydrate (filler)

Time (min)	% drug release						Average values	Stdev
	Tab. 1	Tab. 2	Tab. 3	Tab. 4	Tab. 5	Tab. 6		
0	0.00	0.00	0.00	0.00	0.00	0.00	0.00	0.00
0.5	13.54	7.49	9.33	2.50	8.13	4.16	7.53	3.91
1	65.05	21.74	42.37	35.58	55.66	40.84	43.54	15.21
2	88.05	58.07	76.22	78.93	81.01	69.61	75.31	10.38
3	94.96	82.39	88.30	89.88	92.07	91.68	89.88	4.30
4	96.86	91.63	93.25	93.42	94.89	98.77	94.81	2.62
5	98.99	95.19	95.84	100.03	94.89	97.35	97.05	2.11
7	98.53	96.05	98.82	99.02	96.21	96.33	97.49	1.43
9	98.524	97.47	98.36	98.78	98.33	95.14	97.77	1.36
11	99.4639	99.37	98.13	100.67	97.40	95.85	98.48	1.72
13	98.5277	98.43	97.89	99.50	97.16	97.27	98.13	0.88
15	100.404	99.14	99.07	98.78	97.39	96.56	98.56	1.37
17	100.411	101.28	100.25	97.60	98.34	96.32	99.03	1.91
T (C°)	37.3	37.3	37.3	37.2	37.2	37.1	37.2	0.1

Drug release data of **formulation XI** tablets ($\xi_i=9\%$)
Caffeine powder A (drug) / StaRX1500[®] (dis.) / Lactose monohydrate (filler)

Time (min)	% drug release						Average values	Stdev
	Tab. 1	Tab. 2	Tab. 3	Tab. 4	Tab. 5	Tab. 6		
0	0.00	0.00	0.00	0.00	0.00	0.00	0.00	0.00
0.5	0.30	5.31	9.39	5.33	6.25	9.07	5.94	3.30
1	27.41	31.48	34.66	31.46	34.93	36.91	32.81	3.39
1.5	47.19	46.80	42.55	52.27	53.28	51.20	48.88	4.09
2	61.38	61.52	55.75	65.59	67.86	61.33	62.24	4.17
3	69.98	69.18	76.58	75.34	82.62	77.61	75.22	5.02
4	81.34	85.54	91.69	89.93	96.26	94.28	89.84	5.57
5	92.52	95.62	97.13	98.01	100.96	98.64	97.15	2.87
6	96.65	97.70	100.12	100.65	101.17	99.96	99.38	1.79
7	98.53	96.60	99.95	100.47	100.24	102.39	99.70	1.96
9	97.05	96.22	102.17	101.78	101.17	100.91	99.88	2.57
11	97.04	97.15	101.07	101.60	101.91	100.71	99.91	2.22
13	96.86	96.23	99.77	101.04	98.57	104.45	99.48	3.02
16	95.19	96.59	99.57	99.73	99.67	102.59	98.89	2.63
19	95.36	96.22	100.50	98.61	98.74	97.36	97.80	1.87
T (C°)	37.2	37.3	37.3	37.0	37.2	37.2	37.2	0.1

Drug release data of **formulation XII** tablets ($\xi_t=9\%$)
Caffeine powder A (drug) / StaRX1500[®] (dis.) / Lactose monohydrate (filler)

Time (min)	% drug release						Average values	Stdev
	Tab. 1	Tab. 2	Tab. 3	Tab. 4	Tab. 5	Tab. 6		
0	0.00	0.00	0.00	0.00	0.00	0.00	0.00	0.00
0.5	5.91	8.51	16.16	7.94	20.00	8.50	11.17	5.57
1	54.53	56.67	70.52	79.32	69.42	64.48	65.82	9.28
1.5	86.32	86.71	96.67	96.74	86.88	91.00	90.72	4.94
2	95.04	98.76	100.88	99.42	97.65	100.25	98.67	2.10
3	96.57	99.74	101.27	99.99	101.63	102.33	100.26	2.06
4	97.14	99.56	101.46	99.80	100.89	101.41	100.04	1.63
5	96.58	97.51	102.95	98.31	101.27	100.47	99.52	2.44
6	95.83	98.99	100.72	99.24	100.71	100.47	99.33	1.87
7	94.33	99.18	100.15	98.68	100.70	100.10	98.86	2.33
9	93.39	100.30	100.33	97.38	100.33	100.65	98.73	2.89
11	94.14	97.70	100.52	98.30	98.64	98.05	97.89	2.09
13	93.95	97.13	101.64	98.49	99.01	99.34	98.26	2.57
T (C°)	37.2	37.3	37.3	37.3	37.3	37.0	37.2	0.1

Drug release data of **formulation XIII** tablets ($\xi_t=12\%$)
Caffeine powder A (drug) / StaRX1500[®] (dis.) / Lactose monohydrate (filler)

Time (min)	% drug release						Average values	Stdev
	Tab. 1	Tab. 2	Tab. 3	Tab. 4	Tab. 5	Tab. 6		
0	0.00	0.00	0.00	0.00	0.00	0.00	0.00	0.00
0.5	12.21	21.56	8.62	10.48	10.33	14.05	12.88	4.64
1	60.54	66.60	74.86	87.39	89.07	74.92	75.56	11.22
2	85.82	91.96	94.21	97.80	96.26	91.43	92.91	4.25
3	89.23	93.47	95.94	98.78	101.98	93.01	95.40	4.53
4	94.45	95.60	96.42	97.38	102.24	94.19	96.71	2.96
5	94.47	95.37	96.42	97.60	102.71	98.44	97.50	2.93
7	96.37	99.61	97.83	97.84	101.53	100.01	98.86	1.86
9	98.27	100.80	98.31	95.49	100.81	99.07	98.79	1.98
11	99.22	99.86	97.60	96.66	102.00	100.01	99.23	1.89
13	98.75	100.57	95.95	97.84	101.76	99.07	98.99	2.04
15	99.22	99.86	96.42	98.78	99.39	98.60	98.71	1.21
17	99.46	99.15	95.95	97.38	99.86	98.83	98.44	1.49
T (C°)	37.3	37.3	36.9	37.3	37.3	37.1	37.2	0.17

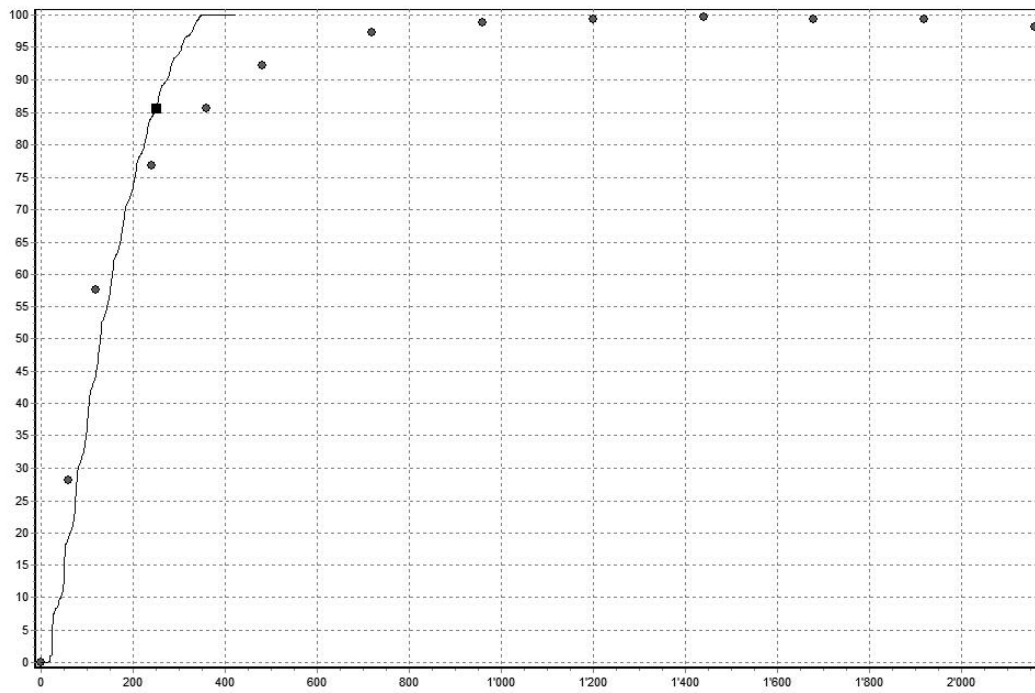
Drug release data of **formulation XIV** tablets ($\epsilon_t=9\%$)
Aspirin (drug) / Lactose monohydrate (filler)

Time (min)	% drug release						Average values	Stdev
	Tab. 1	Tab. 2	Tab. 3	Tab. 4	Tab. 5	Tab. 6		
15	8.73	8.34	6.75	7.54	6.21	7.55	7.52	0.94
30	15.68	15.28	13.99	15.96	13.84	14.64	14.90	0.88
45	21.84	21.45	20.86	23.81	20.35	20.97	21.55	1.22
60	28.76	28.36	27.72	31.28	27.61	27.66	28.57	1.41
75	35.50	35.29	34.20	37.99	34.30	34.56	35.31	1.42
90	40.90	40.31	40.11	44.12	38.91	40.50	40.81	1.75
120	51.63	51.22	50.55	55.93	49.18	50.80	51.55	2.30
150	62.22	61.61	59.90	67.98	58.37	62.09	62.03	3.28
180	70.14	68.38	66.97	74.17	65.84	68.46	68.99	2.93
210	76.31	75.68	73.08	80.10	71.59	74.02	75.13	2.98
240	81.33	79.18	77.67	85.85	77.51	79.20	80.12	3.12
270	85.00	83.98	81.86	88.94	81.93	87.21	84.82	2.85
300	87.89	86.31	85.49	89.73	85.00	88.24	87.11	1.81
330		88.05	85.33	89.73	85.97	90.71	87.96	2.32
360	87.42	88.83	87.22	89.35	87.12	92.25	88.70	1.97
390	88.12	87.69	86.86	88.78	86.94	90.75	88.19	1.45
420	86.59	87.11	86.29	86.88	87.13	89.98	87.33	1.34
450	87.53	86.15	85.53	86.29	84.67	87.89	86.34	1.21
480	87.35	85.38	83.83	85.53	85.02	86.35	85.58	1.19
T (C°)	37.3	37.3	37.3	37.3	37.3	37.3	37.3	0.0

Appendix G *In silico* drug release data

Dissolution simulation data: pure caffeine tablets ($\epsilon_t=30\%$)

Time unit	Time (min)	% drug release	Time unit	Time (min)	% drug release	Time unit	Time (min)	% drug release
3	0.05	0.00	147	2.45	55.95	291	4.85	93.44
7	0.12	0.00	151	2.52	57.96	295	4.92	93.70
11	0.18	0.00	155	2.58	60.29	299	4.98	94.02
15	0.25	0.07	159	2.65	62.30	303	5.05	94.49
19	0.32	0.74	163	2.72	62.99	307	5.12	95.34
23	0.38	1.22	167	2.78	63.64	311	5.18	96.24
27	0.45	7.40	171	2.85	64.59	315	5.25	96.63
31	0.52	8.21	175	2.92	66.18	319	5.32	96.78
35	0.58	8.40	179	2.98	68.08	323	5.38	96.98
39	0.65	9.53	183	3.05	70.06	327	5.45	97.31
43	0.72	10.04	187	3.12	70.95	331	5.52	97.93
47	0.78	10.80	191	3.18	71.49	335	5.58	98.63
51	0.85	15.45	195	3.25	72.25	339	5.65	99.14
55	0.92	18.48	199	3.32	73.24	343	5.72	99.49
59	0.98	19.22	203	3.38	74.76	347	5.78	99.89
63	1.05	20.00	207	3.45	76.55	351	5.85	100.00
67	1.12	20.80	211	3.52	77.85	355	5.92	100.00
71	1.18	21.98	215	3.58	78.31	359	5.98	100.00
75	1.25	25.03	219	3.65	78.86	363	6.05	100.00
79	1.32	29.42	223	3.72	79.55	367	6.12	100.00
83	1.38	30.50	227	3.78	80.63	371	6.18	100.00
87	1.45	31.30	231	3.85	82.21	375	6.25	100.00
91	1.52	32.17	235	3.92	83.59	379	6.32	100.00
95	1.58	33.42	239	3.98	84.12	383	6.38	100.00
99	1.65	35.72	243	4.05	84.58	387	6.45	100.00
103	1.72	39.04	247	4.12	85.10	391	6.52	100.00
107	1.78	41.84	251	4.18	85.77	395	6.58	100.00
111	1.85	42.56	255	4.25	86.94	399	6.65	100.00
115	1.92	43.35	259	4.32	88.30	403	6.72	100.00
119	1.98	44.42	263	4.38	89.07	407	6.78	100.00
123	2.05	46.26	267	4.45	89.46	411	6.85	100.00
127	2.12	48.67	271	4.52	89.80	415	6.92	100.00
131	2.18	51.79	275	4.58	90.24	419	6.98	100.00
135	2.25	52.96	279	4.65	90.98	423	7.05	100.00
139	2.32	53.72	283	4.72	92.26			
143	2.38	54.59	287	4.78	93.11			



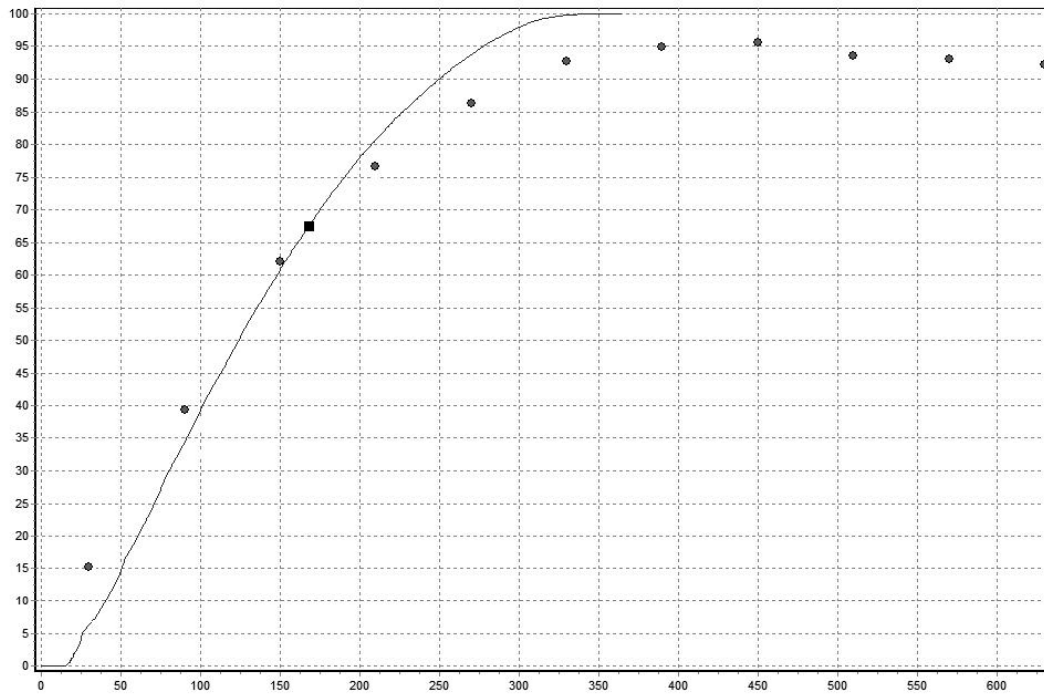
View of the *in silico* dissolution profile of pure caffeine tablets in the DS module interface with uploaded experimental points.

Dissolution simulation data: pure Aspirin tablets ($\epsilon_t=30\%$)

Time unit	Time (min)	% drug release	Time unit	Time (min)	% drug release	Time unit	Time (min)	% drug release
0	0	0.00	71	71	25.05	142	142	57.61
1	1	0.00	72	72	25.54	143	143	57.97
2	2	0.00	73	73	26.07	144	144	58.35
3	3	0.00	74	74	26.61	145	145	58.74
4	4	0.00	75	75	27.15	146	146	59.16
5	5	0.00	76	76	27.73	147	147	59.54
6	6	0.00	77	77	28.32	148	148	59.95
7	7	0.00	78	78	28.91	149	149	60.41
8	8	0.00	79	79	29.48	150	150	60.79
9	9	0.00	80	80	29.95	151	151	61.20
10	10	0.00	81	81	30.36	152	152	61.62
11	11	0.00	82	82	30.78	153	153	61.99
12	12	0.00	83	83	31.22	154	154	62.37
13	13	0.01	84	84	31.61	155	155	62.75
14	14	0.01	85	85	32.09	156	156	63.12
15	15	0.04	86	86	32.58	157	157	63.50
16	16	0.13	87	87	33.05	158	158	63.86
17	17	0.27	88	88	33.48	159	159	64.19
18	18	0.65	89	89	33.89	160	160	64.57
19	19	1.15	90	90	34.39	161	161	64.94
20	20	1.49	91	91	34.86	162	162	65.28
21	21	2.02	92	92	35.34	163	163	65.66
22	22	2.33	93	93	35.80	164	164	66.02
23	23	2.72	94	94	36.27	165	165	66.39
24	24	3.41	95	95	36.76	166	166	66.72
25	25	3.99	96	96	37.22	167	167	67.10
26	26	5.10	97	97	37.72	168	168	67.47
27	27	5.44	98	98	38.27	169	169	67.82
28	28	5.66	99	99	38.76	170	170	68.19
29	29	6.04	100	100	39.28	171	171	68.55
30	30	6.35	101	101	39.74	172	172	68.94
31	31	6.64	102	102	40.29	173	173	69.28
32	32	6.91	103	103	40.83	174	174	69.66
33	33	7.19	104	104	41.28	175	175	70.03
34	34	7.52	105	105	41.75	176	176	70.37
35	35	7.84	106	106	42.21	177	177	70.71
36	36	8.25	107	107	42.63	178	178	71.03
37	37	8.65	108	108	43.07	179	179	71.35
38	38	9.06	109	109	43.45	180	180	71.67
39	39	9.46	110	110	43.88	181	181	72.03
40	40	9.83	111	111	44.28	182	182	72.35
41	41	10.19	112	112	44.67	183	183	72.66
42	42	10.69	113	113	45.12	184	184	72.97
43	43	11.15	114	114	45.53	185	185	73.28
44	44	11.58	115	115	46.00	186	186	73.59
45	45	12.01	116	116	46.45	187	187	73.92
46	46	12.51	117	117	46.91	188	188	74.23
47	47	13.07	118	118	47.36	189	189	74.53
48	48	13.56	119	119	47.79	190	190	74.88
49	49	14.12	120	120	48.24	191	191	75.16
50	50	14.70	121	121	48.71	192	192	75.49
51	51	15.31	122	122	49.18	193	193	75.82
52	52	16.05	123	123	49.63	194	194	76.16
53	53	16.76	124	124	50.07	195	195	76.50
54	54	17.18	125	125	50.54	196	196	76.80
55	55	17.61	126	126	51.03	197	197	77.06
56	56	18.01	127	127	51.45	198	198	77.35
57	57	18.41	128	128	51.89	199	199	77.64
58	58	18.83	129	129	52.35	200	200	77.92
59	59	19.23	130	130	52.80	201	201	78.23
60	60	19.66	131	131	53.22	202	202	78.52
61	61	20.14	132	132	53.58	203	203	78.80
62	62	20.67	133	133	53.97	204	204	79.08
63	63	21.15	134	134	54.35	205	205	79.34
64	64	21.61	135	135	54.76	206	206	79.60
65	65	22.05	136	136	55.17	207	207	79.87
66	66	22.50	137	137	55.57	208	208	80.13
67	67	22.96	138	138	55.95	209	209	80.41
68	68	23.43	139	139	56.36	210	210	80.67
69	69	23.94	140	140	56.76	211	211	80.94
70	70	24.47	141	141	57.18	212	212	81.20

Dissolution simulation data: pure Aspirin tablets ($\epsilon_t=30\%$) (continued)

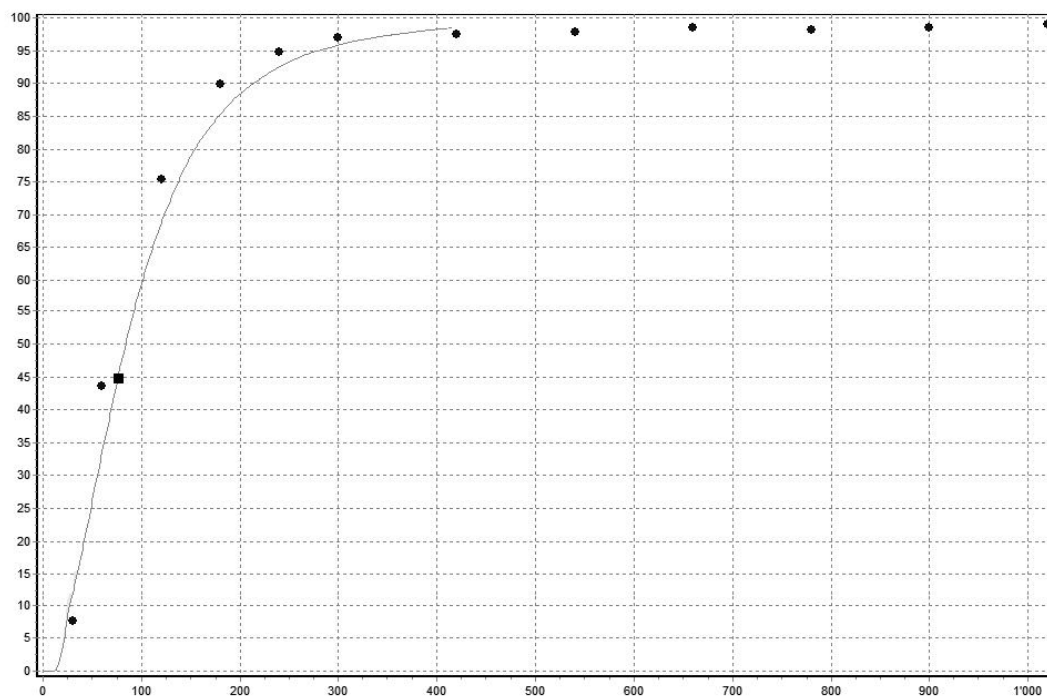
Time unit	Time (min)	% drug release	Time unit	Time (min)	% drug release	Time unit	Time (min)	% drug release
213	213	81.48	264	264	92.77	315	315	99.26
214	214	81.72	265	265	92.93	316	316	99.30
215	215	81.98	266	266	93.09	317	317	99.35
216	216	82.24	267	267	93.26	318	318	99.39
217	217	82.47	268	268	93.43	319	319	99.44
218	218	82.73	269	269	93.60	320	320	99.47
219	219	82.97	270	270	93.79	321	321	99.53
220	220	83.24	271	271	93.96	322	322	99.56
221	221	83.49	272	272	94.13	323	323	99.60
222	222	83.75	273	273	94.28	324	324	99.64
223	223	83.97	274	274	94.44	325	325	99.67
224	224	84.22	275	275	94.59	326	326	99.70
225	225	84.45	276	276	94.77	327	327	99.73
226	226	84.69	277	277	94.95	328	328	99.75
227	227	84.93	278	278	95.08	329	329	99.77
228	228	85.18	279	279	95.23	330	330	99.80
229	229	85.42	280	280	95.38	331	331	99.83
230	230	85.65	281	281	95.54	332	332	99.85
231	231	85.87	282	282	95.70	333	333	99.87
232	232	86.13	283	283	95.83	334	334	99.89
233	233	86.34	284	284	95.96	335	335	99.90
234	234	86.57	285	285	96.10	336	336	99.91
235	235	86.78	286	286	96.23	337	337	99.93
236	236	87.03	287	287	96.35	338	338	99.94
237	237	87.24	288	288	96.47	339	339	99.95
238	238	87.49	289	289	96.60	340	340	99.96
239	239	87.71	290	290	96.74	341	341	99.96
240	240	87.94	291	291	96.87	342	342	99.97
241	241	88.16	292	292	97.00	343	343	99.97
242	242	88.36	293	293	97.13	344	344	99.98
243	243	88.56	294	294	97.24	345	345	99.98
244	244	88.78	295	295	97.37	346	346	99.98
245	245	88.98	296	296	97.47	347	347	99.99
246	246	89.19	297	297	97.60	348	348	99.99
247	247	89.38	298	298	97.72	349	349	99.99
248	248	89.58	299	299	97.82	350	350	99.99
249	249	89.78	300	300	97.94	351	351	99.99
250	250	89.98	301	301	98.05	352	352	100.00
251	251	90.18	302	302	98.16	353	353	100.00
252	252	90.41	303	303	98.27	354	354	100.00
253	253	90.61	304	304	98.37	355	355	100.00
254	254	90.79	305	305	98.47	356	356	100.00
255	255	91.01	306	306	98.56	357	357	100.00
256	256	91.19	307	307	98.65	358	358	100.00
257	257	91.40	308	308	98.73	359	359	100.00
258	258	91.62	309	309	98.82	360	360	100.00
259	259	91.82	310	310	98.90	361	361	100.00
260	260	92.01	311	311	98.98	362	362	100.00
261	261	92.20	312	312	99.06	363	363	100.00
262	262	92.39	313	313	99.13	364	364	100.00
263	263	92.57	314	314	99.19	365	365	100.00



View of the *in silico* dissolution profile of pure Aspirin tablets in the DS module interface with uploaded experimental points.

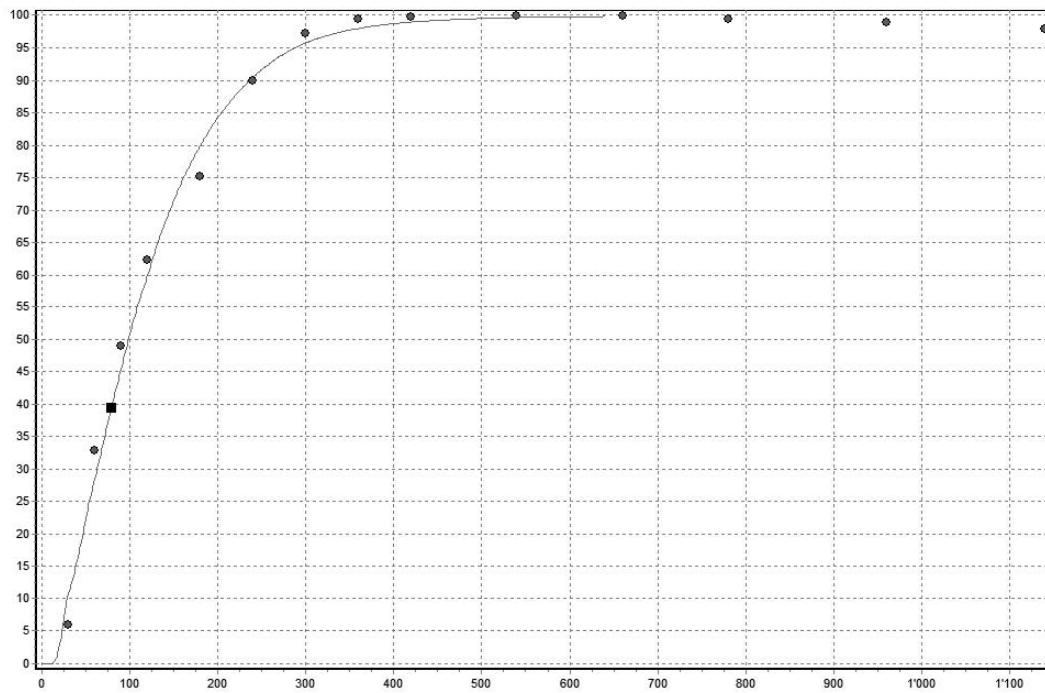
Dissolution simulation data: formulation X tablets ($\epsilon_t=9\%$)

Time unit	Time (min)	% drug release	Time unit	Time (min)	% drug release	Time unit	Time (min)	% drug release
3	0.05	0.00	143	2.38	76.92	283	4.72	95.15
7	0.12	0.00	147	2.45	77.99	287	4.78	95.31
11	0.18	0.02	151	2.52	79.15	291	4.85	95.45
15	0.25	0.76	155	2.58	80.24	295	4.92	95.61
19	0.32	3.10	159	2.65	81.12	299	4.98	95.83
23	0.38	6.19	163	2.72	82.05	303	5.05	95.99
27	0.45	9.97	167	2.78	82.77	307	5.12	96.15
31	0.52	12.71	171	2.85	83.63	311	5.18	96.28
35	0.58	15.30	175	2.92	84.39	315	5.25	96.43
39	0.65	18.06	179	2.98	85.17	319	5.32	96.56
43	0.72	20.91	183	3.05	85.86	323	5.38	96.67
47	0.78	23.81	187	3.12	86.51	327	5.45	96.75
51	0.85	27.08	191	3.18	87.16	331	5.52	96.86
55	0.92	29.89	195	3.25	87.80	335	5.58	96.98
59	0.98	32.75	199	3.32	88.30	339	5.65	97.07
63	1.05	35.70	203	3.38	88.77	343	5.72	97.20
67	1.12	38.43	207	3.45	89.33	347	5.78	97.27
71	1.18	41.32	211	3.52	89.75	351	5.85	97.35
75	1.25	44.15	215	3.58	90.16	355	5.92	97.44
79	1.32	46.90	219	3.65	90.57	359	5.98	97.50
83	1.38	49.42	223	3.72	90.99	363	6.05	97.60
87	1.45	51.86	227	3.78	91.41	367	6.12	97.68
91	1.52	54.30	231	3.85	91.82	371	6.18	97.76
95	1.58	56.53	235	3.92	92.16	375	6.25	97.86
99	1.65	58.88	239	3.98	92.48	379	6.32	97.92
103	1.72	60.99	243	4.05	92.83	383	6.38	97.99
107	1.78	62.98	247	4.12	93.09	387	6.45	98.07
111	1.85	64.80	251	4.18	93.42	391	6.52	98.15
115	1.92	66.56	255	4.25	93.71	395	6.58	98.21
119	1.98	68.27	259	4.32	93.91	399	6.65	98.27
123	2.05	69.88	263	4.38	94.20	403	6.72	98.33
127	2.12	71.33	267	4.45	94.42	407	6.78	98.38
131	2.18	72.79	271	4.52	94.64	411	6.85	98.42
135	2.25	74.15	275	4.58	94.84	415	6.92	98.47
139	2.32	75.51	279	4.65	94.99			

View of the *in silico* dissolution profile of formulation X tablets in the DS module interface with uploaded experimental points.

Dissolution simulation data: formulation XI tablets ($\epsilon_t=9\%$)

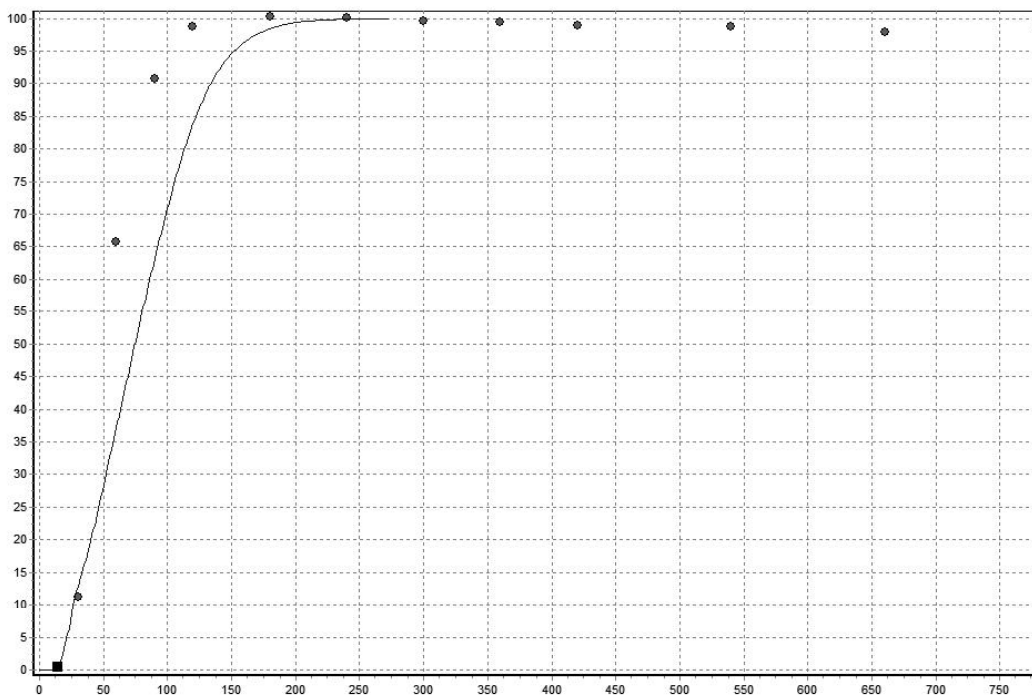
Time unit	Time (min)	% drug release	Time unit	Time (min)	% drug release	Time unit	Time (min)	% drug release
3	0.05	0.00	219	3.65	87.53	435	7.25	99.11
7	0.12	0.00	223	3.72	88.16	439	7.32	99.14
11	0.18	0.01	227	3.78	88.73	443	7.38	99.16
15	0.25	0.54	231	3.85	89.29	447	7.45	99.20
19	0.32	2.30	235	3.92	89.82	451	7.52	99.23
23	0.38	5.00	239	3.98	90.34	455	7.58	99.25
27	0.45	8.76	243	4.05	90.85	459	7.65	99.30
31	0.52	11.12	247	4.12	91.33	463	7.72	99.32
35	0.58	13.07	251	4.18	91.79	467	7.78	99.35
39	0.65	15.39	255	4.25	92.18	471	7.85	99.37
43	0.72	17.66	259	4.32	92.61	475	7.92	99.39
47	0.78	20.18	263	4.38	93.03	479	7.98	99.40
51	0.85	23.08	267	4.45	93.41	483	8.05	99.42
55	0.92	25.60	271	4.52	93.74	487	8.12	99.45
59	0.98	27.79	275	4.58	94.02	491	8.18	99.47
63	1.05	30.06	279	4.65	94.32	495	8.25	99.50
67	1.12	32.33	283	4.72	94.66	499	8.32	99.52
71	1.18	34.65	287	4.78	94.93	503	8.38	99.55
75	1.25	37.11	291	4.85	95.22	507	8.45	99.55
79	1.32	39.52	295	4.92	95.47	511	8.52	99.57
83	1.38	41.68	299	4.98	95.71	515	8.58	99.58
87	1.45	43.73	303	5.05	95.93	519	8.65	99.60
91	1.52	45.91	307	5.12	96.15	523	8.72	99.61
95	1.58	48.07	311	5.18	96.33	527	8.78	99.62
99	1.65	50.23	315	5.25	96.51	531	8.85	99.63
103	1.72	52.27	319	5.32	96.69	535	8.92	99.65
107	1.78	54.19	323	5.38	96.84	539	8.98	99.67
111	1.85	56.04	327	5.45	96.97	543	9.05	99.68
115	1.92	57.77	331	5.52	97.12	547	9.12	99.68
119	1.98	59.55	335	5.58	97.27	551	9.18	99.71
123	2.05	61.30	339	5.65	97.41	555	9.25	99.71
127	2.12	63.06	343	5.72	97.56	559	9.32	99.72
131	2.18	64.72	347	5.78	97.68	563	9.38	99.73
135	2.25	66.25	351	5.85	97.77	567	9.45	99.74
139	2.32	67.65	355	5.92	97.85	571	9.52	99.74
143	2.38	69.11	359	5.98	97.93	575	9.58	99.75
147	2.45	70.53	363	6.05	98.04	579	9.65	99.77
151	2.52	71.89	367	6.12	98.15	583	9.72	99.77
155	2.58	73.16	371	6.18	98.23	587	9.78	99.77
159	2.65	74.31	375	6.25	98.33	591	9.85	99.78
163	2.72	75.55	379	6.32	98.42	595	9.92	99.78
167	2.78	76.60	383	6.38	98.47	599	9.98	99.79
171	2.85	77.69	387	6.45	98.55	603	10.05	99.79
175	2.92	78.75	391	6.52	98.60	607	10.12	99.80
179	2.98	79.68	395	6.58	98.66	611	10.18	99.80
183	3.05	80.57	399	6.65	98.72	615	10.25	99.81
187	3.12	81.50	403	6.72	98.76	619	10.32	99.81
191	3.18	82.42	407	6.78	98.82	623	10.38	99.82
195	3.25	83.33	411	6.85	98.86	627	10.45	99.82
199	3.32	84.13	415	6.92	98.91	631	10.52	99.82
203	3.38	84.82	419	6.98	98.94	635	10.58	99.83
207	3.45	85.48	423	7.05	99.01	639	10.65	99.83
211	3.52	86.23	427	7.12	99.05			
215	3.58	86.82	431	7.18	99.08			



View of the *in silico* dissolution profile of formulation XI tablets in the DS module interface with uploaded experimental points.

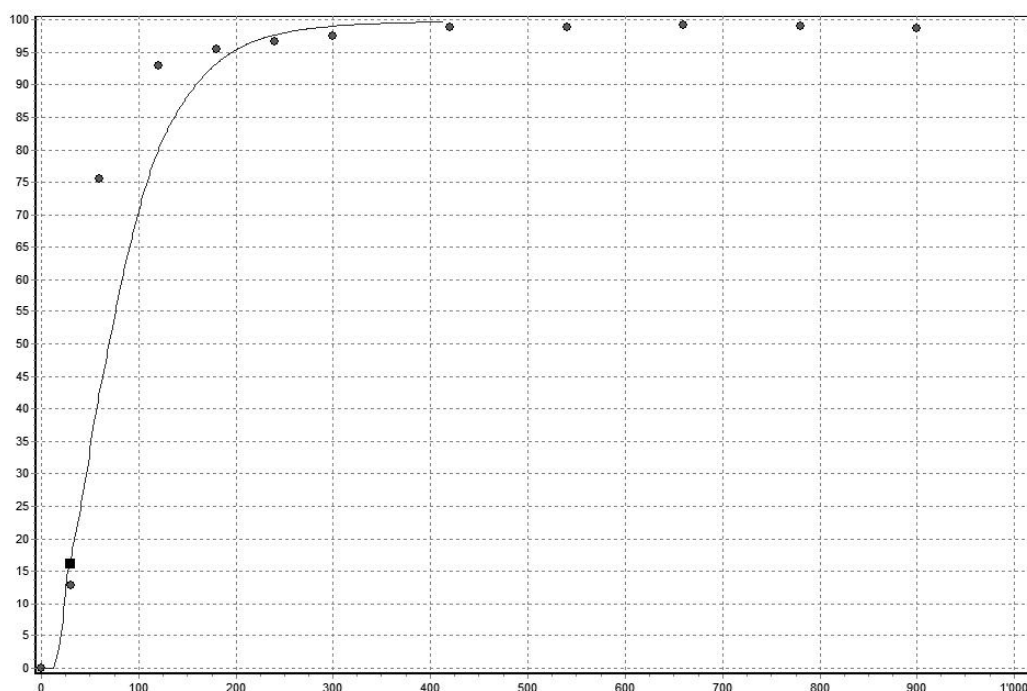
Dissolution simulation data: formulation XII tablets ($\epsilon_t=9\%$)

Time unit	Time (min)	% drug release	Time unit	Time (min)	% drug release	Time unit	Time (min)	% drug release
3	0.05	0.00	95	1.58	67.07	187	3.12	98.86
7	0.12	0.00	99	1.65	70.16	191	3.18	99.05
11	0.18	0.02	103	1.72	73.15	195	3.25	99.21
15	0.25	0.79	107	1.78	75.90	199	3.32	99.33
19	0.32	3.15	111	1.85	78.54	203	3.38	99.44
23	0.38	6.37	115	1.92	81.12	207	3.45	99.53
27	0.45	10.59	119	1.98	83.29	211	3.52	99.59
31	0.52	13.52	123	2.05	85.40	215	3.58	99.65
35	0.58	16.18	127	2.12	87.23	219	3.65	99.70
39	0.65	19.06	131	2.18	88.92	223	3.72	99.74
43	0.72	22.17	135	2.25	90.44	227	3.78	99.80
47	0.78	25.57	139	2.32	91.73	231	3.85	99.83
51	0.85	29.28	143	2.38	92.90	235	3.92	99.85
55	0.92	32.85	147	2.45	93.93	239	3.98	99.89
59	0.98	36.29	151	2.52	94.85	243	4.05	99.90
63	1.05	39.92	155	2.58	95.57	247	4.12	99.92
67	1.12	43.39	159	2.65	96.24	251	4.18	99.94
71	1.18	46.88	163	2.72	96.77	255	4.25	99.94
75	1.25	50.46	167	2.78	97.29	259	4.32	99.95
79	1.32	53.91	171	2.85	97.65	263	4.38	99.95
83	1.38	57.28	175	2.92	98.02	267	4.45	99.96
87	1.45	60.75	179	2.98	98.36	271	4.52	99.97
91	1.52	64.01	183	3.05	98.61			

View of the *in silico* dissolution profile of formulation XII tablets in the DS module interface with uploaded experimental points.

Dissolution simulation data: formulation XIII tablets ($\epsilon_t=12\%$)

Time unit	Time (min)	% drug release	Time unit	Time (min)	% drug release	Time unit	Time (min)	% drug release
3	0.05	0.00	143	2.38	86.60	283	4.72	98.77
7	0.12	0.00	147	2.45	87.51	287	4.78	98.84
11	0.18	0.01	151	2.52	88.41	291	4.85	98.90
15	0.25	1.15	155	2.58	89.17	295	4.92	98.94
19	0.32	4.17	159	2.65	90.01	299	4.98	99.01
23	0.38	8.71	163	2.72	90.73	303	5.05	99.09
27	0.45	14.87	167	2.78	91.40	307	5.12	99.14
31	0.52	17.64	171	2.85	92.02	311	5.18	99.16
35	0.58	20.66	175	2.92	92.60	315	5.25	99.20
39	0.65	23.76	179	2.98	93.11	319	5.32	99.25
43	0.72	27.25	183	3.05	93.64	323	5.38	99.29
47	0.78	30.79	187	3.12	94.10	327	5.45	99.32
51	0.85	34.90	191	3.18	94.54	331	5.52	99.33
55	0.92	38.77	195	3.25	94.93	335	5.58	99.37
59	0.98	42.02	199	3.32	95.32	339	5.65	99.38
63	1.05	44.95	203	3.38	95.62	343	5.72	99.40
67	1.12	48.07	207	3.45	95.94	347	5.78	99.43
71	1.18	51.03	211	3.52	96.23	351	5.85	99.46
75	1.25	54.28	215	3.58	96.51	355	5.92	99.48
79	1.32	57.24	219	3.65	96.73	359	5.98	99.50
83	1.38	60.21	223	3.72	96.93	363	6.05	99.52
87	1.45	62.66	227	3.78	97.21	367	6.12	99.53
91	1.52	65.21	231	3.85	97.36	371	6.18	99.56
95	1.58	67.55	235	3.92	97.50	375	6.25	99.58
99	1.65	69.95	239	3.98	97.64	379	6.32	99.58
103	1.72	72.27	243	4.05	97.75	383	6.38	99.59
107	1.78	74.22	247	4.12	97.89	387	6.45	99.61
111	1.85	76.13	251	4.18	98.04	391	6.52	99.63
115	1.92	77.92	255	4.25	98.13	395	6.58	99.64
119	1.98	79.45	259	4.32	98.28	399	6.65	99.65
123	2.05	80.88	263	4.38	98.37	403	6.72	99.66
127	2.12	82.34	267	4.45	98.46	407	6.78	99.67
131	2.18	83.44	271	4.52	98.56	411	6.85	99.69
135	2.25	84.64	275	4.58	98.63			
139	2.32	85.57	279	4.65	98.70			

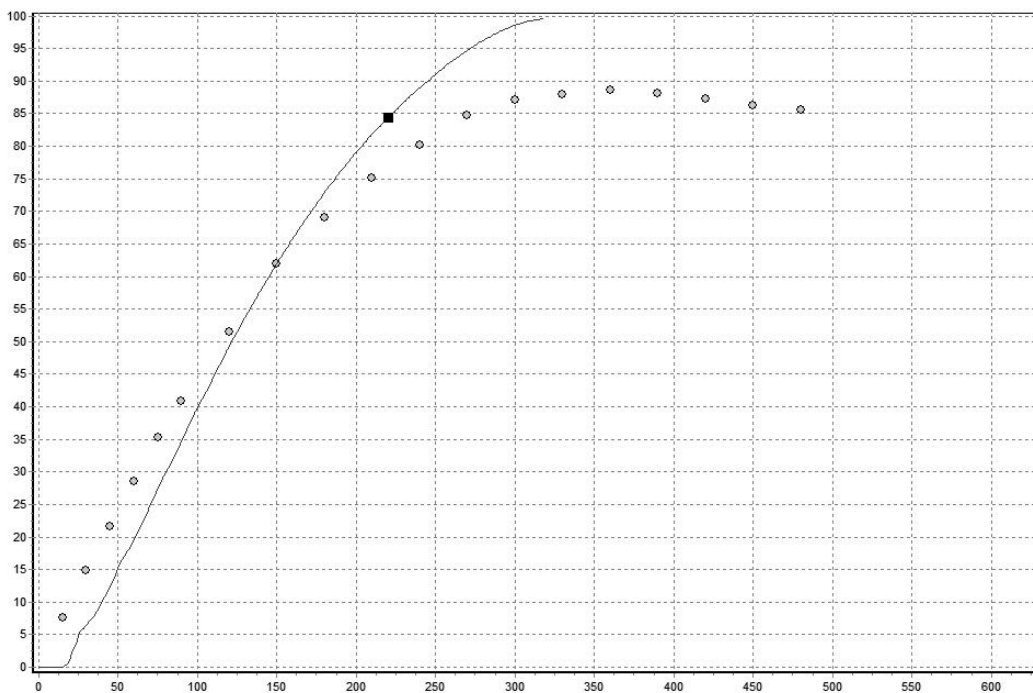
View of the *in silico* dissolution profile of formulation XIII tablets in the DS module interface with uploaded experimental points.

Dissolution simulation data: formulation XIV tablets ($\epsilon_t=14\%$)

Time unit	Time (min)	% drug release	Time unit	Time (min)	% drug release	Time unit	Time (min)	% drug release
0	0	0.00	73	73	26.36	146	146	60.38
1	1	0.00	74	74	26.92	147	147	60.78
2	2	0.00	75	75	27.47	148	148	61.17
3	3	0.00	76	76	28.01	149	149	61.58
4	4	0.00	77	77	28.50	150	150	62.00
5	5	0.00	78	78	28.98	151	151	62.39
6	6	0.00	79	79	29.42	152	152	62.81
7	7	0.00	80	80	29.87	153	153	63.20
8	8	0.00	81	81	30.34	154	154	63.58
9	9	0.00	82	82	30.80	155	155	63.95
10	10	0.00	83	83	31.26	156	156	64.33
11	11	0.00	84	84	31.76	157	157	64.71
12	12	0.00	85	85	32.26	158	158	65.10
13	13	0.01	86	86	32.74	159	159	65.49
14	14	0.03	87	87	33.22	160	160	65.85
15	15	0.07	88	88	33.72	161	161	66.22
16	16	0.14	89	89	34.24	162	162	66.58
17	17	0.27	90	90	34.79	163	163	66.94
18	18	0.49	91	91	35.32	164	164	67.31
19	19	1.04	92	92	35.84	165	165	67.65
20	20	1.60	93	93	36.36	166	166	68.00
21	21	2.28	94	94	36.89	167	167	68.37
22	22	2.80	95	95	37.40	168	168	68.71
23	23	3.28	96	96	37.89	169	169	69.08
24	24	4.05	97	97	38.43	170	170	69.45
25	25	4.82	98	98	38.93	171	171	69.79
26	26	5.54	99	99	39.41	172	172	70.14
27	27	5.73	100	100	39.88	173	173	70.49
28	28	5.94	101	101	40.34	174	174	70.81
29	29	6.21	102	102	40.79	175	175	71.17
30	30	6.47	103	103	41.22	176	176	71.52
31	31	6.73	104	104	41.69	177	177	71.85
32	32	7.04	105	105	42.15	178	178	72.17
33	33	7.36	106	106	42.62	179	179	72.52
34	34	7.68	107	107	43.11	180	180	72.86
35	35	8.01	108	108	43.61	181	181	73.20
36	36	8.40	109	109	44.09	182	182	73.55
37	37	8.82	110	110	44.58	183	183	73.89
38	38	9.29	111	111	45.06	184	184	74.20
39	39	9.73	112	112	45.53	185	185	74.51
40	40	10.16	113	113	46.01	186	186	74.84
41	41	10.60	114	114	46.50	187	187	75.15
42	42	11.04	115	115	46.98	188	188	75.47
43	43	11.49	116	116	47.47	189	189	75.79
44	44	11.96	117	117	47.95	190	190	76.10
45	45	12.42	118	118	48.40	191	191	76.40
46	46	12.94	119	119	48.86	192	192	76.70
47	47	13.48	120	120	49.35	193	193	76.99
48	48	14.04	121	121	49.78	194	194	77.29
49	49	14.63	122	122	50.23	195	195	77.59
50	50	15.22	123	123	50.65	196	196	77.87
51	51	15.84	124	124	51.11	197	197	78.17
52	52	16.37	125	125	51.55	198	198	78.48
53	53	16.78	126	126	51.97	199	199	78.77
54	54	17.13	127	127	52.41	200	200	79.06
55	55	17.55	128	128	52.82	201	201	79.32
56	56	17.90	129	129	53.27	202	202	79.61
57	57	18.31	130	130	53.67	203	203	79.89
58	58	18.73	131	131	54.12	204	204	80.16
59	59	19.20	132	132	54.61	205	205	80.45
60	60	19.65	133	133	55.03	206	206	80.73
61	61	20.16	134	134	55.46	207	207	81.01
62	62	20.66	135	135	55.90	208	208	81.30
63	63	21.15	136	136	56.31	209	209	81.57
64	64	21.64	137	137	56.74	210	210	81.86
65	65	22.12	138	138	57.14	211	211	82.13
66	66	22.62	139	139	57.55	212	212	82.38
67	67	23.15	140	140	57.97	213	213	82.64
68	68	23.67	141	141	58.38	214	214	82.89
69	69	24.20	142	142	58.79	215	215	83.14
70	70	24.75	143	143	59.17	216	216	83.38
71	71	25.28	144	144	59.56	217	217	83.63
72	72	25.81	145	145	59.95	218	218	83.88

Dissolution simulation data: formulation XIV tablets ($\epsilon_t=14\%$)
(continued)

Time unit	Time (min)	% drug release	Time unit	Time (min)	% drug release	Time unit	Time (min)	% drug release
219	219	84.13	253	253	91.67	287	287	97.17
220	220	84.36	254	254	91.87	288	288	97.31
221	221	84.60	255	255	92.06	289	289	97.44
222	222	84.84	256	256	92.27	290	290	97.55
223	223	85.11	257	257	92.45	291	291	97.67
224	224	85.32	258	258	92.64	292	292	97.79
225	225	85.56	259	259	92.82	293	293	97.89
226	226	85.81	260	260	93.01	294	294	98.01
227	227	86.07	261	261	93.18	295	295	98.12
228	228	86.31	262	262	93.35	296	296	98.22
229	229	86.56	263	263	93.52	297	297	98.32
230	230	86.79	264	264	93.69	298	298	98.41
231	231	87.01	265	265	93.86	299	299	98.50
232	232	87.25	266	266	94.03	300	300	98.59
233	233	87.47	267	267	94.20	301	301	98.67
234	234	87.70	268	268	94.39	302	302	98.76
235	235	87.92	269	269	94.57	303	303	98.84
236	236	88.15	270	270	94.75	304	304	98.92
237	237	88.34	271	271	94.92	305	305	98.99
238	238	88.56	272	272	95.08	306	306	99.06
239	239	88.75	273	273	95.24	307	307	99.11
240	240	88.97	274	274	95.41	308	308	99.18
241	241	89.19	275	275	95.53	309	309	99.24
242	242	89.40	276	276	95.69	310	310	99.28
243	243	89.60	277	277	95.83	311	311	99.33
244	244	89.80	278	278	95.99	312	312	99.38
245	245	90.00	279	279	96.13	313	313	99.43
246	246	90.20	280	280	96.27	314	314	99.47
247	247	90.40	281	281	96.41	315	315	99.51
248	248	90.61	282	282	96.55	316	316	99.54
249	249	90.82	283	283	96.67	317	317	99.57
250	250	91.02	284	284	96.79	318	318	99.60
251	251	91.25	285	285	96.91			
252	252	91.47	286	286	97.03			



View of the *in silico* dissolution profile of formulation XIV tablets in the DS module interface with uploaded experimental points.

CURRICULUM VITAE

Personal details:

Name Etienne Krausbauer
Date of birth 2nd of April 1979
Place of origin Strasbourg (France)

Professional education:

2004 (6 months) **MEDIT-SA**, Paris: Development of innovating software for Structure-Based Drug Design (MED-SuMo)
2003 (6 months) **NEURO3D/IFR85**, Strasbourg: build up an original bioinformatic tool to create automatically and to analyse proteinic databases
2002 (2 months) **CNRS**, Strasbourg: creation of a database on macromolecular target used in virtual screening (reversed docking)
2001 (1 month) **SANOFI-SYNTHELABO**, Strasbourg: Ruled scientific library
2000 (1 month) **INSERM**, Strasbourg: Engineer assistant for the development of biomedical equipments

Education:

2004-2007 **PhD study** under the supervision of Prof. Dr. H. Leuenberger at the Institute of Pharmaceutical Technology (University of Basel)
Assistant of practical university course: sterile liquid dosage forms
Tutor of practical and seminar projects: solid dosage forms
IT management at the Institute of Pharmaceutical Technology
2003-2004 **Master "Bioinformatic / molecular modeling"**
Ecole Supérieure de Biotechnologie de Strasbourg (ESBS), France
Thesis: "Development and evaluation of innovating procedures of structure-based drug design"
2001-2003 **IUP "Bioinformatic"**
Université Louis Pasteur de Strasbourg (ULP), France
2000-2001 **DEUG1 "Bio-physico-chemistry"**
ULP, France

Publications, presentations and posters:

Publications:

"Rational estimation of the optimum amount of spherical disintegrant particles applying percolation theory for binary fast-disintegrating formulation"

Etienne Krausbauer, Maxim Puchkov, Gabriele Betz, Hans Leuenberger
Journal of Pharmaceutical Sciences, accepted 13 July 2007

"Manufacturing Pharmaceutical Granules: Is the Granulation Endpoint a Myth?"

Hans Leuenberger, Maxim Puchkov, Etienne Krausbauer, Gabrielle Betz
Submitted to the Powder Technology accepted in 2007

Oral presentations:

“Cellular automata: the model of nature and principals of computational equivalence”

TTC workshop no. 133: Mathematics for process modeling, 27-28 May 2007, Binzen, Germany

“Formulation computer aided design”

Pharmatrans Sanaq 5th Scientific Forum, 16-18 April 2007, Basel

“Computer-aided design of solid dosage forms: a formulation design toolbox for pharmaceutical industry”

FMC Tablet tech 2007 - Solid Dosage Form Manufacturing, 25-26 October, Brussels, Belgium

“Computing formulation design”

TTC workshop no. 120: From Art to Science III: Quality Assurance by Process Understanding, 18-20 September 2007, Binzen, Germany

“Expert system software for solid dosage formulation design”

Pharmaceutical Sciences World Congress 2007, 22-25 April, Amsterdam, Netherlands

“Expert system for formulation design”

TTC (Technology Training Center) workshop no. 119: Robust Dosage Form Design, 6-7 February 2007, Binzen, Germany

“Expert system software for solid dosage formulation design”

Roche, 18 December 2006, Basel, Switzerland

Posters:

“Development of Paracetamol tablet formulations using 3D factorial design.”

E. Krausbauer, M. Tscheulin, M. Puchkov, G. Betz, H. Leuenberger

APV Worldmeeting on Pharmaceutics, Biopharmaceutics and Pharmaceutical Technology, March 2006, Geneva, Switzerland

“Rational estimation of the optimum amount of disintegrant applying percolation theory for binary formulation.”

E. Krausbauer, M. Puchkov, G. Betz, H. Leuenberger

FMC Biopolymer Tablet Tech 2006 (Solid dosage form manufacturing seminar), October 19-20, Brussels, Belgium

“Determination of the critical amount of Ac-Di-Sol[®] for binary formulations with Indomethacin with respect to water uptake.”

M. Puchkov, E. Krausbauer, G. Betz, H. Leuenberger

FMC Biopolymer Tablet Tech 2006 (Solid dosage form manufacturing seminar), October 19-20, Brussels, Belgium

IT Knowledge:

General Algorithmic/Optimisation, Artificial Intelligence, Object-Oriented modelization and development

Network and OS

Operating systems DOS, Windows (2000/XP), UNIX, Linux, MAC OS

Network TCP/IP

Programming

Languages Delphi (Object Pascal), C/C++, Perl, Java, SQL, Mathematica, Matlab

Middleware Corba, ODBC, JDBC, PL/SQL

Databases

modelisation MERISE, UML

softwares Oracle, SQL Server, MySQL

Internet

Dynamic web DHTML, PHP

Presentation web HTML, Javascript, XML

Web servers Netscape Enterprise Server, Apache

Computational

chemistry Molecular modelization, virtual screening.

biology Sequence alignment, gene annotation, proteomic.

pharma. tech. Cellular automata for solid dosage form dissolution simulation

Workshops and conferences:

FMC Biopolymer Tablet Tech.: Solid dosage form manufacturing
25-26 October 2007, Brussels, Belgium

“From Art to Science III”: Quality Assurance by Process Understanding
Technology Training Center (TTC), 18-20 September 2007, Binzen, Germany

Pharmaceutical Sciences World Congress

20-21 (Pre-Satellite for and by PhD Students and Young PostDocs), 22-25 (World congress) April 2007, Amsterdam, Netherlands

FMC Biopolymer Tablet Tech.: Solid dosage form manufacturing seminar

19-20 October 2006, Brussels, Belgium

“From Art to Science II”: Innovative approaches for granulation, coating & drying

Technology Training Center (TTC), 26 - 28 September 2006, Binzen, Germany

“Pharmaceutical Development and Production 2006”

ETH, 13/14 and 19-21 September 2006, Basel, Switzerland

APV Worldmeeting on Pharmaceutics, Biopharmaceutics and Pharmaceutical Technology

27-30 March 2006, Geneva, Switzerland

Thermal Analysis and Calorimetry Conference, 30th anniversary meeting, organised by the swiss society of thermal analysis and calorimetry (STK)

8-9 September 2005, Basel, Switzerland

“From Art to Science”

TTC, 21-23 June 2005, Binzen, Germany

Pharmaceutical Sciences Fair & Exhibition

June 12-17 2005 Nice, France

Visit and practical training in roller compaction (dry agglomeration)

Fitzpatrick, 28 May - 02 June 2005, Saint-Niklaas, Belgium.

“Granulation and tableting”:

TTC, 10-12 May 2005, Binzen, Germany

“Fluid bed drying, granulation and coating”:

TTC, 8-10 March 2005, Binzen, Germany

One day visits of pharmaceutical industries:

Pfizer (Freiburg, Germany), Roche (Basel, Switzerland), Novartis (Stein, Switzerland), Drossapharm Ltd. (Arlesheim, Switzerland)